IDAHO TRANSPORTATION DEPARTMENT

RESEARCH REPORT RP 193

RP 193

Implementation of the MEPDG for Flexible Pavements in Idaho

By

Fouad Bayomy

Professor of Civil Engineering

Sherif El-Badawy

Research Fellow

Ahmed Awed

Graduate Research Assistant

University of Idaho

National Institute for Advanced Transportation Technology,
University of Idaho

Prepared for

Idaho Transportation Department

Research Section,

Transportation Planning Division

http://itd.idaho.gov/planning/research/

October 2011

DISCLAIMER

This document is disseminated under the sponsorship of the Idaho Transportation Department and the United States Department of Transportation in the interest of information exchange. The State of Idaho and the United States Government assume no liability of its contents or use thereof.

The contents of this report reflect the views of the author(s), who are responsible for the facts and accuracy of the data presented herein. The contents do not necessarily reflect the official policies of the Idaho Transportation Department or the United States Department of Transportation.

The State of Idaho and the United States Government do not endorse products or manufacturers. Trademarks or manufacturers' names appear herein only because they are considered essential to the object of this document.

This report does constitute a standard, specification or regulation on report format.

1. Report No.	2. Government Accession No.	3. Recipient's Catalog No.
4. Title and Subtitle Implementation of the MEPDG for Flexible Pavements in Idaho		5. Report Date October 2011
		6. Performing Organization Code KLK557
7. Author(s) Fouad Bayomy, Sherif El-Badawy, and Ahmed Awed		8. Performing Organization Report
9. Performing Organization Name and Address National Institute for Advanced Transportation Technology University of Idaho PO Box 440901; 115 Engineering Physics Building; Moscow, ID 83844-0901		10. Work Unit No. (TRAIS)
		11. Contract or Grant No. RP193
12 . Sponsoring Agency Name and Address Research Section Idaho Transportation Department 3311 West State Street Boise, ID 83707-5881		13. Type of Report and Period Final Draft Report 05/01/2009 to 12/31/2011
		14. Sponsoring Agency Code
15. Supplementary Notes		

16. Abstract

This study was conducted to assist Idaho Transportation Department (ITD) in the implementation of the Mechanistic-Empirical Pavement Design Guide (MEPDG) for flexible pavements. The main research work in this study focused on establishing materials, traffic, and climatic database for Idaho MEPDG implementation. A comprehensive database covering all hierarchical input levels required by MEPDG for hot-mix-asphalt (HMA) and binders, typical in Idaho, were established. The influence of the binder characterization input level on the accuracy of MEPDG predicted dynamic modulus (E*) was investigated. The prediction accuracy of the NCHRP 1-37A viscosity-based Witczak Model, NCHRP 1-40D-binder shear modulus (G*) based Witczak model, Hirsch model, and Gyratory Stability (GS) based Idaho model was also investigated. MEPDG levels 2 and 3 inputs for Idaho unbound materials and subgrade soils were developed. For level 2 subgrade material characterization, 2 models were developed. First, a simple R-value regression model as a function of the soil plasticity index and percent passing No 200 sieve was developed based on historical database of R-value at ITD. Second, a resilient modulus (M_r) predictive model based on the estimated R-value of the soil and laboratory measured M_r values, collected from literature, was developed. For level 3 unbound granular materials and subgrade soils, typical default average values and ranges for R-value, PI, and LL were developed using ITD historical database. For MEPDG traffic characterization, classification and weight data from 25 weigh-in-motion (WIM) sites in Idaho were analyzed. Site-specific (level 1) axle load spectra (ALS), traffic adjustment factors, and number of axles per truck class were established. Statewide and regional ALS factors were also developed. The impact of the traffic input level on MEPDG predicted performance was studied. Sensitivity of MEPDG predicted performance in terms of cracking, rutting, and smoothness to key input parameters was conducted as part of this study. MEPDG recommended design reliability levels and criteria were also investigated. And, finally, a plan for local calibration and validation of MEPDG distress/smoothness prediction models for Idaho conditions was established.

17. Key Word	18. Distribution Statement
MEPDG, Flexible Pavement, Performance, Dynamic Modulus, Binder shear modulus, Resilient modulus, Axle load spectra, Fatigue, Rutting, IRI	Unrestricted. This document is available to the public at http://itd.idaho.gov/planning/research/archived/closed.htm

19. Security Classif. (of this report)	20. Security Classif. (of this page)	21. No. of Pages	22. Price
Unrestricted	Unrestricted	377	

METRIC (SI*) CONVERSION FACTORS

APPROXIMATE CONVERSIONS TO SI UNITS

Symbol	When You Know	Multiply By	To Find	Symbol
		LENGTH		
in	inches	25.4		mm
ft	feet	0.3048		m
yd	yards	0.914		m
mi	Miles (statute)	1.61		km
		AREA		
in^2	square inches	645.2	millimeters squared	cm^2
ft^2	square feet	0.0929	meters squared	m^2
yd^2	square yards	0.836	meters squared	m^2
mi^2	square miles	2.59	kilometers squared	km^2
ac	acres	0.4046	hectares	ha
		MASS (weight)		
oz	Ounces (avdp)	28.35	grams	g
lb	Pounds (avdp)	0.454	kilograms	kg
T	Short tons (2000 lb)	0.907	megagrams	mg
		VOLUME		
fl oz	fluid ounces (US)	29.57	milliliters	mL
gal	Gallons (liq)	3.785	liters	liters
ft^3	cubic feet	0.0283	meters cubed	m^3
yd^3	cubic yards	0.765	meters cubed	m^3

Note: Volumes greater than 1000 L shall be shown in m^3

		TEMPERATURE (exact)		
°F	Fahrenheit temperature	5/9 (°F-32)	Celsius temperature	°C
		ILLUMINATION		
fc	Foot-candles	10.76	lux	lx
fl	foot-lamberts	3.426	candela/m^2	cd/cm^2
		FORCE and PRESSURE or STRESS		
lbf	pound-force	4.45	newtons	N
psi	pound-force per square inch	6.89	kilopascals	kPa

APPROXIMATE CONVERSIONS FROM SI UNITS

Symbol	When You Know	Multiply By	To Find	Symbol
		LENGTH		
mm	millimeters	0.039	inches	in
m	meters	3.28	feet	ft
m	meters	1.09	yards	yd
km	kilometers	0.621	Miles (statute)	mi
		AREA		
mm^2	millimeters squared	0.0016	square inches	in^2
m^2	meters squared	10.764	square feet	ft^2
km^2	kilometers squared	0.39	square miles	mi^2
ha	hectares (10,000 m^2)	2.471	acres	ac
		MASS (weight)		
g	grams	0.0353	Ounces (avdp)	oz
kg	kilograms	2.205	Pounds (avdp)	lb
mg	megagrams (1000 kg)	1.103	short tons	T
		VOLUME		
mL	milliliters	0.034	fluid ounces (US)	fl oz
liters	liters	0.264	Gallons (liq)	gal
m^3	meters cubed	35.315	cubic feet	ft^3
m^3	meters cubed	1.308	cubic yards	yd^3

		TEMPERATURE (exact)		
°C	Celsius temperature	9/5 °C+32	Fahrenheit temperature	°F
		ILLUMINATION		
lx	lux	0.0929	foot-candles	fc
cd/cm^2	candela/m^2	0.2919	foot-lamberts	fl
		FORCE and PRESSURE or STRESS		
N	newtons	0.225	pound-force	lbf
kPa	kilopascals	0.145	pound-force per square inch	psi

Acknowledgements

This project was funded by the Idaho Transportation Department (ITD) under a contract with the National Institute for Advanced Transportation Technology (NIATT), ITD Research Project No. RP193. Many individuals have contributed to the progress of this project.

From ITD, thanks are due to Mike Santi (Assistant Material Engineer) and Ned Parrish (Research Manager) and to their supporting staff for their efforts to help the research team completes the project tasks. Thanks are also due to Scott Fugit (Roadway Data section) for his time, effort, and for providing the traffic data needed for the project.

Mr. Christopher Wagner of FHWA has kindly reviewed this final report as an external peer reviewer. His valuable comments are greatly appreciated. We would like to thank him for his time and effort put into this review process.

The support of the NIATT administrative staff is also acknowledged. Thanks are due to Mrs. Tami Nobel and Ms. Debbie Foster for their dedicated efforts in facilitating the project administration. Authors are very thankful to all their efforts and support

Table of Contents

List of Tables

List of Figures

List of Acronyms

AADT	Annual Average Daily Traffic
AADTT	Annual Average Daily Truck Traffic
AASHO	American Association of State Highway Officials (predecessor to AASHTO)
AASHTO	American Association of State Highway and Transportation Officials
AC	Asphalt Concrete
ADOT	Arizona Department of Transportation
ADTT	Average Daily Truck Traffic
AHTD	Arkansas State Highway and Transportation Department
AI	Asphalt institute
ALS	Axle Load Spectra
ATR	Automatic Traffic Recorder
AVC	Automatic Vehicle Classification
Caltrans	California Department of Transportation
CBR	California Bearing Ratio CBR
CF	Climatic Factor
CI	Cracking Index
CRCP	Continuously Reinforced Concrete Pavement
DOT	Department of Transportation
DSR	Dynamic Shear Rheometer
DTT	Direct Tension Tester
EICM	Enhanced Integrated Climatic Model
ESAL	Equivalent Single Axle Load
FHWA	Federal Highway Agency
FWD	Falling Weight Deflectometer
GS	Gyratory Stability
GWT	Ground Water Table
HMA	Hot Mix Asphalt
HTD	Hourly Truck Distribution
ITD	Idaho Transportation Department
JPCP	Jointed Plain Concrete Pavement
LL	Liquid Limit
LTPP	Long Term Pavement Performance
LVDT	Linear Variable Differential Transformer
MAAT	Mean Annual Air Temperature
MAF	Monthly Adjustment Factor
MEPDG	Mechanistic-Empirical Pavement Design Guide
MnDOT	Minnesota Department of Transportation
NCDOT	North Carolina Department of Transportation
NCHRP	National Cooperative Highway Research Program
NWIS	National Water Information System
PAV	Pressure Aging Vessel

PI	Plasticity Index
PMA	Polymer Modified Asphalt
PMS	Pavement Management System
RD	Rut Depth
RI	Roughness Index
RTFO	Rolling Thing Film Oven
SDDOT	South Dakota Department of Transportation
SGC	Superpave Gyratory Compactor
SHAs	State Highway Agencies
SN	Skid Number
TTC	Truck Traffic Classification
TWRG	Truck Weight Road Group
UDOT	Utah Department of Transportation
UI	University of Idaho
USC	Unified Soil Classification
USGS	United States Geological Survey's
VCD	Vehicle Class Distribution
VDOT	Virginia Department of Transportation
VTTI	Virginia Tech Transportation Institute
WIM	Weigh-In-Motion
WSDOT	Washington State Department of Transportation

Executive Summary

Introduction

The Mechanistic-Empirical Pavement Design Guide (MEPDG) developed under the NCHRP Project 1-37A represents a paradigm shift in design and rehabilitation of pavement structures over the predecessor AASHTO 1993 design guide. While the later was an empirical based on data from the AASHO Road Test, the MEPDG utilized mechanistic principals to analyze the pavement structure and adopted empirical models to predict pavement performance. Hence the MEPDG required massive amount of data to describe the pavement materials, and to represent the real traffic and climate and their effect on the developed pavement design and its predicted performance. The new MEPDG addresses both flexible and rigid pavements.

This study was conducted to assist Idaho Transportation Department (ITD) in the implementation of MEPDG for flexible pavements. The main research work in this study focused on establishing database for the required inputs for MEPDG for Idaho conditions. This includes materials, traffic, and climatic database for Idaho MEPDG implementation.

For materials database, inputs for MEPDG included data for hot-mix-asphalt (HMA) layers, unbound layers and subgrade soils. For HMA, dynamic modulus (E*) tests were conducted on 27 plant-produced mixes that covered most of the utilized mixes in Idaho. These mixes cover the 6 ITD Superpave mix specifications. Dynamic Shear Rheometer (DSR) and Brookfield tests were also performed on 9 typical Superpave binder performance grades. For the tested mixtures and binders a comprehensive database covering all hierarchical input levels required by MEPDG for hot-mix-asphalt (HMA) and binder characterization was established. Gyratory Stability (GS) values of the tested mixes were also determined. The influence of the binder characterization input level on the accuracy of MEPDG predicted E* was investigated. The prediction accuracy of the NCHRP 1-37A η-based Witczak Model, NCHRP 1-40D-G* based Witczak model, Hirsch model, and GS-based Idaho model was also investigated.

For unbound and soil materials, a total of 8233 historical R-value results along with routine material properties of Idaho unbound materials and subgrade soils were used to develop levels 2 and 3 unbound material characterization. For level 2 subgrade material characterization, two models were developed. First, a multiple regression model can be used to predict R-value as a function of the soil plasticity index (PI) and percent passing No 200 sieve. Second, a resilient modulus (M_r) predictive model was developed . The model was based on the estimated R-value of the soil and laboratory measured M_r values, collected from literature. For level 3 unbound granular materials and subgrade soils, typical default average values and ranges of R-value, PI, and liquid limit (LL) were developed using ITD historical database.

For MEPDG traffic characterization, classification and weight data from 25 weight-in-motion (WIM) sites in Idaho were analyzed. Site-specific (level 1) axle load spectra (ALS), traffic adjustment factors, and number of axles per truck class were established. Statewide and regional ALS factors were also developed. The impact of the traffic input level (accuracy) on MEPDG predicted performance was studied.

For climatic database, the MEPDG climatic weather stations in Idaho and the neighboring states that can be used in Idaho have been identified. Also, stations for various counties in Idaho have been identified. Comparative analysis was performed to characterize the weather data at these stations.

Based on this research work, a master database for MEPDG required inputs was created. This database contains MEPDG key input parameters related to HMA, binder, unbound base/subbase granular materials, subgrade soils, traffic, and climate. The developed database was stored in a series of Excel sheets for quick and easy access of the data.

Sensitivity of MEPDG predicted performance in terms of cracking, rutting, and IRI to key input parameters was investigated as part of this study. MEPDG recommended design reliability levels and criteria were investigated using Long Term pavement Performance (LTPP) Projects located in Idaho. Finally, a plan for local calibration and validation of MEPDG distress/smoothness prediction models for Idaho conditions was established.

Research Methodology

The project was conducted in 8 major tasks as follows:

Task 1: Studied the latest version of the MEPDG software (Version 1.10).
Task 2: Reviewed other state agencies MEPDG implementation efforts focusing on Idaho neighboring states.
Task 3: Established input database for HMA, binder, and unbound granular materials and subgrade soils.
Task 4: Established input database for traffic characterization.
Task 5: Established input database for climate.
Task 6: Studied the current MEPDG performance and reliability design criteria.
Task 7: Developed a plan for local calibration and validation of MEPDG performance prediction models.

This report documents all research work conducted under these tasks for ITD.

Key Findings

The key findings of this research work are summarized below:

- To facilitate MEPDG implementation in Idaho, a master database containing MEPDG required key inputs related to materials, traffic, and climate was created. This database is stored in a user-friendly Excel sheets with simple macros for quick and easy access of data.
- Analysis of the E* predictive models of HMA materials in MEPDG using Idaho data revealed the following:

  - The NCHRP 1-37A viscosity-based E* model along with level 3 binder characterization is the least biased methodology for E* prediction among the incorporated E* models in MEPDG. However, this model was found to overestimate E* at the high temperatures.
  - Both Hirsch and MEPDG E* predictive models were found to significantly overestimate E* of Idaho mixtures at the higher temperature regime.
  - The GS-based Idaho E* predictive model predicts E* values that are in excellent agreement with the measured ones (Se/Sy = 0.24 and R2 = 0.94).
  - Among the 4 investigated models, the GS-based E* model was found to yield the lowest bias and highest accuracy in prediction.

- Two simple models for use in MEPDG level 2 inputs for subgrade soils characterization were developed. The first model estimates the R-value of the soil as a function of percent passing No 200 sieve and plasticity index (PI) when direct laboratory measurement of the R-value is unavailable. The second model estimates the Modulus of resilience (M_r) from the R-value.
- Analysis of Idaho WIM traffic data revealed the following:
  - For MEPDG traffic characterization, 12 to 24 months of classification and weight traffic data from 25 WIM sites in Idaho were analyzed using the *TrafLoad* software. Among the 25 sites, only 21 sites possessed enough classification data to produce level 1 traffic inputs for MEPDG. Only 14 WIM sites were found to have weight data that comply with the FHWA recommended procedure.
  - Statewide and regional Axle Load Spectra (ALS) were developed based on the analysis of the weight data from the 14 WIM sites. The developed statewide ALS yielded significantly higher longitudinal and alligator cracking compared to MEPDG default spectra. No significant difference was found in predicted asphalt concrete (AC) layer rutting, total pavement rutting, and IRI based on statewide and MEPDG default spectra.
- A sensitivity analysis was conducted and the following conclusions are observed:
  - Longitudinal cracking was found to be extremely sensitive to most of the investigated parameters. These parameters are related to the HMA layer thickness and properties, base layer thickness, subgrade strength, traffic, and climate.
  - No thermal cracking was predicted for most of the performed MEPDG runs. This is attributed to the use of level 3 data inputs for tensile strength and creep compliance properties of the asphalt mixes. These properties directly affect thermal cracking of asphalt pavement.
  - Alligator cracking and total rutting were found to be mostly sensitive to extremely sensitive to most of the investigated parameters.

  - International Roughness Index (IRI) was not sensitive to most of the parameters investigated in this study.
  - Among all investigated parameters, traffic volume (AADTT) was found to be the most influencing input on MEPDG predicted distresses and IRI.
- Analysis of LTPP projects in Idaho showed that MEPDG yielded highly biased predictions especially for cracking.

In summary, a master database was created. This database contains MEPDG key inputs related to HMA, asphalt binder, unbound granular base/subbase materials and subgrade soils, traffic, and climate. The MEPDG E* predictive models yielded biased E* estimate for Idaho mixes. The GS-Idaho model for E* predictions yielded the most accurate and least biased E* for Idaho mixes compared to MEPDG and Hirsch E* predictive models. The MEPDG nationally calibrated models yielded highly biased distress/IRI predictions based on data from LTPP sites in Idaho, mainly due to the lack of local calibration factors.

Recommendations

Based on the findings of this research the following are recommended:

- MEPDG level 3 is not recommended to characterize Idaho HMA mixtures replacing level 1 due to the highly biased predictions especially at the high temperature values.
- The use of Idaho GS-based E* predictive model for characterizing ITD HMA mixtures is recommended. This model can be used to predict E* at temperatures and frequencies of interest and then input these predicted values into MEPDG as level 1.
- At least, 3 years of traffic data from WIM sites in Idaho should be analyzed to produce traffic data for MEPDG. This analysis should be performed every 3 to 5 years to ensure accurate traffic data. Such analysis should distinguish WIM sites based on similarities in axle load spectra. One way to do that is to develop Truck Road Weight Groups (TRWG) as per MEPDG guidelines.
- As the average annual daily truck traffic (AADTT) was found to be the most significant factor affecting MEPDG predicted distresses and IRI, every effort should be made to accurately determine this parameter.
- To ensure consistency with MEPDG distress prediction, it is recommended that ITD perform pavement condition surveys and update their distress survey method in accordance with LTPP method of data collection.
- Calibrate MEPDG distress/IRI prediction models to Idaho conditions.
- It is recommended that ITD use the current MEPDG design criteria and the associated design reliability levels until local calibration of MEPDG distress/IRI models for Idaho conditions is performed. Once the models are locally re-calibrated, MEPDG recommended design criteria and reliability levels should be investigated.

Chapter 1
Introduction

Background

The AASHTO 1993 Guide for Design of Pavement structures is one of the most widely used design methods in the continental U.S. and the world. This empirical design method is based on results from the original AASHO road test built in the late 1950's in Ottawa, Illinois.[1] The first design methodology based on the results from the AASHO road test was published in 1972 interim design guide. This AASHTO design guide was released in 1986 and was revised in 1993 which is the final version of this design guide. In a survey by FHWA in 2007, based on 50 state departments of transportation (DOT) responders, 63 percent use the 1993 AASHTO Pavement Design Guide, 12 percent use the 1972 interim AASHTO Design Guide, 13 percent use individual state design procedures, 8 percent use a combination of AASHTO and state procedures, and the remaining use other design procedures.[2]

Although, the AASHTO 1993 design method has been and still being used by many state DOTs for design of pavement structures, it is still an empirical and unreliable when applied to conditions different from the original conditions used to develop the guide. The empirical AASHTO 1993 pavement design method has several limitations regarding climate, traffic, subgrade, pavement materials and pavement performance. These limitations are as follows:

1) Limited number of traffic repetitions, axle weights and configuration, truck class and tire pressures.
2) The road test only lasted for about 2 years only while most of the pavements are designed for 20 years or more.
3) Limited AC mixture properties (no Superpave, stone matrix asphalt, and so on).
4) Limited AC binder types (only conventional binders).
5) Limited unbound base/subbase material properties (only two different dense graded base/subbase quality materials).
6) Only 1 subgrade type (A-6) soil.
7) Only 1 climatic location which is represented by Ottawa, Illinois.
8) The design criteria adopted by this method is based upon the concept of pavement severability which is based upon a subjective evaluation.
9) No pavement performance prediction is included.

The limitations of the AASHTO 1993 method raise a question regarding the reliability and applicability of this method to different environmental locations, subgrade (foundation) properties, and larger number of traffic repetitions as nowadays, heavier truck axle weights, different axle configurations and tire pressure compared to the data used in the development of this design method. These inherent limitations motivated the need to develop and implement a new pavement design procedure based on mechanistic principles and performance predictions. This led to the proposal suggested by the AASHTO Joint Task

Force on Pavements, NCHRP, and FHWA, in March 1996, of a research program to develop a pavement design guide based on mechanistic-empirical principles with distress prediction models calibrated with actual field pavement performance data from the long term pavement performance (LTPP) Program.[3, 4] The output of this research project was the NCHRP 1-37A which is the development of the Mechanistic-Empirical Pavement Design Guide of New and Rehabilitated Pavement Structures.[4] This Mechanistic-Empirical Pavement Design Guide (MEPDG) consists of a guide for design/analysis of pavement structures, companion software with documentation and software user manual, and implementation and training materials.[5] A master summary of the key differences (for flexible pavements only) between MEPDG and the AASHTO 1993 guide is shown in Table 1.

Table 1. Comparison of AASHTO 1993 Guide and MEPDG

Parameter	MEPDG	AASHTO 1993
User Friendly Software	Yes	No
Pavement Type:		
New Pavement Design (Flexible or Rigid)	Yes	Yes
Rehabilitation: AC Over Fractures PCC Slab (Crack and Seat, Break and Seat, Rubblized)	Yes	No
Inputs:		
Hierarchical Input levels	Yes	No
Traffic:		
Load Spectra	Yes	No
18-Kip ESALs	Yes	Yes
Hourly, Daily, Monthly Traffic Distribution	Yes	No
Traffic Lateral Displacement (Wander)	Yes	No
Traffic Speed (Rate of Loading)	Yes	No
Special vehicle damage analysis	Yes	No
Climate:		
Wet-Freeze Climate	Yes	Yes, Ottawa, Illinois
Mid-West Climate	Yes	No
Dry or Wet Warm Climate	Yes	No
High Elevation Climate	Yes	No
Coastal Climate	Yes	No
Deep Freeze Climate	Yes	No
Distress Predictions:		
AC and Unbound Materials Rutting	Yes	No
Alligator and Longitudinal Fatigue Cracking	Yes	No
Transverse Cracking	Yes	No
Smoothness	Yes	No
Allows Different Design Reliability for each Distress	Yes	No
Material Characterization:		
Hieratical Input Levels	Yes	No
Nonlinear Unbound Material Characterization	Yes	No
Consider Short and Long Term Age Hardening	Yes	No
HMA Modulus at Different Temperatures and Loading Frequencies	Yes	No
Unbound Material Resilient Modulus Adjusted for Moisture Variation During Pavement Life	Yes	No, only seasonal variations of the modulus considered
Binder Characterization	Yes	No
Models Calibration:		
Nationally Calibrated/Validated Models	Yes	No, only data from AASHO road test
Time length of Performance Dada used in the Calibration	Up to 14 years	Only 2 years of performance data (Serviceability Index)
Traffic Repetition used in Calibration	Up to 27 years	Only 1.1 million ESAL

Problem Statement

The new MEPDG considers mechanistic-empirical design principals to design new and rehabilitated pavements. It also accounts for many factors that affect the design including material variability, and traffic loads. Furthermore, it incorporates a very sophisticated climatic model that accounts for the expected variation of the material properties due to climatic changes. The design criteria in the guide are based on distress models that have been nationally calibrated based on field data from the LTPP program sites across the nation. Unfortunately, even though the LTPP data is considered the most comprehensive in service-data, it is very limited when performance models are to be calibrated for a specific location. Hence, to implement the new guide, an agency needs to identify and establish procedures for how to obtain required data and establish a policy on the acceptance level of the design criteria. The state of Idaho Transportation Department (ITD) needs to develop and execute an implementation plan for the MEPDG in Idaho.

Objectives

The main objectives of this research project were to:

1) Develop material database for the various material layers in the state of Idaho.
2) Develop traffic load spectra for various axle loads operating on various road classes.
3) Establish climatic factors for the various regions of Idaho.
4) Study the sensitivity of MEPDG for the variations considered in traffic, materials, and climate.
5) Develop recommendations for the appropriate design level and reliability levels to be adopted with the implementation plan.
6) Develop a training workshop for ITD engineers on the software and the design process as per the MEPDG procedure.

Report Organization

This report presents the research work completed for the MEPDG implementation in Idaho. It is organized in 11 chapters as described below:

Chapter 1 covers a comparison of AASHTO 1993 and MEPDG procedures, problem statement, and research objectives.

Chapter 2 presents an overview of how a design/analysis can be conducted using MEPDG. The key required inputs and hierarchical inputs levels in MEPDG are also coved in this chapter. Flexible pavement performance models and the evolution and limitations of MEPDG are also presented in this chapter.

Chapter 3 presents an up- to-date thorough literature review of other states implementation plans and calibrations efforts of MEPDG. A comprehensive summary, based on the reviewed literature, of the key design parameters affecting MEPDG predicted distresses is also presented.

Chapter 4 presents the laboratory testing procedures and results conducted for the characterization of typical Idaho mixes and binders. It also investigates the prediction accuracy of MEPDG dynamic modulus prediction models, Idaho, and Hirsch models. This chapter also presents the influence of the binder characterization input level on the MEPDG predicted dynamic modulus of Idaho mixes.

Chapter 5 presents the research work conducted for the characterization of Idaho unbound granular materials and subgrade soils. It presents the development of 2 models: R-value model and M_r model for MEPDG level 2 subgrade soils characterization. It also presents the development of typical default values for the R-value, liquid limit, and plasticity index of Idaho unbound granular materials and subgrade soils.

Chapter 6 reports the development of traffic characterization inputs to facilitate MEPDG implementation in Idaho. It also investigates the impact of traffic inputs on MEPDG predicted distresses and smoothness.

Chapter 7 covers the climatic and ground water table database for MEPDG implementation in Idaho.

Chapter 8 investigates the sensitivity of MEPDG predicted distresses and smoothness to key design parameters.

Chapter 9 investigates current MEPDG recommended performance and design reliability criteria and threshold values of distresses/smoothness. It reports the results of the investigation of the performance of the MEPDG nationally calibrated distress/smoothness models based on Idaho LTPP sites.

Chapter 10 presents a step by step plan for local calibration and validation of MEPDG distress/smoothness models for Idaho conditions. It also addresses the discrepancies between ITD's distress survey method and MEPDG requirements.

Finally, Chapter 11 summarizes the key findings of this research and recommendations for ITD.

The report also includes 6 appendices that document all test results and the developed database. The appendices and the MEPDG Idaho database are included in attached CD's to this report.

Chapter 2
Overview of the Mechanistic-Empirical Pavement Design Guide

Introduction

MEPDG is a comprehensive tool for the analysis and design of new and rehabilitated flexible and rigid pavement structures based on mechanistic-empirical principles. The software mechanistically calculates the structural responses (stresses, strains, and deflections), within a pavement system, using the pavement response model (JULEA multi-layer elastic theory or finite element analysis for flexible pavements and ISLAB2000 for rigid pavements).[4] Moisture and temperature variations within the pavement structure are also calculated internally using the Enhanced Integrated Climatic Model (EICM). The EICM, in MEPDG software Version 1.1, utilizes a comprehensive database from 851 weather stations throughout the United States. Pavement distresses (rutting, bottom-up and top-down fatigue cracking, and thermal cracking) and roughness are predicted, from the mechanistically calculated strains and deformations, using statistical (empirical) transfer functions. In the current software version of the MEPDG (version 1.100, built August 31, 2009), these transfer functions are nationally (globally) calibrated based on field data from 94 LTPP sections distributed all over the United States. The software also allows users to input user defined calibration coefficients (local or regional) to reflect certain conditions.

Inputs Required for MEPDG

In order to perform a pavement design/analysis using MEPDG, more than 100 inputs are required. In general, 4 categories of data are needed for the design guide. The 4 categories are project, traffic, climate, and structure. The project category input group includes general information to identify the project of interest such as the type of design, construction and traffic opening dates …etc. It also includes information regarding the design criteria (threshold values for distresses and roughness) and reliability level for each distress selected in the criteria. Traffic, climate, and structure input categories are the 3 main input groups which must be completed to design/analysis a specific pavement structure. A brief listing of these input parameters related to the flexible pavement design/analysis which are required by each group is presented in Table 2.[4, 6] Appendix A presents a summary of all MEPDG required inputs for new flexible pavements.

Table 2. Flexible Pavement Input Parameters Required for MEPDG Design/Analysis[4, 6]

Input Group		Input Parameter
Truck Traffic		Axle Load Distributions (Single, Tandem, Tridem, and Quad) Truck Volume Distribution Lane & Directional Truck Distributions Tire Pressure Axle Configuration, Tire Spacing Truck Wander
		Traffic Speed
Climate		Temperature, Wind Speed, Cloud Cover, Precipitation, Relative Humidity
Material Properties	**Unbound Layers & Subgrade Materials**	Seasonally Adjusted Resilient Modulus – All Unbound Layers Classification & Volumetric Properties Coefficient of lateral pressure Plasticity index, Gradation Parameters, Effective Grain Sizes, Specific Gravity, Optimum Moisture Contents, Parameters to Define the Soil Water Characteristic Curve (SWCC)
	Bedrock	Elastic Modulus (E)
	Hot-Mix Asphalt (HMA), Recycled HMA	Time-Temperature Dependent HMA Dynamic Modulus (E*) HMA Creep Compliance & Indirect Tensile Strength Volumetric Properties Asphalt Binder Viscosity (Stiffness) Characterization to Account for Aging
All Materials Except Bedrock		Unit Weight Poisson's Ratio Other Thermal Properties; Conductivity; Heat Capacity; Surface Absorptivity
Existing Pavement (in case of overlay design)		Condition of Existing Layers

MEPDG Hierarchical Input Levels

An important feature of MEPDG is the hierarchical levels of the design inputs. This feature provides the user with the highest flexibility in obtaining the design inputs of the project based on its importance and anticipated funding cost. For new flexible pavements, the MEPDG hierarchical approach is applicable on traffic and materials input parameters. Three levels of inputs regarding traffic and material properties are available in the MEPDG. The inputs for the MEPDG may also be obtained using a mix of the 3 hierarchical levels. MEPDG hierarchical input levels are as follows:

- Level 1: represents the highest level of accuracy and lowest level of input errors. Input parameters for this level are measured directly either in the laboratory or in the field. This level of input has the highest cost in testing and data collection. It is important to note that level 1 is more representative of the agency or project specific traffic, materials, and climatic inputs.
- Level 2: represents an intermediate level of accuracy. Parameters are estimated from correlations based on limited routine laboratory test results or selected form an agency database.

- Level 3: represents the lowest level of accuracy. Usually, typical default values (best estimates) of input parameters are used in this level.

Flexible Pavement Design/Analysis Procedure in MEPDG

The overall process of the design/analysis of flexible pavements using the MEPDG is depicted in Figure 1. The current version of the software is an analysis tool rather than a design tool. However, it can be also used in design using the process summarized below:

- Start with assuming a trail pavement structure, layer thicknesses and material properties for a specific environmental location and traffic conditions.
- Define the performance criteria for accepting the pavement and select a threshold value and reliability level for each performance indicator (i.e., total pavement rutting, asphalt concrete (AC) rutting, alligator cracking, longitudinal cracking, and smoothness).
- Process all inputs for traffic, climate, foundation material, and hot-mix-asphalt (HMA) and unbound/bound subbase/base/subgrade materials.
- Run MEPDG software to compute the pavement structural responses then the accumulated damage (distresses) throughout the design/analysis period.
- Estimate smoothness through the International Roughness Index (IRI) which is a function of the distresses, site factors and the initial IRI.
- Evaluate the MEPDG performance outputs (distress and smoothness) against the design criteria and the desired reliability level.
- If the trial section does not meet the specified criteria, revise the trail design inputs and rerun the program until the design meets the criteria.

It should be noted that the AASHTO version of the software called “DARWin-ME” which was released in April, 2011 is a design tool. This software optimizes the design thickness of one layer at a time so that the resulting structure conforms to the specified design criteria.

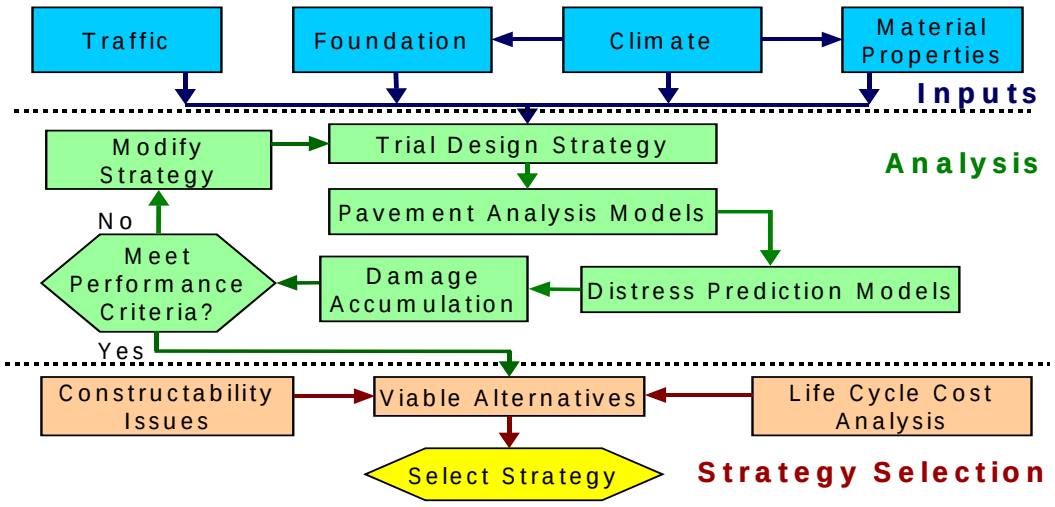

Figure 1. MEPDG Overall Design Process for Flexible Pavements[4, 7]

MEPDG Distress Prediction Models for Flexible Pavements

For prediction of the different load and non-load associated distresses, MEPDG divides the given layers and foundation into small sublayers. The thickness of the sublayers depends upon the layer type, layer thickness, and depth within the pavement structure.[4] For the load-associated distress, the software combines the EICM hourly temperatures (for a given environmental location), at the mid-depth of each HMA sublayer, over a given analysis period (biweekly to one month) into 5 sub-seasons. If the pavement is exposed to freeze and thaw cycles the biweekly time interval is used in the damage computations. The frequency distribution of the temperature is assumed to be normally distributed. For each sub-season, the HMA sublayer temperature is defined by a temperature that represents 20 percent of the frequency distribution of the pavement temperature. This sub-season also represents those conditions when 20 percent of the monthly traffic will occur. This is accomplished by computing pavement temperatures corresponding to standard normal deviations of -1.2816, -0.5244, 0, 0.5244 and 1.2816. These values correspond to accumulated frequencies of 10, 30, 50, 70 and 90 percent within a given month. The program uses these 5 quintile temperatures to calculate the dynamic modulus (E*) at the mid depth of each HMA sublayer taking into account the effect of loading rate (vehicle speed) and temperature variation through the analysis period.

It also calculates the resilient modulus (M_r) at the mid-depth of each unbound sublayer taking into account the moisture variations throughout the analysis period. This is accomplished in either the monthly or semi-monthly basis previously noted. The sublayer moduli are then used for the calculations of the state of stress and the vertical resilient strain at the mid depth of each sublayer for HMA mixtures, stabilized layers, and unbound base/subbase/subgrade layers. The tensile strain is also calculated at the bottom of each bound layer using a grid of horizontal computational points (parallel and perpendicular to the traffic direction) depending on the axle type. This is done in order to ensure that critical strains can be captured by the program.

For the non-load associated thermal fracture distress, EICM processes the HMA temperatures on an hourly basis. The software, then, uses these hourly temperatures to predict the HMA creep compliance and indirect tensile strength values to compute the tensile strength of the surface HMA layer.

The state of stress and critical strain computations are completed using the pavement response model (JULEA) incorporated in the software. These critical strains are used to compute the different pavement distresses as described in the following subsections.

MEPDG Rutting Prediction Models

MEDPG uses 2 different models to predict the permanent deformation (rutting); 1 for the HMA layer (s) and the other model is used for the unbound base/subbase/subgrade layers. These models are as follows:

HMA Layers Rutting Prediction Model

In order the calculate HMA Layers rutting, MEPDG subdivides the HMA layer(s) into sublayers with smaller thicknesses and then uses the set of equations presented in
Figure 2 to calculate the permanent deformation of the HMA layer(s).

$$\Delta_{p(HMA)} = \varepsilon_{p(HMA)} h_{HMA} = \beta_{r1} k_z \varepsilon_{r(HMA)} 10^{k_1} T^{k_2 \beta_{r2}} N^{k_3 \beta_{r3}}$$

$$k_z = (C_1 + C_2 D)0.328196^D$$

$$C_1 = -0.1039(H_{HMA})^2 + 2.4868 H_{HMA} - 17.342$$

$$C_2 = 0.0172(H_{HMA})^2 - 1.7331 H_{HMA} + 27.428$$

where:

$\Delta_{p(HMA)}$	= Accumulated permanent vertical deformation in HMA layer/sublayer, in.
$\varepsilon_{p(HMA)}$	= Accumulated permanent or plastic axial strain in HMA layer/sublayer, in/in.
$\varepsilon_{r(HMA)}$	= Resilient or elastic strain calculated by the structural response model (JULEA) at the mid-depth of each HMA sublayer, in./in.
$h_{(HMA)}$	= Thickness of the HMA layer/sublayer, in.
N	= Number of axle load repetitions.
T	= Pavement temperature, °F.
k_z	= Depth confinement correction function.
$k_{1,2,3}$	= Global field calibration parameters (from the NCHRP 1-40D recalibration; k_1 = -3.35412, k_2 = 1.5606, k_3 = 0.4791).
β_{r1}, β_{r2}, β_{r3},	= Local field calibration constants; for the global calibration effort, these constants were all set to 1.0.
D	= Depth below the surface, in.
H_{HMA}	= Total HMA thickness, in.

Figure 2. MEPDG Equations for the Calculation of HMA Layer(s) Rutting[4, 6]

Rutting Prediction Model for Unbound Materials and Subgrade Soil

MEPDG uses a modified version of the Tseng and Lytton model for the unbound materials and subgrade layer for the permanent deformation calculations. This model takes the form given in Figure 3.[4, 6]

$$\Delta_p = \beta_{s1} k_{s1} \varepsilon_v h \left(\frac{\varepsilon_o}{\varepsilon_r} \right) e^{-\left(\frac{\rho}{N}\right)^{\beta}}$$

$$Log\,\beta = -0.61119 - 0.017638(W_c)$$

$$\rho = 10^9 \left(\frac{C_o}{\left(1 - (10^9)^{\beta}\right)} \right)^{\frac{1}{\beta}}$$

$$C_o = Ln\left(\frac{a_1 M_r^{b_1}}{a_9 M_r^{b_9}} \right)$$

where:

- Δ_p = Permanent or plastic deformation for the layer/sublayer, in.
- N = Number of axle load applications.
- ε_o = Intercept determined from laboratory repeated load permanent deformation tests, in./in.
- ε_r = Resilient strain imposed in laboratory test to obtain material properties ε_o, β, and ρ, in./in.
- ε_v = Average vertical resilient or elastic strain in the layer/sublayer and calculated by the structural response model, in./in.
- h = Thickness of the unbound layer/sublayer, in.
- k_{s1} = Global calibration coefficients; k_{s1}=2.03 for granular materials and 1.35 for fine-grained materials (from the NCHRP 1-40D recalibration).
- β_{s1} = Local calibration constant for the rutting in the unbound layers; the local calibration constant was set to 1.0 for the global calibration effort.
- W_c = Water content, percent.
- M_r = Resilient modulus of the unbound layer or sublayer, psi.
- $a_{1,9}$ = Regression constants; a_1=0.15 and a_9=20.0.
- $b_{1,9}$ = Regression constants; b_1=0.0 and b_9=0.0.

Figure 3. MEPDG Equations for the Calculation of Unbound Granular Materials and Subgrade Rutting

Load Associated Fatigue Cracking Prediction Models

MEDPG predicts 2 types of load-associated fatigue cracking. They are bottom-up alligator cracking and top-down longitudinal cracking. Once the HMA E* and the critical tensile strains at the critical locations are computed (for a given analysis period, traffic load, and environmental location), the allowable number of repetitions to (alligator or longitudinal) fatigue cracking failure (N_f) is calculated, in MEPDG, using the set of equations shown in Figure 4.

$$N_f = 0.00342(k_{f1})(C)(k'_1)(\beta_{f1})\left(\frac{1}{\varepsilon_t}\right)^{k_{f2}\beta_{f2}}\left(\frac{1}{E^*}\right)^{k_{f3}\beta_{f3}}$$

$$C = 10^M$$

$$M = 4.84\left(\frac{V_{be}}{V_a + V_{be}} - 0.69\right)$$

where:

N_f = Allowable number of axle load applications for a flexible pavement.
ε_t = Tensile strain at critical locations and calculated by the structural response model (JULEA), in./in.
E^* = Dynamic modulus of the HMA measured in compression, psi.
k_{f1}, k_{f2}, k_{f3} = Global field calibration parameters (from the NCHRP 1-40D re-calibration; k_{f1} = 0.007566, k_{f2} = -3.9492, and k_{f3} = -1.281).
β_{f1}, β_{f2}, β_{f3} = Local or mixture specific field calibration constants; for the global calibration effort, these constants were set to 1.0.
V_{be} = Effective asphalt content by volume, percent.
V_a = Percent air voids in the HMA mixture.
k'_1 = Thickness correction term taking into account the mode of loading, dependent on type of cracking.

Figure 4. MEPDG Equations for the Calculation of the Allowable Number of Traffic Repetitions to Fatigue Damage[4, 6, 8]

The equations shown in Figure 5 and Figure 6 are used to calculate the thickness correction terms for bottom-up and top-down cracking model, respectively.

$$k'_1 = \frac{1}{0.000398 + \frac{0.003602}{1 + e^{(11.02 - 3.49 * hac)}}}$$

where:

h_{ac} = Total thickness of the asphalt layer, in.

Figure 5. Thickness Correction Equation for Bottom-Up Alligator Cracking Model[4, 6, 8]

$$k'_1 = \frac{1}{0.01 + \frac{12.00}{1 + e^{(15.676 - 2.8186 * hac)}}}$$

where:

h_{ac} = Total thickness of the asphalt layer, in.

Figure 6. Thickness Correction Equation for Top-Down Longitudinal Cracking Model[4, 6, 8]

Incremental (cumulative alligator or longitudinal) fatigue damage (ΔD) is then calculated as the linear sum (Miner's hypothesis) of the ratio of the predicted number of traffic repetitions to the allowable number of traffic repetitions in a specific environmental condition (to some failure level) as shown in Figure 7. This is done in within a specific time increment and axle load interval for each axle type in the analysis.

$$D = \sum (\Delta D)_{j,m,l,p,T} = \sum \left(\frac{n}{N_f} \right)_{j,m,l,p,T}$$

where:

n = Actual number of axle load applications within a specific time period.
N_f = Allowable number of axle load applications for a flexible pavement.
j = Axle load interval.
m = Axle load type (single, tandem, tridem, quad, or special axle configuration).
l = Truck type using the truck classification groups included in the MEPDG.
p = Month.
T = Median temperature for the 5 temperature intervals or quintiles used to subdivide each month, °F.

Figure 7. Formula for Damage Calculation[6]

Finally, in the calibrated alligator cracking version of the MEPDG (no endurance limit used) the fatigue damage is transformed into bottom-up alligator fatigue cracking by using the equation given in Figure 8.

$$FC_{Bottom} = \left(\frac{C_4}{1 + e^{(C_1 * C'_1 + C_2 * C'_2 * \log 10(D))}} \right) * \left(\frac{1}{60} \right)$$

$$C'_1 = -2C'_2$$

$$C'_2 = -2.40874 - 39.748 * (1 + hac)^{-2.856}$$

where:

FC_{Bottom} = Area of alligator cracking that initiates at the bottom of the HMA layers, percent of total lane area.
D = Cumulative damage at the bottom of the HMA layers, percent.
$C_{1,2,4}$ = Transfer function regression constants; C_4= 6,000 (total area of the lane, 12 feet wide * 500 feet length); C_1=1.00; and C_2=1.00

Figure 8. Alligator Fatigue Cracking Transfer Function[6, 8]

For the top-down load associated longitudinal fatigue cracking, the fatigue damage is transformed into longitudinal fatigue cracking with the help of the equations in Figure 9.

$$FC_{Top} = 10.56\left(\frac{C_4}{1+e^{(C_1-C_2*\log 10(D))}}\right)$$

where:

FC_{Top} = Length of longitudinal cracks that initiate at the top of the HMA layer, ft/mile.
D = Cumulative damage near the top of the HMA surface, percent.
$C_{1,2,4}$ = Transfer function regression constants; C_4= 1,000 (maximum length of linear cracks occurring in 2 wheel paths of a 500 ft. section ; C_1=7.0; and C_2=3.5.

Figure 9. Longitudinal Fatigue Cracking Transfer Function[6, 8]

For the cement treated base (CTB) layers, MEDPG uses the models shown in Figure 10 to predict the fatigue behavior of these layers.

$$\log N_{f-CTB} = \frac{(k_{c1} * \beta_{c1} - (\frac{\sigma_t}{M_R})}{k_{c2} * \beta_{c2}}$$

$$FC_{CTB} = C_1 + \frac{C_2}{1+e^{(C_3-C_4*D)}}$$

where

$N_{f\text{-}CTB}$ = Allowable number of axle load applications for a semi-rigid pavement (CTB layer).
σ_t = Maximum traffic induced tensile stress at the bottom of the CTB layer, psi.
M_R = 28-day Modulus of rupture for the CTB layer, psi.
D = Cumulative damage of the CTB or cementitious layer and determined in accordance with the equation in Figure 7, decimal.
$k_{c1,c2}$ = Global calibration factors (in the current version k_{c1}= k_{c2}=1.0)
$\beta_{c1,c2}$ = Local calibration constants; these values are set to 1.0 in the software.
FC_{CTB} = Area of fatigue cracking, ft^2.
$C_{1,2,3,4}$ = Transfer function regression constants; C_1=1.0, C_2=1.0, C_3=0, and C_4=1,000, however, this transfer function was never calibrated.

Figure 10. Fatigue Cracking Prediction Model for CTB Layers[4, 6]

One may notice that the above equation is not nationally (globally) calibrated in the MEPDG software. The reason for that is the difficulty associated with getting the requirements of field section design input and performance data. Once the damage is computed for a specific analysis period, the new damaged modus of the CTB layer for the next analysis period (either 2 or 4 weeks as previously explained) is computed as shown in Figure 11.[4, 6]

$$E_{CTB}^{D(t)} = E_{CTB}^{Min} + \left(\frac{E_{CTB}^{Max} - E_{CTB}^{Min}}{1 + e^{(-4+14(DI_{CTB}))}} \right)$$

where:

$E_{CTB}^{D(t)}$ = Equivalent damaged elastic modulus at time t for the CTB layer, psi.
E_{CTB}^{Min} = Equivalent elastic modulus for total destruction of the CTB layer, psi.
E_{CTB}^{Max} = 28-day elastic modulus of the intact CTB layer, no damage, psi.

Figure 11. Formula for the Calculation of the CTB Layer Damaged Modulus

Non-Loaded Associated Transverse Cracking Prediction Model

In MEPDG, the amount of transverse cracking expected in a pavement system is predicted by relating the crack depth to an amount of cracking (crack frequency) by the expression shown in Figure 12.

$$C_f = \beta_{t1} * N\left(\frac{1}{\sigma}\right) \log\left(\frac{C}{h_{ac}}\right)$$

where:

C_f = Observed amount of thermal cracking, ft/mi.
β_{t1} = Regression coefficient determined through global field calibration (β_{t1}=400).
N = Standard normal distribution evaluated at [z].
σ = Standard deviation of the log of the depth of cracks in the pavement (for the global calibration σ = 0.769), in.
C_d = Crack depth, in.
h_{ac} = Thickness of HMA layers, in.

Figure 12. MEPDG Thermal Cracking Model[4, 6]

For a given thermal cooling cycle that triggers a crack to propagate, the Paris law is used to estimate the crack propagation as explained in Figure 13.

$$\Delta C = A \Delta K^n$$

where:

C = Change in the crack depth due to a cooling cycle.
ΔK = Change in the stress intensity factor due to a cooling cycle.
A, n = Fracture parameters for the HMA mixture.

Figure 13. Paris Law for Crack Propagation[4, 6]

The parameters *A* and *n,* in Figure 13, can be estimated from the indirect tensile creep compliance and strength of the HMA with the help of the expressions shown in Figure 14.

$$A = 10^{\left(k_t \beta_t * (4.389 - 2.52 * \log(E \sigma_m n)\right)}$$

$$n = 0.8\left(1 + \frac{1}{m}\right)$$

where:

k_t = Coefficient determined through global calibration for each input level (in MEPDG version 1.1, k_t = 1.5 for levels 1 and 3 inputs, and 0.5 for level 2 input).
E = HMA indirect tensile modulus, psi.
σ_m = HMA tensile strength, psi.
m = The m-value derived from the indirect tensile creep compliance curve measured in the laboratory.
β_t = Local (regional) calibration factor.

Figure 14. Determination of A and n Parameters[4, 6]

Reflection Cracking Model in HMA Overlays

For the AC over AC and AC over Rigid pavements overlay options MEPDG uses a simple-empirical model, based on field observations, for the prediction of reflective cracking. This model predicts the percentage of cracks that propagate through the overlay as a function of time and AC overlay thickness using the sigmoidal function shown by in Figure 15.

$$RC = \frac{100}{1 + e^{a.c + b.d.t}}$$

where:

RC = Percent of cracks reflected.
t = Time, years.
a, b = Regression fitting parameters calculated as shown Figure 16 and summarized in Table 3.
c, d = User-defined cracking progression parameters.

Figure 15. MEPDG Reflection Cracking Model in HMA Overlay[4, 6, 9]

The regression parameters *a* and *b* are calculated through the equations presented in Figure 16. Typical recommended values for the regression parameters (*a, b)* and user defined parameters *(c, d)* of the reflective cracking model are summarized in in Table 3.

$$a = 3.5 + 0.75\left(H_{eff}\right)$$

$$b = -0.688684 - 3.37302\left(H_{eff}\right)^{-0.915469}$$

where:

H_{eff} = Effective thickness of the overlay layer as defined in Table 3.

Figure 16. MEPDG Reflection Cracking Model Parameters a and b

Table 3. MEPDG Reflection Cracking Model Regression Fitting Parameters[6, 9]

Pavement Type	Fitting and User-Defined Parameters			
	a and b	c	d	
			Delay Cracking by 2 years	Accelerate Cracking by 2 years
Flexible	$H_{eff} = H_{HMA}$	---	---	---
Rigid-Good Load Transfer	$H_{eff} = H_{HMA} - 1$	---	---	---
Rigid-Poor Load Transfer	$H_{eff} = H_{HMA} - 3$	---	---	---
Effective Overlay Thickness, H_{eff}, inches	---	---	---	---
<4	---	1.0	0.6	3.0
4 to 6	---	1.0	0.7	1.7
>6	---	1.0	0.8	1.4

Notes:

1. H_{HMA} = HMA overlay thickness, in.
2. Minimum recommended H_{HMA} thickness is 2 inches for existing flexible pavements, 3 inches for existing rigid pavements with good load transfer, and 4 inches for existing rigid pavements with poor load transfer.

IRI Prediction Model

In MEPDG, the smoothness of the pavement surface is characterized by the IRI. MEPDG predicts the IRI of the pavement over time as a function of the initial pavement IRI, fatigue cracking, transverse cracking, average rut depth, and site factors. For new HMA and HMA overlays of flexible pavements MEPDG uses the nationally calibrated model shown in Figure 17 to predict the IRI of the pavement.

$$IRI = IRI_o + 0.0150(SF) + 0.400(FC_{Total}) + 0.0080(TC) + 40.0(RD)$$

where:

IRI_o = Initial IRI after construction, in./mi.
SF = Site factor, refer to Figure 18.
FC_{Total} = Area of fatigue cracking (combined alligator, longitudinal, and reflection cracking in the wheel path), percent of total lane area. All load related cracks are combined on an area basis – length of cracks is multiplied by 1 foot to convert length into an area basis.
TC = Length of transverse cracking (including the reflection of transverse cracks in existing HMA pavements), ft/mi.
RD = Average rut depth, in.

Figure 17. Equation for the IRI Prediction[6]

The site factor (SF) in the IRI model is calculated with the help of the nationally calibrated equation shown in Figure 18.

$$SF = Age(0.02003(PI + 1) + 0.007947(\mathrm{Pr}ecip + 1) + 0.000636(FI + 1))$$

Where:

Age = Pavement age, years.
PI = Percent plasticity index of the soil.
FI = Average annual freezing index, degree F days.
Precip = Average annual precipitation or rainfall, in.

Figure 18. Equation for the Site Factor Calculation

MEPDG Software Evolution

Several versions of the MEPDG software were released starting with the draft software Version 0.7 in June 2004, Version 0.9 in June 2006, Version 0.91 in September 2006, Version 1.00 in April 2007, Version 1.10 in August 2009, and currently DAWin-ME which was released at the end of April 2011. Version 1.0 was balloted and approved by NCHRP, FHWA, and AASHTIO as an interim AASHTO standard in October 2007. DARWin-ME is production software for use by transportation community which was migrated from the research software resulted from the NCHRP 1-37A and 1-40 projects.

Over time, significant changes, improvements, and bugs elimination have been incorporated in the consecutive versions of the MEPDG software. The most significant improvements from the draft version 0.7 (April 2004) till the 1.10 version (August 2009) includes the following: [10,11, 12, 13, 14, 15, 16, 17, 18]

- Reduction in program running time.
- The moisture prediction models for all the unbound layers were revised based on the findings of the NCHRP 9-23 project. These models includes; new suction models, new Thornthwait moisture index models, new soil weight characteristics curve models,

moisture content models, compaction models, and, specific gravity models, and saturated hydraulic conductivity model.

- Four more years of climatic data from over 800 weather stations throughout the U.S. were added to the original climatic data in MEPDG, this expanded the climatic database to 9 years of hourly climatic data.
- Recalibration of the distress models using more performance data (additional 4 to 5 years of performance data) for the 94 LTPP sections used for the 1-37A original calibration effort. In addition the calibration data were revised and filtered from any errors.
- Incorporation of user adjustment coefficients to the reflective cracking model to allow users to adjust the reflective cracking rate and/or calibrate the model based on field data. In addition, recommend values for the user adjustment coefficients were provided for users of the MEPDG.
- Allowing users to disable the reflective cracking calculation module in cases of using, for example, geotextiles between the existing pavement and the new AC overlay that have a higher possibility of successfully stopping all reflective cracking to occur.
- Incorporation of typical resilient modulus values and ranges for different unbound materials and soil types based on the material classification.
- Incorporation of the fatigue endurance limits with the alligator bottom-up fatigue cracking.
- Incorporation of the binder shear modulus (G*)- based E* Witczak prediction model (NCHRP 1-40D model) into MEPDG software. Thus user have the option to use either the "viscosity based" E* Witczak prediction model (NCHRP 1-37A model) or the "G*-based" E* Witczak prediction model.
- Improved reports for AC over JPCP and AC over CRCP to output reflection cracking prediction properly.
- Improved EICM stability by additional checks on model inputs.
- Variable EICM time-step and nodal spacing to better model thin bonded PCC overlays of existing JPCP.
- For AC over JPCP design, changed the method of JPCP damage analysis from a 2-layer equivalent analysis (pavement/base) to a 3-layer equivalent analysis (AC/PCC/base). The 3-layer analysis method takes into consideration the stresses at the top and bottom of the PCC layer, as well as determination of the equivalent temperature gradients through the asphalt layer.
- Allow users to modify IRI calibration constants in flexible pavements.
- Create traffic export/import capabilities. Allow the user to import/export all of the data need for the traffic files within the interface.
- Used can prepare multiple files with all inputs then upload them in a batch mode so the program runs all the files consecutively.
- Revised thermal fracture prediction models.
- Longer analysis period (design life) for both flexible and rigid pavements.

The significant improvements of the DARWin-ME production software over the research software versions include the following:

- Design optimization.
- Significant reduction in the running time of the flexible pavement.
- Incorporation of local data libraries.
- Incorporation of the SI units in addition to the U.S. customary units.
- Better batch mode capabilities.
- Backcalculated variables into rehab.
- Improved graphical user interface and output reports.

Software Limitations

There are some factors that the current research software (MEPDG version 1.10) does not handle in the flexible pavement structures module. In addition, there are some distress prediction models that are not nationally calibrated. Some of the MEPDG limitations (in the flexible pavement structures module) include: [6, 19]

- MEPDG is an analysis tool rather than a design tool; it does not provide the structural thickness as an output. Users can only find the design thicknesses through trial and error process.
- The current software is only available in U.S. customary units.
- The fatigue damage model for the chemically stabilized mixtures (CSM) is not calibrated in the current version of the software.
- The geosynthetics and other reinforcement materials cannot be simulated.
- MEPDG does not predict mixture durability such as raveling and stripping.
- MEPDG does not have the capability to consider the volume changes potential in frost susceptible and expansive soils.

However some of these limitations have been overcome in the production software (DARWin-ME) as previously presented.

Chapter 3
State Highway Agencies Implementation Efforts

Introduction

The AASHTO Joint Task Force on Pavements has sponsored several research projects and training workshops, so as to advance the adoption and implementation of the MEPDG by the state department of transportations (DOTs) throughout the U.S. One of the major projects for the MEPDG implementation was the NCHRP 1-40: Facilitating the Implantation of the Guide for the Design of New and Rehabilitated Pavement Structures. This project includes the following:

- NCHRP 1-40A: Independent Review of the Recommended Mechanistic-Empirical Design Guide and Software.
- NCHRP 1-40B: User Manual and Local Calibration Guide for the Mechanistic-Empirical Pavement Design Guide and Software.
- NCHRP 1-40D (01 & 02): Technical Assistance to NCHRP and NCHRP 1:40A: Versions 0.9 and 1.0 of the M-E Pavement Design Software.

Moreover, a group was formed from 19 different states named “Lead States”, in conjunction with AASHTO, NCHRP, and FHWA, in order to promote and facilitate the refinement, implementation, and evolution of the MEPDG.[20] The lead states are: Arizona, California, Florida, Kentucky, Maine, Maryland, Minnesota, Mississippi, Missouri, Montana, New Jersey, New Mexico, New York, Pennsylvania, Texas, Utah, Virginia, Washington, and Wisconsin.

This chapter presents a literature review of other states, including some of the lead states, implementation activates for MEPDG with the focus on Idaho neighboring states. The purpose of this review is to learn from other states what steps and activities need to be performed in order to successfully implement MEPDG in Idaho.

MEPDG States Implementation Efforts

In a recent survey in year 2007 by FHWA based on 52 state highway agencies (SHAs) responders, about 80% of the SHAs stated that they have plans for implementation of the MEPDG.[21] An older FHWA survey that was conducted in 2003 showed at that time only 42 percent of the SHAs had implementation plans for the MEPDG.[22] This means that MEPDG is gaining more attention with time. The next subsections focus upon reviewing the Idaho neighboring states and other states implementation activities of MEPDG including some of the lead states.

Utah

An implementation plan of the MEPDG was completed by the Applied Research Associates, Inc. for the Utah Department of Transportation (UDOT). This plan was initiated in 2003 with the objectives of 1) determining the suitability of MEPDG for Utah, 2) define needed modifications to MEPDG, 3) improving materials characterization and obtain necessary new equipment, 3) prioritizing and implementing needed modifications incrementally based on their impact on pavement design, and finally 4) providing training to UDOT staff on how to use the MEPDG software.[23]

The Utah MEPDG implementation project consists of 2 phases. Phase I involved 1) determination of LTPP data to be used for validation and local calibration of MEPDG, 2) a sensitivity analysis, 3) a comparison of MEPDG and the existing UDOT pavement design methods, and finally 4) preparation of a scope for future work required for the full implementation of MEPDG. Phase II of the UDOT MEPDG implementation plan focused on the validation of the MEPDG nationally calibrated distress prediction models using data from both LTPP and UDOT pavement management system. In addition, local calibration factors for the distress prediction models based on Utah conditions were developed. Utah study included 4 pavement types: 1) new or reconstructed flexible pavements, 2) AC over AC rehabilitation, 3) new or reconstructed jointed plain concrete pavement (JPCP), and 4) older JPCP subjected to concrete pavement restoration that includes diamond grinding. It should be mentioned that the MEPDG software Version 0.8 was used during Phase I of the implementation while Version 1.0 was used for the Phase II validation/calibration efforts for Utah.

For the distress/IRI local calibration, 12 to 15 new and reconstructed projects and only 2 to 3 AC over AC rehabilitation projects were used. Level 2 truck volumes and truck ALS and level 3 tire pressures, truck speed, and truck wander represented the inputs in the MEPDG traffic module. Most of the HMA, base/subbase, and foundation material characterization database were only available at level 3 and few material characterization were available at level 2. The research team used the database from the Natural Resources Conservation Services (NRCS) regarding the subgrade soils characterization. Climatic data from the weather stations attached with MEPDG for Utah and its surrounding states were used to create virtual site specific climatic date for use in the calibration/implementation efforts in Utah. This is considered level 2 climatic data inputs.

The Utah calibration study showed that for newly flexible pavements and AC over AC rehabilitation design, the nationally calibrated MEPDG alligator cracking model predictions for Utah conditions were relatively good for low to moderate cracking. There were no roads in Utah with significant alligator cracking to check the model predictions at these conditions. The nationally calibrated transverse cracking model predictions were adequate for the newly constructed pavements with Superpave binders and inadequate for the older constructed pavements using conventional binders. No local calibration coefficients were determined for the transverse cracking model. A good agreement was found between measured and predicted IRI using the MEPDG nationally calibrated IRI model. The research team reported that only the rutting prediction models needed to be recalibrated to reflect Utah conditions.[23] The local calibration factors found for the rutting models for Utah roads are summarized in Table 4.

Table 4. Utah Local Calibration Coefficients for the Rutting Models[23]

Pavement Type	Rutting Submodels Local Calibration Coefficients		
	HMA (β_{r1})	Base (β_{s1})	Subgrade (β_{s1})
New flexible pavement and AC over AC rehabilitation	0.560	0.604	0.400

Finally, a draft user's guide for UDOT Mechanistic-Empirical Pavement Design using MEPDG Version 1.0 was completed as a part of the implementation activities.[24] This draft user's guide shows all the inputs needed for pavement design using MEPDG with recommendations of typical inputs for Utah pavements. Moreover, a sensitivity analysis was performed using the locally calibrated MEPDG models for new and reconstructed HMA pavements based on Utah conditions. A summary of the sensitivity results is shown in Table 5.

Table 5. Summary of MEPDG Sensitivity Results of Utah Flexible Pavements[24]

Design/Material Variable	Distress/Smoothness			
	Alligator Cracking	Rutting	Transverse Cracking	IRI
HMA Thickness	High	Moderate	Low	Moderate
Tire load, Contact Area, and Pressure	Moderate	High		
HMA Tensile Strength			High	
HMA Coefficient of Thermal Contraction			Moderate	
Mixture Gradation	Moderate	High		
HMA Air Voids In-Situ	High	Moderate	Moderate	Moderate
Effective HMA Binder Content	High	Moderate	Moderate	Low
Binder Grade	Moderate	Moderate	High	High
Bonding with Base	High	Low		
Base Type/Modulus	High	High		
Base Thickness	Low			
Subgrade Type/Modulus	Moderate	Moderate		
Ground Water Table	Low	Low		
Climate	Moderate	Moderate	High	Low
Truck Volume	High	High		
Truck Axle Load Distribution	Moderate	Moderate		
Truck Speed	Moderate	High		
Truck Wander	Moderate	Moderate		
Initial IRI				High

Montana

Montana MEPDG implementation effort focused upon locally calibrating MEPDG distress models for Montana conditions. This effort was divided into 3 phases. Phase I involved the identification of the test sections and developing data collection procedures. Phase II effort included the data collection and analysis of the MEPDG distress prediction models to match the climate, materials, and design strategies in Montana. Three reports were published covering this work.[25, 26, 27] Phase III was the future assistance from an outside agency to continue with the data collection efforts for updating the calibration factors for the MEPDG performance models.

Pavement sections, in Montana, with performance data, HMA mixture types, unbound and subgrade material properties for new HMA, reconstructed HMA, and rehabilitated pavements were selected for a factorial study using MEPDG. In addition, LTPP test sections from Idaho, North and South Dakota, Wyoming, and Alberta and Saskatchewan (Canada) were also selected. The reason that these sections were not from Montana was that Montana does not have the full experimental factorial planned by the implementation team such as Spuerpave mixtures, drainage layer and so on. The total number of test sections was 89 LTPP and 13 non-LTTP sections. Of the 89 LTPP sections, only 34 sections are located in Montana and 55 are located in the adjacent states and Canada.

Field samples were taken to assure that the inventory properties of the pavement materials and soils collected from the as-built construction plans match the field test results. Two field cores were taken from the non-LTPP test sections for layer thickness measurements, and HMA volumetric properties such as aggregate gradation, air voids, asphalt content, and binder viscosity. Additional 12 field cores were cut and tested for creep compliance, modulus, and layer strength for use in distress predictions. A total of 2, 20-ft, borings were also drilled through the pavement for the determination of the unbound base/subbase and foundation materials routine properties. In addition, in place moisture content and dry density, optimum moisture content, maximum dry density, and Atterberg limits were determined for each unbound layer and the subgrade soils. Laboratory tests were also performed on samples of unbound base and subgrade materials to determine material classification and M_r at optimum moisture content (level 1). Cores were also taken from the cement treated base layers for compressive strength, indirect tensile strength and elastic modulus measurements. The cores and borings were also used to determine the rutting beneath the HMA layers and the direction of crack propagation. For the non-LTPP sections the field investigation showed that most of the rutting occurred at the surface was found to be in the HMA layer. For the LTTP sections, there was no visual observation on the direction of crack propagation or the rutting in the individual layers.

A long term monitoring program was designed and conducted to monitor the performance of the test sections. This program included Falling Weight Deflectometer (FWD) tests to measure the load response characteristics and to back-calculate the elastic modulus for each layer and the foundation (for overlay sections), longitudinal and transverse profile measurements, and condition distress surveys to determine IRI and rut depth.

For the climatic data required by MEPDG, the closest weather station data built in the MEPDG (within 25 miles) to the test section was selected. For test sections with unavailable weather station at or near the test section site, a virtual weather station was built using the MEPDG software using up to 6 weather stations surrounding that site. The ground water table (GWT) depth was set to 20 ft below the surface for all sections used in this study and no seasonal variation in the GWT was included because of data limitations.

Traffic data from 21 WIM stations in Montana were used to characterize traffic for the local validation/calibration effort of MEPDG. In general, these data showed that for the majority of Montana roads, class 9 trucks was the most widely truck using Montana roads followed by class 13 trucks. However, for the low volume roads and county roads, class 6 trucks contributes the majority of the truck traffic. ALS at Montana WIM sites were found to be close enough to the MEPDG default values. The statewide average values (level 3) of the monthly adjustment factors (MAF) for the 3 major truck categories in Montana were used for all Montana test sections as WIM data were insufficient to calculate these factors for the specific sites. Montana statewide MAF are summarized in Table 6. On the other hand, the traffic monthly adjustment factors for the test sections in the states adjacent to Montana and the Canadian provinces were taken as the default values in the MEPDG (all values are 1.0 in MEPDG).

Table 6. Montana Statewide Monthly Adjustment Factors[25]

Month	Single Unit Trucks (Truck Class 5 or 6)	Combination Trucks (Truck Class 9 or 10)	Multi-trailer Trucks (Truck Class 13)
January	0.84	0.91	0.99
February	0.79	0.92	0.89
March	0.76	0.94	0.88
April	0.86	0.99	0.99
May	1.10	1.06	1.03
June	1.30	1.09	0.96
July	1.43	1.02	0.92
August	1.39	1.06	1.11
September	1.14	1.00	1.09
October	1.06	1.15	1.12
November	0.87	1.00	1.00
December	0.76	0.84	0.87

Site specific traffic data (level 1) were used for the initial 2-way average annual daily truck traffic (AADTT), number of lanes, percentage of trucks in design lane, percentage of trucks in design direction, operational speed, lane width, and traffic growth factor. Default values (level 3) were used for axle spacing, dual tire spacing, tire pressure, and ALS. The research team stated that, generally many of the Montana WIM station data are in agreement with the MEPDG default values for the ALS yet; considerable variability appeared in the 2000-2001 data. They suggested that this variability may be due to scale calibration problems. The values of the number of axles for each truck class used in the local calibration effort for Montana are shown in Table 7.

Table 7. Number of Axles for each Truck Class Used for the Verification/ Calibration Study in Montana[25]

Truck Class	Axle Type		
	Single	Tandem	Tridem
4	1.50	0.50	0.00
5	2.00	0.00	0.00
6	1.00	1.00	0.00
7	1.00	0.00	1.00
8	2.00	0.50	0.00
9	1.00	2.00	0.00
10	1.00	1.00	1.00
11	4.75	0.25	0.00
12	4.00	1.00	0.00
13	3.00	1.75	0.25

All the data collected from the test sections were stored in a database and used to calibrate the MEPDG (Version 0.9) distress models. Running the MEPDG globally calibrated distress models in with Montana database reveled the following:[25]

- MEPDG significantly over-predicted total rutting. Higher rutting values were predicted in the unbound layers and subgrade soils.
- MEPDG over-predicted the load associated alligator cracking in case of new constructed flexible pavements. On the other hand, it under-predicted alligator cracking of AC over AC overlay pavements.
- MEPDG over-predicted the alligator fatigue cracking of new flexible pavements and overlays for test sections with pavement preservation techniques applied in their early life.
- The bias for the predicted longitudinal cracking within wheel path was insignificant; however, the residual error was large.
- For the non-load related transverse cracking, MEPDG over-predicted the length of the transverse cracks of the test sections located in Montana and under predicted the crack lengths for the test sections located in the areas adjacent to Montana.

Based on these findings, the research team suggested that the distress transfer functions in the MEPDG needed to be locally calibrated for Montana conditions. A local adjustment factor for the unbound layers rutting (β_{s1} = 0.20) for both coarse and fine grained materials was suggested.

New input parameters related to the HMA mixture properties were suggested to be incorporated in the MEPDG for the calibration of the HMA rutting and alligator fatigue cracking models. These new inputs are the gradation index which is defined as the absolute difference between the actual gradation and the 0.45 maximum density line using sieves sizes 3/8", #4, #8, #16, #30, and #50, design air voids, optimum asphalt content by weight and volume (from design reports), and fine and coarse aggregate angularity indices.[25] One may notice that some of these new parameters are not easy to find as they require testing results that are not usually conducted. Despite the fact that this new calibration methodology revealed

reasonable agreement between the field measure and predicted distresses using MEPDG for Montana conditions, yet the new suggested calibration methodology with the new inputs when initially incorporated into the MEPDG software and tried with various pavement sections and conditions, it resulted in significant erroneous predictions especially for the HMA rutting. Thus, the NCHARP 1-40D research team decided not to pursue the suggested calibration method in the MEPDG software.[28, 28]

Montana research team reported that they could not find any good local calibration factors for the MEPDG longitudinal fatigue cracking model. They suggested not using the present model in Montana, and if used the original global calibration factors should be used in design. For the transverse cracking prediction model, a local calibration factor for level 3 inputs of (β_{s3} = 0.25) was suggested. The global calibration factors for the IRI model were found to be adequate for use in Montana. A summary of the local calibration factors suggested for use in Montana for new flexible and AC over AC pavements are given in Table 8.

Table 8. Montana Local Calibration Coefficients[25]

Distress Model	Distress Type/Layer	Calibration Coefficient
Rutting	HMA	New Method Proposed
	Granular Base, (β_{B1})	0.20
	Subgrade, (β_{s1})	0.20
Fatigue Cracking	Alligator Damage/Cracking	New Method Proposed
	Longitudinal Damage/Cracking	Global Values
Transverse Cracking	Non-Load Related (β_{s3})	0.25
IRI	Smoothness	Global Values

Washington

Since the first release of MEPDG in 2004, the Washington State Department of Transportation (WSDOT) has worked on the evaluation, calibration, and implementation of the guide to replace the AASHTO 1993 method currently used in Washington state.[29] Data obtained from the Washington state pavement management system was used to locally calibrate the MEPDG (Version 1.0) distress prediction models. The *TrafLoad* software was used to process traffic data and produce all traffic inputs required by MEPDG. Traffic data collected at 38 WIM sites located in Washington State was used for traffic characterization. One group of ALS, which used in the calibration, was found to be representative for the entire state of Washington.[29, 30] MEPDG default weather stations, located in Washington, close to the selected pavement sections for calibration were used in the local calibration process. WSDOT calibration process involved a combination of split-sample and jackknife approaches and consisted of 5 steps: bench testing, model analysis, calibration, validation, and iteration. The first step of the calibration (bench testing) was basically a sensitivity analysis of the software distress predictions to key design inputs and comparing the prediction to actual performance. This step concluded a reasonable agreement between MEPDG predictions and actual performance of Washington state pavements. Table 9 presents the typical design

parameters used for the sensitivity analysis. The sensitivity of the predictions to key design parameters are summarized in Table 10.

Table 9. Typical WSDOT Design parameters used for the Sensitivity Analysis[29]

Design Parameter	Input Value
AC Thickness (in.)	4.2, 5, 8, 12
PG Binder Grade	PG 58-22, PG 64-28, PG 58-34
Base Type	Asphalt Treated, Granular
Base Thickness (in.)	4.2, 6, 8, 12
AADTT (Design Lane)	100, 1000, 2000
Annual Growth Rate (%)	2, 4, 6
Soil Type	A-4, A-5, A-7-5, A-7-6
Subgrade Modulus (psi)	7500, 12500, 15000, 17500
Climate	Camas, Spokane, Pullman, Seattle, Stampede Pass

Table 10. Inputs Sensitivity for Flexible Pavement Distress Conditions[29]

Input Factor	Longitudinal Cracking	Transverse Cracking	Alligator Cracking	AC Rutting	IRI
Climate	Medium	High		High	High
PG Binder Grade	High	Medium	Medium	Medium	
AC Thickness	High	Medium	Medium	High	
Base Type	Medium			High	
AADTT	Medium			High	Medium
AC Mix Stiffness			High		Medium
Soil Type	Medium				

An elasticity analysis was conducted by running MEPDG several times using various design inputs and calibration factors in order to access the influence of the calibration factors on the pavement distress models. This analysis indicated that, asphalt concrete fatigue damage models (alligator and longitudinal) should be calibrated before the damage to cracking transfer functions. Calibration factors β_{r2} and β_{r3} should be adjusted before the calibration factor β_{r1}. Only 2 flexible pavement sections representative of east and west Washington with medium traffic levels (AADTT = 222 and 295) were used in the calibration of the distress models. A summary of the local calibration coefficients of the MEPDG distress/IRI models is shown in Table 11. For the transverse cracking model the global calibration coefficients produced reasonable results. The research team indicated some sort of software bug related to the IRI model calibration. However, after calibrating the rutting and cracking models, the MEPDG globally calibrated IRI model always produced values that are lower than the actual roughness. Nevertheless, the differences in the predictions were small.[29]

Table 11. Washington State Local Calibration Coefficients[29]

Distress Model	Distress Type/Layer	Calibration Coefficient
Rutting	HMA, (β_{r1}, β_{r2}, β_{r3})	1.05, 1.109, 1.1
	Granular Base, (β_{B1})	default
	Subgrade, (β_{s1})	0.0
Fatigue Cracking	Fatigue Model, (β_{f1}, β_{f2} *and* β_{f3})	0.96, 0.97, 1.03
	Bottom-Up Transfer Function (C_1, C_2)	1.071, 1.0
	Top-Down Transfer Function (C_1, C_2)	6.42, 3.596
IRI	Smoothness (C_1, C_2, C_3, C_4)	Could not locally calibrate due to software bug

The research team concluded that before MEPDG implementation, calibration to local condition is deemed essential. For local implementation of the design guide, a user guide covering how to use the software, sensitivity level of each input, and definition and reasonable range of each high-sensitivity-level input and identification of software problems that might be faced are important. In addition, preparing design files with comprehensive database to be used with the software and training the pavement designers on the MEPDG are important for the implementation success.

Oregon

The initial effort to implement MEPDG in Oregon started with the traffic characterization. A study was conducted using traffic data from 4 WIM sites in the state of Oregon. ADTT volume of 5000, 1500, and 500 were chosen to represent the high, moderate, and low traffic volumes, respectively. Seasonal adjustment factors (winter, spring, summer, and fall) were developed and a "virtual" truck classification was created in the MEPDG program in order to implement the Oregon WIM data into the software.[31] The traffic data specific to Oregon to be used in the MEPDG were found to be hourly truck volume distribution, site-specific axle weight data, average number of axles per truck, and average axle spacing. Work is still in progress with Oregon State University to develop design inputs and evaluate the fatigue cracking, rutting and thermal cracking models in MEPDG.

California

California is one of the leading states for the MEPDG implementation. A joint research effort between the University of California Pavement Research Center and the California Department of Transportation (Caltrans) resulted in the development of default truck traffic inputs pertinent to California conditions to be used with the MEPDG and the Caltrans Mechanistic-Empirical Pavement Design (CalME) methods. In the California study, Class 9 truck traffic volume was used to represent the main truck flow at all locations. ALS and truck traffic volume data obtained from 108 WIM sites located throughout the state of California, with traffic data collected between 1991-2003, were analyzed and clustered into 8 groups.[32] Default traffic inputs, for pavement sections in California where WIM traffic data are unavailable, were then developed for each group. Microsoft Access database was prepared using this default data for information retrieval.

Arizona

Being one of the lead states for the MEPDG implementation, Arizona Department of Transportation (ADOT) involved with Arizona State University in a long term research project, initiated in 1999. The main objective of this project was to develop performance related specifications for asphalt pavements in Arizona based on the MEPDG.[33] This project focused upon the development of MEPDG typical design input parameters related to asphalt binders, asphalt mixtures, base and subgrade materials, climate, and traffic characteristics for Arizona. This project was divided into 11 projects. Only projects relevant to the MEPDG implementations are briefed in this report.

Project 2: ADOT AC Binder Characterization Database. In this project, laboratory Superpave tests were performed on 6 typical AC binders commonly used in ADOT construction projects. These binders are PG 58-22, PG 64-16, PG 64-22, PG 76-16, PG 70-10, and PG 76-16. The conducted tests were as follows:

- Penetration at 59 °F and 77 °F.
- Ring and ball softening point.
- Absolute viscosity at 140 °F.
- Rotational viscosity at 140, 176, 212, 250, 275 and 250 °F
- Low temperature flexural creep stiffness parameters (S and m-values) at 3 temperatures in 32 °F to -40 °F range.
- Dynamic Shear Rheometer (DSR) to determine binder G* and phase Angle (δ) at 58, 77, 95, 113, 140, 158, 176, 203, 221 and 239 °F under the oscillatory loading frequencies of 1, 10 and 100 radians per second.
- Direct Tension Tester (DTT) in temperature range of 32 °F to –36 °F to determine the low temperature ultimate tensile strain. These tests were conducted at 4 different aging conditions, 1) original or tank condition; 2) construction phase aging of asphalt binder using the Rolling Thin Film Oven (RTFO), and 3) accelerated in-service aging of asphalt binder using the Pressure Aging Vessel (PAV) at both 212 °F and 230 °F.

The output from these tests was stored in Excel database files for the binder characterization module in the MEPDG.

Project 3: ADOT AC Mix Stiffness Characterization Database. Laboratory tests were conducted on 11 lab blended conventional HMA mixtures using 5 different aggregates to develop a comprehensive E* master curve database associated with typical ADOT mixtures. E* test was conducted at temperatures of 14, 40, 70, 100, and 130 °F with loading frequencies of 0.1, 0.5, 1, 5, 10, and 25 Hz. The applied stress levels ranged from 10 to 100 psi for temperatures (14 °F to 70 °F) and 2 to 10 psi for higher temperatures. These test results are fundamental inputs required for the MEPDG level 1 inputs to characterize the HMA stiffness at different loading rates and temperatures.

Project 4: ADOT AC Thermal Fracture Characterization. This project dealt with the development of a comprehensive database for the thermal fracture properties (tensile creep and tensile strength) of typical ADOT mixtures. A total of 11 ADOT lab blended conventional HMA mixtures using 5 different aggregates

were tested for creep compliance and tensile strength. The creep compliance and tensile strength are fundamental material inputs required for MEPDG levels 1 and 2 for the prediction of the thermal cracking stress.

Project 8: ADOT Unbound Materials Modulus Database. in this project a set of typical k_1-k_2-k_3 material parameters for a range of 4 typical Arizona base materials, and 4 typical subgrade soils were established based on the repeated load resilient modulus testing. In addition, the test results from this project were used to validate the coefficients used to adjust the predicted M_r values using the MEPDG universal M_r prediction model for in-situ moisture and density conditions.

Project 10: Implementing EICM to Arizona Climatic Conditions. In this project, the state of Arizona was divided into 9 different environmental zones with each environmental zone having similar climatic characterizes. Specific weather stations, built in the MEPDG, were suggested for use within each climatic zone. In addition, software "*Climatic.exe"* was developed to generate and retrieve the climatic input files needed by MEPDG.

Project 11: Development of Design Guide Traffic Files for ADOT. This project dealt with the development of a computerized traffic database (in Excel format) of the entire Arizona highway network to be used with MEPDG in the analysis and design of Arizona roads.

In addition, a research effort was exerted to develop local calibration factors for the permanent deformation, load associated alligator and longitudinal cracking, distress models and IRI of new flexible pavements. A total of 22, 25, and 37 pavement sections in Arizona with performance and material characterization data obtained from LTPP and ADOT databases were used for the local calibration study for fatigue cracking, rutting, and IRI prediction models, respectively.[34] A trial and error method was used in order to find the optimum calibration coefficients which produce the least squared error and zero sum of standard error between field measured and MEPDG predicted performance values for each distress/IRI models. The recommended calibration coefficients for Arizona based on this study are summarized in Table 12.

Table 12. Arizona Local Calibration Coefficients[34]

Distress Model	Distress Type/Layer	Calibration Coefficient
Rutting	HMA, (β_{r1}, β_{r2}, β_{r3})	3.63, 1.10, 0.70
	Granular Base, (β_{s1})	0.111
	Subgrade, (β_{s1})	1.380
Fatigue Cracking	HMA Fatigue Model, (β_{f1}, β_{f2} *and* β_{f3})	0.729, 0.800, 0.800
	Bottom-Up Transfer Function (C_1, C_2)	0.732, 0.732
	Top-Down Transfer Function (C_1, C_2)	1.607, 0.803
IRI	Smoothness (C_1, C_2, C_3, C_4)	5.455, 0.354, 0.008, 0.015

Arkansas

Arkansas State Highway and Transportation Department (AHTD) has launched a long term research program with the help of the University of Arkansas in order to implement MEPDG. The implementation activities started with the assessment of the relative sensitivity of the MEPDG distress models in both flexible and rigid pavements to key design inputs.[35] For flexible pavements, the sensitivity analysis was conducted using 2 standard pavement sections typical in Arkansas. They are shown in Figure 19. One should notice that the resilient modulus of the subgrade material is 17,000 psi while the resilient modulus of the crushed stone granular base material is 10,000 psi (typical M_r range for crushed stone is 20,000 to 45,000 psi) which is very unusual in pavement design and should have a huge impact on the predicted cracks in the asphalt layer and the rutting in both base and subgrade layers. All sensitivity runs were performed at one traffic level (AADTT=1000) and one climatic location (Fayetteville with GWT depth = 20 ft). All inputs were held constant and one input was varied each time. A total of 2 HMA aggregate gradations (12.5 mm and 25.0 mm) were used in the study. In general, the values of the inputs that were varied in the sensitivity runs are shown in Table 13.

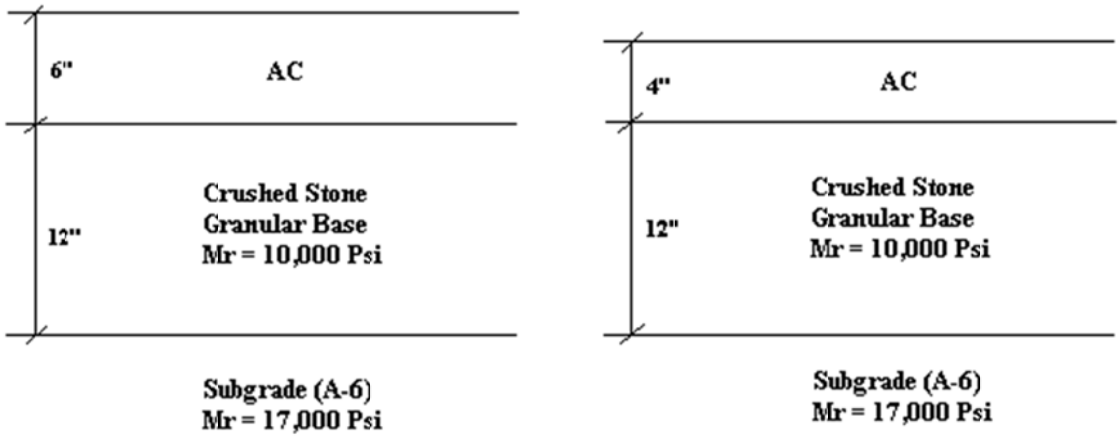

Figure 19. Flexible Pavement Sections used in the MEPDG Simulation Runs

Table 13. Input Levels for the Sensitivity Analysis of the HMA Material Inputs[35]

Input Variable	Value
Poisson's Ratio, (in./in.)	0.30, 0.35, 0.40
Surface Shortwave Absorptivity	0.80, 0.85, 0.90
Heat Capacity, (BTU/lb-°F)	0.1, 0.23, 0.50
Thermal Conductivity, (BTU/hr-ft-°F)	0.50, 0.67, 1.0
Air Voids (12.5mm mixes), (%)	3.0, 4.0, 4.5, 5.0, 6.0, 8.0
Air Voids (25.0mm mixes), (%)	3.0, 4.0, 4.5, 5.0, 6.0, 8.0
Binder Grade (12.5mm mixes)	PG 64-22, PG 70-22, PG 76-22
Binder Grade (25.0mm mixes)	PG 64-22, PG 70-22, PG 76-22
Total Unit Weight (12.5mm mixes), (pcf)	122, 135, 148
Total Unit Weight (25.0mm mixes), (pcf)	122, 135, 148
Effective Binder content (12.5mm mixes), (% volume)	7.5, 8.2, 8.4, 8.6, 8.7, 9.1, 10.1, 10.8

A one-way analysis of variance (ANOVA) was performed on the resulted damage from the sensitivity runs to check the impact of changing each of the varied inputs on the predicted damage. The results of Arkansas sensitivity analysis are summarized in Table 14.

Table 14. Summary of the Sensitivity Analysis of the HMA Material Inputs[35]

HMA Material Characteristics	Performance Models			
	Longitudinal Fatigue Cracking	Alligator Fatigue Cracking	Rutting	IRI
Poisson's Ratio	I	I	I	I
Surface Shortwave Absorptivity	I	I	I	I
Heat Capacity	I	I	I	I
Thermal Conductivity	I	I	I	I
Air Voids (12.5mm mixes)	I	I	I	I
Air Voids (25.0mm mixes)	S	S	I	S
Binder Grade (12.5mm mixes)	I	S	I	I
Binder Grade (25.0mm mixes)	I	I	I	I
Total Unit Weight (12.5mm mixes)	I	I	I	I
Total Unit Weight (25.0mm mixes)	I	I	I	I
Percent Binder Effective (12.5mm mixes)	S	S	I	S
Percent Binder Effective (25.0mm mixes)	I	S	I	I

S = Significant to the performance models
I = Insignificant to the performance models

It is of great importance to note that this study was performed using an earlier version of the MEPDG (Version 0.8). This means that the global calibration parameters of the distress models were different from the ones in the current version. In addition, the IRI model itself was different from the current model.

As part of Arkansas MEPDG implementation activities, classification and weight data from 55 WIM sites (reduced to 25 WIM sites after quality control checks performed on the classification data), operated from 2003 through 2005, was used to develop statewide traffic inputs for MEPDG.[36] First the researchers tried to use the *TrafLoad* computer program for generating traffic inputs for MEPDG, however they reported that the software could not read the W-card files.[36] Thus 2 computer programs were developed using Microsoft Excel® to generate the traffic inputs for MEPDG. Based on classification data collected at the 25 WIM sites, statewide volume adjustment factors were developed for the state of Arkansas. Researchers observed that the monthly and hourly adjustment factors were not significant for pavement performance while vehicle class distribution factors were found significant.[37] Moreover, statewide single, tandem, and tridem ALS were developed for Arkansas. Only few quad axles were found in Arkansas. The developed Arkansas statewide ALS factors were found to be different compared to the default nationwide values in the MEPDG. These differences were found to have significant influence on the predicted distresses using MEPDG Version 0.8.[36, 38] This study also showed that only 10 WIM stations out of 55 provided suitable data for the development of the Arkansas statewide ALS.

For simplifying the MEPDG implementation in the state of Arkansas, a centralized database system for MEPDG required inputs was prepared, using the Microsoft Access® and a user friendly interface (*PrepME*).[39, 40] This software stores, checks the data quality, and generates climate, traffic, material, and performance data for the state of Arkansas to be used with the MEPDG.

Local calibration factors for the MEPDG distress models to fit Arkansas pavements were also developed. A total of 26 sections from LTPP and AHTD pavement management system were used for the local calibration effort.[41] Default values of monthly adjustment, hourly truck distribution, and general traffic inputs (Level 3 input) were used in this effort. Site-specific vehicle class distribution (data was used whenever it was available (Level 1 input); otherwise, recommended values from MEPDG were used according to Truck Traffic Classification (TTC) groups (Level 2 input). Statewide ALS values were used in the local calibration study (Level 3 input). A summary of the local calibration factors developed for Arkansas are shown in Table 15.

Table 15. Arkansas Local Calibration Coefficients[41]

Distress Model	Distress Type/Layer	Calibration Coefficient
Rutting	HMA, (β_{r1}, β_{r2}, β_{r3})	1.2, 1.0, 0.80
	Granular Base, (β_{s1})	1.0
	Subgrade, (β_{s1})	0.50
Fatigue Cracking	HMA Fatigue Model, (β_{f1}, β_{f2} *and* β_{f3})	Default values
	Bottom-Up Transfer Function (C_1, C_2)	0.688, 0.294
	Top-Down Transfer Function (C_1, C_2)	3.016, 0.216

MEPDG predicted transverse cracking for Aransas sections used in the calibration were all zeros. The researchers contributed that to the implementation of the Performance Graded (PG) binders for HMA in Arkansas. However, field distress surveys for these sections showed recorded transverse cracking suggesting that additional cracking mechanisms may be predominate in Arkansas. Thus, according to the researchers, because of the nature of the data, MEPDG transverse cracking model was not calibrated in this study. In addition, the IRI model was not also calibrated.

Iowa

MEPDG implementation effort in Iowa focused upon studying the sensitivity of MEPDG predicted performance to the HMA properties, traffic, and climatic conditions based on field data from 2 existing Iowa flexible pavement systems. A total of 23 input parameters were varied in this study. Limited set of runs were also conducted to study the 2-way interaction among the input variables.[42] The results of the sensitivity analyses are summarized in Table 16. A summary of the extremely sensitive and sensitive to very sensitive input parameters affecting MEPDG distress predictions based on Iowa study are given in Table 17.

It should be noted that these results were found using an earlier version of MEPDG. Additionally, one should surmise that the above results are only valid for the pavement structural sections used in this analysis. Pavements with different AC thickness values might result in totally different conclusions especially for cracking. This study recommend that Iowa should seek to implement the MEPDG as the preferred approach to pavement design and evaluation in 3 to 5 years and train the pavement engineers on the software.

Table 16. Summary of Iowa Sensitivity Analysis[43]

	Flexible Pavement Inputs	Performance Models								
		Cracking			Rutting					IRI
		Longitudinal	Alligator	Transverse	AC Surface	AC Base	Subbase	Subgrade	Total	
AC General Property	AC Thickness	S	I	I	I	I	I	I	I/LS	I
AC Mix Properties	Nominal Max. Size	S	I	I	I/LS	I	I	I	I/LS	I
	PG Grade	ES	I	ES	LS/S	I	I	I	LS/S	LS/S
	Volumetric (Vbe/Va/ VMA)	VS	I	VS/ES	LS	I	I	I	LS	LS/S
	Unit Weight	LS/S	I	I	I/LS	I	I	I	I/LS	I
	Poisson's Ratio	LS/S	I	I	S	I	I	I	S	I
AC Thermal Properties	Thermal Conductivity	S	I	LS	I/LS	I	I	I	I	I
	Heat Capacity	VS	I	VS	LS/S	I	I	I	LS/S	LS
Traffic	Tire Pressure	VS	I	I	LS	I	I	I	LS	I
	AADT	VS	LS/S	I	ES	S	I	S	ES	I
	Traffic Distribution	VS	I	I	LS	I	I	I	LS	I
	Speed	VS	I	I	S/VS	I	I	I	S/VS	I
	Wander	LS/S	I	I	I	I	I	I	I	I
Climate	Climate	VS	I	ES	S	I/LS	I	I/LS	S	S
Base	Thickness	S/VS	S/VS	I	VS	I/LS	I	I/LS	VS	LS
	Quality (Mr)	LS/S	ES	I/LS	VS	I/LS	I/LS	I/LS	VS	VS/S
Subbase	Thickness	LS/S	I	I	I	I	I	I/LS	I	I
	Quality (Mr)	I	I	I	I	I	I	I	I	I
Subgrade	Type (Mr)	ES	LS	I	I	I	I	I/LS	I/LS	I/LS
Others	Aggregate Thermal Coefficient	I	I	I	I	I	I	I		I

ES = Extreme Sensitivity

VS = Very Sensitive

S = Sensitive

LS = Low Sensitivity

I = Insensitive

Table 17. Summary of Iowa Sensitive to Very Sensitive Input Parameters[43]

Performance Model	Extremely Sensitive	Sensitive to Very Sensitive
Longitudinal Cracking	Performance Grade (PG) Binder Type of Subgrade	HMA Layer Thickness Nominal Maximum Size Volumetric Thermal Conductivity Heat Capacity Tire Pressure AADT Traffic Distribution Traffic Velocity Climate Data from Different Stations Base Layer Thickness
Transverse Cracking	Performance grade (PG) binder Climate data from different stations	Volumetric Thermal Conductivity Heat Capacity
Rutting	AADT	Poisson's Ratio Traffic Velocity Climate Data from Different Stations Base Layer Thickness Type of Base
Smoothness		Climate Data from Different Stations Type of Base

Kansas

An implementation effort for MEPDG in Kansas was initiated with the objectives of evaluation of the software, performing sensitivity analysis of input variables, and attempting local calibration of the distress models. Laboratory tests to determine E* at 5 temperatures, 4, 10, 20, 30, 35 °C and 5 loading frequencies, 10, 5, 1, 0.5 0.1 Hz as well as creep compliance and tensile strength at -10 ^{o}C were performed on 8 asphalt mixtures usually used in Kansas roadways. In addition, the volumetric properties of the mixes and the shear moduli of the binders were also determined. A comparison study showed that MEPDG underestimated E* and overestimated the creep compliance of Kansas Superpave mixes at -10 ^{o}C.[44]

In addition, a calibration effort was conducted to locally calibrate MEPDG distress models for Kansas conditions. Several projects typical in Kansas roadways including dense graded HMA mixtures with conventional, neat, Polymer Modified Asphalt (PMA) and Superpave mixtures were used in the calibration. Table 18 summarizes the local calibration factors for Kansas conventional pavements. Table 19 and Table 20 show these factors for Kansas roads constructed with PMA and Superpave mixtures, respectively.

Table 18. Kansas Local Calibration Coefficients, Conventional Pavements[45]

Distress Model	Distress Type/Layer	Calibration Coefficient
Rutting	HMA, (β_{r1}, β_{r2}, β_{r3})	1.5, 0.90, 1.00
	Granular Base, (β_{B1})	0.5
	Subgrade, (β_{s1})	0.5
Fatigue Cracking	Fatigue Model, (β_{f1}, β_{f2} *and* β_{f3})	0.05, 1.0, 1.0
	Bottom-Up Transfer Function (C_1, C_2)	1.0, 1.0
	Top-Down Transfer Function (C_1, C_2)	2.0
IRI	Smoothness (C_1, C_2, C_3, C_4)	Global Values

Table 19. Kansas Local Calibration Coefficients, PMA Pavements[45]

Distress Model	Distress Type/Layer	Calibration Coefficient
Rutting	HMA, (β_{r1}, β_{r2}, β_{r3})	2.5, 1.15, 1.00
	Granular Base, (β_{B1})	0.5
	Subgrade, (β_{s1})	0.5
Fatigue Cracking	Fatigue Model, (β_{f1}, β_{f2} *and* β_{f3})	0.005, 1.0, 1.0
	Bottom-Up Transfer Function (C_1, C_2)	1.0,1.0
	Top-Down Transfer Function (C_1, C_2)	2.0
IRI	Smoothness (C_1, C_2, C_3, C_4)	Global Values

Table 20. Kansas Local Calibration Coefficients, Superpave Pavements[45]

Distress Model	Distress Type/Layer	Calibration Coefficient
Rutting	HMA, (β_{r1}, β_{r2}, β_{r3})	1.5, 1.2, 1.00
	Granular Base, (β_{B1})	0.5
	Subgrade, (β_{s1})	0.5
Fatigue Cracking	Fatigue Model, (β_{f1}, β_{f2} *and* β_{f3})	0.0005, 1.0, 1.0
	Bottom-Up Transfer Function (C_1, C_2)	1.0,1.0
	Top-Down Transfer Function (C_1, C_2)	3.5
IRI	Smoothness (C_1, C_2, C_3, C_4)	Global Values

Minnesota

The Minnesota Department of Transportation (MnDOT) and the Local Road Research Board (LRRB) initiated a research study in 2009 for the MEPDG implementation. The objectives of this study were: 1) evaluation of the MEPDG default inputs, 2) identification of deficiencies in the MEPDG software, 3) evaluation of prediction capabilities of the MEPDG performance prediction models for Minnesota conditions, and finally 4) recalibration of MEPDG performance models for Minnesota conditions. Several sensitivity analyses were conducted using different versions of the MEPDG and the research team confirmed that Version 1.0 represented a major improvement over the previous versions.[46]

Local calibration of the MEPDG rutting model was performed based on properties and field measured rutting values from MnROAD cells. The research team found that the rutting models for the base and

subgrade of flexible pavements could not be properly calibrated by adjusting the MEPDG model parameters. They suggested the following methodology for the local calibration of the rutting model:[46]

1. Run MEPDG Version 1.0 to determine each layer rutting at the end of the design period, and rutting in the base and subgrade layers for the first month for the 50 percent reliability level.
2. Use the equations in Figure 20 to determine the total rutting at the end of the design period at the 50 percent reliability level.

$$Total\_Rutting = Rutting\_AC + Rutting\_Base^* + Rutting\_Subgrade^*$$

$$Rutting\_Base^* = Rutting\_Base - Rutting\_Base\_1$$

$$Rutting\_Subgrade^* = Rutting\_Subgrade - Rutting\_Subgrade\_1$$

where:

Total_Rutting = Predicted surface rutting
Rutting_AC = Predicted rutting in the asphalt layer only
*Rutting_Base** = Modified predicted rutting in the base layer only
*Rutting_Subgrade** = Modified predicted rutting in the subgrade only
Rutting_Base = Predicted rutting in the base layer only using the original MEPDG predictions
Rutting_Subgrade = Predicted rutting in the subgrade only using the MEPDG original predictions
*Rutting_Base*_1 = Predicted rutting in the base layer only after one month
Rutting_Subgrade_1 = Predicted rutting in the subgrade only after one month

Figure 20. Minnesota Equations for MEPDG Rutting Models Calibration

3. Using the output from the design guide, find the rutting corresponding to the specified reliability.

The research team anticipated that the current longitudinal cracking model most likely will be modified under an ongoing NCHRP project. Thus, this model was not locally calibrated. The IRI model was not also calibrated in this study since the longitudinal cracking models was not calibrated. A summary of the local calibration coefficients suggested for Minnesota is shown in Table 21.

Table 21. Minnesota Local Calibration Coefficients[46]

Distress Model	Distress Type/Layer	Calibration Coefficient
Rutting	HMA, (β_{r1}, β_{r2}, β_{r3})	New Method proposed
	Granular Base, (β_{B1})	New Method proposed
	Subgrade, (β_{s1})	New Method proposed
Fatigue Cracking	HMA Fatigue Model, (β_{f1}, β_{f2} *and* β_{f3})	0.1903
	Bottom-Up Transfer Function (C_1, C_2)	Not calibrated
Transverse Cracking	HMA Non-Load Related (β_{s3})	1.85
IRI	Smoothness (C_1, C_2, C_3, C_4)	Not calibrated

North Carolina

In order to implement and calibrate MEPDG in North Carolina, 53 pavement sections were selected for the calibration/validation of rutting and alligator cracking distress models. These pavement sections consisted of 30 LTPP sections (16 new flexible and 14 rehabilitated sections), and 23 North Carolina Department of Transportation (NCDOT) sections. All the necessary data were obtained from the LTPP and the NCDOT databases. The *TrafLoad* software version 1.08 was used to obtain the vehicle classification, ALS and number of axles per truck data from the WIM raw data files (C-card and W-card) at or near the pavement sections used for the calibration[47]. To obtain the local calibration coefficients, it was assumed that the alligator damage model is an accurate simulation of actual field conditions. Thus, an iterative fitting process was used to minimize the sum of the squared errors of the predicted and measured cracking values (from the transfer function) by varying the C1 and C2 parameters. A summary of the local calibration factors developed for North Carolina is given in Table 22.[47, 48]

Table 22. North Carolina Local Calibration Coefficients[48]

Distress Model	Distress Type/Layer	Calibration Coefficient
Rutting	HMA, (β_{r1}, β_{r2}, β_{r3})	0.983, 1.00, 1.00
	Granular Base, (β_{B1})	1.58
	Subgrade, (β_{s1})	1.10
Fatigue Cracking	Fatigue Model, (β_{f1}, β_{f2} *and* β_{f3})	1.0, 1.0, 1.0
	Bottom-Up Transfer Function (C_1, C_2)	0.437, 0.150

South Dakota

The research effort for MEPDG implementation in South Dakota started with a sensitivity analysis of selected inputs related to 5 typical South Dakota Department of Transportation (SDDOT) pavement designs.[49] These sections contained 3 new construction designs (rural JPCP, rural AC, and continuously reinforced concrete pavement (CRCP) interstate) and 2 rehabilitation designs (AC overlay over existing rural AC and AC overlay over rubblized rural JPCP). MEPDG software (Version 0.9) was run to find the influence of changing selected MEPDG inputs on predicted distresses and IRI. Only results of the studies

related to flexible pavements and AC over AC overlays are presented in this report. A total number of 56 MEPDG simulation runs were conducted by varying key design inputs based on local South Dakota conditions on newly constructed flexible pavements. For the AC over AC pavement section, 78 MEPDG computer simulation runs were conducted by varying key design inputs based on local South Dakota conditions. Table 23 and Table 24 summarize the key design inputs that were found to have significant influence on the distress predictions for newly constructed and AC over an existing AC pavements, respectively. In addition to the conducted sensitivity analyses, the research team proposed a plan outlined the tasks needed by the SDDOT over 3-year period for successful implementation of the MEPDG.

Table 23. Summary of South Dakota Sensitive Input Parameters for New Flexible Pavements[49]

Performance Indicator	Input Parameter/Predictor
Longitudinal Cracking	AC Layer Thickness AADTT Base Resilient Modulus AC Binder Grade
Alligator Cracking	AADTT AC Binder Grade AC Layer Thickness Base Resilient Modulus
AC Rutting	Initial 2-way AADTT AC layer thickness AC binder grade Location (climate)
Total Rutting	AADTT AC Layer Thickness Subgrade Resilient Modulus GWT AC Binder Grade Base Resilient Modulus
IRI	Alligator Cracking Total Rutting

Table 24. Summary of South Dakota Sensitive Input Parameters for AC Over Existing AC Pavements[49]

Performance Indicator	Input Parameter/Predictor
Longitudinal Cracking	AC Overlay Binder Grade AADTT Base Resilient Modulus Existing AC Pavement Rating
Alligator Cracking	Existing AC Pavement Rating Existing AC binder grade
Reflective Cracking	Existing AC Pavement Rating AC Overlay Thickness
AC Rutting	AADTT AC Overlay Thickness Existing AC Pavement Rating Climate (Location) AC Overlay Binder Grade Total Rutting in Existing Pavement
Total Rutting	Total Rutting in Existing AC Pavement AADTT AC Overlay Thickness
IRI	Total Rutting

Virginia

Virginia is one of the lead states who had MEPDG implementation and local calibration plans in place. Virginia Tech Transportation Institute (VTTI) established a research project focusing on the characterization of fundamental engineering properties of asphalt paving mixtures used in Virginia.[50] This objective was achieved by collecting and testing loose samples of 11 HMA mixes (3 surface, 4 intermediate, and 4 base mixes) from different plants across Virginia. Maximum theoretical specific gravity, asphalt content using the ignition oven method, and gradation of the reclaimed aggregate tests were applied on representative samples. Specimens were prepared for various tests using Superpave Gyratory Compactor (SGC) with target air voids of (7 ± 1 percent) after coring and cutting process. The project examined E*, creep compliance, and tensile strength of the investigated mixes. In addition, the resilient modulus test, which is not required by the MEPDG, was performed on different mixes to investigate any possible correlations with E*. The testing results confirmed that E* is the effective way to fully characterize the mechanical behavior of HMA at different temperatures and loading frequencies. E* was found susceptible to the mix ingredients (aggregate type, aggregate gradation, asphalt content, etc.). Based on the results of the investigation, it was recommended that the Virginia Department of Transportation (VDOT) use Level 1 input data to characterize E* of the HMA for the most significant projects. Levels 2 and 3 dynamic modulus prediction equation reasonably estimated the measured E*. The research team concluded that they could be used for smaller projects. The research team also recommended quantifying the effect of changing the dynamic modulus on the asphalt pavement design by performing a sensitivity analysis. Since the indirect tension strength and creep tests needed for low-temperature cracking model did not produce any reasonable results, level 2 or 3 was recommended to be used.

MEPDG States Implementation Summary

Based on the presented review of the SHAs implementation and calibration activities of the MEPDG it can be concluded that, for successful MEPDG implementation, a comprehensive input database (input libraries) for material characterization, traffic, and climate should be established. In addition, distress prediction models should be locally calibrated based on the state conditions for more accurate and less biased predictions. Defining the sensitivity of each input and establishing reasonable ranges based on local conditions for each design key inputs are extremely important. Moreover, training pavement designers on the software is a very important task toward a successful MEPDG implementation. From the presented literature review, the following can also be highlighted:

- Traffic ALS can be characterized using data collected at WIM sites. However, the quality of the data should be assessed and the WIM stations should be calibrated regularly.
- Some SHAs used the *TrafLoad* software for processing the WIM data to be used with the MEPDG. Other states reported problems opening the WIM data files with this software and therefore they developed their own software to analyze WIM data and generate required traffic inputs for MEPDG.
- Although level input 1 is the most accurate input data level, many of the SHAs have used levels 2 and 3 data inputs for traffic and material characterization as this is the level of data usually available.
- All SHAs used the default weather station climatic database that comes with the software for climatic characterization.
- Pavement performance data measured accurately over time in a manner consistent with MEPDG requirements is essential for implementation and local calibration of the guide. Many state DOTs have pavement management data containing cracking and rutting. However, the way that the pavement distresses are measured by many of the state DOTs (including ITD) is inconsistent with the MEPDG recommended method.

Many SHAs performed sensitivity analyses to study and determine the key inputs that significantly affect the performance of new flexible pavements based on local pavement conditions. In general, the most significant design inputs based on many sensitivity analyses found in literature are summarized in

- Table 25.[29, 35, 43, 49, 51, 52, 52, 53]
- Many SHAs developed local calibration coefficients (adjustment factors) for the MEPDG distress models based on their specific conditions as a part of the implementation efforts of the design guide. A summary of the local calibration coefficients for rutting, fatigue cracking (alligator and longitudinal), thermal cracking, and IRI prediction models developed for different states are shown in Table 26 through Table 29, respectively.

Table 25. Summary of Very Significant to Significant Key Design Input Parameters for New Flexible Pavements

Performance Indicator	Input Parameter/Predictor
Longitudinal Cracking	AADTT AC Layer Thickness AC Binder Grade Effective Asphalt Content AC Mixture In-Situ Air Voids AC Mixture Stiffness Foundation Quality Environmental Location
Alligator Cracking	AADTT AC Binder Grade Effective Asphalt Content AC Mixture In-Situ Air Voids AC Layer Thickness AC Mixture Stiffness (Insignificant at Very Thick AC Layers) Foundation Quality Environmental Location
AC Rutting	AADTT AC Mixture Stiffness AC Layer Thickness AC Binder Grade AC Mixture In-Situ Air Voids Environmental Location
Total Rutting	AADTT Total Pavement Thickness GWT AC Binder Grade Foundation Quality Base Resilient Modulus Climatic Location
Transverse Cracking	AC Thickness AC Binder Grade AC Mixture In-Situ Air Voids AC Mixture Tensile Strength Environmental Location
IRI	Alligator Cracking Total Rutting Environmental Location Initial IRI

Table 26. Summary of Local Calibration Factors for the MEDPG Rutting Model

State		HMA			Granular Base	Subgrade
		β_{r1}	β_{r2}	β_{r3}	β_{B1}	β_{s1}
Utah		0.56	1.00*	1.00*	0.604	0.40
Montana		New Method Proposed			0.20	0.20
Washington		1.05	1.109	1.10	1.00*	0.00
Arizona		3.63	1.10	0.70	0.111	1.38
Arkansas		1.20	1.00*	0.80	1.0*	0.50
Kansas	**Conventional Pavements**	1.50	0.90	1.00*	0.50	0.50
	PMA Pavements	2.50	1.15	1.00*	0.50	0.50
	Superpave Pavements	1.50	1.20	1.00*	0.50	0.50
Minnesota		New Method Proposed				
N. Carolina		0.983	1.00*	1.00*	1.58	1.10

*Default global (national) calibration value

Table 27. Summary of Local Calibration Factors for the MEDPG Fatigue Model

State		HMA Fatigue Model			HMA Bottom-Up Transfer function		HMA Top-Down Transfer Function	
		β_{f1}	β_{f2}	β_{f2}	C_1	C_2	C_1	C_2
Utah		1.00*	1.00*	1.00*	1.00*	1.00*	7.00*	3.50*
Montana		1.00*	1.00*	1.00*	New Method Proposed		7.00*	3.50*
Washington		0.96	0.97	1.03	1.071	1.00*	6.42	3.596
Arizona		0.729	0.8	0.8	0.732	0.732	1.607	0.803
Arkansas		1.00*	1.00*	1.00*	0.688	0.294	3.016	0.216
Kansas	**Conventional Pavements**	0.05	1.00*	1.00*	1.00*	1.00*	-	-
	PMA Pavements	0.005	1.00*	1.00*	1.00*	1.00*	-	-
	Superpave pavements	0.0005	1.00*	1.00*	1.00*	1.00*	-	-
Minnesota		0.1903	1.00*	1.00*	1.00*	1.00*	-	-
N. Carolina		1.00*	1.00*	1.00*	0.437	0.15	-	-

*Default global (national) calibration value
- Not calibrated

Table 28. Summary of Local Calibration Factors for the MEDPG Transverse Cracking Model

State		Calibration Factor (β_{s3})
Utah		-
Montana		0.25
Washington		-
Arizona		-
Arkansas		-
Kansas	Conventional Pavements	2
	PMA Pavements	2
	Superpave pavements	3.5
Minnesota		1.85
N. Carolina		-

- Not calibrated

Table 29. Summary of Local Calibration Factors for the MEDPG IRI Model

Calibration Coefficients		C_1	C_2	C_3	C_4
Utah		40*	0.4*	0.008*	0.015*
Montana		40*	0.4*	0.008*	0.015*
Washington		-	-	-	-
Arizona		5.455	0.354	0.008	0.015
Arkansas		-	-	-	-
Kansas	Conventional Pavements	40*	0.4*	0.008*	0.015*
	PMA Pavements	40*	0.4*	0.008*	0.015*
	Superpave pavements	40*	0.4*	0.008*	0.015*
Minnesota		-	-	-	-
N. Carolina		-	-	-	-

*Default global (national) calibration value
- Not calibrated

Chapter 4
HMA Material Characterization

Introduction

The most important hot-mix asphalt (HMA) property influencing the structural response of flexible pavements is the HMA dynamic modulus. It is the primary stiffness property for the characterization of HMA in all of the hierarchical input levels of MEPDG. Critical stresses, strains, and deflections in the AC layer(s) are calculated as a function of E* using the pavement response model incorporated in MEPDG software.

This chapter presents the laboratory tests and analyses conducted on different HMA mixes commonly used by ITD in pavement construction projects in Idaho to establish database for HMA material characterization. This database covers all 3 input levels, in MEPDG, for HMA characterization. The experimental laboratory work is comprised of both binder and mix investigation. Laboratory testing results were also used to investigate the prediction accuracy of the MEPDG E* predictive models as well as Hirsch and Idaho models. In addition, the influence of the binder input level on the MEPDG E* predictive models is investigated.

HMA Hierarchical Input Levels

As previously explained, for HMA material characterization, MEPDG has 3 different levels of input data. For HMA characterization, level 1 input data requires conducting E* laboratory tests at different loading frequencies and temperatures. The laboratory measurements are used by the software to develop the E* master curve. Once the master curve is established, E* at any given temperature and loading frequency (vehicle speed) can then be calculated. MEPDG both levels 2 and 3 input data do not require E* testing. E* at any temperature and loading frequency can be obtained directly from built-in predictive models. The software utilizes 2 different E* predictive models (NCHRP 1-37A viscosity (η)-based and NCHRP 1-40D binder shear modulus (G*)-based models) according to users selection. Figure 21 represents a flow chart of how HMA materials are characterized according to MEPDG input level.[4]

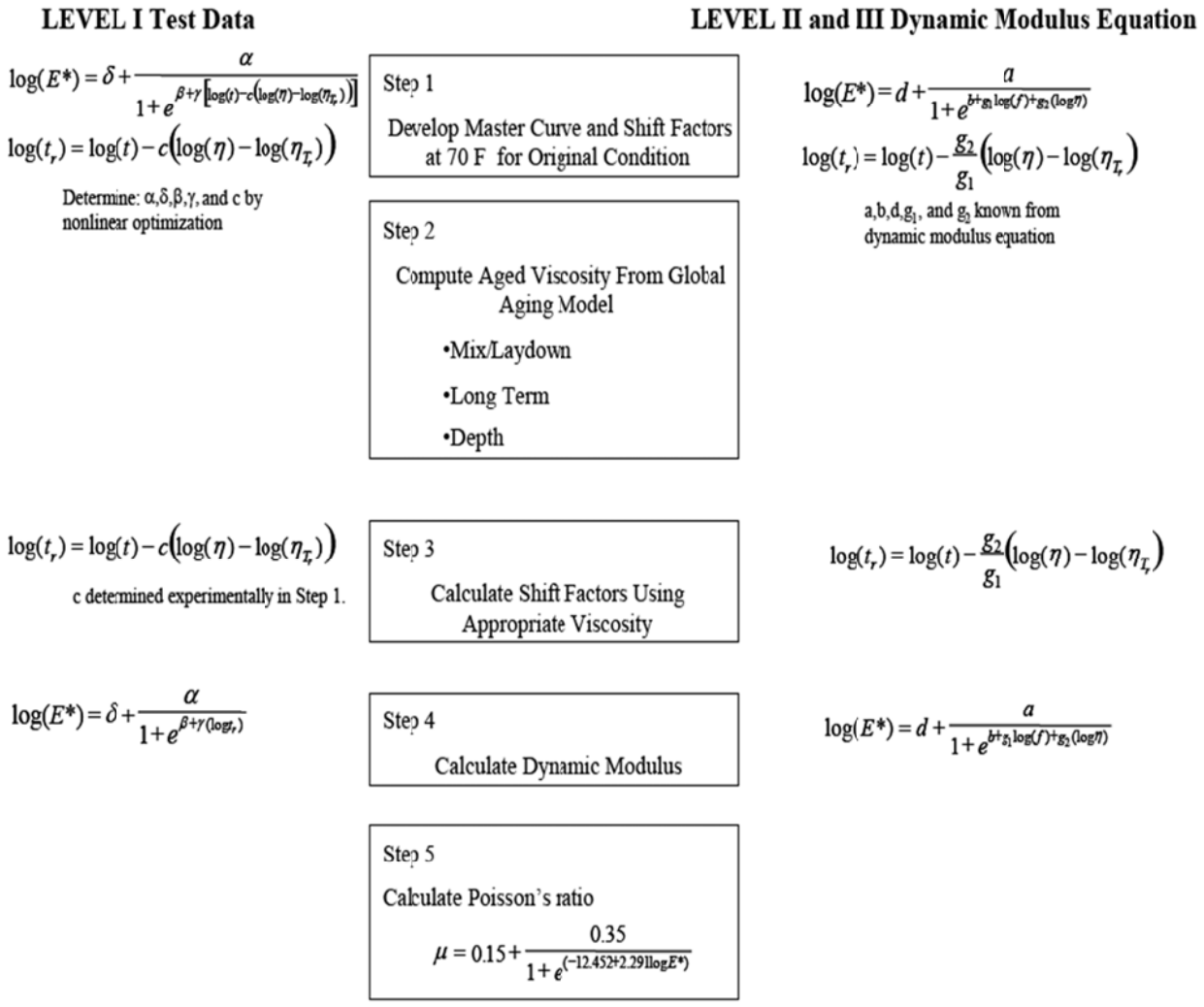

Figure 21. HMA Material Characterization Flow Chart[(4)]

For MEPDG binder characterization, there are also 3 input levels. For Superpave performance grade binders, level 1 (same as level 2) inputs requires DSR test results at angular frequency (ω = 10 rad/sec) over a range of temperatures. For conventional binder grading systems, level 1 input data requires conventional binder testing results such as penetration at 25 ^{o}C, ring and ball softening point, absolute and kinematic viscosities, and Brookfield viscosity. For level 3 binder inputs, users are only asked to select either the Performance Grade (PG) for superpave binders, or viscosity or penetration grade for conventional binders. The MEPDG required input data for the HMA material characterization at the different input levels are summarized in Table 30.

Table 30. MEPDG Required Inputs at the Different Hierarchical Levels[4]

HMA Components	Asphalt Material Properties		
	Level 1	Level 2	Level 3
Aggregate		Cumulative % Retained 3/4 inch Sieve	Cumulative % Retained 3/4 inch Sieve
		Cumulative % Retained 3/8 inch Sieve	Cumulative % Retained 3/8 inch Sieve
		Cumulative % Retained #4 sieve	Cumulative % Retained #4 sieve
		% Passing # 200 Sieve	% Passing # 200 Sieve
Asphalt Binder	Dynamic Shear Modulus (Pa) and Phase Angle (°) at ω = 10 rad/sec or Conventional Binder Tests	Dynamic Shear Modulus (Pa) and Phase Angle (°) at ω = 10 rad/sec or Conventional Binder Tests	Binder Performance Grade
Asphalt Mix	% Effective Binder Content by Volume	% Effective Binder Content by Volume	% Effective Binder Content by Volume
	% Air Voids	% Air Voids	% Air Voids
	Total Unit Weight (pcf)	Total Unit Weight (pcf)	Total Unit Weight (pcf)
	Measured E* values at Different Temperatures and Frequencies (psi)		

MEPDG E* Predictive Models

If users choose either level 2 or level 3 HMA characterization, then MEPDG uses one of 2 different E* predictive models according to the user selection. Both MEPDG E* models were developed by Witczak and his colleagues. Details of these models are presented next.

NCHRP 1-37A Viscosity-based E* Model

This model was implemented in the first version of MEPDG (Version 0.7). It was developed based on 2750 measured E* data points from 205 different HMA mixtures, including modified and unmodified binders, that have been periodically collected by Witczak and his colleagues since 1969.[54] It predicts E* at different temperatures as a function of the mix aggregate gradation, volumetric properties, loading frequency and binder viscosity. The model is presented in Figure 22.

$$\log_{10} E^* = -1.249937 + 0.02923\rho_{200} - 0.001767(\rho_{200})^2 - 0.002841\rho_4 - 0.058097V_a$$
$$-0.82208\frac{V_{beff}}{V_{beff}+V_a} + \frac{3.871977 - 0.0021\rho_4 + 0.003958\rho_{38} - 0.000017(\rho_{38})^2 + 0.00547\rho_{34}}{1+e^{(-0.603313-0.313351\log f-0.393532\log\eta)}}$$

where:

E^* = HMA dynamic modulus, 10^5 psi
η = Binder viscosity at the age and temperature of interest, 10^6 poise
f = Loading frequency, Hz
V_a = Percent air voids in the mix, by volume
V_{beff} = Percent effective binder content, by volume
ρ_{34} = Percent cumulative retained weight on the ¾ in. sieve, by total aggregate weight
ρ_{38} = Percent cumulative retained weight on the 3/8 in. sieve, by total aggregate weight
ρ_4 = Percent cumulative retained weight on the # 4 sieve, by total aggregate weight
ρ_{200} = Percent passing No. 200 sieve

Figure 22. NCHRP 1-37A Viscosity Based E* Model[4, 54]

The main disadvantage of the 1-37A model presented above is that it characterizes the binder in terms of conventional viscosity rather than the shear modulus and phase angle of the binder.[55, 57] The binder G* and δ are commonly used as a part of the superpave performance grade (PG) binder specification.

NCHRP 1-40D G*-based E* Model

In order to overcome the disadvantage of the NCHRP 1-37A model concerning binder characterization, the MEPDG flexible pavement research team incorporated, in addition to the 1-37A model, another E* predictive model which characterizes the binder in terms of G* and δ. This was done as a part of the NCHRP 1-40D (02) project which is the Technical Assistance to NCHRP and NCHRP Project 1-40A: Versions 0.9 and 1.0 of the M-E Pavement Design Software.[12] This model is a modified version of the Bari and Witczak's E* predictive model originally developed in 2005.[12, 16, 17] It was implemented in the MPEDG since Version 1.0. The E* database used in this model development contains 7400 data points from 346 mixtures. This database included the data used for the development of the 1-37A model. The model is presented in Figure 23.

$$\log_{10} E^* = 0.02 + 0.758\left(|G_b^*|^{-0.0009}\right)\times\left(\begin{array}{l}6.8232 - 0.03274\rho_{200} + 0.00431\rho_{200}^{\ 2} + 0.0104\rho_4 - 0.00012\rho_4^{\ 2} \\ + 0.00678\rho_{38} - 0.00016\rho_{38}^{\ 2} - 0.0796V_a - 1.1689\left(\frac{V_{beff}}{V_a + V_{beff}}\right)\end{array}\right)$$
$$+\frac{1.437 + 0.03313V_a + 0.6926\left(\frac{V_{beff}}{V_a + V_{beff}}\right) + 0.00891\rho_{38} - 0.00007\rho_{38}^{\ 2} - 0.0081\rho_{34}}{1 + e^{(-4.5868 - 0.8176\log|G_b^*| + 3.2738\log\delta)}}$$

where:

$|G_b^*|$ =Dynamic shear modulus of binder (G*), psi

δ = Phase angle of the binder, degrees

All other variables are as previously defined in Figure 22.

Figure 23. NCHRP 1-40D G*-based E* Model[12]

Comparison of MEPDG 1-37A and 1-40D E* Predictive Models

Both MEPDG 1-37A and 1-40D models predict E* of HMA as a function of mix volumetric properties, mix aggregate gradation, and binder stiffness parameter. Both Witczak models follow the form of a sigmoid function. The main disadvantage of the 1-37A model is that is characterizes the binder stiffness in terms of conventional viscosity. The 1-40D model expresses it in terms of binder shear modulus and phase angle. Further, the 1-40D model was developed based on a larger database compared to the 1-37A model. The1-37A model database only contained lab blended mixtures that were not short term aged, while the 1-40D database contained non-aged, short term oven aged for 4 hours at 135 ^{o}C, plant mixes, asphalt rubber mixes, and field cores.[17] Table 31 presents a comparison of the goodness-of-fit statistics of the investigated models based on the original database used for each model development. The goodness-of-fit statistics shown in this table are the coefficient of determination (R^2) and the standard error divided by the standard deviation of measured E* values about the mean (S_e/S_y). It is clear from the tabular data that both models have "excellent" goodness-of-fit statistics, based on the original database used for each model development.

Table 31. Goodness-of-Fit Statistics of Witczak E* Predictive Models based on Original Data used for the Development of the Models[4, 12, 58]

	1-37A Model	1-40D Model
Total Number of Mixes	205	346
Number of E* Measurements	2750	7400
Goodness-of-Fit in Logarithmic Scale		
S_e/S_y	0.24	0.30
R^2	0.94	0.91

MEPDG E* Prediction Methodology

As discussed before, the presented E* predictive models are function of the binder characteristics. There are 2 levels of binder inputs in MEPDG; level 1 and level 3 (level 2 is the same as level 1). For level 1 binder characterization, MEPDG requires the G* and δ of the binder (aged at RTFO condition) at different temperatures and one angular frequency of 10 rad/sec. The software then uses the relationship shown in Figure 24 to compute the viscosity at different temperatures as a function of G* and δ.[4, 58, 59]

$$\eta = \frac{G^*}{10}\left(\frac{1}{\sin\delta}\right)^{4.8628}$$

where:

G^* = Binder complex shear modulus, Pa
η = Binder viscosity, Pa.s
δ = Binder phase angle, degree

Figure 24. Determination of Viscosity from Binder Shear Modulus and Phase Angle

Consequently, the ASTM D2493 viscosity-temperature relationship is established as shown in Figure 25.

$$\log\log\eta = A + VTS\log T_R$$

where:

η = Binder viscosity, cP
T_R = Testing temperature, Rankine
A = Regression intercept
VTS = Regression slope of the viscosity-temperature susceptibility

Figure 25. ASTM D2493 Viscosity-Temperature Relationship[60]

The A and VTS parameters in Figure 25 are determined by conducting linear regression on the viscosity-temperature data. The above relationship is then used directly to estimate the binder viscosity at the temperature of interest and then use the 1-37A model (Figure 22) for E* computation. For the 1-40D model, once the A and VTS are determined, the set of equations shown in Figure 26 are used to compute G* and δ at the temperature and frequency of interest in order to compute the E* at these temperatures and frequencies.

$$\log\log \eta_{f_s,T} = A' + VTS' \log T_R$$

$$A' = 0.9699 * f_s^{-0.0527} * A$$

$$VTS' = 0.9668 * f_s^{-0.0575} * VTS$$

$$f_s = f_c / 2\pi$$

$$\delta_b = 90 - 0.1785 * \log(\eta_{f_s,T})^{2.3814} * (f_s)^{(0.3507 + 0.0782 VTS)}$$

$$|G_b^*| = 1.469 * 10^{-9} * \log(\eta_{f_s,T})^{12.0056} * f_s^{0.7418} (\sin \delta)^{0.6806}$$

where:

f_c = Loading frequency in dynamic compression loading mode as used in the E* testing, Hz
f_s = Loading frequency in dynamic shear loading mode as used in the G_b* testing, Hz
A' = Adjusted "A" (adjusted for loading frequency)
VTS' = Adjusted "VTS" (adjusted for loading frequency)
$\eta_{fs,T}$ = Binder viscosity as a function of both loading frequency (f_s) and temperature (T_R), cP
δ = Binder phase angle, degree
G^* = Complex binder shear modulus, Pa

Figure 26. Equations to Estimate G* and δ[12, 58, 59]

The set of equations presented in Figure 26 were developed based on asphalt binder properties database containing 8940 data points from 41 different virgin and modified asphalt binders.[12, 17] Finally, E* at any temperature and frequency of interest can then be calculated using the 1-40D model shown in Figure 23. It must be noted that the NCHRP 1-40 D G*-based E* predictive model was developed based on estimated, rather than laboratory measured, G* and δ at the same temperature and frequency of E* from default A and VTS values (based on conventional binder characterization testing).

For Level 3, binder input, the program uses its internal default values of A and VTS for the selected binder grade. Then it follows the previous procedure explained for level 1 binder characterization to predict E* either from the NCHRP 1-37A model or the NCHRP 1-40D model as selected by the user.

In summary, the above analysis indicates that the E* prediction methodology, in MEPDG, using either the 1-37A or 1-40D E* predictive models, is based on the A-VTS regression parameters from binder characterization. The 1-37A model, estimates the binder viscosity as a function of temperature (no influence of frequency on binder viscosity) through the ASTM equation shown in Figure 25. On the other hand, the 1-40D model estimates G* and δ at different temperatures and frequencies form A and VTS through the series of regression equations presented in Figure 26. It is important to note that the A and VTS used in the development of both E* predictive models are the default values in the MEDPG which were based on conventional viscosity binder testing data. Some researchers questioned the validity of the

typical (default) A and VTS values in MEPDG to superpave performance grade binders, since the superpave binders use DSR data.[58, 59, 61, 62, 63]

Investigated Mixtures

In coordination with ITD, 27 different plant-produced HMA mixtures widely used in flexible pavement construction in Idaho were recruited from ITD for the purpose of establishing HMA material characterization for MEPDG implementation. All these mixtures were designed according to the ITD superpave mixture requirements illustrated in Table 32. These mixes cover the 6 various Superpave specifications in the state of Idaho. The investigated mixtures contain 6 different superpave performance grade binder types (PG58-28, PG58-34, PG64-28, PG 64-34, PG70-28, and PG 76-28), varied mix aggregate gradation, and mix volumetric properties.

Properties of the Investigated Mixtures

Table 33 presents a list of the field mixtures investigated along with the project that each mixture belongs to, project number, and key number. It should be noted that, out of the 27 investigated mixtures, 7 mixtures were extracted from the database of ITD Project No. RP 181.[64] Table 34 lists the gradations, volumetric properties, design number of gyrations, and the binder PG grades extracted for the Job Mix Formula (JMF) reports of these mixes. In this table it can be seen that the SP3-5 mix was split into 5 mixes (SP3-5-1, SP3-5-2, SP3-5-3, SP3-5-4, and SP3-5-5). This was due to the small variation in the asphalt content between these mixes.

Table 32. ITD Superpave Mixture Requirements

ITD Mixture Type	SP1	SP2	SP3	SP4	SP5	SP6
Design ESALs [a] (millions)	< 0.3	0.3 -< 1	1 -< 3	3 -< 10	10 - < 30	≥ 30
LA Wear (AASHTO T96) Max % loss	40	35	30	30	30	30
Fractured Face, Coarse Aggregate [b] % Minimum	50/-	65/-	75/60	85/80	95/90	100/100
Uncompacted Void Content of Fine Aggregate % Minimum	--	40	40	45	45	45
Sand Equivalent, % Minimum	35	35	40	45	45	50
Flat and Elongated [c] % Maximum	--	10	10	10	10	10
Gyratory Compaction:						
Gyrations for Nini	6	6	7	8	8	9
Gyrations for Ndes	40	50	75	90	100	125
Gyrations for Nmax	60	75	115	160	160	205
Relative Density, %Gmm@Nini	<91.5	≤ 90.5	≤89.0	≤89.0	≤89.0	≤89.0
Relative Density, %Gmm@ Ndes	96.0	96.0	96.0	96.0	96.0	96.0
Relative Density, %Gmm@Nmax	≤98.0	≤98.0	≤98.0	≤98.0	≤98.0	≤98.0
Air Voids, %	4.0	4.0	4.0	4.0	4.0	4.0
Dust to Binder Ratio [f] Range*	0.6-1.2	0.6-1.2	0.6-1.2	0.6-1.2	0.6-1.2	0.6-1.2
Voids Filled with Asphalt [e] Range, Percent	70-80	65-78	65-75	65-75	65-75	65-75

a The anticipated project traffic level expected on the design lane over a 20-year period.

b 85/80 denotes that 85 percent of the coarse aggregate has one fractured face and 80 percent has 2 or more fractured faces.

c This criterion does not apply to No. 4 nominal maximum size mixtures.

d A 2 percent tolerance will be allowed for coarse aggregate having 100% 2 or more fractured faces.

e For 1 1/2" nominal maximum size mixtures, the specified lower limit of the VFA shall be 64% for all design traffic levels.

f For No. 4 nominal maximum size mixtures, the dust-to-binder ratio shall be 0.9 to 2.0

g For 1 inch nominal maximum size mixtures, the specified lower limit of the VFA shall be 67% for design traffic levels of < 0.3 million ESALs.

h For design traffic levels of > 3 million ESALS, 3/8" nominal maximum size mixtures, the specified VFA range shall be 73% to 76 % and for No. 4 nominal maximum size mixtures shall be 75 to 78%.

Table 33. Investigated Mixtures

Mix ID	Project ID	Project #	Key#	ITD Class
SP1-1	STC-3840, Ola Highway, Kirkpatrick Rd North	A 011(945)	11945	SP1
SP2-1	Cat Cr. Sum-mit to MP 129 to Camas Co.	A 009(867)	9864 & 9867	SP2
SP2-2 *	Washington State Line to US 95/SH6	S07209A	8883	SP2
SP3-1	Sage JCT to Debois, SBL	A 010(010)	10010	SP3
SP3-2	JCT US-26 to Bonneville Co. Ln.	STP 6420(106)	9239	SP3
SP3-3	Bellevue to Hailey	A 009(865)	9865	SP3
SP3-4	Rigby North & South US-20	NH 6470(134)	9005	SP3
SP3-5	Oak Street, Nez Perce	ST 4749(612)	9338	SP3
SP3-6 *	Topaz to Lava Hot Springs	NH A010(455)	10455	SP3
SP3-7 *	Lapwai to Spalding	NH 4110(144)	8353	SP3
SP3-8 *	US 20 MP 112.90 to MP 124.63	NH 3340(109)	9106	SP3
SP3-9 *	Pullman to Idaho State Line, WA 270 (1/2 inch Mix)	01A-G71985(270)	7120	SP3
SP3-10 *	Pullman to Idaho State Line, WA 270 (1 inch Mix)	01B-G71974(270)	7120	SP3
SP4-1	Broadway Ave. Rossi St. to Ridenbaugh Cnl. Br.	A 009(812)	9812	SP4
SP4-2	Cleft to Sebree	A 010(533)	10533	SP4
SP4-3	Alton Road to MP 454 / Dingle	NH 1480(127)	9543	SP4
SP4-4 *	Jerome IC	IM 84-3(074)165	8896	SP4
SP5-1	Ten Mile Rd to Meridian IC, Reconstruction	A 0011(003)	11003	SP5
SP5-2	Deep Creek to Devil Creek IC	A 011(094)	11094	SP5
SP5-3	EP Ramps to Fairview Ave.	A 010(527)	10527	SP5
SP5-4	Moscow Mountain Passing Ln.	A 011(031)	11031	SP5
SP6-1	Burley to Declo & Heyburn IC O'Pass	IM 84-3(071)211	9219	SP6
SP6-2	Garrity Br IC & 11th Ave to Garrity	A 010(915) & A 011(974)	10915 & 11974	SP6

* Field mixtures extracted from the database of ITD Project No RP 181 “Development and Evaluation of Performance Tests to Enhance Superpave Mix Design and its Implementation in Idaho”.

Table 34. Job Mix Formula of the Investigated Field Mixtures

Mix ID	SP1-1	SP2-1	SP2-2	SP3-1	SP3-2	SP3-3	SP3-4
Project ID	STC-3840, Ola Highway, Kirkpatrick Rd North	Cat Cr. Sum-mit to MP 129 to Camas Co.	Washington State Line to US 95/SH6	Sage JCTto Debois, SBL	JCT US-26 to Bonneville Co. Ln.	Bellevue to Hailey	Rigby North & South US-20
Project #	A 011(945)	A 009(867)	S07209A	A 010(010)	Stp 6420(106)	A 009(865)	NH 6470(134)
Key#	11945	9864 & 9867	8883	10010	9239	9865	9005
Class	SP1	SP2	SP2	SP3	SP3	SP3	SP3
ESALs (millions)	< 0.3	0.3 -< 1	0.3 -< 1	1 -< 3	1 -< 3	1 -< 3	1 -< 3
N-Design	40	50	50	75	75	75	75
Mix Properties							
G_{mm}	2.393	2.408	2.510	2.453	2.429	2.421	2.437
G_{mb}	2.273	2.312	2.321	2.343	2.317	2.323	2.342
P_b (% by Mix Wt.)	6.40	5.93	6.10	5.55	5.30	5.37	4.95
VMA, %	16.5	14.9	18.2	15.2	14.4	14.6	14.6
Va, %	4.0	4.2	3.7	4.0	3.9	4.4	4.0
VFA, %	76.0	73.2	78.0	74.0	72.2	73.0	72.5
Binder Properties							
PG	58-28	58-28	58-34	64-28	64-28	58-28	70-28
G_b	1.024	1.029	1.009	1.032	1.032	1.034	1.035
Mixing Temp., °F	305	302	318	325	325	290	325
Comp. Temp., °F	285	280	290	292	295	277	305
Aggregates Properties							
G_{sb}	2.549	2.556	2.731	2.611	2.562	2.575	2.607
G_{se}	2.601	2.630	2.744	2.653	2.608	2.619	2.626
Absorption, %	1.4	1.9	1.7	1.4	2.1	1.5	0.6
% Passing, Sieves							
25mm (1")	100	100	100	100	100	100	100
19mm (3/4")	100	100	100	100	100	100	99
12.5mm (1/2")	98	99	95	93	83	81	89
9.5mm (3/8")	86	86	78	79	70	69	73
4.75mm (#4)	54	57	53	56	48	46	46
2.36mm (#8)	39	39	35	38	31	29	29
1.18mm (#16)	29	27	22	25	21	20	20
600µm (#30)	21	18	15	15	15	15	15
300µm (#50)	13	11	12	10	10	11	12
150µm (#100)	8	7	9	6	7	7	8
75µm (#200)	5.2	5.1	6.8	4.1	4.9	5.2	4.8

G_{mm} = maximum theoretical specific gravity, G_{mb} = bulk specific gravity of mix, P_b = percent asphalt content by mix weight, VMA = voids in mineral aggregate, Va = percent air voids, VFA = voids filled with binder, PG = binder performance grade, G_b = specific gravity of binder, G_{sb} = bulk specific gravity of aggregate, and G_{se} = effective specific gravity of aggregate.

Table 34. Job Mix Formula for the Investigated Field Mixtures *(continued)*

Mix ID	SP3-5-1	SP3-5-2	SP3-5-3	SP3-5-4	SP3-5-5	SP3-6	SP3-7
Project ID	Oak Street, Nez Perce	Oak Street, Nez Perce	Oak Street, Nez Perce	Oak Street, Nez Perce	Oak Street, Nez Perce	Topaz to Lava Hot Springs	Lapwai to Spalding
Project #	ST 4749(612)	ST 4749(612)	ST 4749(612)	ST 4749(612)	ST 4749(612)	NH A010(455)	NH 4110(144)
Key#	9338	9338	9338	9338	9338	10455	8353
Class	SP3	SP3	SP3	SP3	SP3	SP3	SP3
ESALs (millions)	1 -< 3	1 -< 3	1 -< 3	1 -< 3	1 -< 3	1 -< 3	1 -< 3
N-Design	75	75	75	75	75	75	75
Mix Properties							
G_{mm}	2.599	2.599	2.599	2.599	2.599	2.408	2.586
G_{mb}	2.483	2.478	2.507	2.497	2.484	2.229	2.413
P_b (% by Mix Wt.)	5.99	5.98	5.82	5.60	6.11	4.49	5.70
VMA, %	16.1	16.3	15.1	15.3	16.2	13.4	15.9
Va, %	4.0	4.0	4.0	4.0	4.0	3.4	3.3
VFA, %	72.0	72.3	76.9	74.5	72.8	67.1	75.0
Binder Properties							
PG	58-28	58-28	58-28	58-28	58-28	64-34	70-28
G_b	1.034	1.034	1.034	1.034	1.034	1.025	1.034
Mixing Temp., °F	300	300	300	300	300	335	323
Comp. Temp., °F	280	280	280	280	280	307	293
Aggregates Properties							
G_{sb}	2.782	2.782	2.782	2.782	2.782	2.553	2.771
G_{se}	2.860	2.860	2.860	2.860	2.860	2.568	2.808
Absorption, %	1.9	1.9	1.9	1.9	1.9	1.5	1.9
% Passing, Sieves							
25mm (1")	100	100	100	100	100	100	100
19mm (3/4")	100	100	100	100	100	100	97
12.5mm (1/2")	96	96	96	96	96	83	83
9.5mm (3/8")	85	85	85	85	85	65	71
4.75mm (#4)	55	55	55	55	55	37	51
2.36mm (#8)	37	37	37	37	37	25	34
1.18mm (#16)	24	24	24	24	24	18	23
600µm (#30)	17	17	17	17	17	14	16
300µm (#50)	14	14	14	14	14	11	11
150µm (#100)	10	10	10	10	10	7	8
75µm (#200)	8.2	8.2	8.2	8.2	8.2	4.7	5.9

Table 34. Job Mix Formula for the Investigated Field Mixtures *(continued)*

Mix ID	SP3-8	SP3-9	SP3-10	SP4-1	SP4-2	SP4-3	SP4-4
Project ID	US 20 MP 112.90 to MP 124.63	Pullman to Idaho State Line, WA 270 (1/2 inch Mix)	Pullman to Idaho State Line, WA 270 (1 inch Mix)	Broadway Ave. Rossi St. to Ridenbaugh Cnl. Br.	Cleft to Sebree	Alton Road to MP 454 / Dingle	Jerome IC
Project #	NH 3340(109)	01A-G71985(270)	01B-G71974(270)	A 009(812)	A 010(533)	NH 1480(127)	IM 84-3(074)165
Key#	9106	7120	7120	9812	10533	9543	8896
Class	SP3	SP3	SP3	SP4	SP4	SP4	SP4
ESALs (millions)	1 -< 3	1 -< 3	1 -< 3	3 < 10	3 < 10	3 < 10	3 < 10
N-Design	75	75	75	100	100	100	100
Mix Properties							
G_{mm}	2.458	2.581	2.460	2.434	2.435	2.462	2.442
G_{mb}	2.283	2.417	2.274	2.328	2.315	2.339	2.273
P_b (% by Mix Wt.)	4.90	5.90	5.10	5.31	5.70	5.10	4.80
VMA, %	13.9	16.7	14.9	14.6	15.0	14.7	13.6
Va, %	4.3	3.8	4.5	4.0	4.4	4.1	4.1
VFA, %	71.2	68.0	81.0	73.0	73.3	72.8	70.6
Binder Properties							
PG	70-28	70-28	70-28	70-28	76-28	64-34	70-28
G_b	1.021	1.036	1.036	1.021	1.019	1.028	1.021
Mixing Temp., °F	330	328	328	333	345	329	330
Comp. Temp., °F	305	305	305	305	315	297	305
Aggregates Properties							
G_{sb}	2.589	2.822	2.822	2.582	2.567	2.604	2.586
G_{se}	2.648	2.847	2.656	2.626	2.628	2.631	2.639
Absorption, %	1.9	1.4	1.7	1.1	1.3	1.3	1.3
% Passing, Sieves							
25mm (1")	100	100	98	100	100	100	98
19mm (3/4")	100	100	90	100	100	100	86
12.5mm (1/2")	79	96	74	82	99	84	73
9.5mm (3/8")	66	87	66	70	86	70	64
4.75mm (#4)	45	58	40	50	56	40	41
2.36mm (#8)	32	36	25	33	39	25	27
1.18mm (#16)	23	22	16	23	27	15	18
600µm (#30)	16	17	12	16	18	11	13
300µm (#50)	9	13	10	10	11	9	10
150µm (#100)	5	8	7	7	8	6	5
75µm (#200)	4	6.4	5.7	4.7	5.4	4.6	4

Table 34. Job Mix Formula for the Investigated Field Mixtures *(continued)*

Mix ID	SP5-1	SP5-2	SP5-3	SP5-4	SP6-1	SP6-2
Project ID	Ten Mile Rd to Meridian IC, Reconstruction	Deep Creek to Devil Creek IC	EP Ramps to Fairview Ave.	Moscow Mountain Passing Ln.	Burley to Declo & Heyburn IC O'Pass	Garrity Br IC & 11th Ave to Garrity
Project #	A 0011(003)	A 011(094)	A 010(527)	A 011(031)	IM 84-3(071)211	A 010(915)
Key#	11003	11094	10527	11031	9219	10915
Class	SP5	SP5	SP5	SP5	SP6	SP6
ESALs (millions)	10 -< 30	10 -< 30	10 -< 30	10 -< 30	≥ 30	≥ 30
N-Design	100	100	100	100	125	125
Mix Properties						
G_{mm}	2.412	2.421	2.443	2.555	2.466	2.406
G_{mb}	2.315	2.317	2.341	2.459	2.355	2.309
P_b (% by Mix Wt.)	5.31	4.60	5.07	5.45	4.70	5.10
VMA, %	13.9	13.8	14.5	16.2	13.7	13.7
Va, %	4.2	3.9	4.3	4.0	4.2	4.0
VFA, %	71.0	72.1	72.0	75.0	71.0	71.0
Binder Properties						
PG	70-28	64-34	70-28	70-28	76-28	76-28
G_b	1.034	1.028	1.034	1.034	1.033	1.033
Mixing Temp., °F	325	325	330	325	335	325
Comp. Temp., °F	290	295	308	295	306	306
Aggregates Properties						
G_{sb}	2.549	2.563	2.598	2.770	2.601	2.539
G_{se}	2.607	2.579	2.630	2.808	2.634	2.591
Absorption, %	1.3	1.8	1.3	1.9	0.5	1.6
% Passing, Sieves						
25mm (1")	100	100	100	100	100	100
19mm (3/4")	98	100	100	99	99	98
12.5mm (1/2")	85	87	84	83	83	86
9.5mm (3/8")	70	71	71	67	71	76
4.75mm (#4)	54	40	47	44	49	54
2.36mm (#8)	41	27	32	27	33	40
1.18mm (#16)	31	20	22	16	23	29
600µm (#30)	22	14	15	11	16	19
300µm (#50)	13	10	10	9	11	10
150µm (#100)	7	7	6	7	7	6
75µm (#200)	3.8	3.5	4.1	5.5	4.7	3.6

Laboratory Testing

The E* and Gyratory Stability (GS) tests were conducted on the 27 plant-produced HMA mixes. In addition, DSR and Brookfield laboratory tests were conducted on the investigated binders.

Dynamic Modulus Sample Preparation and Testing

Dynamic modulus tests were performed on 2 replicates per mix. Specimens were compacted using a SGC to achieve cylindrical specimens 150 mm (5.91 in.) in diameter and 170 mm (6.69 in.) in height with target air voids 9±0.5%. Specimens were then cored from the middle of the 150 x 170 mm cylindrical specimen to produce a specimen with 100 mm (3.94 in.) diameter. The height was trimmed from the top and the bottom to reach a final height of 150 mm (5.91 in.). The target air voids for the cored E* specimens was 7±1.0%. Sample preparation and compaction, and cutting and coring of the specimens are shown in Figure 27 and Figure 28, respectively.

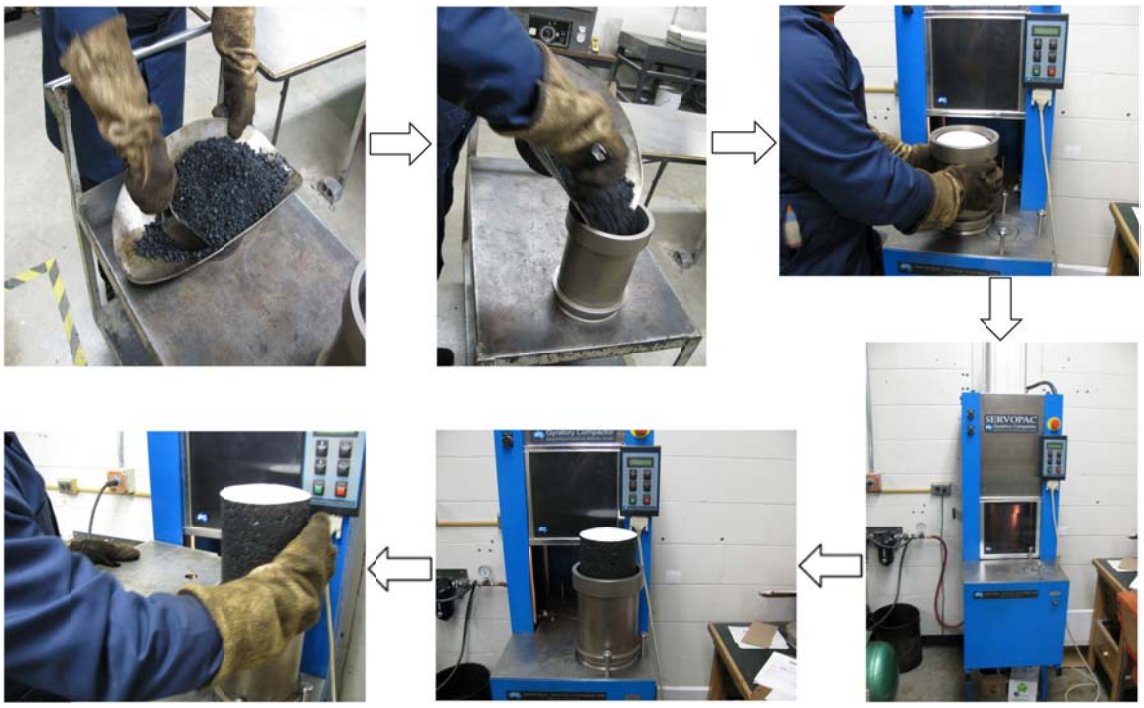

Figure 27. Sample Preparation and Compaction

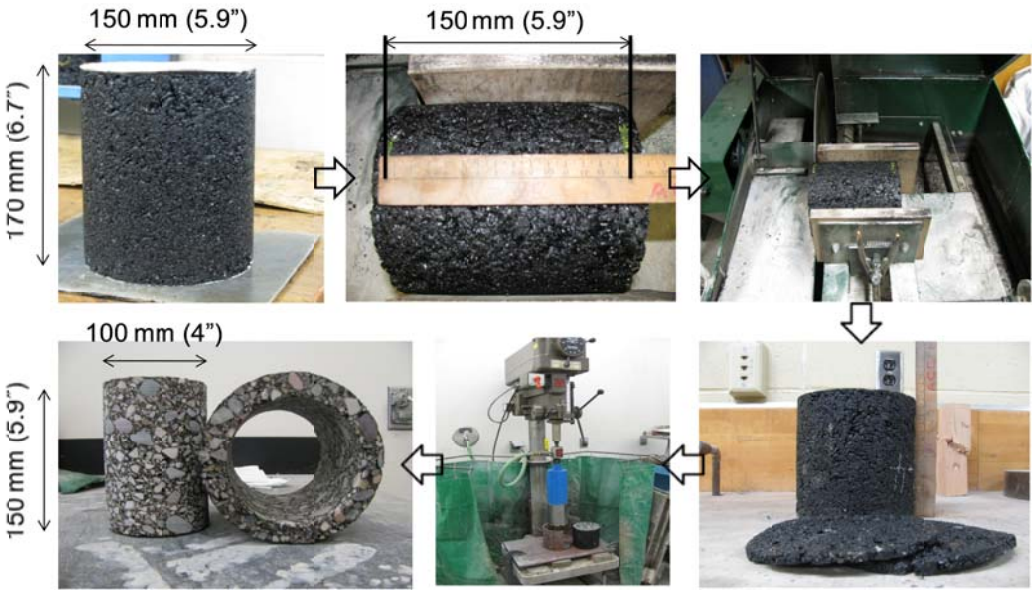

Figure 28. E* Samples Cutting and Coring Process

Dynamic modulus tests were carried out on the prepared specimens using the Asphalt Mixture Performance Tester (AMPT) in accordance with AASHTO TP 62-07.[65] The AMPT is shown in Figure 29. The tests were conducted at 40, 70, 100, 130 °F (4.4, 21.1, 37.8, and 54.4 °C). It should be pointed out that, no E* tests were conducted at 14 °F as recommended in the AASHTO TP 62-07 protocol as, it was always difficult and time consuming to achieve and maintain this very low temperature using the environmental chamber of the AMPT machine. At each temperature, the test was conducted at loading frequencies of 0.1, 0.5, 1.0, 5.0, 10, and 25 Hz. Each specimen was instrumented with 3 vertical Linear Variable Differential Transformers (LVDTs) to measure the vertical strain induced due to the applied load throughout the test.

Figure 29. Asphalt Mixture Performance Tester

Gyratory Stability Sample Preparation and Testing

For each mix, GS was determined based on the compaction results of 2 samples. These samples were compacted using SGC to the design number of gyrations of each mix which is shown in Table 34. SGC compaction was performed in accordance with AASHTO PP 60-09.[66]

Binder Dynamic Shear Rheometer (DSR) Testing

DSR tests were conducted on 9 superpave performance grade (PG) binders typical in Idaho. The investigated mixes contain 6 out of the 9 binders. The DSR tests were run according to AASHTO T315-06 procedure.[67] All tested binders were RTFO aged before testing to simulate aging during mixing and field compaction. All DSR tests were performed at the same temperature and frequency of the E* testing. All DSR tests were conducted by the Idaho Asphalt Supply.

Brookfield Rotational Viscometer Testing

In addition to the DSR tests, the Brookfield rotational viscometer tests were also performed on the investigated binders at 3 different temperatures. These tests were also run by the Idaho Asphalt supply in accordance with AASHTO TP48-97.[68]

E* Test Results and Analysis

HMA dynamic modulus (E*) and phase angle (ϕ) results of the investigated mixes at different temperatures and loading frequencies are summarized in Appendix B. E* values at different temperatures and frequencies are required inputs for level 1 HMA characterization in MEPDG. The software uses the measured E* values at different temperatures and loading frequencies to create a master curve for each HMA layer. This master curve is then used to determine the E* value at the temperature and frequency of interest for stress-strain computations. To ensure the generation of accurate sigmoidal function for E* master curve, MEPDG requires measured E* values at a minimum of 3 different temperatures. The minimum temperature for E* measurement should fall between 10 to 20 ^{o}F, the maximum temperature should be in the range of 125 to 135 ^{o}F, and at least 1 intermediate temperature between 60 and 90 ^{o}F. As explained before, it was difficult and time consuming to achieve the minimum temperature required by the software using the AMPT machine. Thus the minimum temperature was set to 40 ^{o}F. In order to overcome this, the sigmoidal master curve was established for each tested sample, and extrapolation was performed to determine the E* at 14 ^{o}F.

E* Master Curves

Master curves are constructed in order to account for temperature and rate of loading effects on the E*. They are constructed using the principle of time-temperature superposition. First, a standard reference temperature is selected (in this case, 70 °F), and then data at various temperatures are shifted with respect to time until the curves merge into a single smooth function. The master curve of modulus as a function of time formed in this manner describes the time dependency of the material. The amount of

shifting at each temperature required to form the master curve describes the temperature dependency of the material. Thus, both the master curve and the shift factors are needed for a complete description of the rate and temperature effects. Figure 30 presents an example of a master curve constructed in this manner and the resulting shift factors. For the tested mixtures, E* master curves were constructed using the sigmoidal function presented in Figure 31.

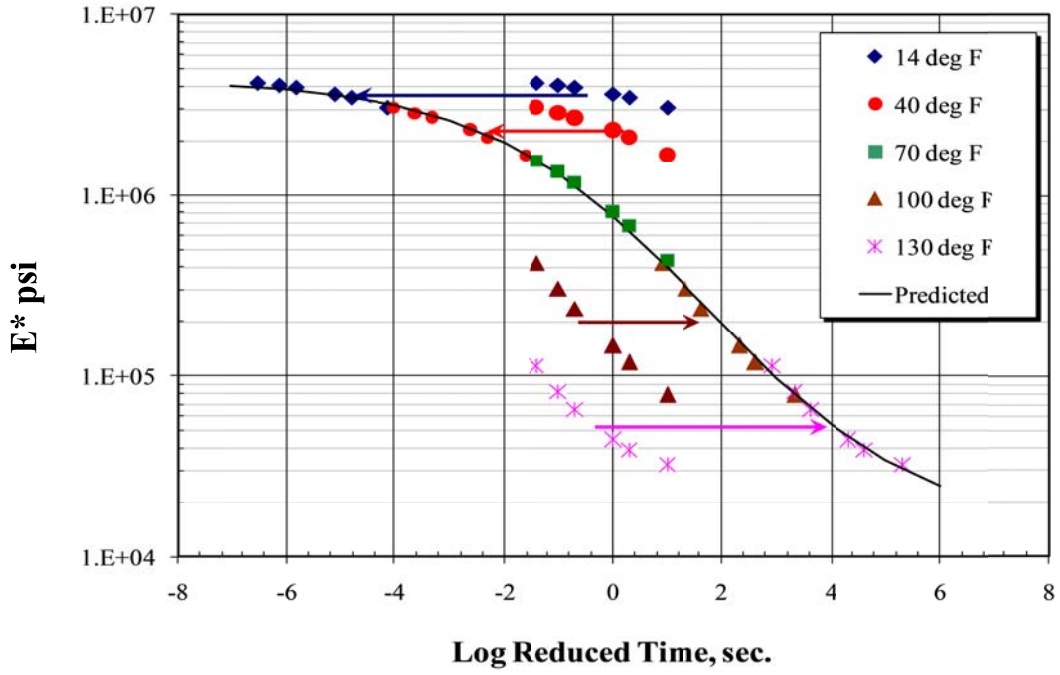

a. Master Curve

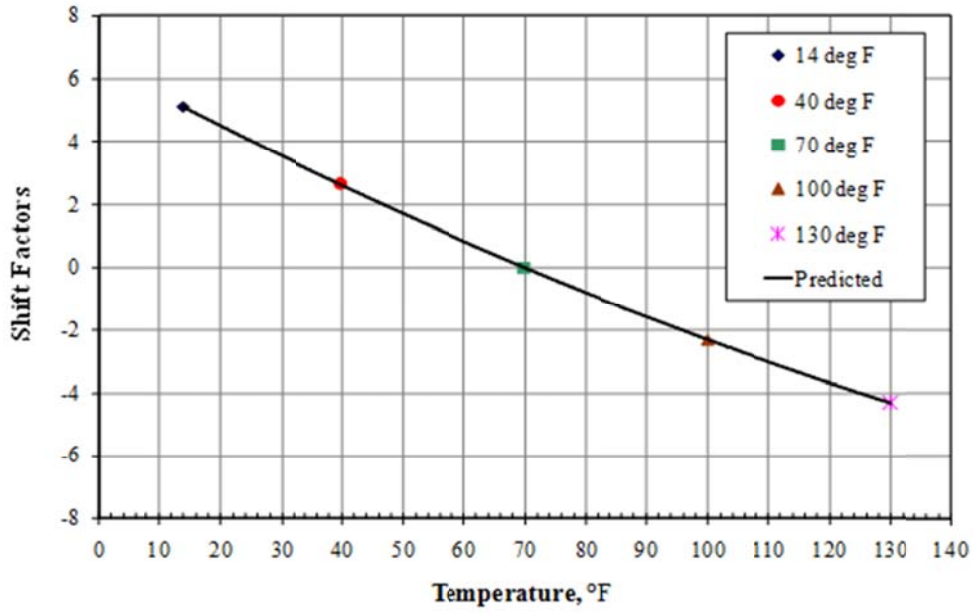

b. Shift Factors.

Figure 30. Schematic of Master Curve and Shift Factors[12]

$$\log\left|E^*\right| = \delta + \frac{\alpha}{1+\exp(\beta+\gamma\log f_r)}$$

where:

$|E^*|$ = Dynamic modulus of the mixture, psi
δ, α, β, and γ = Fitting parameters
f_r = Reduced frequency, Hz

Figure 31. E* Master Curve Sigmoidal Function[69]

The reduced frequency in Figure 31 is computed using time-temperature shift factors based on the second-order polynomial function shown in Figure 32.

$$\log f_r = \log f + a_1(T_R - T) + a_2(T_R - T)^2$$

where:

f_r = Reduced frequency at the reference temperature, Hz
f = Loading frequency at the test temperature, Hz
a_1, a_2 = Fitting coefficients
T_R = Reference temperature, 70°F
T = Test temperature, °F

Figure 32. Equation to Calculate the Reduced Frequency[69]

The fitting parameters were determined by numerical optimization using the "Solver" function in Microsoft Excel®. Starting with seed (initial) values for these parameters, the "Solver" function was used to minimize the sum of the squared errors between the logarithms of the average measured dynamic moduli at each temperature/frequency combination by varying the fitting parameters of the sigmoid function. Table 35 contains the fitting parameter values which used in developing E* master curves. Figure 33 through Figure 40, show the E* master curves of the investigated AC mixtures at a reference temperature of 70 °F. The figures clearly show that the master curve of the mixtures even within the same ITD specification can vary widely. This is expected and it is believed that the main reasons of this variability are the variability in the aggregate gradation, binder grade and the volumetric properties of the mixtures.

Table 35. Master Curve Fitting Parameters for the Investigated Mixtures[70]

Mix ID	Master Curve Fitting Parameters					
	α	β	δ	γ	a_1	a_2
SP1-1	4.475	-1.318	-0.966	-0.373	0.07015	0.00026
SP2-1	3.572	-0.940	-0.182	-0.590	0.06017	0.00018
SP2-2	3.789	-1.168	-0.490	-0.532	0.06715	0.00025
SP3-1	4.698	-1.375	-1.057	-0.392	0.07025	0.00022
SP3-2	3.855	-1.091	-0.293	-0.454	0.06885	0.00031
SP3-3	3.177	-1.008	0.218	-0.673	0.06813	0.00039
SP3-4	4.137	-1.207	-0.578	-0.494	0.06348	0.00018
SP3-5-1	4.581	-1.316	-1.076	-0.397	0.06827	0.00017
SP3-5-2	4.585	-1.371	-1.140	-0.420	0.07098	0.00026
SP3-5-3	4.500	-1.355	-1.047	-0.431	0.07208	0.00036
SP3-5-4	4.840	-1.478	-1.308	-0.385	0.07099	0.00028
SP3-5-5	4.159	-1.428	-0.789	-0.437	0.07150	0.00025
SP3-6	3.235	-0.496	0.112	-0.574	0.06319	0.00025
SP3-7	3.705	-1.159	-0.306	-0.482	0.06696	0.00028
SP3-8	4.038	-1.298	-0.563	-0.425	0.06581	0.00021
SP3-9	3.852	-1.287	-0.396	-0.439	0.06667	0.00020
SP3-10	4.319	-1.214	-0.959	-0.445	0.06525	0.00015
SP4-1	3.283	-1.039	0.069	-0.537	0.06840	0.00033
SP4-2	3.789	-1.266	-0.257	-0.400	0.06741	0.00015
SP4-3	3.379	-0.496	0.072	-0.522	0.06320	0.00021
SP4-4	3.615	-1.300	-0.039	-0.504	0.06703	0.00024
SP5-1	3.001	-1.086	0.254	-0.597	0.07786	0.00070
SP5-2	3.209	-0.615	0.175	-0.556	0.06176	0.00024
SP5-3	3.748	-1.253	-0.214	-0.439	0.06965	0.00023
SP5-4	3.260	-0.946	0.168	-0.535	0.06574	0.00023
SP6-1	3.166	-1.300	0.196	-0.547	0.06207	0.00011
SP6-2	3.572	-1.287	-0.085	-0.450	0.07151	0.00027

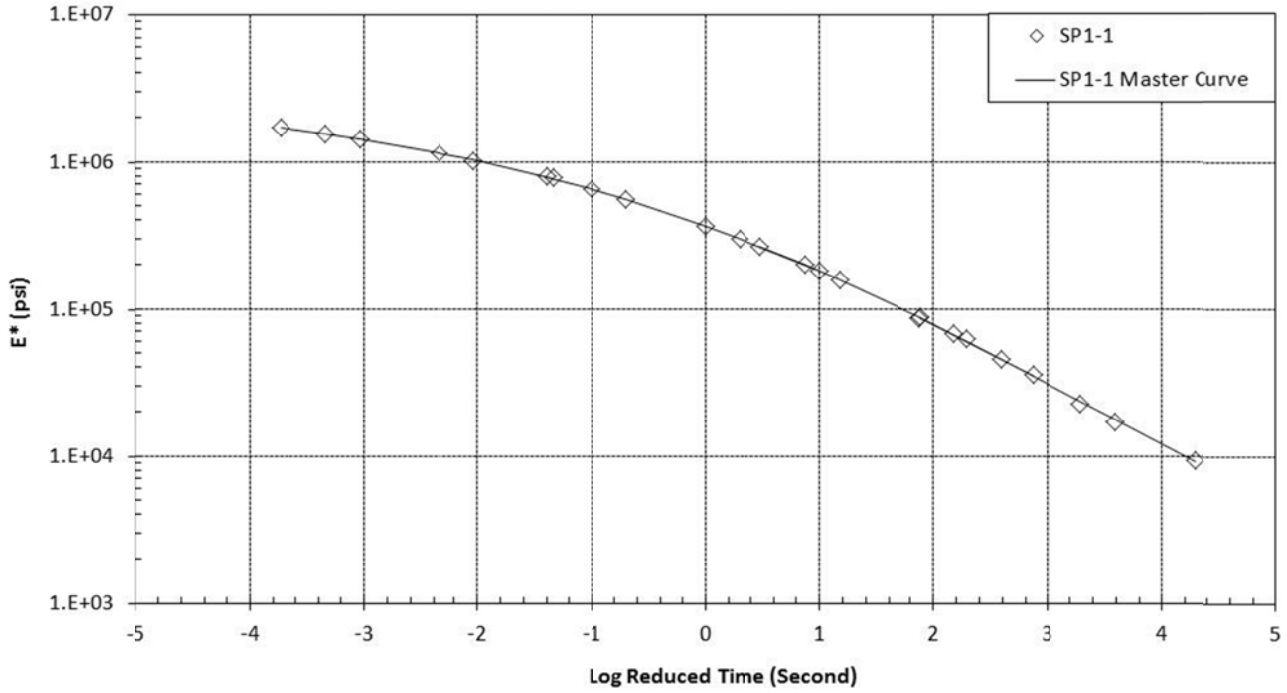

Figure 33. E* Master Curves of SP1 Mixtures

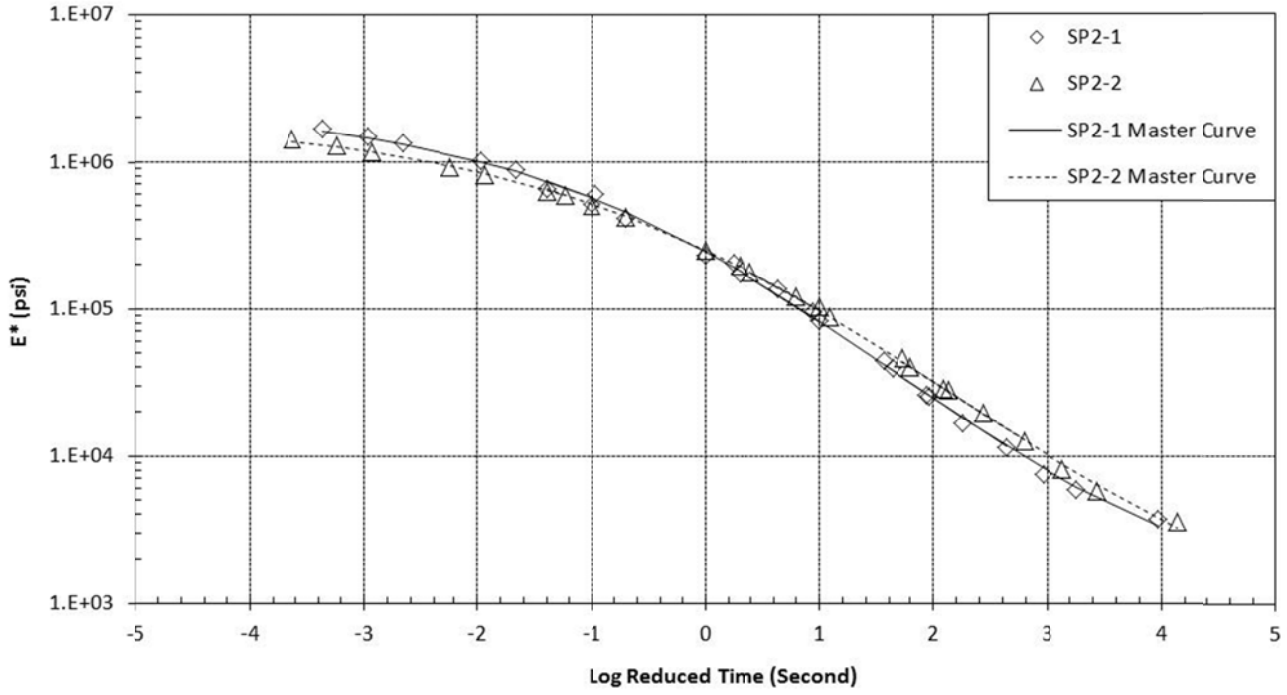

Figure 34. E* Master Curves of SP2 Mixtures

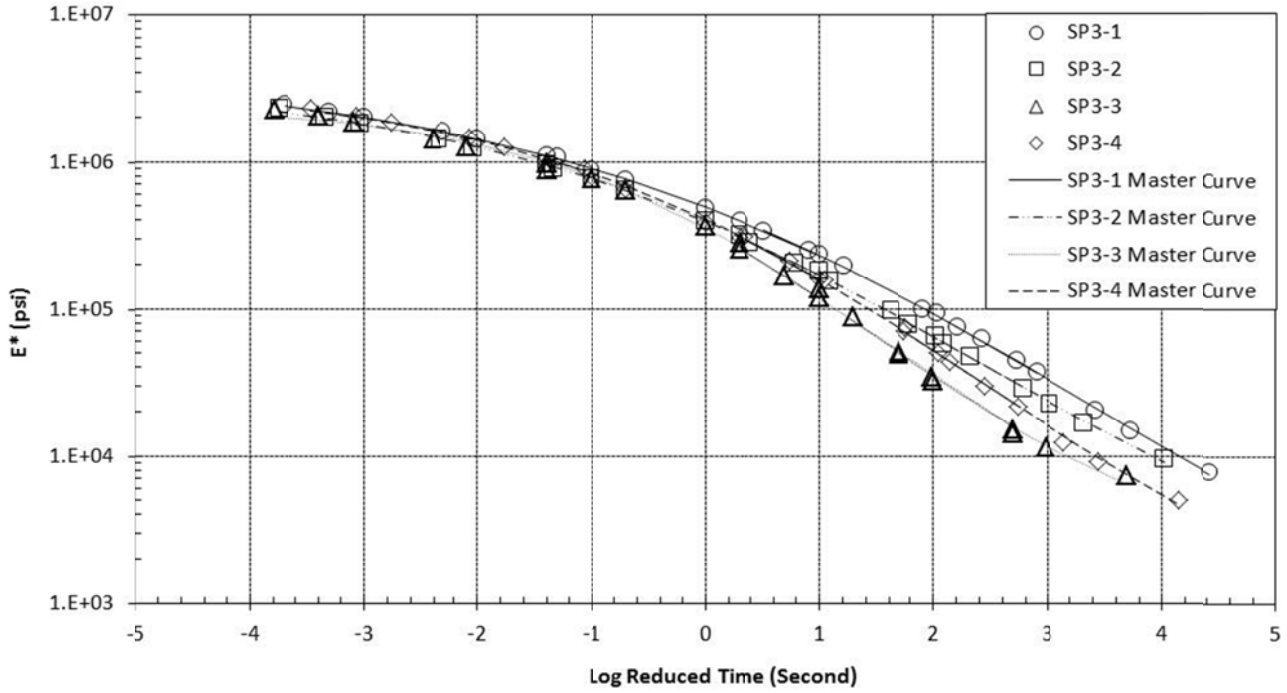

Figure 35. E* Master Curves of SP3-1 to SP3-4 Mixtures

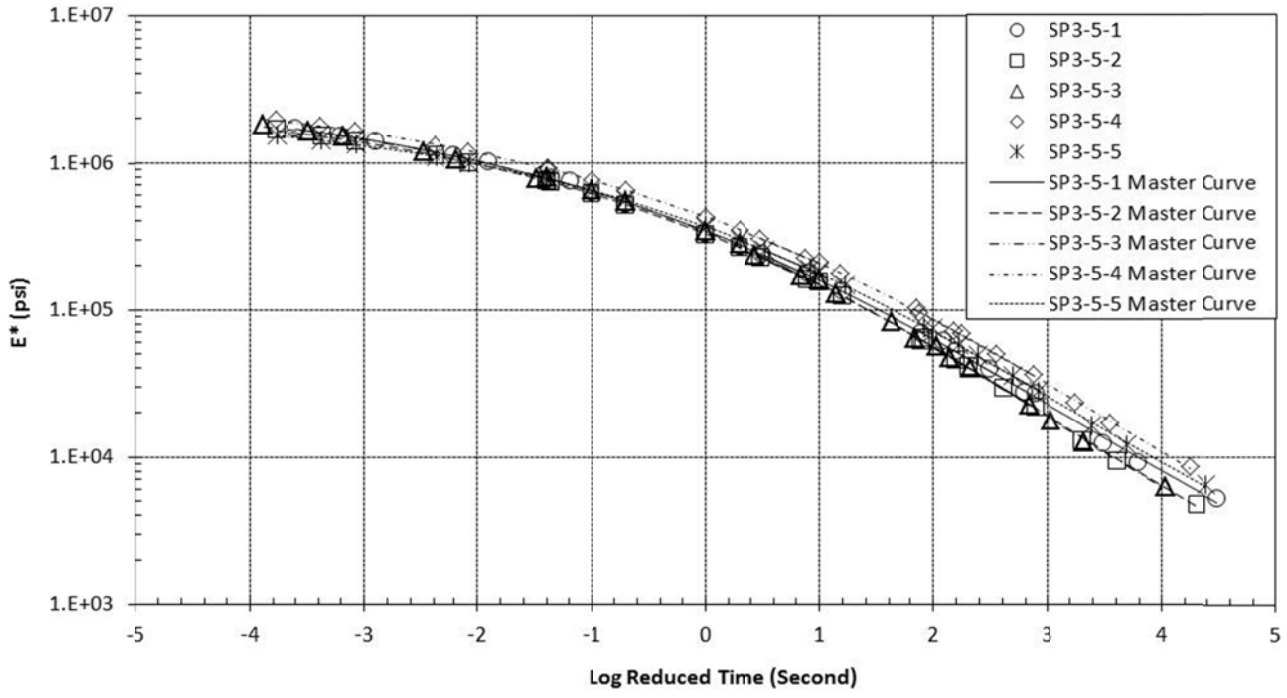

Figure 36 E* Master Curves of SP3-5 Mixtures

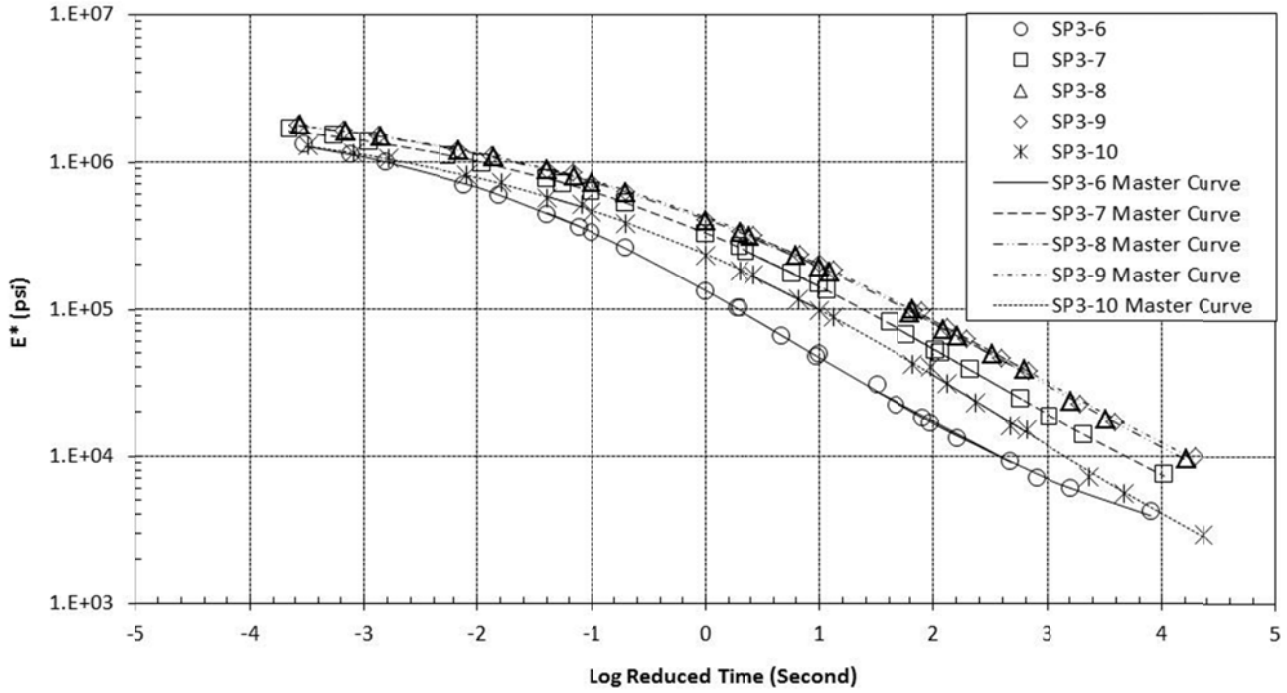

Figure 37. E* Master Curves of SP3-6 to SP3-10 Mixtures

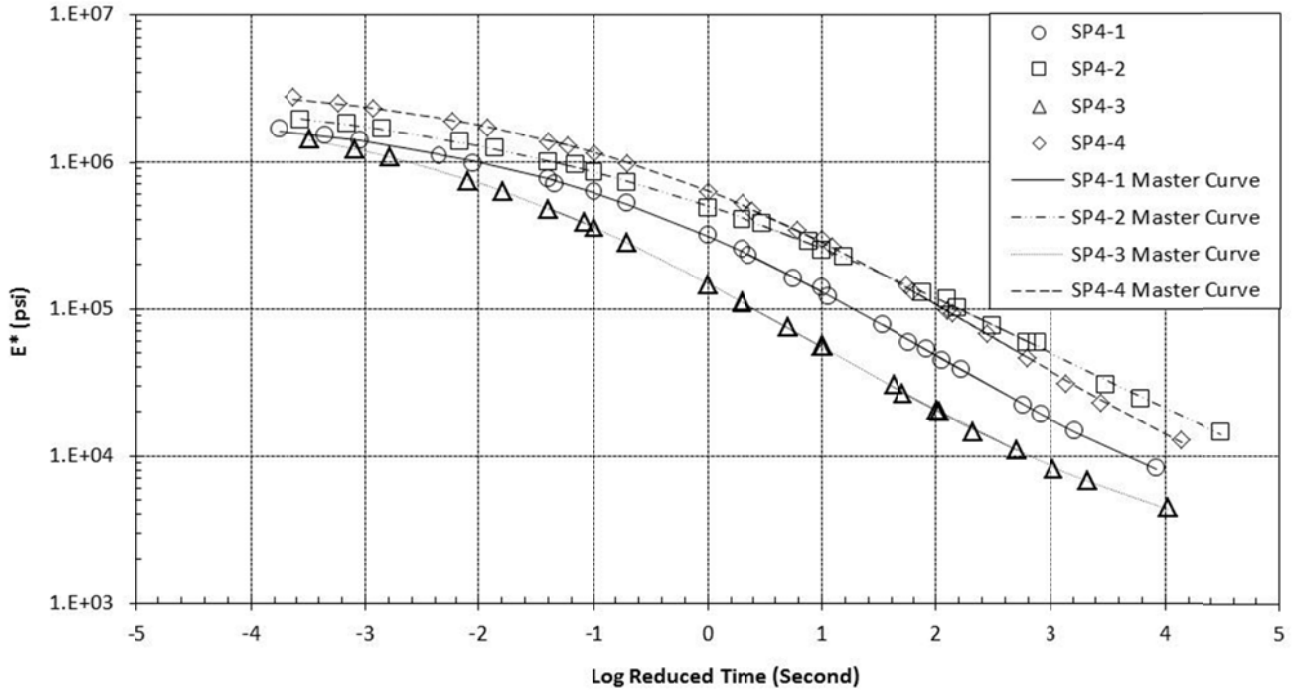

Figure 38. E* Master Curves of SP4 Mixtures

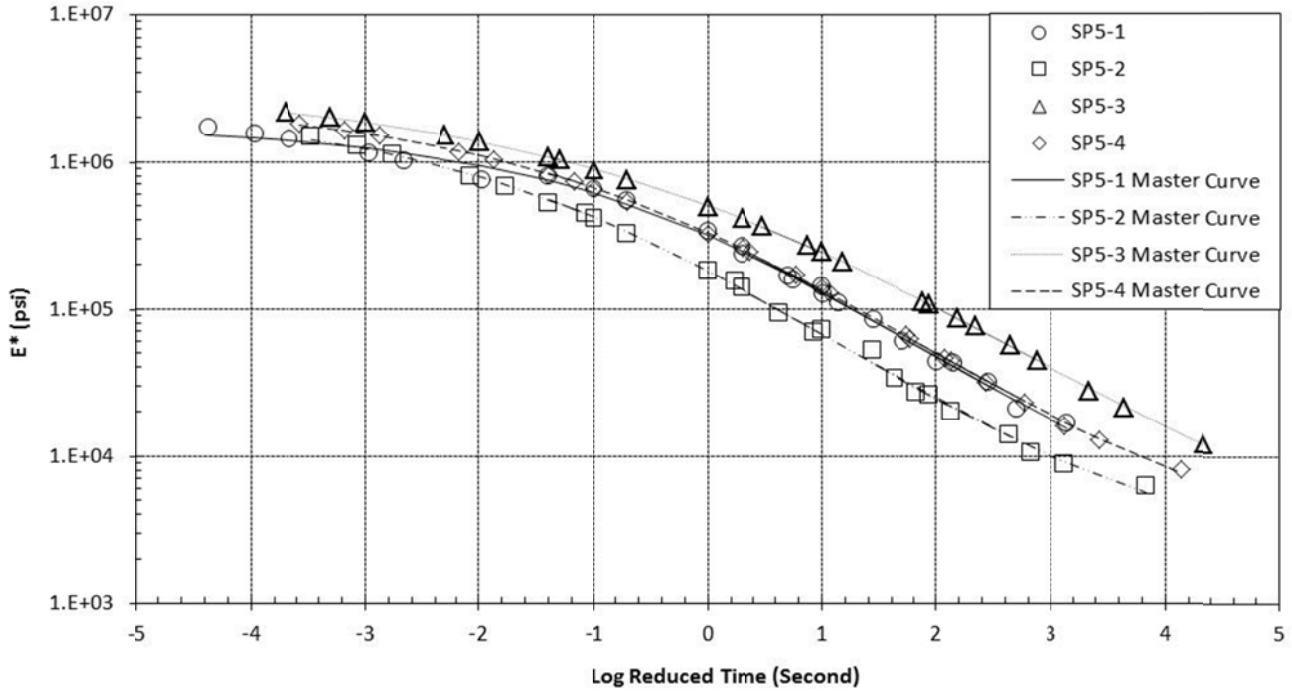

Figure 39. E* Master Curves of SP5 Mixtures

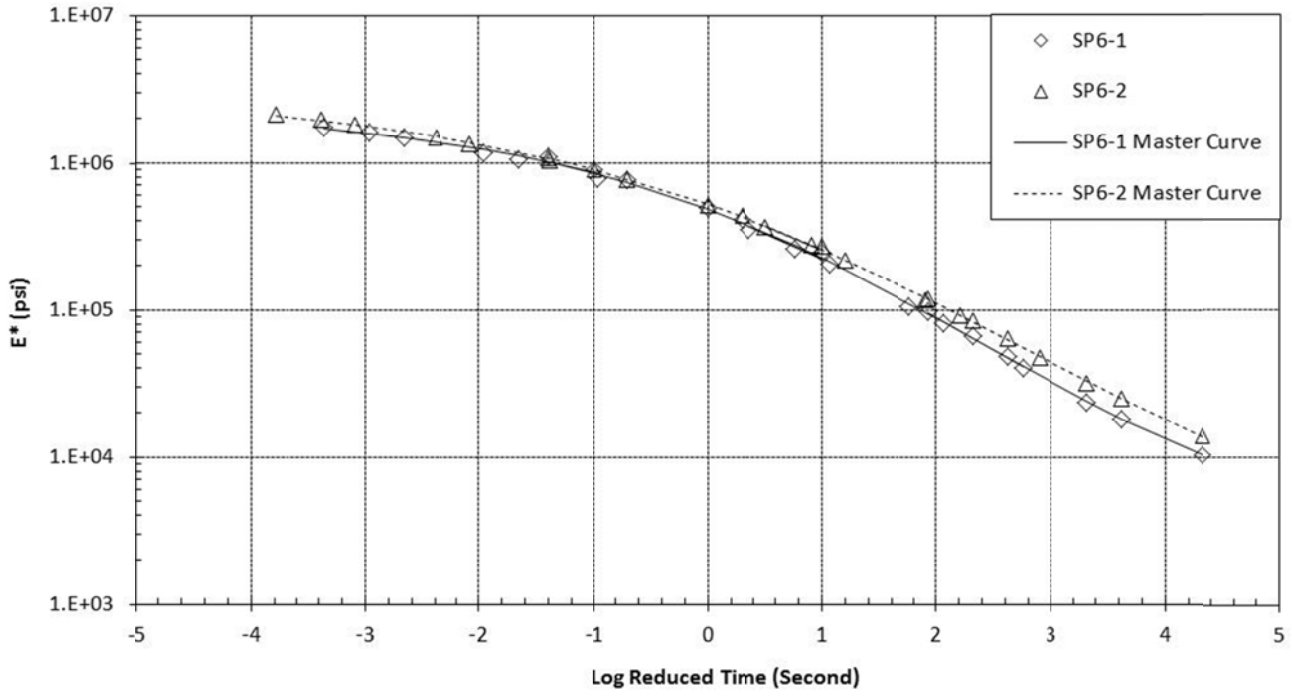

Figure 40. E* Master Curves of SP6 Mixtures

Gyratory Stability

Gyratory Stability is a parameter that reflects the mix internal structure. It is a measure of the accumulated shear energy in the sample during compaction from the point of aggregate contacts to the end of design number of gyrations. Based on the research done at the University of Idaho (UI) the GS was found to be a simple and quick parameter to measure.[64, 71, 72, 73, 74, 75, 76, 77, 78] It is reproducible and independent of the compactor type. The GS can be measured using the compaction data from any SGC equipped to report stresses generated in HMA sample during compaction. Aggregate properties determined by image analysis indicated that aggregate texture correlated with the GS. The GS concept was validated for a large array of asphalt mixes including various levels of Superpave mixes in Idaho (SP1 through SP6).

To determine GS, forces applied on the sample during gyratory compaction are analyzed, and the internal shear force at mid-height (S_i) at any gyration number (i) is determined. The GS is then calculated as the sum of shear energy increments that are dissipated in the sample during part B of the compaction process as shown in Figure 41.[79, 80, 81] GS can be determined using the equation shown in Figure 42.

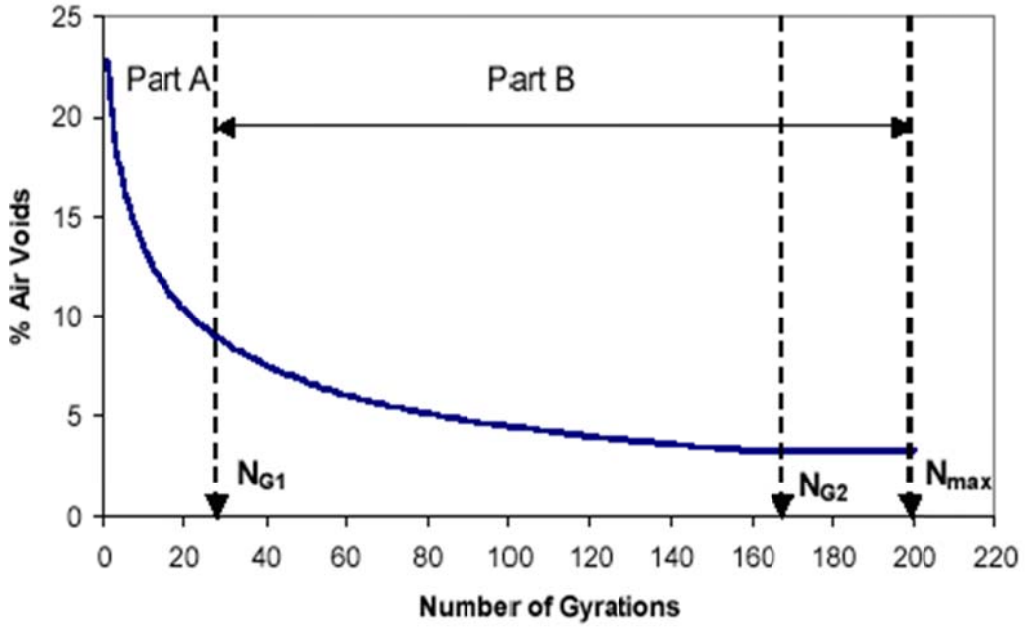

Figure 41.Typical Compaction Curve[77]

$$GS = \sum_{i=N_{G1}}^{N_{design}} S_i \Delta d_i$$

where:

GS = Gyratory Stability, kN.m

N_{G1} = Initial number of gyrations

N_{design} = Designed number of gyrations

S_i: = Shear force at half sample height at number of gyration (i), kN

Δd_i = Change in sample height between number of gyrations (i) and (i-1), meters

Figure 42. Gyratory Stability Equation

The sum of the energy product $S_i \Delta d_i$ is determined over a range of number of gyrations from N_{G1} to $N_{G2}=N_{design}$. N_{G1} is determined at the point where the change of slope of the compaction curve is steady (linear) where the third derivative of the compaction curve is zero. In physical terms, it is the point where the change in sample height starts to be related to the particles orientation and forming particle contacts in the mix rather than to merely volumetric change. Mechanistically, the shear strength development in the mix will be related to particle contacts and to the properties of the mastic around the coarse particles. At the initial number of gyrations (N_{G1}), mix deforms rapidly, and change in sample height is mainly due to volumetric change. Starting from N_{G1}, mix starts to develop shear resistance and it continues to increase until it reaches maximum value at N_{G2}. The shear strength stays unchanged to N_{max}. However, if compaction continues beyond this point, a possibility of damage to the sample may occur and sample may lose its shear strength due to micro fractures at the particle contacts. The algorithm developed for calculating GS is based on the range N_{G1} to $N_{G2}=N_{design}$. The GS may vary from specimen to another within the same asphalt mixture depending on the structure of each specimen. [79, 80, 81]

Based on the aforementioned method to calculate GS, Bayomy et al. at UI developed a spreadsheet to determine the GS of the mix.[71, 80]. This spreadsheet was revised and modified overtime. As part of this research work, visual basic software was developed to compute the GS and it is named "*G-Stab 2010*".[70] This software is user-friendly and easy to use due to the enhancements which were added to it. It calculates the GS of HMA specimens using the compaction volumetric and shear data. Figure 43 shows the main windows of the *G-Stab 2010* software. The GS values for the investigated mixtures along with the design number of gyrations, design air voids at the design number of gyrations, G_{mb} and G_{mm} are listed in Table 36.

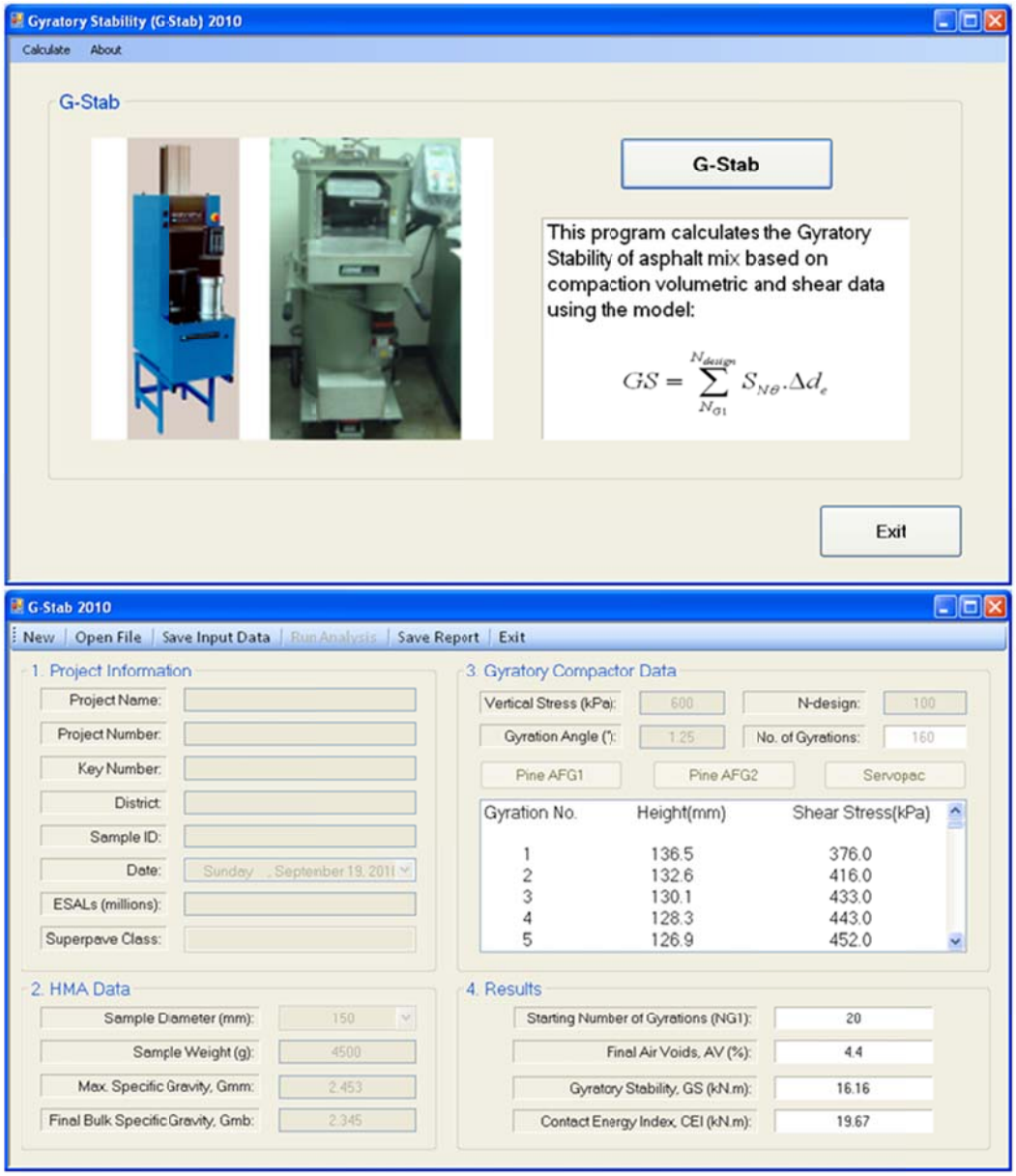

Figure 43. Screen Shots of the Main Windows of *G-Stab 2010* Software[70]

Table 36. Gyratory Stability Values of the Investigated Mixtures[70]

Mix ID	N_{design}	Air Voids @ N_{design} (%)	Final G_{mb}	Mix G_{mm}	GS (kN.m)	Average GS
SP1-1	40	4.8	2.278	2.393	11.77	13.30
	40	4.6	2.282	2.393	14.83	
SP2-1	50	4.8	2.293	2.408	9.85	9.35
	50	4.5	2.299	2.408	8.84	
SP2-2	50	3.7	2.417	2.510	11.23	11.23
SP3-1	75	4.3	2.347	2.453	13.84	12.93
	75	4.2	2.349	2.453	12.02	
SP3-2	75	4.5	2.320	2.429	14.42	13.56
	75	5.0	2.307	2.429	12.7	
SP3-3	75	3.3	2.340	2.421	13.38	12.68
	75	3.3	2.340	2.421	11.98	
SP3-4	75	4.1	2.338	2.437	9.15	10.57
	75	3.8	2.344	2.437	11.98	
SP3-5-1	75	4.5	2.483	2.599	14.63	14.63
SP3-5-2	75	4.7	2.478	2.599	11.37	11.37
SP3-5-3	75	3.5	2.507	2.599	12.95	12.95
SP3-5-4	75	3.9	2.497	2.599	12.27	12.27
SP3-5-5	75	4.4	2.484	2.599	13.62	13.62
SP3-6	75	3.4	2.327	2.408	14.26	14.26
SP3-7	75	3.3	2.502	2.586	15.19	15.19
SP3-8	75	4.3	2.352	2.458	16.31	16.31
SP3-9	75	3.8	2.484	2.581	14.07	14.07
SP3-10	75	4.5	2.35	2.46	12.89	12.89
SP4-1	90	3.0	2.360	2.434	12.56	13.95
	90	3.1	2.359	2.434	15.33	
SP4-2	90	4.3	2.331	2.435	15.03	14.75
	90	4.5	2.326	2.435	14.47	
SP4-3	90	3.0	2.388	2.462	11.45	11.92
	90	3.9	2.365	2.462	12.39	
SP 4-4	90	4.1	2.342	2.442	17.61	17.61
SP5-1	100	4.1	2.313	2.412	15.22	16.63
	100	4.1	2.312	2.412	18.04	
SP5-2	100	4.7	2.307	2.421	15.48	14.19
	100	4.5	2.312	2.421	12.9	
SP5-3	100	4.3	2.339	2.443	13.19	14.39
	100	4.5	2.333	2.443	15.59	
SP5-4	100	3.2	2.474	2.555	14.14	13.65
	100	3.2	2.474	2.555	13.15	
SP6-1	125	4.9	2.344	2.466	17.7	17.33
	125	4.8	2.347	2.466	16.95	
SP6-2	125	3.1	2.332	2.406	16.55	16.86
	125	3.1	2.331	2.406	17.17	

Brookfield Rotational Viscometer Testing Results

The results of the Brookfield rotational viscometer tests performed on the investigated binders are summarized in Table 37. These tests were conducted at 3 different temperatures as shown in the table. Brookfield viscosity results were used in this research to investigate the binder input level on the prediction accuracy of MEPDG E* predictive models. This will be explained later in the chapter.

Table 37. Brookfield Rotational Viscometer Test Results

PG Grade	PG58-28	PG58-34	PG64-22	PG64-28	PG64-34	PG70-22	PG70-28	PG70-34	PG 76-28
Viscosity at 135°C (Pa.s)	0.303	0.470	0.443	0.600	1.108	0.892	1.053	1.392	1.925
Viscosity at 150°C (Pa.s)	0.158	0.249	0.219	0.301	0.533	0.442	0.529	0.721	0.900
Viscosity at 165°C (Pa.s)	0.088	0.149	0.120	0.167	0.321	0.254	0.294	0.450	0.430

The data illustrated in Table 37 were used to determine the ASTM A-VTS parameters of the investigated binders. This is shown in Figure 44.

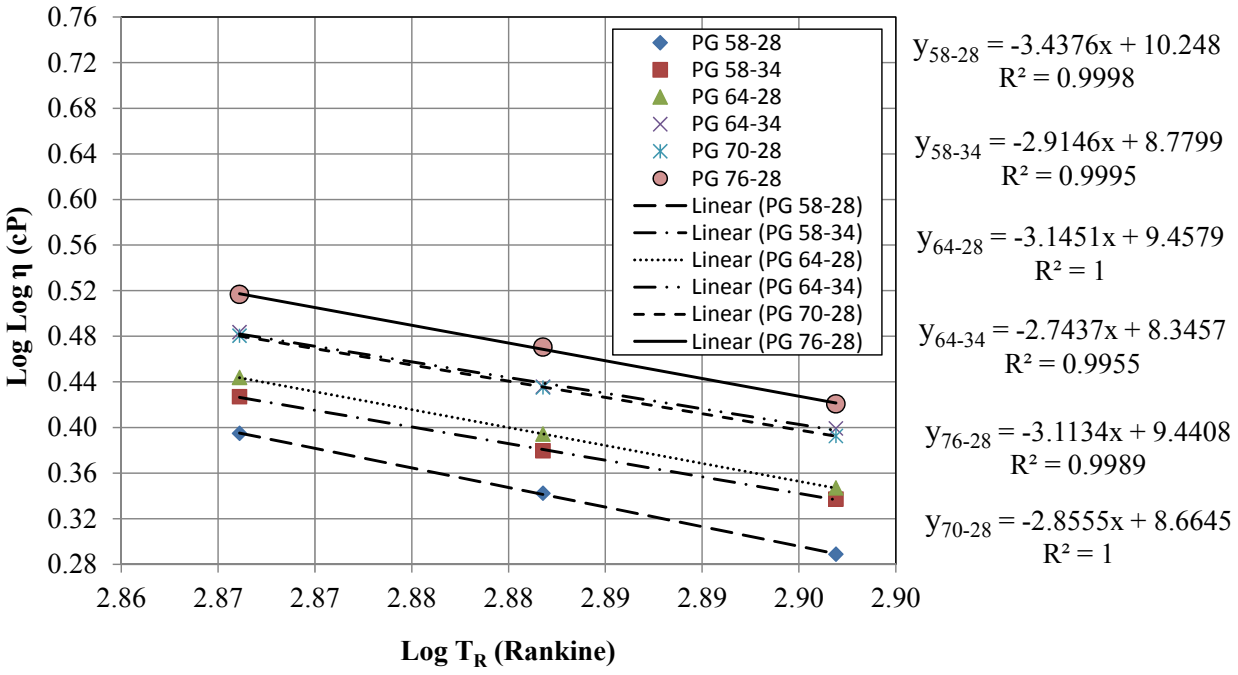

Figure 44. Brookfield Viscosity-Temperature Relationships of the Investigated Binders

DSR Testing Results

The binder G* master curves for the 9 typical superpave performance grade binders investigated in this research are shown in Figure 45. The DSR testing results of these binders are tabulated in Appendix C. This data includes binder phase angle (δ), complex shear modulus (G*), elastic modulus (G' = G*cos δ), viscous modulus (G"= G*sin δ), and viscosity (η*) at different test temperatures and loading frequencies.

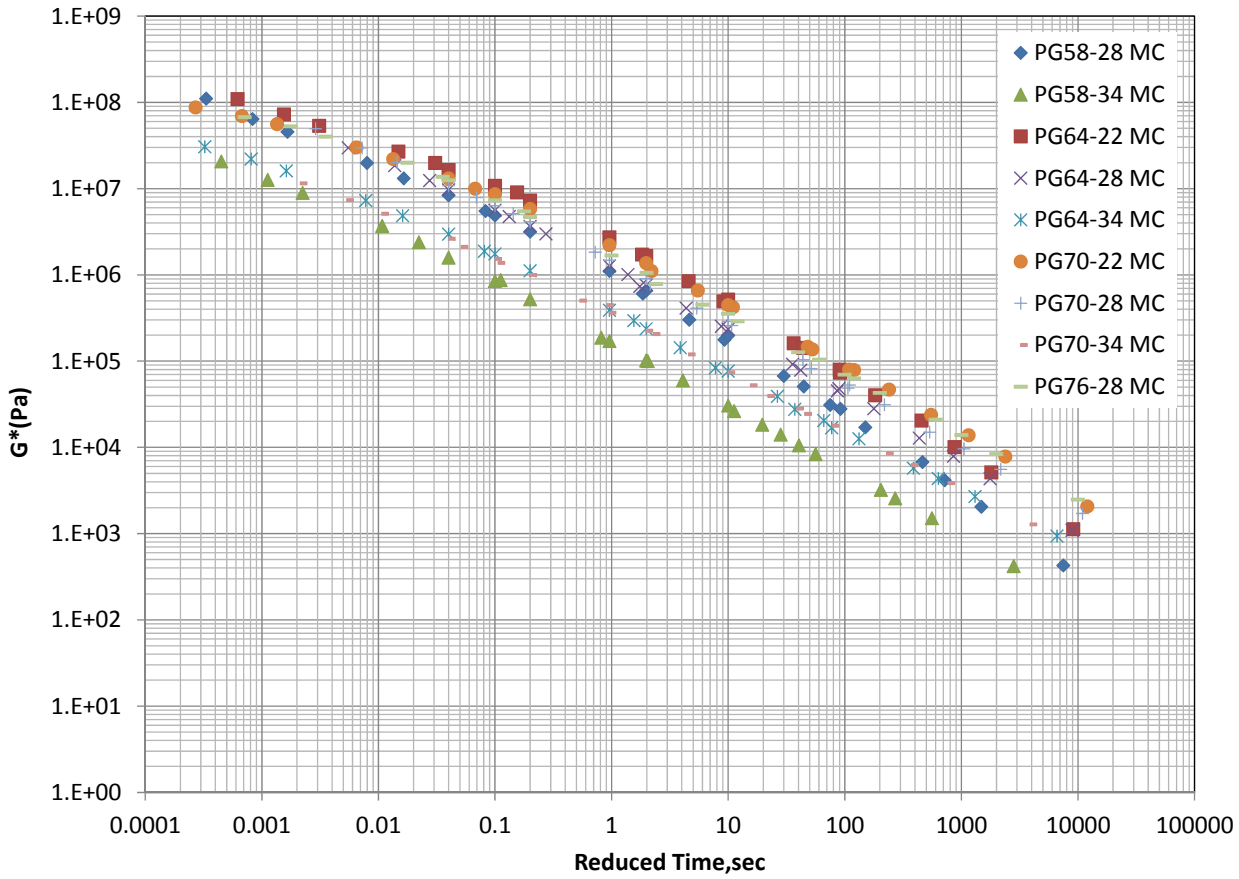

Figure 45. Binder Shear Modulus Master Curves at Reference Temperature of 70 ^{o}F

In order to investigate the accuracy of the MEPDG E* predictive models, it was important to determine the A and VTS parameters of the investigated binders as previously explained. For MEPDG level 1 input binder characterization, only G*and δ data at a loading frequency of 10 rad/sec (1.59 Hz) and different temperatures are required. These values are provided in Table 38. This data along with the equation presented in Figure 24 were first used to determine the binder viscosity at the different test temperatures. A liner regression was then conducted on the viscosity-temperature data for each binder using the equation presented in Figure 25. The viscosity-temperature plots along with the ASTM A-VTS parameters and the coefficient of determination (R^2) of the 6 binders used in the investigated mixes based on the DSR data are depicted in Figure 46.

Table 38. G*and δ Values at 1.59 Hz Loading Frequency (MEPDG Level 1 Binder Data)

Binder	Temp (°F)	G* (Pa)	δ (°)
PG58-28	40	2.46E+07	57.96
	70	1.40E+06	60.92
	100	6.84E+04	73.70
	130	5.78E+03	82.02
PG58-34	40	4.49E+06	56.13
	70	2.28E+05	63.32
	100	2.51E+04	68.09
	130	3.49E+03	70.34
PG64-22	40	3.22E+07	52.79
	70	3.29E+06	57.38
	100	1.96E+05	73.98
	130	1.42E+04	82.12
PG64-28	40	5.89E+06	58.87
	70	1.62E+06	60.97
	100	1.04E+05	66.79
	130	1.07E+04	73.77
PG64-34	40	8.42E+06	46.93
	70	5.04E+05	60.75
	100	3.91E+04	66.87
	130	5.95E+03	61.47
PG70-22	40	3.31E+07	37.09
	70	2.70E+06	56.14
	100	1.77E+05	63.19
	130	1.87E+04	70.86
PG70-28	40	9.96E+06	58.22
	70	1.89E+06	59.61
	100	1.11E+05	61.85
	130	1.34E+04	67.88
PG70-34	40	2.57E+06	54.17
	70	4.65E+05	57.37
	100	5.70E+04	67.80
	130	8.29E+03	62.47
PG76-28	40	2.20E+07	42.28
	70	2.19E+06	59.11
	100	1.34E+05	58.16
	130	1.86E+04	63.63

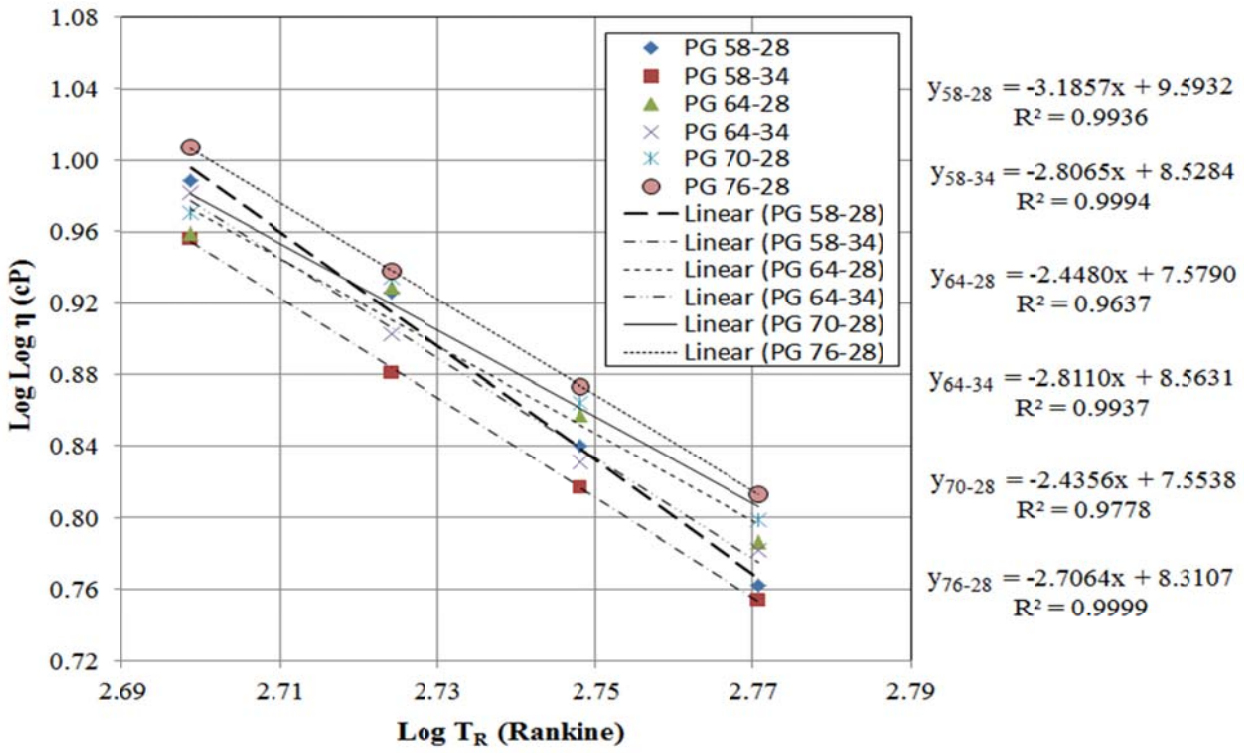

Figure 46. Viscosity-Temperature Relationships from DSR Testing Results

Influence of the Binder Input Level on MEPDG E* Prediction Accuracy

As discussed earlier in this chapter, both MEPDG E* predictive models are function of the binder characteristics. Thus, It is important to study the influence of the MEPDG binder data input level on the predicted E* from the 2 MEPDG models. Based on the prescribed MEPDG binder input levels, 5 cases, for each E* predictive model, were investigated in this study:

- Case 1 (MEPDG-level 1 conventional binder data): measured viscosity from Brookfield rotational viscometer results on short-term aged binders.
- Case 2 (MEPDG-level 1 Superpave performance binder data): G* and δ from DSR test on short-term aged binders interpolated at 10 rad/sec angular frequency and different temperatures.
- Case 3 (MEPDG-level 3 binder default values): recommended typical MEPDG A-VTS values based on the binder performance grade.
- Case 4: predicted viscosity from DSR test on short-term aged binders interpolated at 10 rad/sec angular frequency and different temperatures.
- Case 5: measured η, δ, and G* from DSR test on short-term aged binders at the same frequencies (0.1, 0.5, 1, 5, 10, and 25 Hz) and temperatures (40, 70, 100, and 130 °F) of dynamic modulus testing.

In case 1, for each binder, the A-VTS parameters were determined using the ASTM equation (Figure 25) based on the Brookfield viscosity testing results as depicted previously in Figure 44. In Case 2 binder characterization, DSR tests were run to determine *G** and *δ* at different frequencies and temperatures and then data at 10 rad/sec angular frequency for different temperatures was found by interpolation. Binder viscosity values were then estimated at each tested temperature as illustrated by the equation in Figure 24. The ASTM equation (Figure 25) was again used to determine the A and VTS values for each binder. This is shown in Figure 46. In case 3 binder characterization, the MEPDG software has built-in default values of A-VTS parameters for each binder grade. The MEPDG typical default values of A-VTS parameters were used based on the binder performance grade. In case 4 binder characterization, measured *η* values from the DSR tests at different frequencies and temperatures were used to find *η* values at 10 rad/sec angular frequency for different temperatures by interpolation. The ASTM viscosity-temperature relationship was again used to determine the A and VTS values for each binder. This is shown in Figure 47.

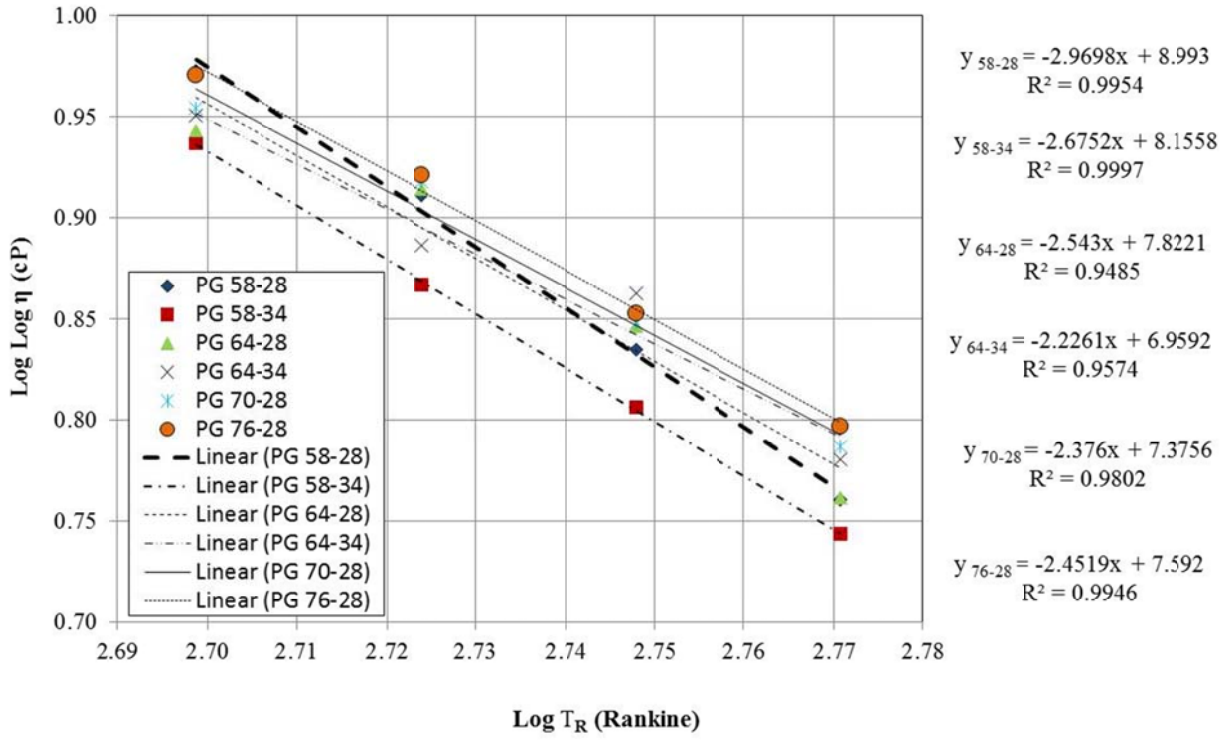

Figure 47. Case 4 Viscosity-Temperature Relationships of the Investigated Binders

In case 5, actual *η*, *δ*, and *G** values from the DSR test results on short-term aged binders were used directly to characterize the binder for both MEPDG E* predictive models at the same frequencies (0.1, 0.5, 1, 5, 10, and 25 Hz) and temperatures (40, 70, 100, and 130°F) of dynamic modulus testing. It should be noted that this case cannot be conducted using the MEPDG directly.

Table 39 compares the A and VTS values of the investigated binders based on the first 4 cases of binder input levels. Data given in in this table shows that, A-VTS values obtained from the 4 cases are different. The MEPDG typical default A-VTS (Case 3) values are the largest, while A-VTS values obtained from Case 4 are the smallest.

Table 39. Binder Viscosity-Temperature (A-VTS) Parameters for the Binders (RTFO-Aged)

Binder Grade	Case 1 (Brookfield)		Case 2 (DSR @ 10 rad/s)		Case 3 (Default MEPDG)		Case 4 (Predicted η from DSR @ 10 rad/s)	
	MEPDG Level 1 (Conventional)		MEPDG Level 1 (Superpave)		MEPDG Level 3			
	A	VTS	A	VTS	A	VTS	A	VTS
PG58-28	10.2477	-3.4376	9.5932	-3.1857	11.0100	-3.7010	8.9930	-2.9698
PG58-34	8.7799	-2.9146	8.5284	-2.8065	10.0350	-3.3500	8.1558	-2.6752
PG64-28	9.4579	-3.1451	7.5790	-2.4480	10.3120	-3.4400	7.8221	-2.5430
PG64-34	8.3457	-2.7437	8.5631	-2.8110	9.4610	-3.1340	6.9592	-2.2261
PG70-28	8.6645	-2.8555	7.5538	-2.4356	9.7150	-3.2170	7.3756	-2.3760
PG76-28	9.4408	-3.1134	8.3107	-2.7064	9.2000	-3.0240	7.5920	-2.4519

Comparison of MEPDG E* Predictions

A comparison of laboratory measured and predicted E* was conducted using both E* predictive models incorporated in MEPDG for the aforementioned 5 cases of binder characterization. Figure 48 through Figure 52 show measured versus predicted E* from the 2 MEPDG predictive models based on the 5 cases of binder data. In these figures, the dotted 45 degree lines represent the lines of equality. The closer the points to this line the higher is the prediction accuracy of the predictive procedure. Also shown in these figures the number of E* measurements (n), R^2 and S_e/S_y.

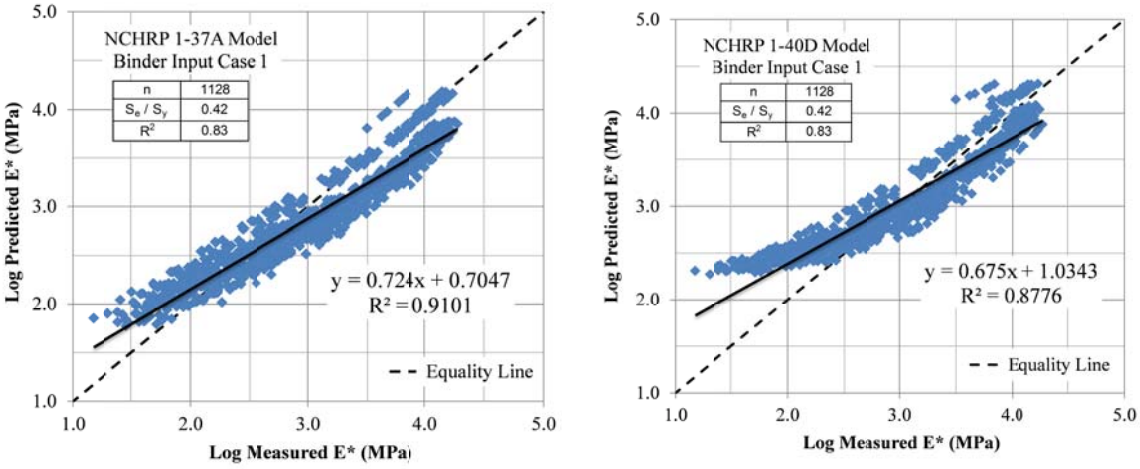

a) NCHRP 1-37A Model **b) NCHRP 1-40D Model**

Figure 48. Predicted versus Measured E* based on Case 1 Binder Data

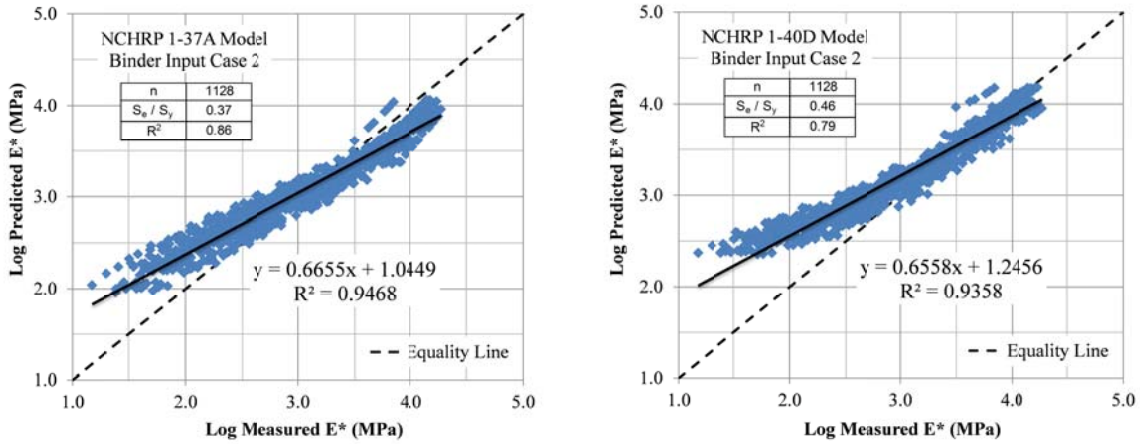

a) NCHRP 1-37A Model **b) NCHRP 1-40D Model**

Figure 49. Predicted versus Measured E* based on Case 2 Binder Data

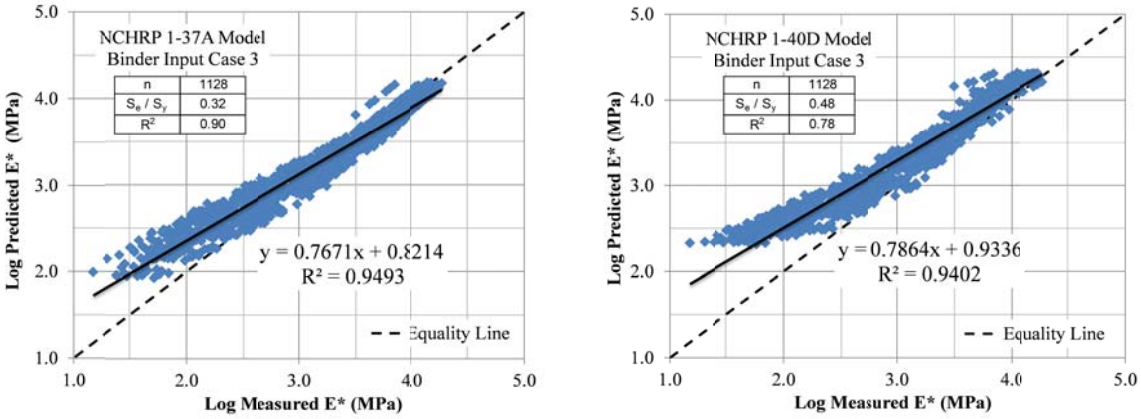

a) NCHRP 1-37A Model **b) NCHRP 1-40D Model**

Figure 50. Predicted versus Measured E* based on Case 3 Binder Data

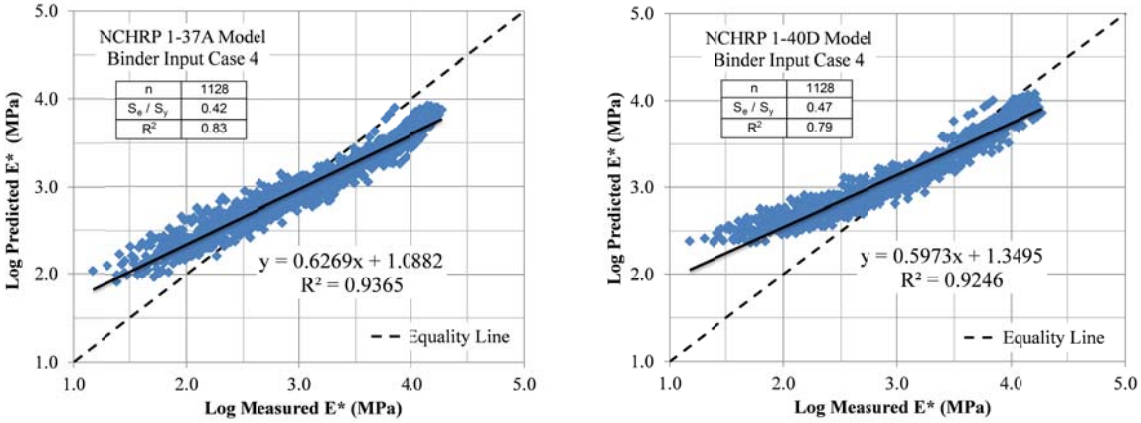

a) NCHRP 1-37A Model **b) NCHRP 1-40D Model**

Figure 51. Predicted versus Measured E* based on Case 4 Binder Data

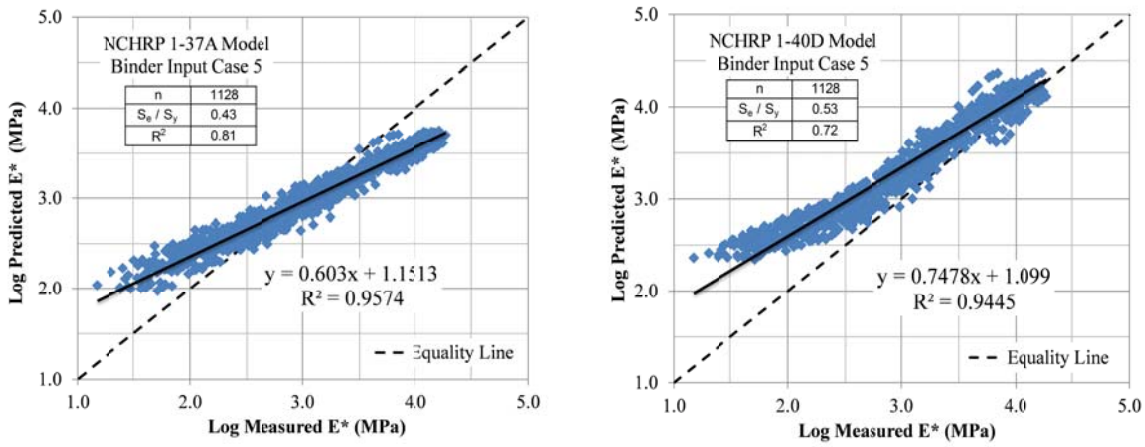

a) NCHRP 1-37A Model **b) NCHRP 1-40D Model**

Figure 52. Predicted versus Measured E* based on Case 5 Binder Data

Goodness-of-Fit Statistics and Relative Bias

To assess the performance of the investigated predictive procedures, correlation of the predictive and measured values was evaluated using goodness-of-fit statistics according to the conceptual criteria shown in Table 40. This criteria is based on R^2 and S_e/S_y. The R^2 is simply the square of the correlation coefficient between the measured and predicted E* (higher R^2 indicates higher accuracy). The S_e/S_y is an indicator of the relative improvement in accuracy. Smaller S_e/S_y value points out better accuracy.

Table 40. Criteria for Goodness-of-Fit Statistical Parameters[82]

Criteria	R^2	S_e/S_y
Excellent	≥ 0.90	≤ 0.35
Good	0.70 - 0.89	0.36 – 0.55
Fair	0.40 – 0.69	0.56 - 0.75
Poor	0.20 – 0.39	0.76 – 0.89
Very Poor	≤ 0.19	≥ 0.90

The goodness-of-fit statistical parameters are calculated with respect to the line of equality using the formulas shown in Figure 53.

$$S_y = \sqrt{\frac{1}{n-1}\sum_{i=1}^{n}\left(E^*_{mi} - \overline{E}^*_m\right)^2}$$

$$e_i = \sum_{i=1}^{n}\left(E^*_{pi} - E^*_{mi}\right)$$

$$S_e = \sqrt{\frac{\sum_{i=1}^{n} e_i^2}{n - p}}$$

$$R^2 = 1 - \frac{n-p}{n-1}\cdot\left(\frac{S_e}{S_y}\right)^2$$

where:

n = Number of data points
p = Number of model parameters
E^*_{mi} = Measured dynamic modulus
E^*_m = Mean value of measured dynamic modulus
E^*_{pi} = Predicted dynamic modulus
S_y = Standard deviation of the measured E* values about the mean measured
e_i = Error between the predicted and measured E* values
S_e = Standard error (i.e., standard deviation of error)
R^2 = Coefficient of determination

Figure 53. Equations to Compute the Goodness-of-Fit Statistics(82)

The E* database used in this analysis is based on 1128 data points from 27 common Idaho mixtures. A summary of the goodness-of-fit statistics is shown in Table 41. Generally, all 5 binder characterization cases along with the NCHRP 1-37A and NCHRP 1-40D E* predictive models yielded high R^2 and low S_e/S_y. Nevertheless, the 1-37A model always yielded biased E* predictions at the high temperature values for all binder input cases. At the low temperatures, this model showed biased E* predictions at some binder input cases. The 1-40D model showed highly biased E* estimates at the lowest and highest temperatures with case 1 binder data (Figure 48-b). With Cases 2 and 4 binder data, this model overestimated the E* at the highest temperatures (Figure 49-b and Figure 51-b), while with cases 3 and 5 binder data, it overestimated the E* for almost all tested temperatures (Figure 50-b and Figure 52-b). When comparing the performance (accuracy and bias) of the1-37A model with the 1-40D model for each binder characterization case, it can be concluded that, the 1-37A model performance superseded the 1-40D model for Idaho mixtures. Because of the highly biased E* estimates of both Witczak models for Idaho mixes, Hirsch and Idaho models for HMA E* predictions were investigated.

Table 41. Evaluation of the MEPDG E* Predictive Procedures in Logarithmic Space

MEPDG E* Models	Binder Level	R^2	S_e/S_y	Evaluation
NCHRP 1-37A (1999 η-based)	Case 1	0.83	0.42	Good/Good
	Case 2	0.86	0.37	Good/Good
	Case 3	0.90	0.32	Excellent/Excellent
	Case 4	0.83	0.42	Good/Good
	Case 5	0.81	0.43	Good/Good
NCHRP 1-40D (2007 G*-based)	Case 1	0.83	0.42	Good/Good
	Case 2	0.79	0.46	Good/Good
	Case 3	0.78	0.48	Good/Good
	Case 4	0.79	0.47	Good/Good
	Case 5	0.72	0.53	Good/Good

To measure the relative degree of bias of each of the investigated cases, linear regressions were conducted between measured and predicted E* values. The closer the slope of the unconstrained regression lines to unity and the intercept to 0, the less is the bias in the predictions. These unconstrained regression lines and the line of equality are also shown in Figure 48 through Figure 52.

Figure 54 and Figure 55 present a comparison of the accuracy and relative bias measures of the MEPDG E* models for the different binder input data cases. All parameters were normalized such that the closer the value of the parameter to 0, the less the bias or the higher the accuracy (less scatter). The scatter parameters are R^2 and S_e/S_y, while the slope and intercept of the unconstrained regression lines are measures of the bias. Among the NCHRP 1-37A model with the 5 binder characterization cases, binder characterization case 3 (MEPDG Level 3 binder characterization) produced the most accurate predictions (R^2=0.90 and S_e/S_y=0.32). The bias (1-slope = 0.23) was lower than case 1 (1-slope = 0.28), case 2 (1-slope = 0.33), case 4 (1-slope = 0.37), and case 5 (1-slope = 0.40). However, this case showed a slight bias and scatter in the E* predictions at the higher temperatures as shown in Figure 50-a. In addition, the NCHRP 1-37A with binder characterization case 3 showed an intercept value of 0.82 which is slightly higher than case 1 (intercept = 0.73). This result was expected as the 1-37A model was developed based on level 3 binder data.

On the contrary, among the NCHRP 1-40D model with the 5 binder characterization cases, Case 1 which is based on Brookfield results yielded the highest R^2 (0.83) and the lowest S_e/S_y (0.42). This case also produced the lowest bias (1-slope = 0.33) compared to case 2 (1-slope = 0.34) and case 4 (1-slope = 0.40). However it produced high bias compared to case 3 (1-slope = 0.21) and case 5 (1-slope = 0.25). In addition, NCHRP 1-40D with binder characterization case 3 showed an intercept value of (0.93) which is lower than case 1 (intercept = 1.03).

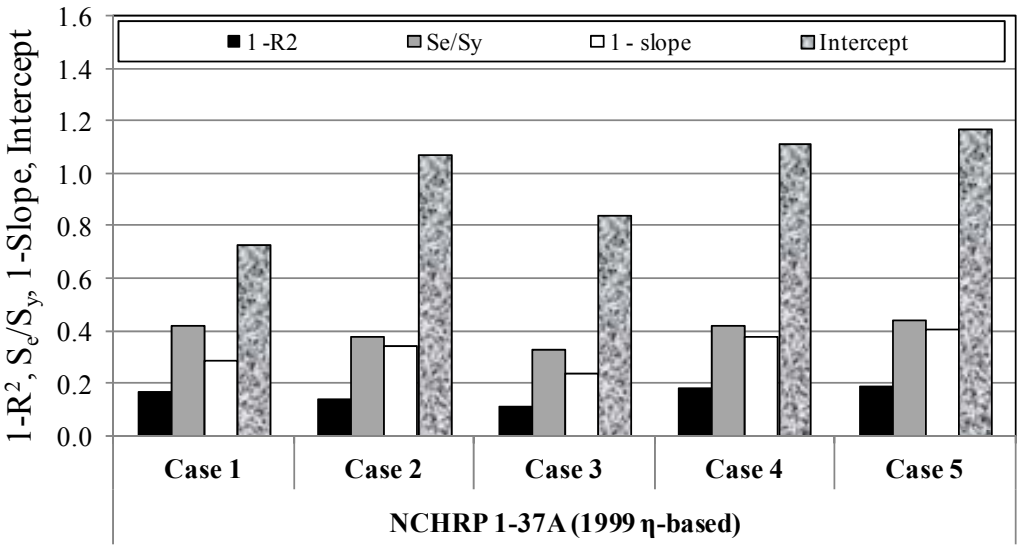

Figure 54. Accuracy and Bias of the NCHRP 1-37A E* Model

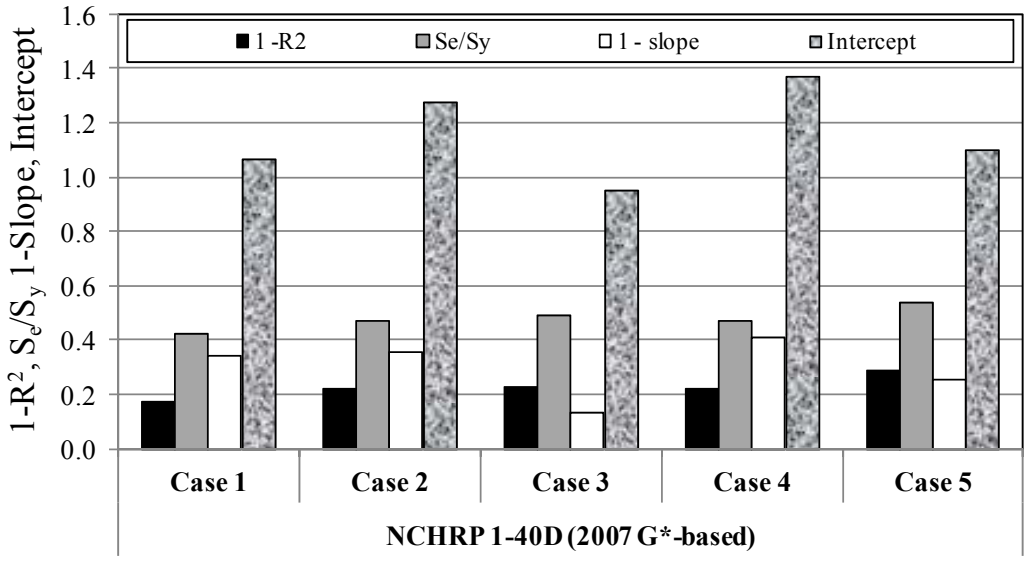

Figure 55. Accuracy and Bias of the NCHRP 1-40D E* Model

Comparison of MEPDG with Hirsch and Idaho E* Predictive Models

Based on the previous comparison of the prediction accuracy and bias of both Witczak E* models along with the different binder characterization methods, the following 2 E* predictive models and binder characterization levels were chosen to be compared with both Hirsch (2003 P_c-based E* predictive model) and Idaho (2008 GS-based E* predictive model) models:

- 1999 η-based E* predictive model (NCHRP 1-37A model with case 3 binder input).

- 2007 G*-based E* predictive model (NCHRP 1-40D model with case 1 binder input).

They above binder characterization cases were selected as they yielded the best E* estimates and lowest bias among the investigated binder input cases for each model. A brief background regarding Hirsch and Idaho models for E* predictions is presented in the flowing 2 subsections.

Hirsch Model

Christensen et al. developed an E* predictive model for HMA based upon an existing version of the law of mixtures, called the Hirsch model, which combines series and parallel elements of phases.[83] The original Hirsch model is presented in Figure 56 while the alternate version of the modified Hirsch model is shown in Figure 57. In this figure the relative proportion of material in parallel arrangement, called the contact volume, is not constant but varies with time and temperature. In Figure 56 and Figure 57, the subscripts p and s refer to the parallel and series phases, respectively. In Figure 57, Va refers to the aggregate volume exclusive of the contact volume; Vm refers to the binder volume; and Vv refers to the air void volume.

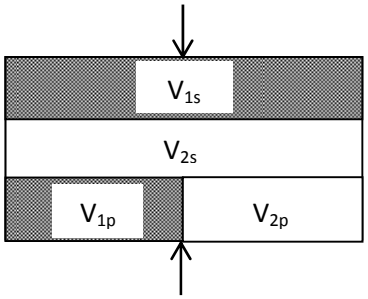

Figure 56. Schematic Representation of Composite Model for Hirsch Arrangement of Phases[83]

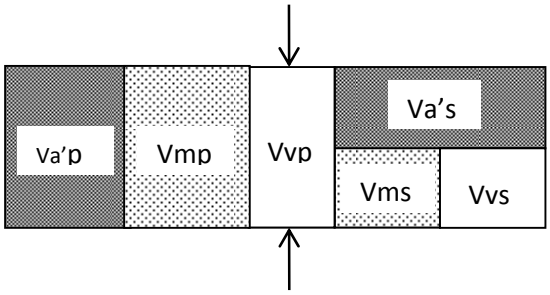

Figure 57. Schematic Representation of the Alternate Version of the Modified Hirsch Model[83]

Based on the schematic shown in Figure 57, a semi-empirical model that directly relates the dynamic modulus of HMA to the binder shear modulus, voids in mineral aggregate, and voids filled with asphalt was developed. This model is presented in Figure 58.

$$|E^*|_{mix} = Pc\left[4{,}200{,}000\left(1-\frac{VMA}{100}\right)+3|G^*|\left(\frac{VFA\times VMA}{10{,}000}\right)\right]$$
$$+(1-Pc)\times\left[\frac{1-\frac{VMA}{100}}{4{,}200{,}000}+\frac{VMA}{3\times VFA\times|G^*|}\right]^{-1}$$

$$Pc=\frac{\left(20+\frac{VFA\times 3|G^*|}{VMA}\right)^{0.58}}{650+\left(\frac{VFA\times 3|G^*|}{VMA}\right)^{0.58}}$$

where:

|E*| = Dynamic modulus of the mixture, psi
|G*| = Shear modulus of the binder, psi
VMA = Voids in the mineral aggregates, percent
VFA = Voids filled with Asphalt, percent
P_c = Contact factor

Figure 58. Hirsch Model[83]

As reported by the researchers, G* can be determined experimentally using DSR or a similar device. It can also be determined from mathematical models. G* should be determined at the same temperature and loading frequency of E* and in consistent units.[83] This model was developed based on 206 E* measurements from 18 different HMA mixtures containing 8 different binders.

One of the advantages of this model over Witczak models is that Hirsch model form is simpler. However, it was found to lose its prediction accuracy when applied to the database used for the development of the latest Witczak model.[16,17] Furthermore, it was also reported by various researchers that Hirsch model, similar to Witczak models, always yields significantly biased E* estimates at the extreme low and high temperatures.[16, 17, 58, 59, 64].

Gyratory Stability-based Idaho E* Predictive Model

Researchers at UI developed a model for the prediction of the dynamic modulus of Idaho superpave mixes.[64,71] This model is based on the inclusion of the GS as a parameter that reflects the mix internal structure. The model also includes other volumetric parameters. In the theoretical development of the model form, the theory of dimensional analysis was used to determine the model parameters and the shape form of the model.[71] The model is presented Figure 59. [64,71]

$$E^* = 1.08\left(\frac{\rho_w . G^* . GS . G_{mb}}{P_b(1-P_b)}\right)^{0.558}$$

Where:

E* = Dynamic modulus of the mixture, MPa
G* = Dynamic shear modulus for RTFO aged binder, MPa
P_b = Binder content by mix weight
GS = Gyratory Stability, kN.m
G_{mb} = Bulk specific gravity of the mix
ρ_w = Density of water, kg/m^3

Figure 59. Idaho GS-based E* Predictive Model

The aforementioned model was developed based on dynamic modulus measurements form 17 different laboratory mixtures containing 4 different aggregate structures and gradations, 3 binder contents per 2 aggregate structures (optimum asphalt content ± 0.5 percent from optimum), and 8 superpave performance grade binders. The model was also verified using 7 HMA field mixtures commonly used in pavement construction in Idaho.

Goodness-of-Fit Statistics of Original MEPDG, Hirsch, and Idaho E* Models

A summary of the number of mixes as well as the number of E* measurements for the NCHRP 1-37A, NCHRP 1-40D, Hirsch, and Idaho E* predictive models is given in Table 42. The goodness-of-fit statistics, in both logarithmic and arithmetic scales, of these models based on the original data used for their development are shown in this table. The goodness-of-fit statistics of the 4 models are relatively similar. However, the number of mixes and E* measurements used for the development of each of these models are significantly different.

Table 42. Goodness-of-Fit Statistics of Witczak, Hirsch, and Idaho E* Predictive Models based on Original Data used for their Developments[12, 54, 71, 83]

Parameter	E* Predictive Models			
	Witczak (1-37A)	Witczak (1-40D)	Hirsch	Idaho
No. of Mixes	205	346	18	17
Data Points	2750	7400	206	408
	Goodness-of-Fit in Arithmetic Scale			
S_e/S_y	0.34	0.44	NR	0.45
R^2	0.89	0.81	NR	0.80
	Goodness-of-Fit in Logarithmic Scale			
S_e/S_y	0.24	0.30	NR	0.22
R^2	0.94	0.91	0.98	0.95

Accuracy and Bias of the Investigated E* Predictive Models for Idaho Mixes

A master database for all parameters required by the 4 investigated models along with the laboratory measured E* values was established. E* values were then predicted using each of the 4 models. A comparison of laboratory measured and predicted E* values from NCHRP 1-37A, Hirsch, NCHRP 1-40D, and Idaho E* predictive models is shown in Figure 60.

Table 43 summarizes the goodness-of-fit statistics of the investigated models based on the 1128 data points from 27 typical Idaho mixtures in logarithmic scale. The goodness-of-fit statistics reveals that, the 4 models predict E* values that are in good /excellent agreement with the measured ones. The GS-based Idaho model yielded better E* predictions (S_e/S_y = 0.24, R^2=0.94) compared to NCHRP 1-37A (S_e/S_y = 0.33, R^2=0.90), Hirsch (S_e/S_y = 0.33, R^2=0.89) and NCHRP 1-40D (S_e/S_y = 0.42, R^2=0.83) models.

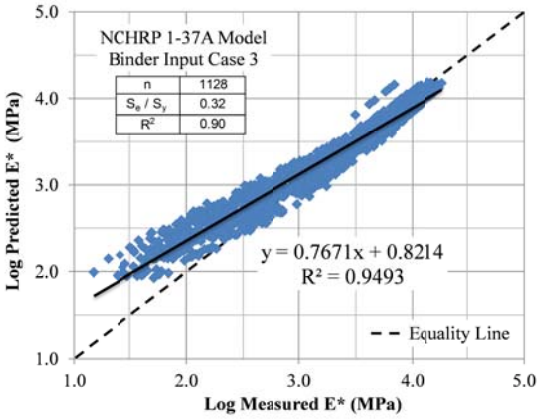

a) NCHRP 1-37A Model (Case 3 Binder Input)

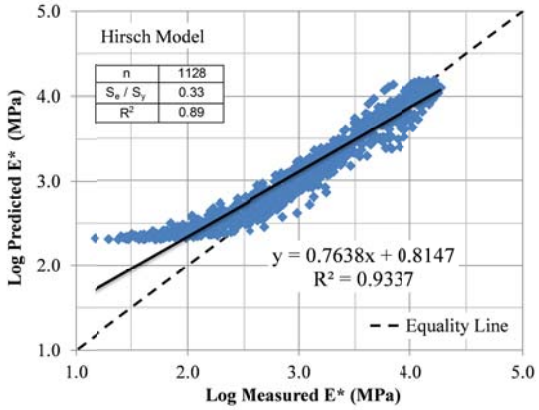

b) Hirsch Model

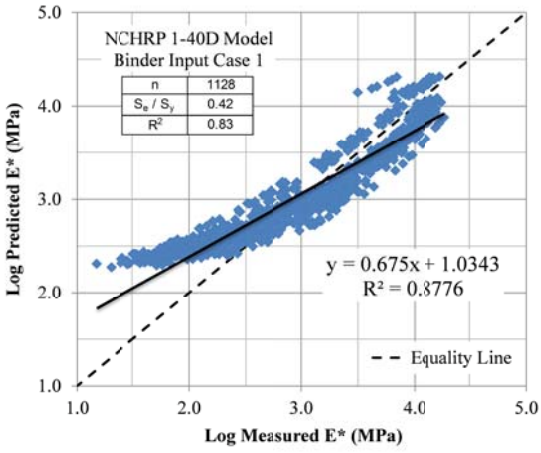

c) NCHRP 1-40D Model (Case 1 Binder Input)

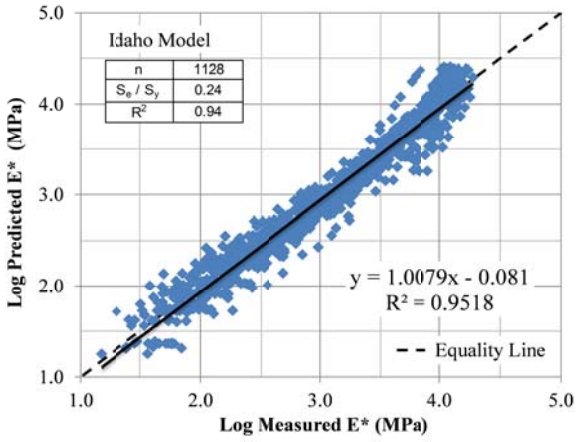

d) Idaho Model

Figure 60. Predicted versus Measured E* for Idaho Mixes

Table 43. Goodness-of-Fit Statistics of the Investigated Models in the Logarithmic Scale

E* Models	R^2	S_e/S_y	Evaluation
NCHRP 1-37A (1999 η-based)	0.90	0.32	Excellent /Excellent
Hirsch (2003 Pc-based)	0.89	0.33	Good/Excellent
NCHRP 1-40D (2007 G*-based)	0.83	0.42	Good/Good
Idaho (2008 GS-based)	0.94	0.24	Excellent/Excellent

Figure 61 shows a comparison of the unconstrained linear regression lines of the measured versus predicted E* resulted from the 4 models all in the same plot. This figure also shows the constrained line of equality (slope = 1 and intercept = 0). This figure clearly shows the bias of each of the 4 investigated models relative to the line of equality. One can infer from this figure and the slope of the unconstrained regression line of each model that NCHRP 1-37A, Hirsch and NCHRP 1-40D models produce highly biased E* predictions for Idaho mixtures, especially at the higher temperature and lower frequency range. It must be noted that E* values at high temperature and low frequency represent the critical values at which rutting occurs. Thus, NCHRP 1-37A, Hirsch and NCHRP 1-40D models may produce stiffer E* values compared to the actual values and consequently lower predicted rutting than the actual rutting. On the other hand, from Figure 61, one can infer that, the GS-based Idaho model showed the least biased E* estimates among the 4 investigated models. Only slight bias at the very low temperatures and the very high loading frequencies, (critical for pavement response for cracking) was found with this model.

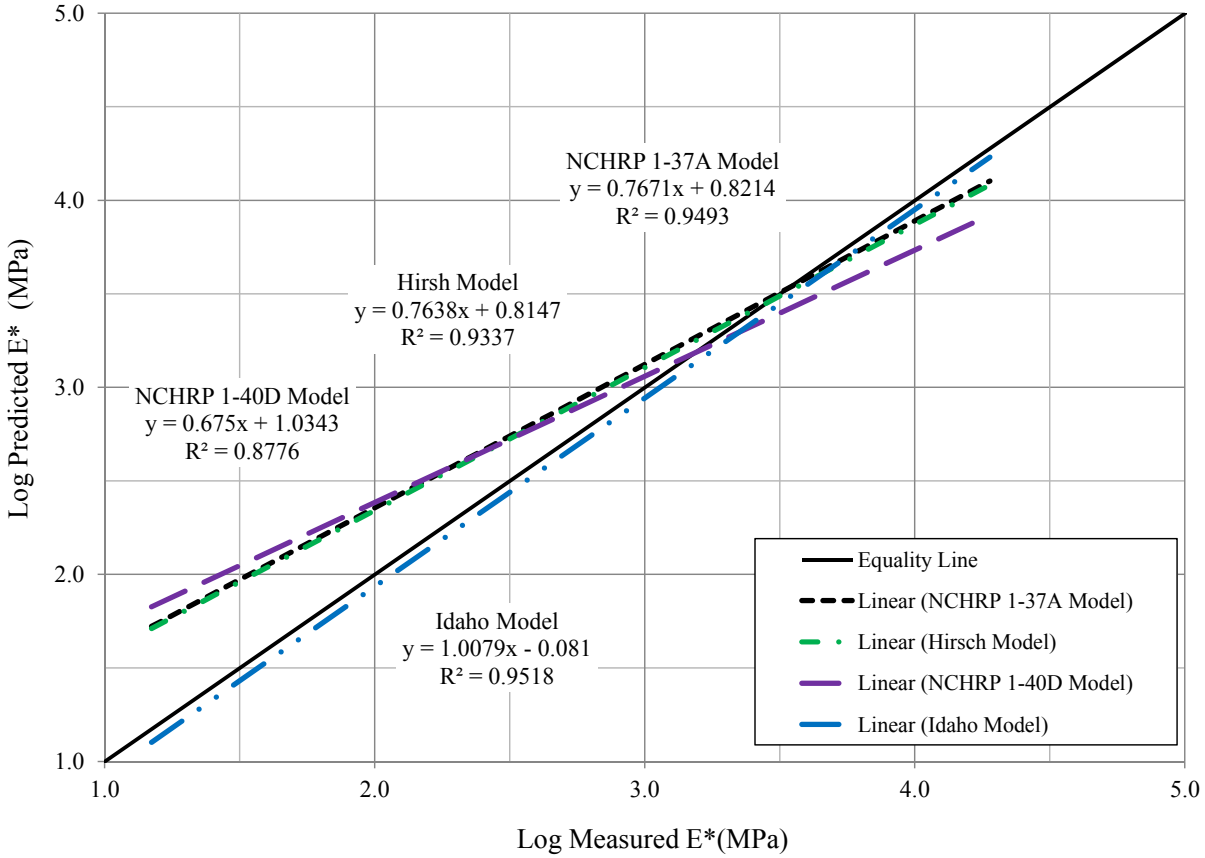

Figure 61. Unconstrained Linear Regression Lines of E* Predictions of the Investigated Models

A comparison of the bias and accuracy parameters of the investigated models in logarithmic scale is depicted graphically in Figure 62. All parameters were normalized such that, the closer the value of the parameter to 0, the less the bias or the higher the accuracy (less scatter). Figure 62 indicates that, among the investigated models, Idaho model has the lowest amount of bias and the highest accuracy in the prediction.

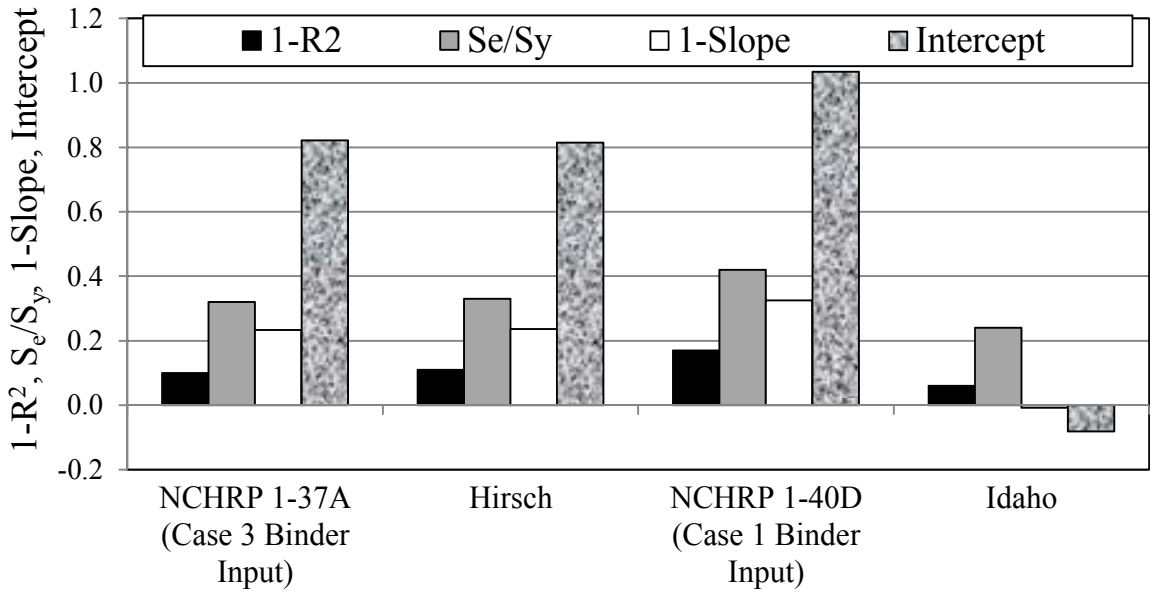

Figure 62. Comparison of the Bias and Accuracy of the Investigated Models

Based on the recommendations of the E* prediction comparisons, *E-Star 2010* software was built with the Visual Basic language to predict E* for HMA mixtures based on the Idaho GS-based model which is a function of specimen volumetric properties, binder characterization and GS. Figure 63 presents the main screens of *E-Star 2010* software.

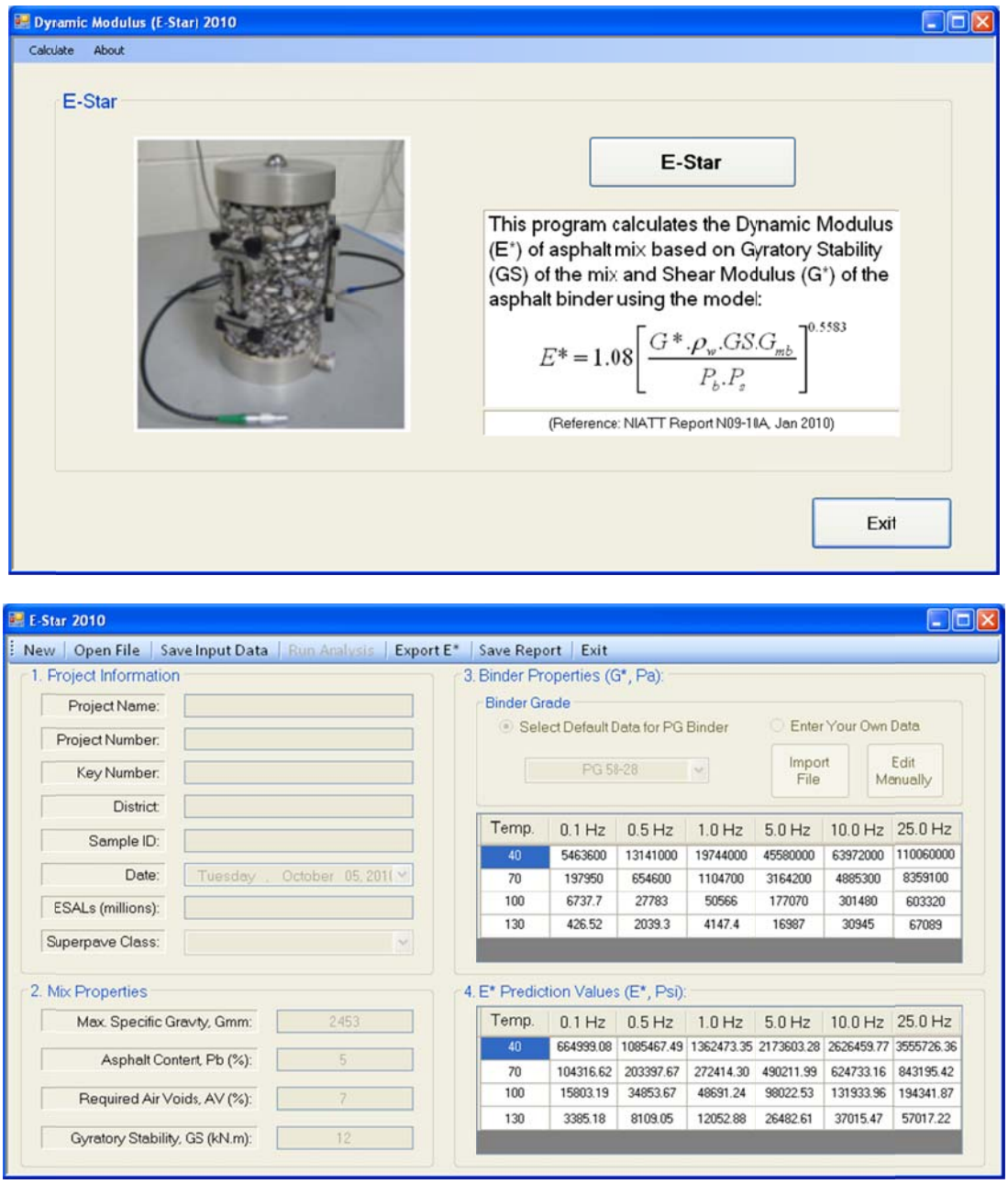

Figure 63. Screen Shots of the Main Screens of the *E-Star 2010* Software[(70)]

HMA and Binder Database

A user-friendly Excel spreadsheet containing ITD established database for MEPDG was created using simple macros. The HMA materials and binder database contains input parameters required for MEPDG HMA materials characterization. For each tested mix, the database contains the required MEPDG level 1 and levels 2 and 3 E* inputs (levels 2 E* data is the same as level 3). It also contains binder G* and δ at 10 rad/sec (levels 1 and 2 binder inputs) and binder PG grade (level 3 binder input). The gyratory stability data are also contained in the database. This data can be used with Idaho model for E* prediction. The HMA materials database also includes the master curve for each tested mixture and the fitting parameters of the master curves as well. Appendix D presents a user's guide for the developed database spreadsheet.

Chapter 5
Unbound Materials and Subgrade Soils Characterization

Resilient modulus of granular materials and subgrade soils is an important input parameter for pavement structure design. AASHTO 1993 and MEPDG require this parameter as the main input for the characterization of unbound granular base/subbase materials and subgrade soils. This chapter describes the unbound granular base/subbase materials and subgrade soils characterization effort for MEPDG implementation in Idaho. It presents the development of 2 models for level 2 MEPDG unbound granular and subgrade materials input. First, a multiple regression model that can be used to predict R-value of the unbound granular and subgrade materials as a function of the soil plasticity index and percent passing No 200 sieve. Second, a resilient modulus predictive model based on the estimated R-value is presented. This Chapter also presents the development of typical default values for the R-value, liquid limit, and plasticity index of Idaho unbound granular materials and subgrade soils.

MEPDG Hierarchical Input Levels

MEPDG requires the resilient modulus at optimum moisture content as the main input to characterize the unbound base/subbase and subgrade materials. It is used for the structural response computation models.[4] Resilient modulus can be either measured directly in the laboratory or obtained through the use of correlations with other material strength properties such as California Bearing Ratio (CBR), R-value, or soil index properties. There are 3 different levels in the MEPDG for the resilient modulus input of the unbound granular materials and subgrade soils. In level 1, the resilient modulus values are determined from cyclic triaxial tests on representative samples prepared at optimum moisture content and maximum dry density. The resilient modulus test results at the anticipated stress state are used to estimate the coefficients k_1, k_2, and k_3 using the constitutive model presented in Figure 64. The coefficients k_1, k_2, and k_3, not the actual M_r test data, are the direct input in the MEPDG for level 1 unbound granular base/subbase and subgrade characterization.

For level 2, the resilient modulus is estimated from correlations with soil index and strength properties. Models used in MEPDG for estimating M_r for level 2 inputs are given in Table 44. For MEPDG Level 3 inputs, user has the option to input an estimated value of M_r at optimum conditions. In addition, the software has built –in default values for the Mr at optimum moisture conditions for different soil classes according to the AASHTO and Unified Soil Classification (USC) systems. These Mr estimates are based on in-situ CBR values using the equation presented in Figure 65 which were adjusted for optimum moisture conditions using the relationship given in Figure 66.

$$M_r = k_1 p_a \left(\frac{\theta}{P_a}\right)^{k_2} \left(\frac{\tau_{oct}}{P_a} + 1\right)^{k_3}$$

where:

M_r = Resilient modulus, psi

θ = Bulk stress = $\sigma_1 + \sigma_2 + \sigma_3$

σ_1 = Major principal stress

σ_2 = Intermediate principal stress = σ_3 for M_r test on cylindrical specimen

σ_3 = Minor principal stress/confining pressure

τ_{oct} = Octahedral shear stress

$$= \frac{1}{3}\sqrt{(\sigma_1 - \sigma_2)^2 + (\sigma_1 - \sigma_3)^2 + (\sigma_2 - \sigma_3)^2}$$

P_a = Atmospheric pressure = 14.7 psi

k_1, k_2, k_3 = Regression constants

Figure 64. MEPDG Resilient Modulus Prediction Equation

Table 44. Models Relating Material Index and Strength Properties to M_r[4]

Strength/Index Property	Model	Comments	Test Standard
CBR	$M_r = 2555(CBR)^{0.64}$ Mr, psi	CBR = California Bearing Ratio, percent	AASHTO T193, "The California Bearing Ratio"
R-value	$M_r = 1155 + 555R$ Mr, psi	R = R-value	AASHTO T190, "Resistance R-Value and Expansion Pressure of Compacted Soils"
AASHTO layer coefficient	$M_r = 30000\left(\frac{a_i}{0.14}\right)$ Mr, psi	a_i = AASHTO Layer Coefficient	AASHTO Guide for the Design of Pavement Structures
PI and Gradation*	$CBR = \frac{75}{1 + 0.728(wPI)}$	wPI = P200*PI P200= Percent Passing No. 200 Sieve Size PI = Plasticity Index, Percent	AASHTO T27. "Sieve Analysis of Coarse and Fine Aggregates" AASHTO T90, "Determining the Plastic Limit and Plasticity Index of Soils"
DCP*	$CBR = \frac{292}{DCP^{1.12}}$	CBR = California Bearing Ratio, percent DCP =DCP Index, mm/blow	ASTM D 6951, "Standard Test Method for Use of the Dynamic Cone Penetrometer in Shallow Pavement Applications"

*Estimates of CBR are used to estimate M_r

$$M_r = 2555(CBR)^{0.64}$$

where:

M_r = Resilient modulus, psi

CBR = California bearing ratio, percent

Figure 65. Mr-CBR Relationship[4, 14]

$$M_{ropt} = \left[2.11 - 2.78 \cdot 10^{-5}\left(M_{r\ insitu}\right)\right] M_{r\,\text{insitu}}$$

where:

M_{ropt} = Resilient modulus at optimum moisture condition, psi

$M_{r\ insitu}$= Resilient modulus at in-situ moisture condition, psi

Figure 66. Equation to Estimate Mr at Optimum Moisture Condition[14]

A summary of the resilient modulus values at optimum conditions computed from the equations in Figure 64 and Figure 66 is given in Table 45 and Table 46 for soils classified using the USC and AASHTO classification systems, respectively. These tables are currently embedded in the MEPDG software. However, the Interim Mechanistic-Empirical Pavement Design Guide Manual of Practice is recommending the M_r values shown in Table 47 to be used as level 3 inputs for unbound base/subbase and subgrade for flexible and rigid pavements. These recommended values for the unbound granular and subgrade soils in flexible pavements are based on back-calculated moduli data from field FWD tests obtained from the LTPP database. The back-calculated moduli were corrected to reflect values at optimum moisture conditions. One may notice that the modulus values shown in Table 46 are more conservative compared to the values shown in Table 47.

Table 45. Current MEPDG Typical Resilient Modulus Values based on USC Classification[4, 14]

USCS Classification	Modulus at Optimum (ksi)	
	Range	Default Value
CH	5 - 13.5	8.0
MH	8 - 17.5	11.5
CL	13.5 - 24	17.0
ML	17 - 25.5	20.0
SW	28 - 37.5	32.0
SP	24 - 33	28.0
SW – SC	21.5 - 31	25.5
SW – SM	24 - 33	28.0
SP – SC	21.5 - 31	25.5
SP – SM	24 - 33	28.0
SC	21.5 - 28	24.0
SM	28- 37.5	32.0
GW	39.5 - 42	41.0
GP	35.5 - 40	38.0
GW – GC	28 - 40	34.5
GW – GM	35.5 - 40.5	38.5
GP – GC	28 - 39	34.0
GP – GM	31 - 40	36.0
GC	24 - 37.5	31.0
GM	33 - 42	38.5

Table 46. Current MEPDG Typical Resilient Modulus Values based on AASHTO Soil Classification[4, 14]

AASHTO Soil Classification	Modulus at Optimum (ksi)	
	Range	Default Value
A-1-a	38.5 - 42	40
A-1-b	35.5 - 40	38
A-2-4	28 - 37.5	32
A-2-5	24 - 33	28
A-2-6	21.5 - 31	26
A-2-7	21.5 - 28	24
A-3	24 - 35.5	29
A-4	21.5 - 29	24
A-5	17 - 25.5	20
A-6	13.5 - 24	17
A-7-5	8 - 17.5	12
A-7-6	5 - 13.5	8

Table 47. Recommended Resilient Modulus at Optimum Moisture According to the Interim MEPDG Manual of Practice[6]

AASHTO Soil Classification	Recommended Resilient Modulus at Optimum Moisture (AASHTO T 180), ksi		
	Base/Subbase for Flexible and Rigid Pavements	Embankment & Subgrade for Flexible Pavements	Embankment & Subgrade for Rigid Pavements
A-1-a	40	29.5	18
A-1-b	38	26.5	18
A-2-4	32	24.5	16
A-2-5	28	21.5	16
A-2-6	26	21.0	16
A-2-7	24	20.5	16
A-3	29	16.5	16
A-4	24	16.5	15
A-5	20	15.5	8
A-6	17	14.5	14
A-7-5	12	13.0	10
A-7-6	8	11.5	13

Level 2 Unbound Granular and Subgrade Materials Characterization for Idaho

The laboratory resilient modulus test procedure is tedious, complex, time consuming, and requires expensive equipment. It is envisioned that this test will not be used as a routine laboratory test for material characterization. At least in the near future it is not practical to rely on it for unbound granular and subgrade materials characterization. In addition, many states have an extensive database of either CBR or R-value for the subgrade soils. Furthermore, in the current MEPDG software version, using level 1 for the unbound base/subbase or subgrade material characterization requires many hours for 1 simulation run. This is not practical. Thus, MEPDG levels 2 and 3 inputs are expected to be used more commonly by SHAs for unbound and subgrade material characterization. In the meantime it is suggested that Idaho uses correlations with other material parameters to estimate the resilient modulus of the unbound granular materials and subgrade soils for their design.

Like some of the western states, Idaho is using the R-value for the unbound base/subbase and subgrade material characterization. MEPDG uses the Asphalt Institute (AI) relationship to estimate the resilient modulus from the R-value. This is considered level 2. The AI equation is also recommended by the AASHTO 1993 guide. The equation takes the form shown in Figure 67.

$$M_r = 1155 + 555*R$$

where:

M_r = Resilient modulus, psi

R = R-value

Figure 67. Asphalt Institute M_r-R-Value Equation[4, 84]

Literature R-Value Models

In a recent research project, completed by UI researchers, a multiple regression model for R-value prediction of ITD unbound granular and subgrade materials was developed. This model is based on historical ITD geotechnical soil testing results that were collected from ITD materials reports and soil-profile scrolls.[85] This historical data contains 8233 data records (dated from 1953 through 2008) representing all 25 classes of soils prescribed by the USC system. It was noticed during this research effort that the R-value tests before 1971 were conducted using an exudation pressure of 300 psi while the R-value tests after 1971 were conducted using an exudation pressure of 200 psi according to Idaho T-8. This necessitated a statistical adjustment of the pre-1971 R-values testing results to bring them into close general agreement with the post-1971 R-values testing results. This adjustment was completed by performing statistical hypothesis testing using a student's t-statistic on 2 sample means at a level of significance equals 0.05.[85] In case there was a significant difference between the sample means, the pre-1971 R-values for were then adjusted by a value equal to the difference between the 2 sample means. The distribution of the historical soil types (by district) used for the development of the R-value model is shown in Table 48. The frequency distribution of the R-values contained within this database is shown in Figure 68.

Table 48. Distribution of Soil Types by District used to Develop the R-Value Model (Values are Approximate Percentages of the Database Totals which is 8233 Points)[85]

District	CL	ML	CL-ML	Other Fine Soils	SC	SM	SC-SM	GC	GM	GC-GM	Other Coarse Soils
1	18	21	7	2	2	17	3	3	9	< 1	18
2	32	8	6	18	8	17	1	3	3	1	3
3	20	15	9	4	6	23	5	2	7	1	8
4	16	35	17	< 1	3	13	2	1	6	< 1	5
5	27	18	14	2	2	8	2	6	6	3	11
6	17	14	12	< 1	4	16	5	4	7	3	18
All	21	18	12	3	4	15	4	4	6	2	11

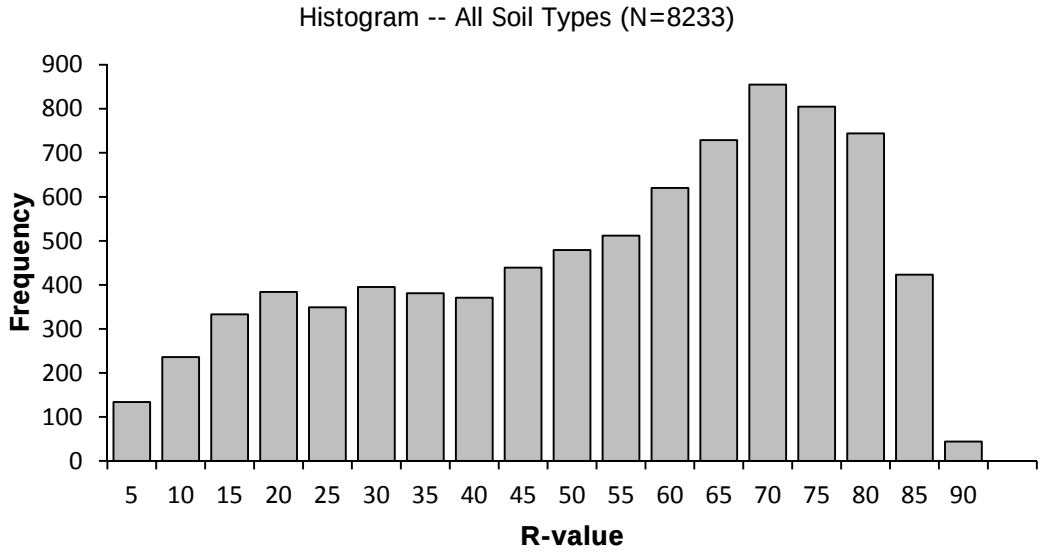

Figure 68. Frequency Distribution of the R-Values in the Database

Multiple regression models were then developed to predict R-value as a function of soil index properties using the whole database as well as database specific to each district. These models are summarized in Table 49.

Table 49. Multiple Regression Idaho R-Value Models[(85)]

District	Model	Number of Data Points	R^2
All	$R = 55.91 + 1.10(USC) - 0.41(PI) - 2.49[\sqrt[3]{(PI \times P200)}]$	8233	0.635
1	$R = 57.62 + 0.92(USC) - 0.51(PI) - 2.99[\sqrt[3]{(PI \times P200)}]$	428	0.676
2	$R = 57.099 + 0.43(USC) - 0.18(PI) - 2.96[\sqrt[3]{(PI \times P200)}]$	346	0.625
3	$R = 52.09 + 1.32(USC) - 0.11(PI) - 2.78[\sqrt[3]{(PI \times P200)}]$	2188	0.612
4	$R = 59.03 + 0.85(USC) - 0.34(PI) - 2.36[\sqrt[3]{(PI \times P200)}]$	1117	0.464
5	$R = 57.32 + 1.61(USC) - 0.90(PI) - 1.89[\sqrt[3]{(PI \times P200)}]$	2409	0.704
6	$R = 54.66 + 1.12(USC) - 0.83(PI) - 2.10[\sqrt[3]{(PI \times P200)}]$	1745	0.672

R = R-Value
USC = Numerical code, from 1 to 25, assigned to each USC class as shown in Table 50
PI = Plasticity index
P200 = Percentage passing #200 U.S. sieve

Table 50. USC Soil Class Code[85]

USC Soil Class	Code	USC Soil Class	Code
OH	1	SP-SC	14
OL	2	SW-SC	15
CH	3	SP-SM	16
MH	4	SW-SM	17
CL	5	GP-GC	18
CL-ML	6	GW-GC	19
ML	7	GP-GM	20
SC	8	GW-GM	21
GC	9	SP	22
SC-SM	10	SW	23
GC-GM	11	GP	24
SM	12	GW	25
GM	13		

Excluding the model for district 4, the models presented in Table 49 generally show reasonable R^2 values. However, because of the model forms shown above, there is a possibility that these models yield negative R-values especially in case of highly plastic clays. Thus, it was important to revise or develop a new model to predict the R-value of Idaho unbound granular base/subbase materials and subgrade soils. Another model form found in literature, and is used by ADOT was investigated. This model predicts the R-value as a function of percent passing 200 U.S. sieve (P200) and plasticity index (PI).The ADOT model is shown in Figure 69.

$$R = 10^{(2-0.006*P200-0.017*PI)}$$

Figure 69. ADOT R-Value Model[86, 87]

When this model was applied to the ITD database it yielded very poor predictions.

Development of a Revised R-Value Model for Idaho

The same ADOT model form (Figure 69) was used to develop an R-value model for Idaho. The ADOT model form was optimized, using the ITD's historical R-value database, based on minimizing the sum of squared error. The revised model yielded reasonable goodness-of-fit statistics (S_e = 13.56, S_e/S_y = 0.60, and R^2 = 0.637). The new revised model is shown in Figure 70.[88]

$$R = 10^{(1.893-0.00159*P200-0.022*PI)}$$

Figure 70. Revised R-Value Model for Idaho Unbound Granular and Subgrade Materials

Figure 71 shows the relationship between measured and predicted R-values using the proposed model (Figure 70). The frequency distribution of the residuals is depicted in Figure 72. This figure clearly shows that the residuals follow a relatively symmetrical normal distribution with a mean equals to 0 and a relatively small standard deviation. This model may be used to estimate the R-value of unbound granular materials and subgrade soils through simple index material properties when direct laboratory measurement of the R-value is unavailable.

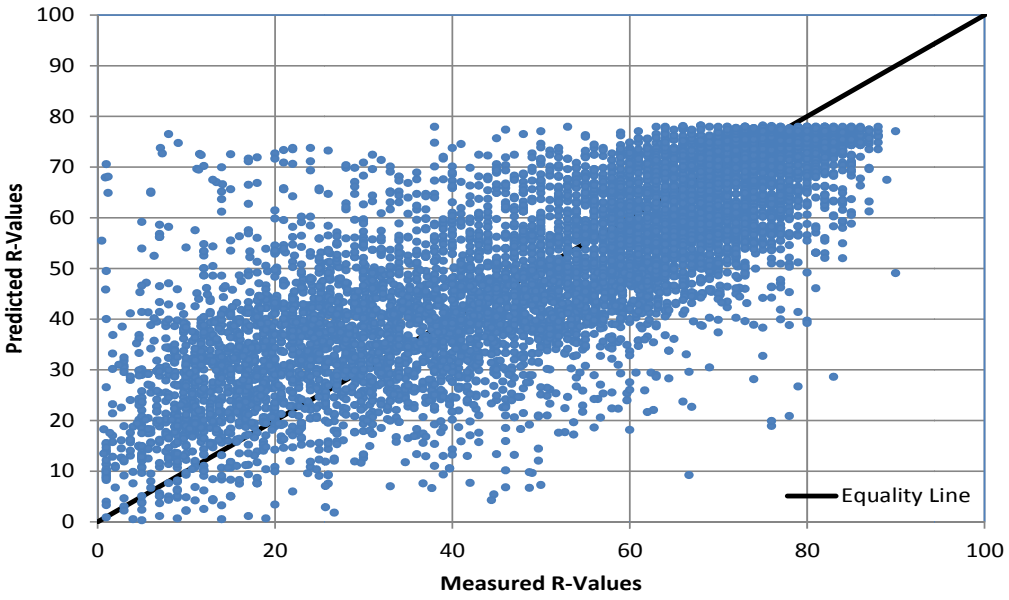

Figure 71. Measured versus Predicted R-values using the Proposed Model

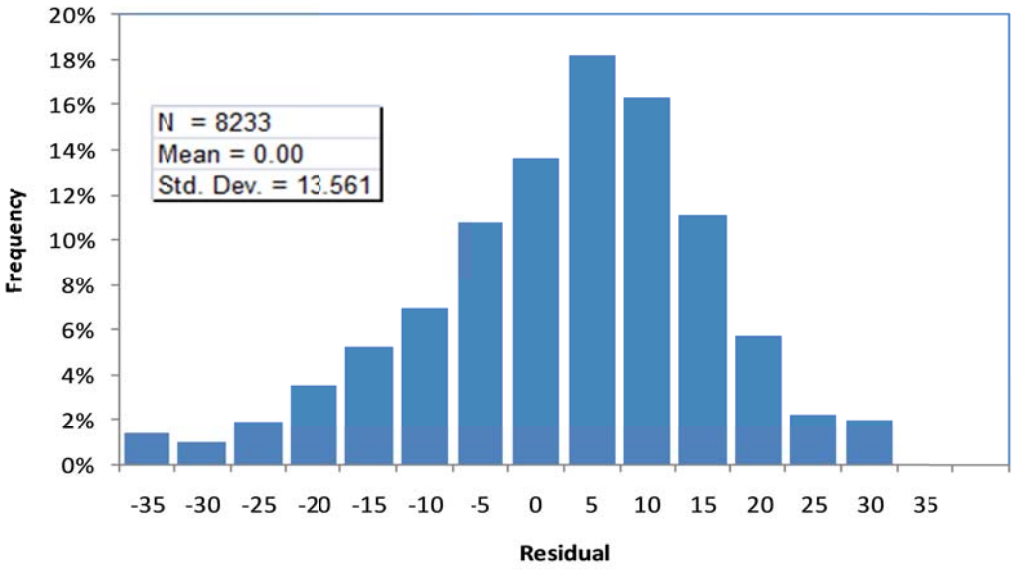

Figure 72. Frequency Distribution of the Residuals of the Proposed Model

Accuracy of the Asphalt Institute Model for M_r Prediction

For MEPDG level 2 unbound material characterization, once the R-value of the material is known, MEPDG uses the AI equation (Figure 67) to compute the resilient modulus. However, the AI manual advised that the accuracy of this equation drops for R-values larger than 20.[84] For larger R-values, this relationship tends to overestimate the modulus. In addition, this equation was developed based on very limited data points (only 6 different soil samples). Furthermore, Souliman reported that M^r values estimated from R-values using the AI equation for Arizona subgrade soils were at least 20 to 30 percent higher than M_r values estimated from CBR and the typical default M_r values in MEPDG (level 3) based on subgrade type.[34] Because of all these reasons, it is important to validate the prediction accuracy of the AI equation.

In order to verify the accuracy of the developed R-value model along with the AI M_r predictive model, laboratory measured M_r values of different subgrade soils were gathered from literature. These soils are representative of Indiana, Mississippi, Louisiana, Arizona, Ohio, and the soils used for the development of the AI equation.[33, 34, 84, 89, 90, 91, 92] The great majority of these subgrade soils were fine-grained materials. The percent fines ranged from 1 percent to 98 percent while the plasticity index ranged from zero (non-plastic) to 49. For these soils, some moduli values were measured directly in the lab at the anticipated field stresses [σ_3 = 13.8 kPa (2 psi), σ_1 = 41.4 kPa (6 psi)] and at the optimum moisture content for each soil. While for other soils, the moduli were estimated at the anticipated state of stress based on the k_1, k_2, k_3 values determined from laboratory test data at optimum or close to optimum moisture contents using the MEPDG model previously presented in Figure 64. The R-value of each soil was computed using the index soil properties with the help of the developed model (Figure 70). The estimated R-values were in the range of 5 to 78. It should be noted that for the AI soils, the R-value for each soil was measured in the laboratory. The moduli were then computed from the R-values using the AI model (Figure 67). Comparison between laboratory measured M_r values (gathered from literature) and Mr values predicted from the AI equation is shown in Figure 73. This figure shows that the AI equation yields very highly biased M_r estimates.

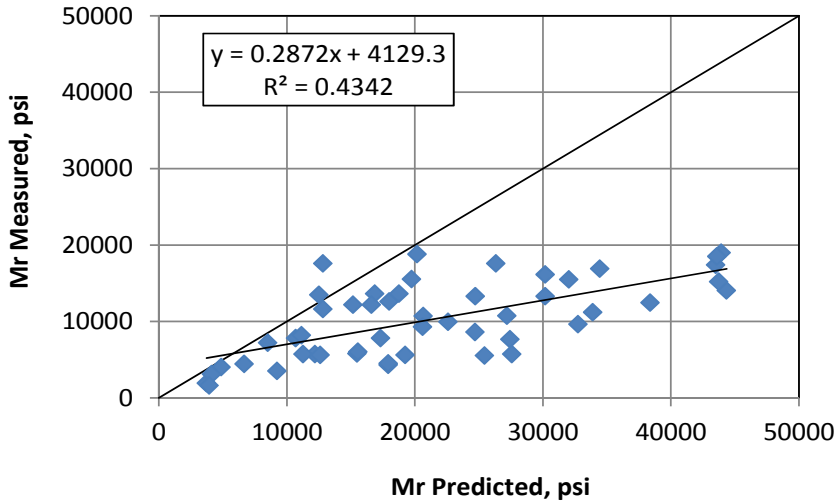

Figure 73. Comparison of Measured versus predicted M_r using the AI Model

Accuracy of the Other Literature M_r-R-Value Relationships

Additional literature Mr-R relationships were also investigated in this research. These relationships are used by ITD, WSDOT, and ADOT. These relationships are shown in Figure 74 through Figure 76.

$$Log\ M_r = (222+R)/67$$

where:

M_r = Resilient modulus, psi

R = R-value

Figure 74. ITD M_r-R Relationship

$$M_r = 720.5\ (e^{(0.0521*R)}-1)$$

where:

M_r = Resilient modulus, psi

R = R-value

Figure 75. WSDOT M_r-R Relationship

$$M_r = \frac{1815+225(Rmean)+2.40(Rmean)^2}{0.6(SVF)^{0.6}}$$

where:

M_r = Resilient modulus, psi

R = R-value

$Rmean$ = Weighted average R-value

SVF = Seasonal variation factor (SVE was set to 1 in this analysis)

Figure 76. ADOT M_r-R Relationship

Table 51 shows the literature data along with the predicted R-value and M_r using different literature relationships. Figure 77 through Figure 79 show comparison between laboratory measured and predicted M_r values of the literature soils using ITD, WSDOT, and ADOT models, respectively. Analyzing these results reveals that all investigated literature M_r-R relationships yielded highly biased predictions. Both AI and ADOT models significantly over predict the moduli. On the contrary, both ITD and WSDOT models were found to significantly under predict the moduli.

Table 51. Comparison of Measured and Predicted M_r using Different Relationships from Literature

Soil Type	P200	PI	Predicted R-Value	Predicted Resilient Modulus, psi				Measured M_r psi	Soil Source
				Asphalt Institute Model	ITD Model	WSDOT Model	ADOT Model		
CH	48	23	20	11017	3790	1098	7511	13489	Indiana
CL	37	16	30	15792	5094	2126	9710	12588	
CL	11	15	35	18091	5873	2812	10677	10698	
CL	18	21	25	13336	4375	1540	8617	12165	
CL	25	16	32	16450	5306	2308	9992	13607	
CL	24	9	45	23039	7979	4901	12614	17563	
CL–ML	21	5.2	56	27978	10833	8216	14399	15506	
CL–ML	23	4.6	57	28604	11262	8757	14617	9632	
CL–ML	22	14.7	34	17671	5723	2676	10504	18814	
CL–ML	24	6.2	52	26374	9809	6967	13834	13276	
CL	55	6.1	47	23783	8355	5307	12891	10718	Mississippi
CL-ML	56	8	42	21631	7313	4205	12080	13282	
SM-SC	40	7	47	23995	8466	5428	12970	7659	
CL	60	12.4	33	17302	5593	2560	10351	15513	
CL	96	13.1	28	14815	4795	1877	9284	13613	
SM	28	1	67	33497	15248	14283	16263	12429	
CL-ML	42	4.9	52	26373	9809	6966	13833	16137	
CL	98	13.3	28	14579	4725	1820	9179	12171	
CL	95	15	26	13607	4449	1598	8741	5800	Louisiana
CL	97	20	20	10750	3728	1053	7378	5700	
CL	94	15	26	13653	4462	1608	8762	6000	
CL	72	28	15	8167	3177	671	6016	3500	
CL	84	29	13	7534	3055	591	5657	7200	
CL	53	12	35	18060	5862	2802	10664	9300	
CL	80	23	18	9927	3543	921	6960	5700	
CL	82	24	17	9433	3436	847	6702	7800	
CL	87	20	21	11108	3812	1114	7556	5600	
CH	93	34	10	5946	2769	409	4696	4400	
ML	94	3	48	24108	8525	5494	13012	5700	
CH	76	43	7	4387	2514	255	3635	4000	
Cl	80	13	30	15713	5069	2105	9676	4300	
CL	80	13	30	15713	5069	2105	9676	4500	
CH	95	49	5	3380	2362	167	2851	1900	
CH	96	46	5	3735	2414	197	3140	3100	
SC	21.6	9.9	44	22249	7598	4499	12316	5504	Arizona
GP	1.2	0	78	38686	21025	23698	17916	14043	
SC	31.5	17.2	29	15209	4913	1975	9457	7819	
SC	25	12.1	39	19791	6525	3423	11362	9945	
GW	5.1	0	77	38153	20343	25508	17750	15191	
SP	3.8	0	77	38330	20567	22896	17805	18979	
SP-SM	6.5	0	76	37964	20106	22099	17691	17392	
SP-SM	6.0	0	76	38032	20190	22244	17712	18490	
Sand	-	-	60*	34455	16179	15694	15128	16900	Asphalt Institute
Silt	-	-	59*	33900	15633	14861	14963	11200	
Sandy Loam	-	-	21*	12810	4235	1431	7642	11600	
Silty Clay loam	-	-	21*	12810	4235	1431	7642	17600	
Silty Clay loam	-	-	18*	11145	3820	1120	6913	8200	
Heavy Clay	-	-	5*	3930	2444	214	3004	1600	
CL	56.3	8	42	21609	7303	4194	12072	11018	Ohio
CL	68.8	12.3	33	16870	5445	2429	10169	9282	

*Laboratory measured R-values

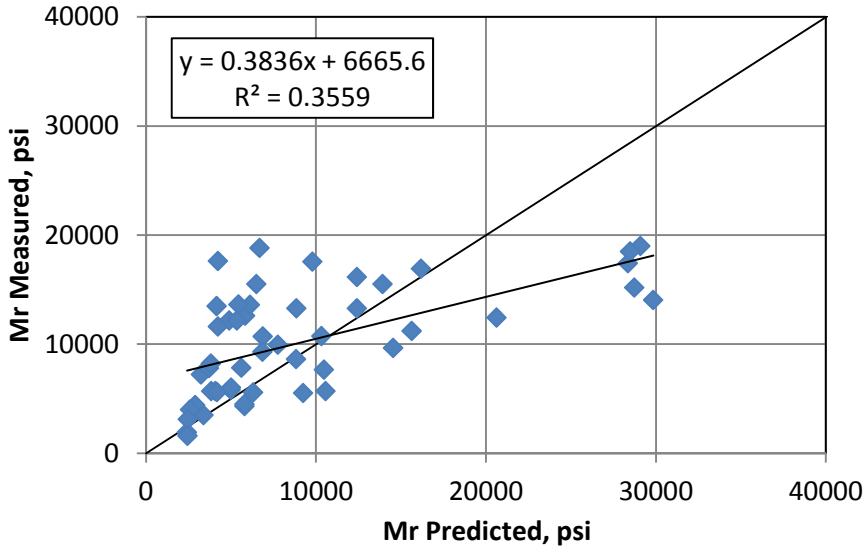

Figure 77. Comparison of Measured versus Predicted M_r using ITD Model

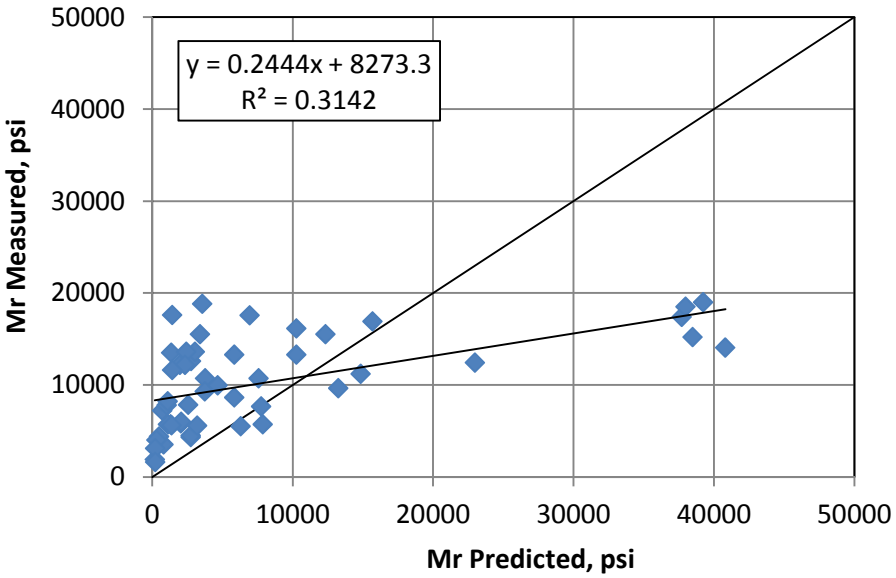

Figure 78. Comparison of Measured versus Predicted M_r using WSDOT Model

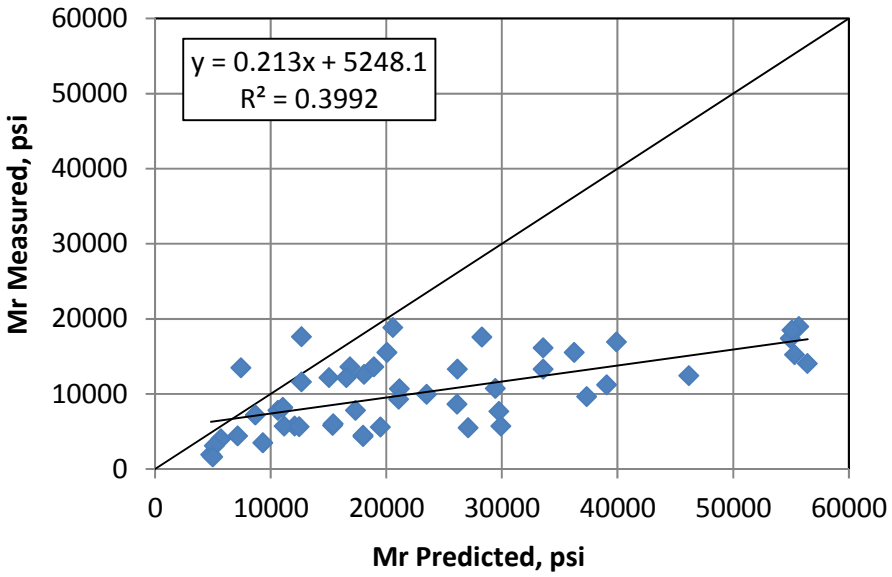

Figure 79. Comparison of Measured versus predicted M_r using the ADOT Model

Development of M_r-R-Value Model for Idaho

Based on the limited data found in literature and using regression analysis, a new model correlating M_r to R-value was developed. The model is shown in Figure 80.[88]

$$M_r = 1004.4\,(R)^{0.6412}$$

Figure 80. Proposed M_r-R-value Relationship for Idaho

This model yielded a reasonably fair goodness-of-fit statistics (S_e=0.169, S_y = 0.260, S_e/S_y=0.649, and R^2= 0.579). The M_r-R-vale relationship is shown in Figure 81. The scatter of the new model is lower than the AI model and the investigated literature models. Moreover, the new model has a significantly lower bias compared to investigated models.

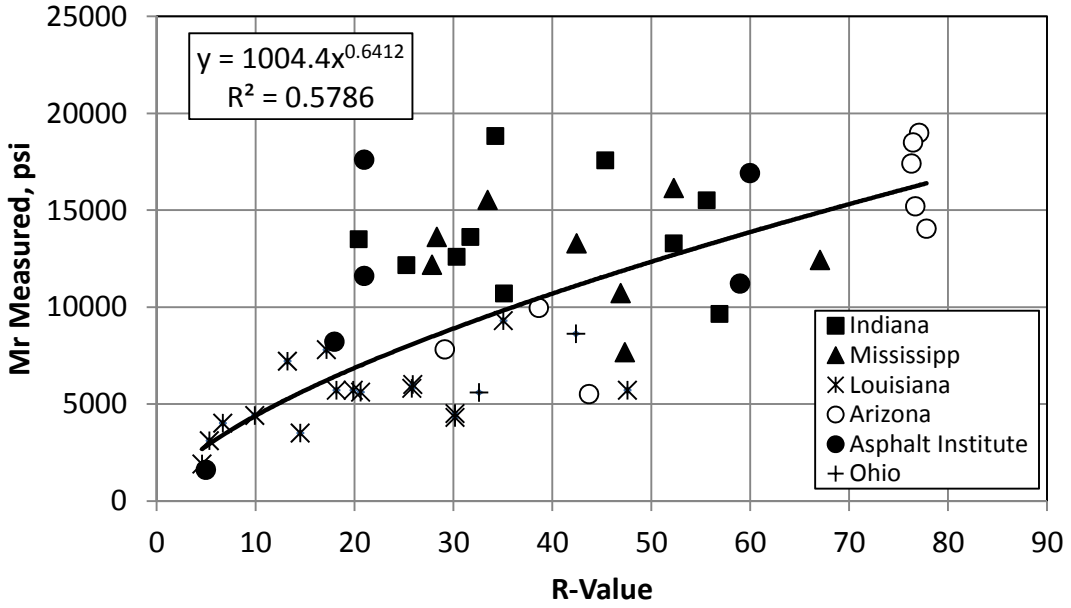

Figure 81. Relationship between R-value and Resilient Modulus based on Literature Data

It is recommended that ITD uses the developed predictive model for the R-value (if direct laboratory measurements are not available) along with the M_r-R value relationship (Figure 80) for MEPDG level 2 subgrade strength characterization. Because most of the literature data used in the development of the relationship shown in Figure 80 was for fine-graded soils, it is therefore recommended that this model only be used for similar types of subgrade soils.

Typical Level 3 R-Values for Idaho Unbound Granular/Subgrade Materials

ITD historical geotechnical testing results including the R-value and the USC soil class was used to develop typical default values and ranges of R-values for Idaho unbound granular materials and subgrade soils. These values can be used as the basis for estimating the resilient modulus for MEPDG level 3 inputs for unbound granular and subgrade materials characterization.

In order to develop typical R-values for the Idaho materials, first, the data was sorted and divided according to each USCS material class. A statistical analysis was then performed on the R-values contained in the database to compute the mean, median, standard deviation, minimum, maximum, and the confidence interval of the mean at 95 percent level of significance. The output of this statistical analysis is summarized in Table 52. The results summarized in this table show that, for all practical purposes, the average (mean) and median are in very close agreement. Thus, the average R-value for each soil class is chosen as the recommended typical default value for MEPDG level 3 unbound granular and subgrade characterization for Idaho. Recommended ranges of R-values for MEPDG level 3 material characterization for each USC class are shown in Table 53. These ranges are estimated based on +/- 1 standard deviation of the mean of each soil class.

Table 52. Descriptive Statistics of the ITD Historical Measured R-Values of the Unbound Granular and Subgrade Materials

Soil Type	Mean	Median	Standard Deviation	Minimum	Maximum	No. of Observations	95% Confidence Level
OH	32	30	17	14	57	5	21
OL	44	44	14	18	68	33	5
CH	15	11	11	1	49	130	2
MH	28	26	16	3	69	51	5
CL	27	25	14	1	70	1764	1
CL-ML	45	47	14	1	74	1005	1
ML	60	63	13	0.5	81	1508	1
SC	35	34	18	2	80	314	2
GC	38	38	18	1	76	283	2
SC-SM	53	56	17	5	84	290	2
GC-GM	60	62	14	21	90	171	2
SM	66	69	14	1	86	1247	1
GM	72	75	13	13	89	532	1
SP-SC	15	7	17	5	41	4	28
SW-SC	71	72	9	56	82	10	6
SP-SM	74	77	10	6	83	118	2
SW-SM	77	78	5	64	88	112	1
GP-GC	65	70	17	11	85	31	6
GW-GC	68	75	15	17	84	59	4
GP-GM	78	80	9	8	88	123	2
GW-GM	79	80	6	45	88	214	1
SP	74	75	4	65	83	63	1
SW	75	76	5	64	87	26	2
GP	77	78	7	50	86	54	2
GW	79	81	8	46	90	87	2

Table 53. Recommend Default R-Values and Ranges for Idaho Unbound Granular Materials and Subgrade Soils (MEPDG Level 3)

Soil Classification	Recommended R-Value	Recommended R-Value Range	
		Lower Bound	Upper Bound
OH*	32	15	49
OL	44	30	58
CH	15	3	26
MH	28	12	45
CL	27	12	41
CL-ML	45	31	60
ML	60	47	73
SC	35	17	54
GC	38	20	56
SC-SM	53	35	70
GC-GM	60	46	73
SM	66	52	80
GM	72	59	84
SP-SC*	15	1	32
SW-SC	71	62	80
SP-SM	74	64	84
SW-SM	77	72	82
GP-GC	65	49	82
GW-GC	68	53	83
GP-GM	78	69	86
GW-GM	79	73	85
SP	74	71	78
SW	75	69	80
GP	77	70	84
GW	79	72	87

*Only few data points were available for this soil class

For MEPDG level 3 unbound granular base material characterizations, a minimum R-value of 80 is recommended for granular base layers as per ITD specifications. A resilient modulus value of 38,000 to 40,000 psi is recommended for granular base layers.

Typical Index Properties for Level 3 Unbound Granular and Subgrade Material Characterization

The index material properties required by the MEPDG software are plasticity index, liquid limit, and material gradation. Actual testing results or default values for these properties are essential inputs, preferably the actual values. In order to find typical default values of the plasticity index (PI) and the liquid limit (LL) for Idaho unbound materials and subgrade soils, the ITD historical database collected from the different Idaho districts was statistically analyzed. Table 54 and Table 55 summarize the statistical analyses for the PI and LL of Idaho unbound granular materials and subgrade soils, respectively. The statistical results show that, generally the mean and median of the PI and LL for each soil type are very close. Thus, the mean value for the PI and LL of each soil type was selected to represent the typical value for ITD materials. These values are summarized in Table 56 and Table 57 for the PI and LL, respectively. Additionally, recommended ranges of PI and LL values for MEPDG level 3 unbound/subgrade materials characterization for each USC material class are also shown in Table 56 and Table 57. These ranges are estimated based on +/- 1 standard deviation of the mean of each soil class. For the recommended plasticity index values, the minimum value for non-plastic material (shown as 0 in the table) should be preferably set to 1 as this is required by the software for drainage reasons. It should be noted that the historical database included 4896 LL observations. Some soil types had very limited LL data records. For these soil types, it was decided that the available LL data points are not enough to recommend typical values and ranges.

Table 54. Statistical Summary of the Plasticity Index of ITD Unbound Materials and Subgrade Soils

Soil Type	Mean	Median	Standard Deviation	Minimum	Maximum	No. of Observations	95% Confidence Level
OH*	21	21	3	16	25	5	4
OL	7	5	6	0	20	33	2
CH	39	34	16	7	109	130	3
MH	24	23	10	0	47	51	3
CL-ML	5	5	1	4	10	1005	0
GC-GM	5	5	1	4	7	171	0
SM	0	0	1	0	4	1247	0
SP-SC*	16	11	13	6	35	4	21
SW-SC	10	5	9	4	25	10	6
SP-SM	0	0	0	0	3	118	0
SW-SM	0	0	0	0	3	112	0
GP-GC	8	7	3	4	16	31	1
GW-GC	11	10	6	4	28	59	2
GP-GM	0	0	1	0	3	123	0
GW-GM	0	0	1	0	4	214	0
SP	0	0	0	0	0	63	0
SW	0	0	1	0	5	26	0
GP	1	0	2	0	13	54	1
GW	1	0	2	0	7	87	0

* Only few number of data points were available

Table 55. Statistical Summary of the Liquid Limit of ITD Unbound Materials and Subgrade Soils

Soil Type	Mean	Median	Standard Deviation	Minimum	Maximum	No. of Observations	95% Confidence Level
OH*	62	60	4	57	68	5	5
OL	33	31	7	25	47	28	3
CH	65	59	20	50	169	130	3
MH	67	65	14	41	99	50	4
CL	35	33	10	2	130	1585	0
CL-ML	27	26	4	5	53	909	0
ML	24	24	4	2	49	601	0
SC	36	33	13	14	83	314	1
GC	33	31	8	10	78	269	1
SC-SM	25	24	5	2	41	290	1
GC-GM	26	25	4	17	40	171	1
SM	23	21	6	3	59	275	1
GM	24	22	7	0	53	86	2
SP-SC*	46	32	33	25	96	4	53
SW-SC	26	27	2	23	30	10	2
SP-SM*	23	23	1	22	24	2	13
SW-SM	19	18	2	16	21	11	1
GP-GC	26	24	6	20	50	31	2
GW-GC	30	29	10	4	71	59	3
GP-GM*	22	22	2	20	25	5	3
GW-GM	21	20	4	15	37	36	1
SP*	18	18	2	16	19	2	19
SW*	8	0	14	0	25	3	36
GP*	27	27	7	20	34	4	11
GW	23	22	5	18	38	16	3

* Only few number of data points are available

Table 56. Recommended Typical Values and Ranges of the Plasticity Index of ITD Unbound Subbase Materials and Subgrade Soils

Soil Type	Recommended PI	Recommended PI Range	
		Lower Bound	Upper Bound
OH*	21	17	24
OL	7	1	12
CH	39	23	56
MH	24	14	34
CL	15	8	21
CL-ML	5	4	7
ML	1	0	2
SC	16	6	25
GC	13	7	20
SC-SM	5	4	6
GC-GM	5	4	7
SM	0	0	1
GM	0	0	1
SP-SC*	16	3	29
SW-SC	10	2	19
SP-SM	0	0	0
SW-SM	0	0	1
GP-GC	8	5	11
GW-GC	11	5	17
GP-GM	0	0	1
GW-GM	0	0	1
SP	0	0	0
SW	0	0	1
GP	1	0	3
GW	1	0	2

*Only few number of data points are available

Table 57. Recommended Typical Values and Ranges of the Liquid Limit of ITD Unbound Materials and Subgrade Soils

Soil Type	Recommended LL	Recommended LL Range	
		Lower Bound	Upper Bound
OH	62	57	66
OL	33	26	40
CH	65	46	85
MH	67	53	81
CL	35	25	45
CL-ML	27	23	31
ML	24	20	28
SC	36	24	49
GC	33	25	40
SC-SM	25	20	30
GC-GM	26	21	30
SM	23	16	29
GM	24	16	31
SP-SC	46	13	79
SW-SC	26	24	29
SP-SM*	-	-	-
SW-SM	19	17	21
GP-GC	26	19	32
GW-GC	30	20	40
GP-GM	22	20	24
GW-GM	21	17	25
SP*	-	-	-
SW*	-	-	-
GP	27	20	34
GW	23	18	28

* Available data is not enough find typical values and ranges

Unbound and Subgrade Materials Database

The developed models are incorporated in the developed Excel spreadsheet database provided with this report. The typical R-value, LL, and PI for Idaho unbound granular materials and subgrade soils for each USC class are also stored this spreadsheet for quick and easy access of data. Appendix D presents a user's guide for the developed database spreadsheet.

Chapter 6
Traffic Characterization

Background

Traffic data is one of the most important inputs for any pavement design procedure. It is required for estimating the frequency and magnitude of loads that are applied to a pavement throughout its design life. Unlike AASHTO 1993 design methodology that requires the number of 18-kips Equivalent Single Axle Loads (ESALs) and ITD design methodology which requires the Traffic Index (TI) which is a function of ESALs as the only traffic input, MEPDG requires an extensive amount of traffic inputs for the design/analysis of pavement systems.

This chapter reports the development of traffic characterization inputs to facilitate MEPDG implementation in Idaho. It also investigates the impact of traffic inputs on MEPDG predicted distresses and smoothness. It should be noted that the analyses performed in this chapter was limited because traffic analysis was beyond the scope of this research work.

MEPDG Traffic Hierarchical Inputs

As for material characterization, MEPDG offers 3 hierarchical traffic input levels based on the amount of traffic data available.[4] Level 1 is considered the most accurate and it requires detailed knowledge of historical load, volume, and classification data at or near the project location. Level 2 is moderately accurate and it requires modest knowledge of traffic characteristics. It requires regional ALS instead of site-specific data. Level 3 is the least accurate as it only requires estimates of truck traffic volume data and statewide default ALS with no site-specific knowledge of traffic characteristics at the project site. An estimate of traffic inputs based on local experience is also considered level 3. Table 58 lists the differences between the MEPDG traffic input levels.

Table 58. MEPDG Traffic Input Levels

Traffic Input Level	Understanding of Traffic	Traffic Classification/Weight Data
Level 1	Very Good	Site/Segment-Specific
Level 2	Fair	Regional Summaries
Level 3	Poor	National/Statewide Default Summaries

MEPDG Traffic Inputs

Traffic inputs in MEPDG are very comprehensive and more sophisticated compared to other design procedures. MEPDG requires an extensive traffic data in certain formats. There are 4 basic traffic input categories in MEPDG as follows:

- Base year truck traffic volume
- Traffic volume adjustment
    - Monthly adjustment factors
    - Vehicle class distribution
    - Hourly truck distribution
    - Traffic growth factors
- Axle load distribution factors
- General Traffic inputs.
    - Number of axles per truck.
    - Axle configuration
    - Wheel base

MEPDG required traffic data can be obtained through WIM, automatic vehicle classification (AVC), and vehicle counts. The base year truck traffic volume and traffic volume adjustment factors can be obtained from WIM, AVC, and vehicle counts. ALS can only be determined from WIM data.

Idaho Traffic Data

WIM data severs as the primary source for the MEPDG traffic inputs. Traffic data collected at 25 WIM stations located in Idaho was provided by ITD. Most of this data was collected in 2009 with few sites with data for both 2008 and 2009. Table 59 summaries the location information of the recruited WIM sites. The provided WIM data is divided into 2 types; vehicle classification data and vehicle weight data. The vehicle classification data contains hourly truck traffic volume by truck class while the weight data contains hourly weights for each truck class and axle type as well as axle spacing. The format of the classification and weight data follows the FHWA C-card and W-card formats, respectively. More details regarding the C-cards and W-cards format can be found in the FHWA's Traffic Monitoring Guide (TMG).[93]

Table 59. Investigated WIM Stations

WIM Site ID	Functional Classification	Route	Mile Post	Nearest City
79	Principal Arterial -Interstate (Rural)	I-15	27.7	Downey
93	Principal Arterial -Interstate (Rural)	I-86	25.05	Massacre Rocks
96	Principal Arterial -Other (Rural)	US-20	319.2	Rigby
115	Principal Arterial -Interstate (Rural)	I-90	23.37	Wolf Lodge
117	Principal Arterial -Interstate (Rural)	I-84	231.7	Cottrell
118	Principal Arterial-Other (Rural)	US-95	24.1	Mica
119	Principal Arterial-Other (Rural)	US-95	85.2	Samuels
128	Principal Arterial -Interstate (Rural)	I-84	15.1	Black canyon
129	Principal Arterial-Other (Rural)	US-93	59.8	Gerome
133	Minor Arterial (Rural)	US-30	205.5	Filer
134	Principal Arterial -Other (Rural)	US-30	425.785	Georgetown
135	Principal Arterial -Other (Rural)	US-95	127.7	Mesa
137	Principal Arterial -Other (Rural)	US-95	37.075	Homedale
138	Principal Arterial -Other (Rural)	US-95	22.72	Marsing
148	Principal Arterial -Other (Rural)	US-95	363.98	Potlatch
155	Minor Arterial (Rural)	US-30	229.62	Hansen
156	Minor Arterial (Rural)	SH-33	21.94	Howe
166	Principal Arterial -Interstate (Rural)	I-84	-	Eden
169	Principal Arterial -Other (Rural)	US-95	56.002	Parma
171	Principal Arterial -Interstate (Rural)	I-84	114.5	Hammett
173	Principal Arterial -Interstate (Rural)	I-15	177.86	Dubois
179	Principal Arterial -Interstate (Rural)	I-86B	101.275	American Falls
185	Principal Arterial-Other (Rural)	US-12	163.01	Powell
192	Principal Arterial-Other (Rural)	US-93	16.724	Rogerson
199	Principal Arterial-Other (Rural)	US-95	441.6	Alpine

Generating MEPDG traffic inputs from WIM data requires an extensive effort. The *TrafLoad* software developed as part of the NCHRP 1-39 Project was used to process and generate the required MEPDG traffic data at the investigated WIM sites.[94] This is explained in the subsequent sections.

Idaho Traffic Classification Data

For truck traffic classification, MEPDG uses the 10 FHWA truck classes (Class 4 to class 13). These truck classes are shown in Figure 82. Classification data from the 25 WIM sites were analyzed in this study. In order to process the classification data using the *TrafLoad* software to generate MEPDG site-specific (level 1 data), continuous classification data for at least 12 consecutive months must be available. Analysis of the provided data showed that 21 out of the 25 WIM sites contained sufficient classification

data for at least 12 consecutive months. The rest of the WIM stations were missing the classification data for some months within the analysis period. Thus, truck volume distribution by class and month of the year were generated using the *TrafLoad* software for the 21 stations with sufficient data. The following subsections present the MEPDG level 1 classification data inputs for the analyzed WIM sites

Base Year Truck Traffic Volume and Directional and Lane Distribution Factors

Level 1 MEPDG Traffic volume inputs at the analyzed WIM sites are summarized in Table 60. This table shows the number of lanes in each direction, AADTT, direction of travel, and percentage of trucks in design direction and lane. The directional distribution factors of the trucks, shown in Table 60 ranged from 0.50 to 0.68 with an average of 0.56 and a standard deviation of 0.05. This value is very close the MEPDG default value which is 0.55. The design lane factor for the 4-lane roads ranged from 0.89 to 0.97 with an average of 0.93 and a standard deviation of 0.03. Again, this value agrees quite well with the MEPDG default value for of 0.90. For the 2-lane roads the lane and directional distribution factors are both equal to unity.

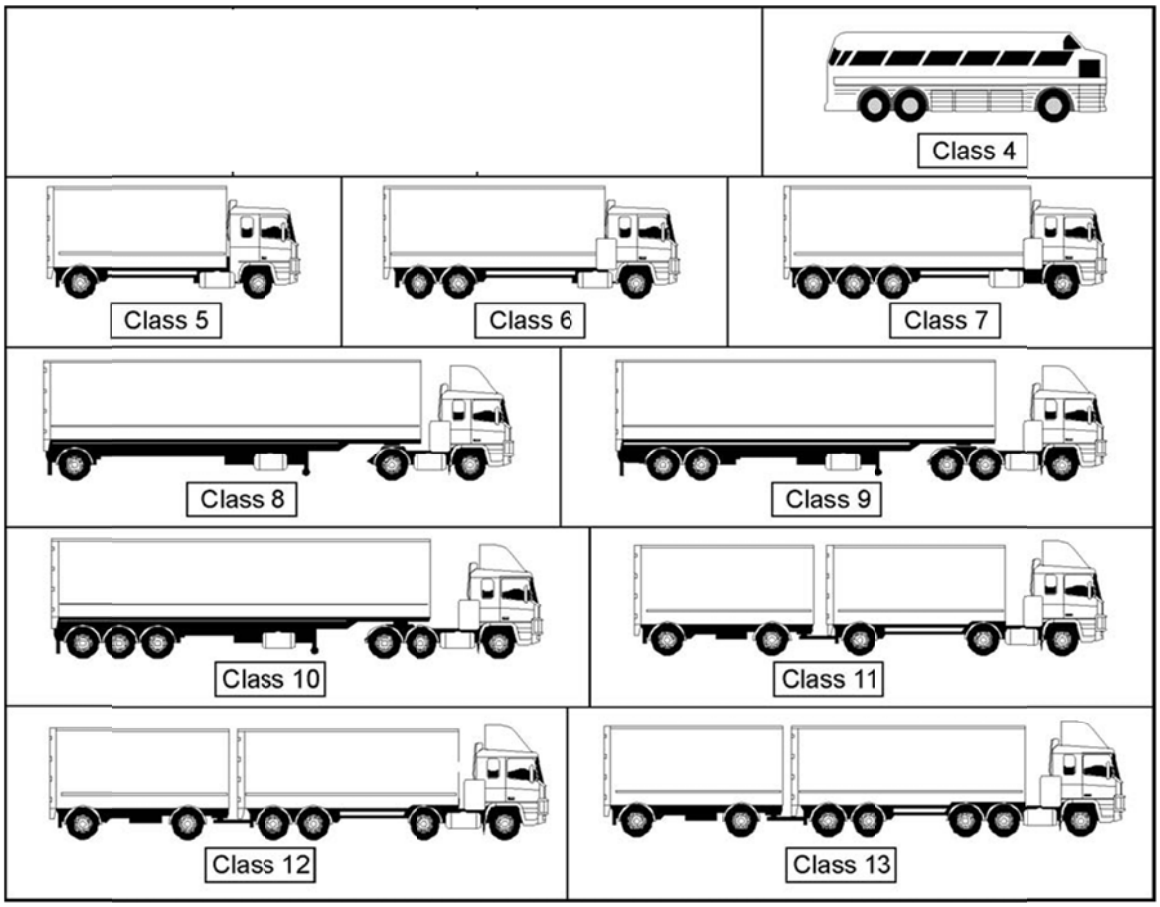

Figure 82. FHWA Vehicle Classes used in MEPDG[(95)]

Table 60. Traffic Volume Characteristics of the Analyzed WIM Sites

WIM Site ID	No. of Lanes in Design Direction	AADTT	Travel Direction	Percent Trucks in Design Direction	Percent Trucks in Design Lane
79	2	1917	NB/SB	55/45	97
93	2	912	EB/WB	54/46	97
96	2	2213	NEB/SWB	51/49	89
115	2	1013	EB/WB	32/68	89
117	2	2449	SEB/NWB	65/35	95
118	2	963	NEB/SWB	49/51	95
128	1	4736	SEB/NWB	50/50	100
129	1	871	NB/SB	45/56	100
133	1	671	NB/SB	44/56	100
134	1	863	EB/WB	45/55	100
135	1	403	EB/WB	43/57	100
137	1	413	EB/WB	51/49	100
138	1	377	SEB/NWB	54/46	100
148	1	290	EB/WB	54/0.46	100
155	1	302	NB/SB	50/50	100
156	1	93	NB/SB	43/57	100
171	2	3978	SEB/NWB	50/50	95
179	1	569	NB/SB	43/57	100
185	1	75	NB/SB	45/55	100
192	2	541	NB/SB	54/46	93
199	2	1829	EB/WB	35/65	47

NB = North Bound, SB = South Bound, EB = East Bound, WB = West Bound, NEB = North East Bound, NWB = North West Bound, SEB = South East Bound, SWB = South West Bound

Vehicle Class Distribution

Vehicle class distribution represents the percent of truck volume by truck class within the base year AADTT. Table 61 summarizes the site-specific VCD. Data in this table shows that at the majority of the sites, the predominant truck class is class 9 followed by class 5 trucks.

In case of the absence of accurate truck traffic classification, there are 17 TTC groups in MEPDG that can be used based on the user's selection. MEPDG TTC groups represent default (level 3) truck traffic combinations based on the analysis of traffic data from 133 LTPP sites. MEPDEG default TTC groups are shown in Table 62. The criterion used for the development of the 17 TTC groups is illustrated in Table 63.

Table 61. Percentage Vehicle Class Distribution

WIM Site ID	Vehicle Class									
	4	**5**	**6**	**7**	**8**	**9**	**10**	**11**	**12**	**13**
79	1.77	21.20	2.13	0.50	8.35	49.07	5.19	1.11	1.01	9.67
93	0.99	11.21	1.31	0.11	4.09	52.90	12.73	0.76	0.59	15.33
96	1.94	45.59	6.60	0.95	7.64	27.43	6.73	0.18	0.32	2.62
115	2.62	29.15	7.15	10.82	5.31	33.57	7.92	0.26	1.03	2.18
117	1.03	5.96	3.86	7.20	4.56	52.35	15.06	1.45	1.33	7.20
118	2.50	48.01	11.18	14.05	4.19	8.84	10.52	0.02	0.04	0.65
128	1.25	16.44	1.75	0.22	5.49	54.73	9.96	2.28	1.54	6.34
129	5.10	37.84	6.61	0.64	7.29	22.21	11.36	0.45	0.17	8.33
133	1.34	46.53	10.18	7.73	7.54	18.56	5.12	0.08	0.01	2.92
134	2.15	21.28	1.90	0.36	5.51	61.01	3.43	0.19	0.27	3.91
135	1.84	42.40	4.74	0.82	9.71	30.16	7.54	0.53	0.08	2.19
137	5.37	8.56	10.73	0.32	6.94	52.33	8.71	0.61	0.18	6.26
138	1.14	3.82	2.39	0.03	5.18	72.76	6.35	2.23	0.58	5.54
148	2.11	7.69	13.66	1.16	5.02	24.87	41.78	0.00	0.12	3.59
155	17.94	7.73	11.46	3.10	8.46	16.75	15.21	2.07	2.33	14.95
156	1.01	4.00	5.12	0.00	4.96	39.99	12.72	0.00	0.08	32.12
171	1.17	3.37	1.51	0.24	3.46	69.49	9.24	1.64	1.48	8.41
179	0.35	10.37	9.84	0.53	2.64	35.85	13.36	0.00	0.00	27.07
185	0.26	4.77	9.10	0.45	8.05	46.29	21.53	0.00	0.00	9.55
192	3.40	4.90	2.18	0.60	7.24	75.47	3.68	0.50	0.26	1.78
199	2.98	38.76	9.94	12.49	5.12	11.90	11.67	0.68	1.06	5.40

Table 62. MEPDG TTC Group Description and Corresponding VC Distribution Values[6]

TTC Group	TTC Description	Vehicle/Truck Class Distribution (percent)									
		4	5	6	7	8	9	10	11	12	13
1	Major Single-Trailer Truck Route (Type I)	1.3	8.5	2.8	0.3	7.6	74	1.2	3.4	0.6	0.3
2	Major Single-Trailer Truck Route (Type II)	2.4	14.1	4.5	0.7	7.9	66.3	1.4	2.2	0.3	0.2
3	Major Single- and Multi-Trailer Truck Route (Type I)	0.9	11.6	3.6	0.2	6.7	62	4.8	2.6	1.4	6.2
4	Major Single-Trailer Truck Route (Type III)	2.4	22.7	5.7	1.4	8.1	55.5	1.7	2.2	0.2	0.4
5	Major Dingle- and Multi-Trailer Truck Route (Type II).	0.9	14.2	3.5	0.6	6.9	54	5.0	2.7	1.2	11.0
6	Intermediate Light and Single-Trailer Truck Route (I)	2.8	31.0	7.3	0.8	9.3	44.8	2.3	1.0	0.4	0.3
7	Major Mixed Truck Route (Type I)	1.0	23.8	4.2	0.5	10.2	42.2	5.8	2.6	1.3	8.4
8	Major Multi-Trailer Truck route (Type I)	1.7	19.3	4.6	0.9	6.7	44.8	6.0	2.6	1.6	11.8
9	Intermediate Light and Single-Trailer Truck Route (II)	3.3	34.0	11.7	1.6	9.9	36.2	1.0	1.8	0.2	0.3
10	Major Mixed Truck Route (Type II)	0.8	30.8	6.9	0.1	7.8	37.5	3.7	1.2	4.5	6.7
11	Major Multi-Trailer Truck Route (Type II)	1.8	24.6	7.6	0.5	5.0	31.3	9.8	0.8	3.3	15.3
12	Intermediate Light and Single-Trailer Truck Route (III)	3.9	40.8	11.7	1.5	12.2	25.0	2.7	0.6	0.3	1.3
13	Major Mixed Truck Route (Type III)	0.8	33.6	6.2	0.1	7.9	26	10.5	1.4	3.2	10.3
14	Major Light Truck Route (Type I)	2.9	56.9	10.4	3.7	9.2	15.3	0.6	0.3	0.4	0.3
15	Major Light Truck Route (Type II)	1.8	56.5	8.5	1.8	6.2	14.1	5.4	0.0	0.0	5.7
16	Major Light and Multi-Trailer Truck Route	1.3	48.4	10.8	1.9	6.7	13.4	4.3	0.5	0.1	12.6
17	Major Bus Route	36.2	14.6	13.4	0.5	14.6	17.8	0.5	0.8	0.1	1.5

Table 63. MEPDG Truck Traffic Classification Criterion[4]

TTC Group	Vehicle Type	Percent of AADTT			
		Class 9	Class 5	Class 13	Class 4
1	Truck	>70	<15	<3	-
2	Truck	60 – 70	<25	<3	-
3	Truck	60 – 70	5 – 30	3-12	-
4	Truck	50 – 60	8 – 30	0 - 7.5	-
5	Truck	50 – 60	8 – 30	>7.5	-
6	Truck	40 - 50	15 – 40	<6	-
7	Truck	40 - 50	15 – 35	6-11	-
8	Truck	40 - 50	9-25	>11	-
9	Truck	30 - 40	20 -45	<3	-
10	Truck	30 - 40	25 - 40	3-8	-
11	Truck	30 - 40	20 - 45	>8	-
12	Truck	20 - 30	25 - 50	0 - 8	-
13	Truck	20 - 30	30 - 40	>8	-
14	Truck	<20	40 - 70	<3	-
15	Truck	<20	45 - 65	3-7	-
16	Truck	<20	50 - 55	>7	-
17	Bus	-	-	-	>35

The same criterion shown in Table 63 was used to establish TTC groups for Idaho Traffic data. The developed TTC groups for Idaho are shown in Table 64. As this table shows, 6 WIM sites classification data did not match any of the MEPDG recommended TTC groups.

Table 64. Idaho Truck Traffic Classification Groups

WIM Site ID	TTC Group
79	7
93	5
96	12
115	9
117	NA
118	14
128	4
129	13
133	14
134	3
135	12
137	4
138	NA
148	NA
155	NA
156	NA
171	3
179	NA
185	NA
192	1
199	NA

NA = Not Applicable

Monthly Adjustment Factors (MAF)

Truck traffic monthly adjustment factors (MAF) are used to proportion the annual truck traffic for each month of the year. They are expresses as shown in Figure 83.

$$\mathrm{MAF}_i = \frac{AMDTT_i}{\frac{1}{12}\sum_{i=1}^{12} AMDTT_i}$$

where:

MAF_i = Monthly adjustment factor for month i
$AMDTT_i$ = Average monthly daily truck traffic for month i
i = Month of the year

Figure 83. Equation to Calculate Monthly Adjustment Factors[(4)]

Before the determination of the MAF at the investigated WIM sites, the normalized monthly VC distribution plots were created for each WIM data. These plots help identifying any unexpected change in the vehicle mix. These plots are presented in Appendix E. The normalized monthly VC distribution plots can be categorized into 2 cases as follows:

- Case 1: no shift in the normalized monthly VC distribution. The normalized VC distribution curves were consistent. Site 79 is an example of this case. This is shown in Figure 84.
- Case 2: some change in the normalized monthly VC distribution curves. The normalized monthly VC distribution curves showed some shift. WIM site 117 represents an example of this case. This is shown in Figure 85. However, for most of the WIM sites only 12 months of classification data were used in the analysis which is not enough assess these trends.

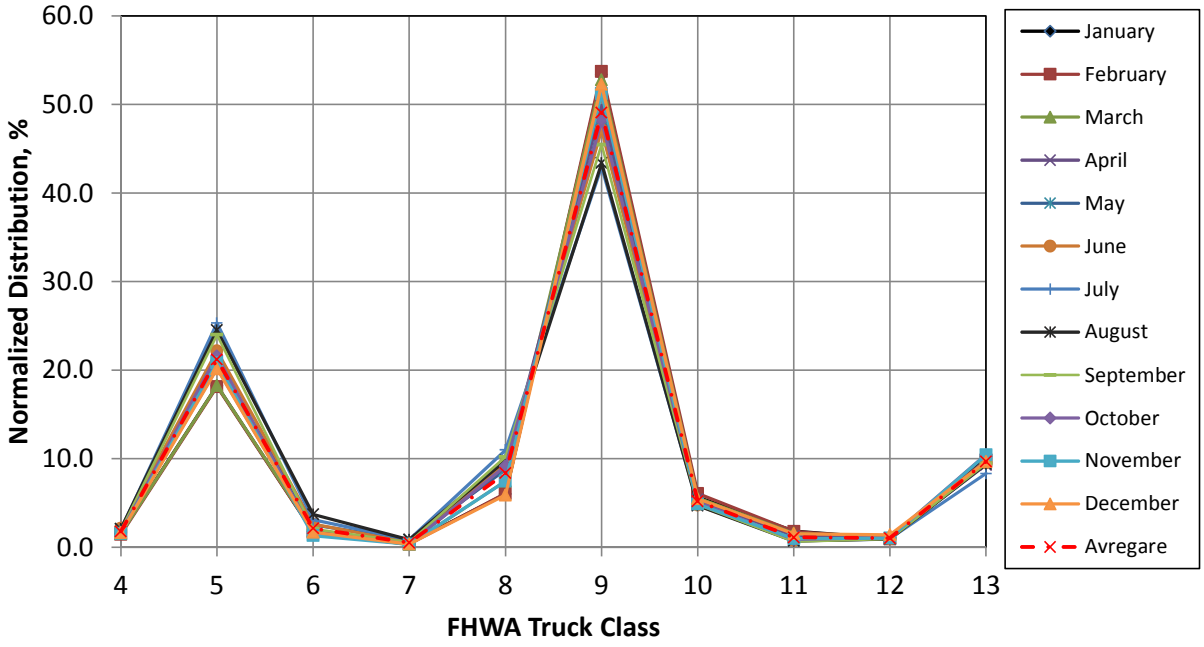

Figure 84. Normalized Monthly VC Distribution at WIM Site 79

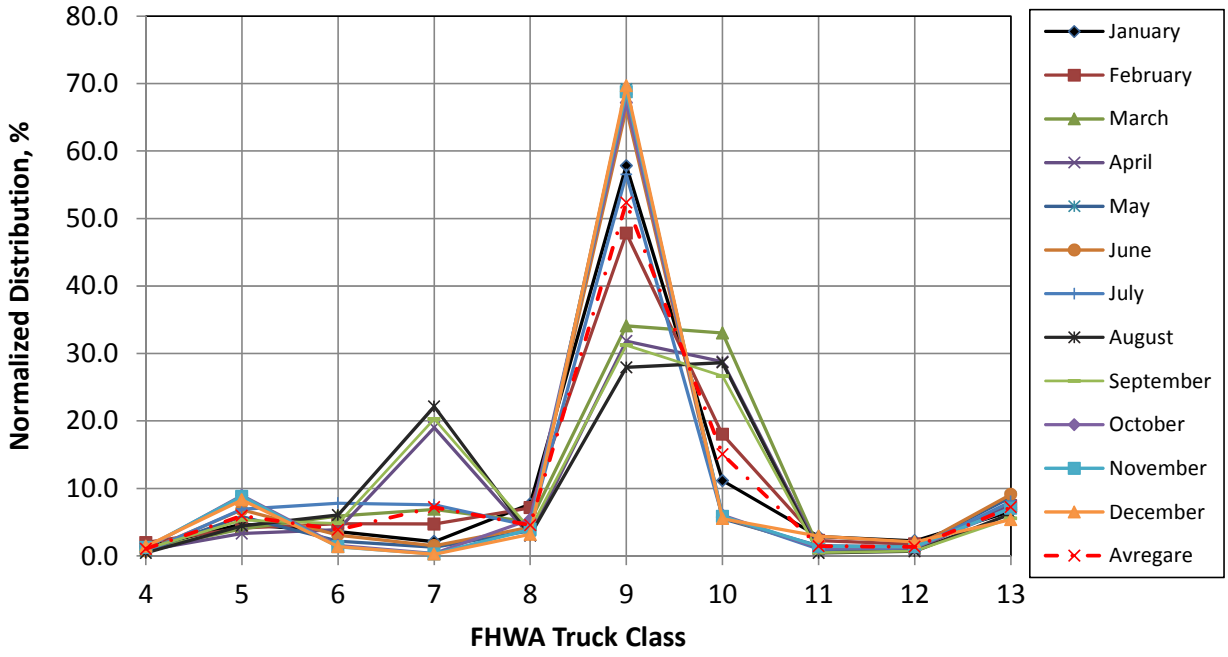

Figure 85. Normalized Monthly VC Distribution at WIM Site 117

Site-specific 1 MAF were established for each vehicle class using the *TrafLoad* software. Figure 86 exemplifies the MAF for WIM site 79. The MAF for the analyzed WIM stations are provided in electronic format. For each truck class the sum of MAF should be 12, while for all truck classes the average should be 1. The developed factors show that truck volumes vary from month to month. In MEPDG, a typical default (level 3) MAF value of 1.0 is suggested for all truck classes and all months when level 1 data is unavailable.

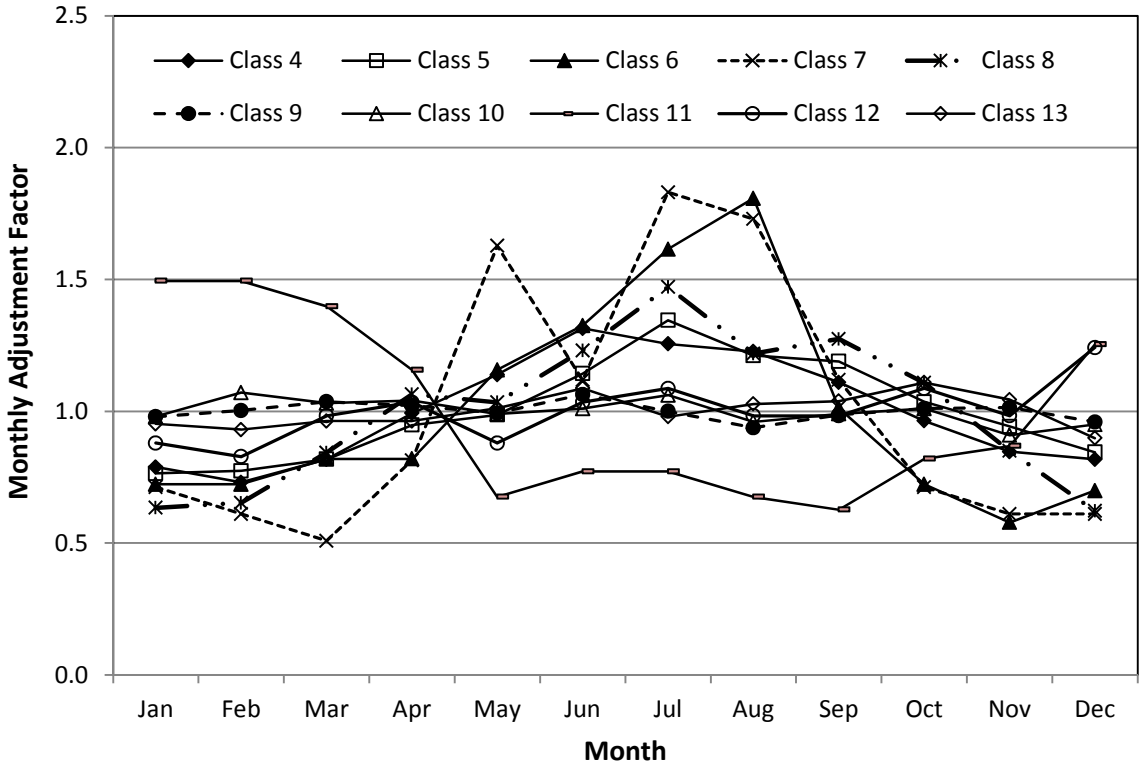

Figure 86. Monthly Adjustment Factors for WIM Site 79

Hourly Truck Distribution

This parameter represents the percentage of truck traffic for each hour of the day. For flexible pavements, hourly truck distribution factors have negligible impact on the predicted distresses and IRI.[6] This is because analysis of flexible pavement is related to temperature which is processed monthly. Thus, MEPDG default hourly truck distribution factors can be used.

Determination of Axle Load Distribution Factors

The axle load distribution factors (spectra) present the percentage of the total axle applications within each load interval for each axle type (single, tandem, tridem, and quad) and vehicle class (FHWA vehicle class 4 to 13).[4] The axle load distribution or spectra can only be determined form WIM data. MEPDG requires the following axle load distribution:

- Axle load distribution for each axle type and load interval:
  - Single axles: 3,000 lb to 41,000 lb at 1,000 lb intervals.
  - Tandem axles: 6,000 lb to 82,000 lb at 2,000 lb intervals.
  - Tridem axles: 12,000 lb to 102,000 lb at 3,000 lb intervals.
  - Quad axles: 12,000 lb to 102,000 lb at 3,000 lb intervals.

- For each axle type, load distribution is required for each month (January through December) and truck class (class 4 through 13).

MEPDG provides users with default ALS (level 3) based on the analysis of LTPP WIM data. These load spectra were normalized on annual basis as no systematic year-to-year or month-to-month differences were found.[4] The following subsections present the results of the analyses of Idaho WIM data to develop level 1 (site-specific), level 2 (regional), and level 3 (statewide) axle load spectra for Idaho.

Development of Site-Specific ALS

In order to develop the site-specific ALS for each WIM site data, all truck weight record files for all 12 months of the analysis year were uploaded and run by the *TrafLoad* software. The software outputs the load spectrum for each axle type and vehicle class per season (month) of the analysis year. Because heavier trucks usually use the outside (right) lane, all weight analyses for roadways with more than one lane in one direction were performed on the trucks using this lane. Among the investigated WIM sites, only data from 2 sites resulted in errors and could not be run through the *TrafLoad* software. These sites are 171 and 191. Figure 87 and Figure 88 show examples of the monthly single and tandem axle load distribution for class 9 truck at WIM site 138, respectively. The annual load spectra for each site, vehicle class and axle type, were then established by averaging the monthly load spectra data. Figure 89 shows an example of a comparison of the southbound and northbound annual tandem axle load spectra for class 9 truck using data from WIM site 169. This figure clearly shows that the axle load distribution may also vary by direction of travel. Figure 90 presents a comparison of the tandem axle load spectra for class 9 truck at WIM site 137 for 2 different years. This figure show fairly similar ALS in 2008 and 2009.

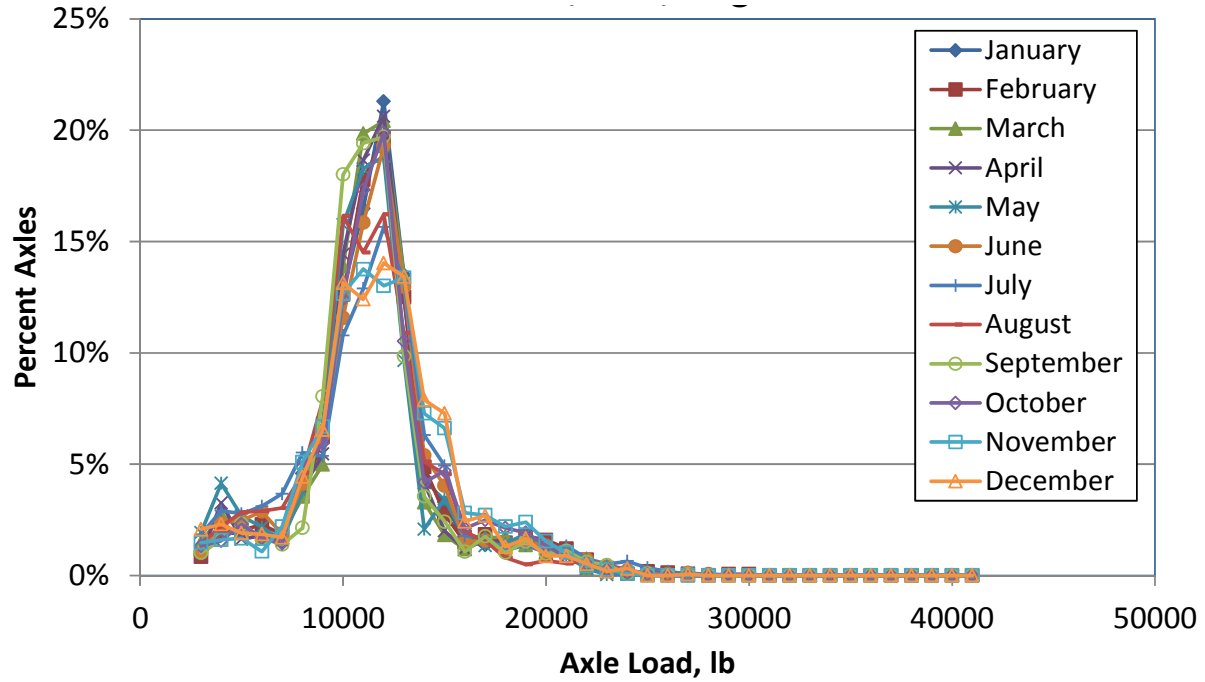

Figure 87. Monthly Variation in Single Axle Spectra for Class 9 Truck at WIM Site 192 Southbound Direction

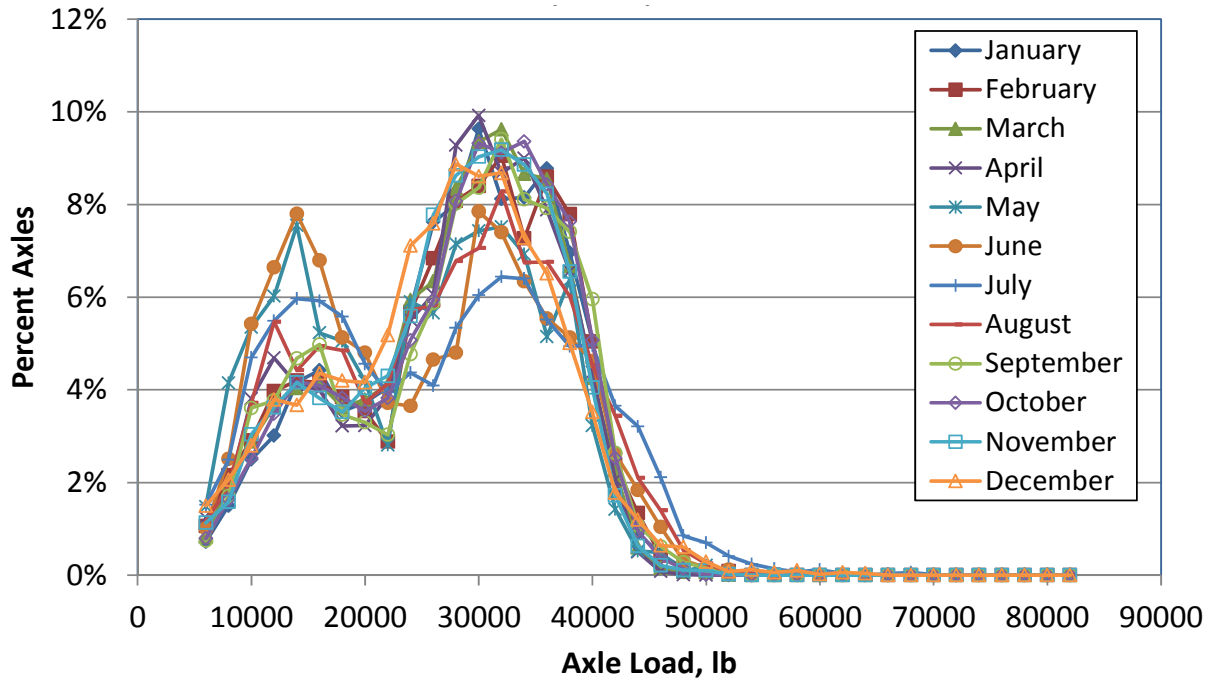

Figure 88. Monthly Variation in Tandem Axle Spectra for Class 9 Truck at WIM Site 138 Southbound Direction

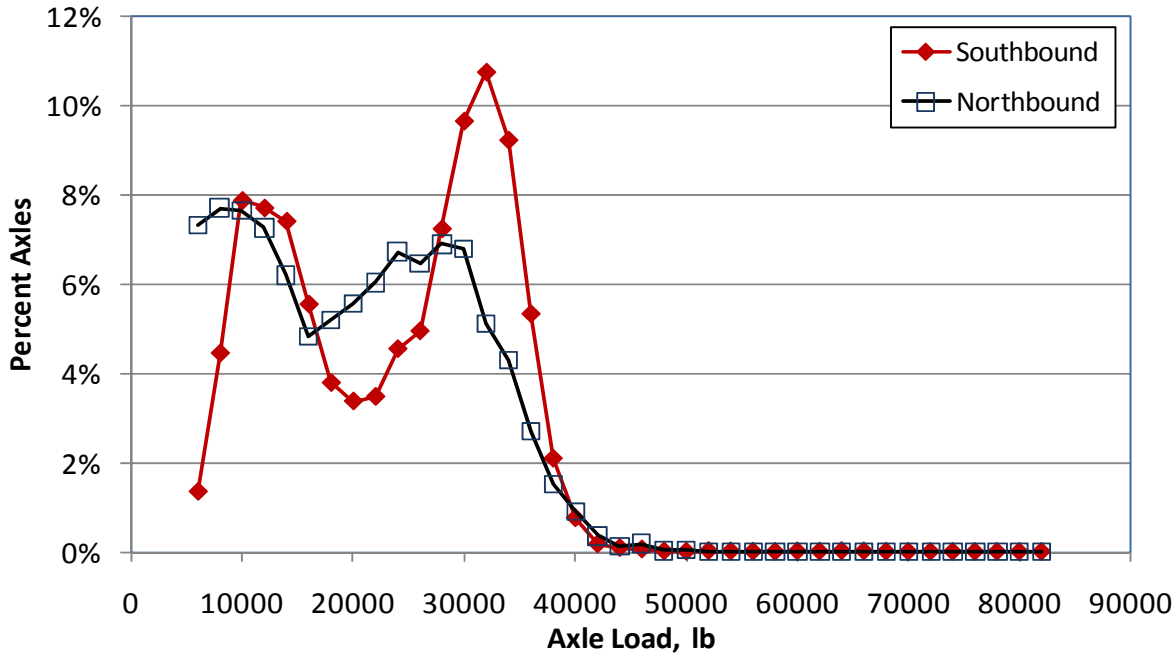

Figure 89. Comparison of the Southbound and Northbound Annual Tandem Axle Load Spectra for Class 9 Truck at WIM Site 169

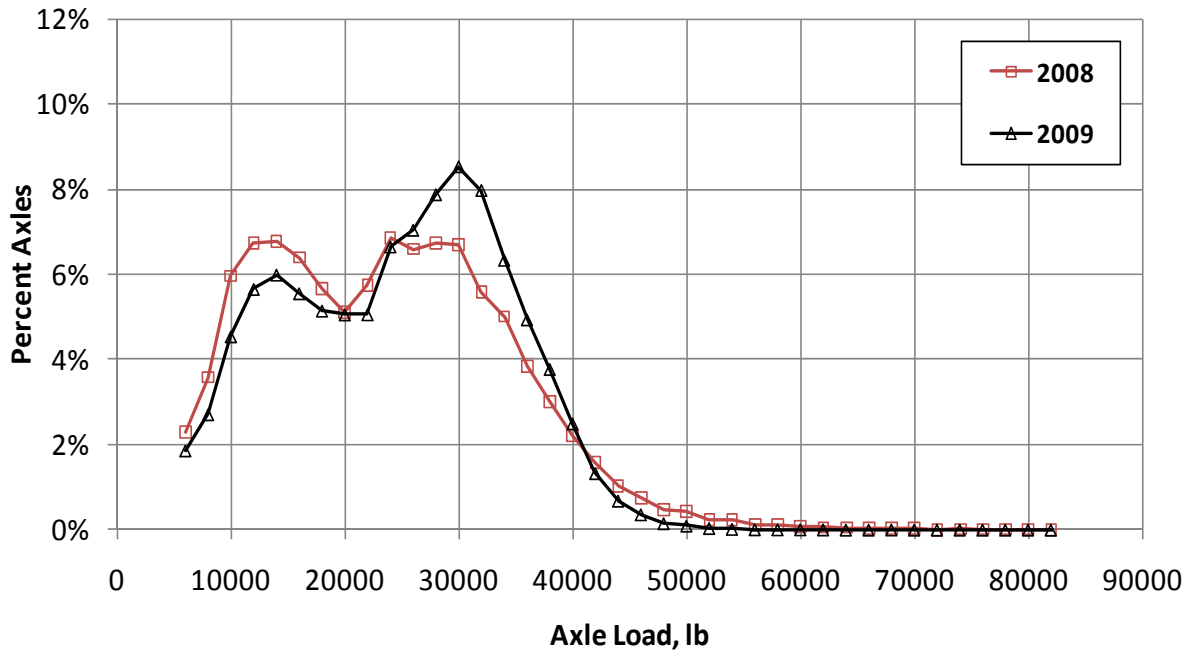

Figure 90. Comparison of 2008 and 2009 Tandem Axle Load Spectra for Class 9 Truck at WIM Site 137

The developed ALS for each site were examined to check any erroneous data that may be resulted from calibration problems of the WIM scales. Limited quality checks were conducted on the analyzed weight data. One important check, which is recommended by FHWA, is that regardless of the gross vehicle weight, the steering axle weight (single axle) of class 9 truck should peak between 8,000 and 12,000 pounds.[93] In addition, the drive tandem axle weight for the fully loaded class 9 truck should peak between 30,000 and 36,000 pounds.

Out of the 25 investigated WIM sites, only 14 WIM sites were found to comply with the aforementioned quality checks. These sites are: 79, 93, 96, 117, 129, 134, 137, 138, 148, 155, 156, 169, 185 and 192. In fact, the quality of WIM data is always questionable. WSDOT reported that out of 38 WIM data, only 12 possessed valid data.[30] In addition, Arkansas reported that out of 55 WIM data, only 10 stations provided good weight data.[36, 37]

For the WIM Stations that passed the quality checks of the weight data, the load spectra for each station, vehicle class, and axle type, were established. This data is provided in electronic format as shown later in Appendix D.

Development of Statewide Axle Load Spectra

All axle weight data for each axle type and truck class at the 14 sites with valid data were combined together in one database. The statewide annual axle load spectra were then determined by averaging the normalized axle load spectra for each axle type and truck class collected at all sites. This is considered input level 3 in the design guide. Table 65 through Table 68 present the developed statewide

single, tandem, tridem, and quad ALS, respectively. Figure 91 to Figure 94 show the developed statewide axle load spectra for single, tandem, tridem, and quad axles, respectively.

A comparison of the developed statewide and MEPDG default ALS is shown in Figure 95 through Figure 98. These figures show that the developed load spectra for ITD is fairly similar to the MEPDG default load spectra in the location of the peaks for most of the truck classes and axle types. However, some truck classes and axle types showed high variability in the location of the peaks and the percentages of axles within these peaks.

Table 65. Statewide Single Axle Load Spectra

Axle Load (lb)	Vehicle Class									
	4	5	6	7	8	9	10	11	12	13
3000	4.07	9.14	1.82	5.81	15.18	2.13	1.16	9.74	8.25	5.21
4000	1.91	10.92	2.83	3.02	10.52	2.15	0.78	6.44	5.84	5.81
5000	3.18	10.80	3.51	2.44	9.48	2.64	1.72	9.26	4.66	5.87
6000	6.18	12.22	5.14	5.03	9.05	3.02	2.74	9.79	6.56	6.65
7000	6.30	7.69	6.82	6.59	7.04	4.89	3.53	7.82	7.12	7.75
8000	10.77	8.31	9.85	8.93	10.41	7.45	7.30	9.01	10.57	7.20
9000	8.39	6.94	9.12	9.03	6.37	9.20	10.35	6.72	9.77	8.34
10000	9.01	5.70	10.59	9.35	7.18	13.36	15.49	7.70	11.94	11.01
11000	7.49	4.60	9.13	9.15	4.45	14.00	13.92	5.83	9.51	8.15
12000	7.39	4.47	10.23	9.18	4.00	14.58	15.04	4.73	7.04	8.59
13000	6.94	3.31	8.47	7.99	3.11	9.22	10.78	3.34	4.67	5.86
14000	6.22	2.50	5.75	5.07	2.09	4.02	3.94	2.74	2.80	3.48
15000	6.21	2.40	5.67	3.51	2.15	3.42	3.28	2.82	2.55	3.78
16000	3.46	1.80	2.97	3.84	1.19	2.05	1.22	2.23	1.78	2.50
17000	2.68	1.81	2.48	3.13	1.18	1.77	0.96	2.03	1.39	2.63
18000	1.83	1.48	1.41	2.21	1.01	1.34	0.60	1.72	1.04	1.87
19000	1.58	1.42	1.18	1.49	1.26	1.18	1.21	1.53	0.71	1.54
20000	1.02	0.94	0.70	0.87	0.82	0.79	2.29	1.06	0.49	0.96
21000	0.88	0.74	0.75	0.75	1.01	0.67	1.61	0.83	0.59	0.69
22000	0.83	0.45	0.80	0.40	0.60	0.52	0.66	0.74	0.31	0.41
23000	0.74	0.43	0.38	0.66	0.41	0.47	0.24	0.84	0.27	0.27
24000	0.55	0.29	0.10	0.51	0.23	0.27	0.32	0.56	0.37	0.30
25000	0.58	0.15	0.12	0.25	0.14	0.14	0.29	0.31	0.31	0.31
26000	0.43	0.17	0.03	0.13	0.14	0.15	0.11	0.17	0.27	0.12
27000	0.32	0.19	0.02	0.21	0.11	0.10	0.04	0.22	0.14	0.09
28000	0.24	0.29	0.02	0.09	0.10	0.06	0.05	0.12	0.11	0.06
29000	0.15	0.19	0.01	0.16	0.07	0.03	0.02	0.14	0.06	0.06
30000	0.09	0.11	0.00	0.01	0.07	0.07	0.06	0.25	0.06	0.06
31000	0.09	0.08	0.00	0.01	0.06	0.04	0.02	0.17	0.06	0.04
32000	0.11	0.07	0.00	0.04	0.06	0.03	0.01	0.16	0.06	0.04
33000	0.10	0.04	0.02	0.03	0.06	0.02	0.03	0.15	0.04	0.02
34000	0.07	0.04	0.00	0.00	0.05	0.05	0.05	0.13	0.05	0.04
35000	0.04	0.03	0.00	0.00	0.05	0.03	0.02	0.15	0.05	0.03
36000	0.04	0.04	0.00	0.01	0.04	0.01	0.01	0.09	0.08	0.02
37000	0.01	0.04	0.01	0.01	0.04	0.03	0.01	0.08	0.09	0.04
38000	0.01	0.02	0.00	0.01	0.03	0.02	0.01	0.06	0.08	0.03
39000	0.03	0.01	0.00	0.00	0.04	0.01	0.02	0.06	0.06	0.03
40000	0.01	0.04	0.02	0.05	0.05	0.01	0.03	0.08	0.09	0.04
41000	0.05	0.13	0.05	0.03	0.15	0.06	0.08	0.18	0.16	0.10

Table 66. Statewide Tandem Axle Load Spectra

Axle Load (lb)	Vehicle Class									
	4		4		4		4		4	
6000	4.34	0.00	5.52	11.08	30.69	1.69	3.74	21.91	7.33	6.03
8000	2.25	0.00	6.01	6.54	11.45	2.92	5.89	9.97	4.42	6.60
10000	2.60	0.00	6.93	9.47	9.39	5.61	6.01	15.71	8.03	7.20
12000	3.52	0.00	7.25	9.73	11.11	8.14	7.41	20.39	8.45	9.54
14000	2.64	0.00	7.09	7.18	7.52	6.94	7.82	13.50	8.20	5.77
16000	4.20	0.00	6.27	5.76	6.04	6.23	8.24	4.49	10.64	6.20
18000	4.40	0.00	6.45	5.82	4.66	5.35	5.73	2.91	13.47	6.00
20000	5.91	0.00	5.45	4.39	3.58	5.22	5.06	1.91	7.83	5.97
22000	9.56	0.00	5.47	4.15	2.42	4.87	5.70	1.04	8.38	4.79
24000	10.61	0.00	5.74	4.68	3.64	5.67	6.39	0.57	6.51	5.46
26000	7.87	0.00	6.18	4.54	3.15	5.93	4.06	0.43	3.84	6.28
28000	6.64	0.00	5.36	3.97	1.51	6.03	5.21	0.57	3.13	6.13
30000	6.89	0.00	4.73	3.93	0.90	6.35	5.75	0.86	2.59	5.67
32000	6.93	0.00	3.75	2.64	0.66	5.48	5.30	0.84	1.88	3.80
34000	4.51	0.00	3.39	3.24	0.59	5.31	4.04	0.85	1.28	3.37
36000	3.71	0.00	2.63	3.07	0.55	4.76	2.85	0.89	0.79	2.95
38000	2.90	0.00	2.43	2.07	0.40	3.81	2.13	0.30	0.68	1.84
40000	1.72	0.00	1.83	1.68	0.24	2.74	1.83	0.27	0.35	1.79
42000	1.30	0.00	1.56	1.42	0.18	2.25	1.59	0.20	0.42	1.14
44000	0.79	0.00	1.88	0.59	0.18	1.47	0.66	0.21	0.36	0.91
46000	0.76	0.00	1.26	0.45	0.15	1.18	0.54	0.23	0.42	0.53
48000	0.51	0.00	0.96	0.40	0.12	0.62	0.42	0.17	0.15	0.33
50000	1.07	0.00	0.46	0.42	0.10	0.38	0.57	0.14	0.10	0.28
52000	1.41	0.00	0.24	0.35	0.12	0.17	0.24	0.08	0.15	0.44
54000	0.91	0.00	0.19	0.26	0.08	0.31	0.15	0.10	0.09	0.36
56000	0.60	0.00	0.55	0.29	0.08	0.19	0.09	0.18	0.04	0.12
58000	0.16	0.00	0.12	0.15	0.05	0.12	0.08	0.12	0.04	0.06
60000	0.03	0.00	0.07	0.18	0.04	0.05	0.08	0.13	0.03	0.09
62000	0.09	0.00	0.07	0.40	0.05	0.05	0.04	0.06	0.06	0.03
64000	0.22	0.00	0.03	0.32	0.05	0.04	0.02	0.11	0.04	0.06
66000	0.24	0.00	0.02	0.21	0.08	0.04	0.13	0.12	0.03	0.05
68000	0.38	0.00	0.01	0.11	0.06	0.03	0.51	0.13	0.05	0.03
70000	0.16	0.00	0.02	0.08	0.02	0.01	0.71	0.16	0.06	0.01
72000	0.00	0.00	0.02	0.10	0.01	0.00	0.68	0.09	0.06	0.06
74000	0.01	0.00	0.03	0.07	0.01	0.00	0.24	0.08	0.04	0.03
76000	0.01	0.00	0.01	0.05	0.01	0.00	0.02	0.03	0.02	0.01
78000	0.00	0.00	0.01	0.09	0.02	0.00	0.01	0.02	0.00	0.01
80000	0.00	0.00	0.00	0.04	0.04	0.03	0.01	0.05	0.01	0.01
82000	0.15	0.00	0.01	0.08	0.05	0.01	0.05	0.18	0.03	0.05

Table 67. Statewide Tridem Axle Load Spectra

Axle Load (lb)	Vehicle Class									
	4		4		4		4		4	
12000	0.00	0.00	42.61	13.22	14.86	40.49	12.16	3.66	30.50	19.41
15000	0.00	0.00	7.04	3.73	9.56	12.48	7.10	3.84	6.29	7.94
18000	0.00	0.00	7.37	4.61	25.09	9.37	5.68	16.10	14.17	5.64
21000	0.00	0.00	9.01	6.32	22.10	7.78	5.51	22.67	3.32	3.85
24000	0.00	0.00	8.84	5.22	13.32	3.49	4.62	9.36	1.36	3.05
27000	0.00	0.00	7.59	6.66	2.38	4.49	4.11	8.81	4.76	4.87
30000	0.00	0.00	7.06	7.04	1.71	6.07	7.31	1.71	8.20	7.18
33000	0.00	0.00	1.46	6.45	1.08	2.40	6.40	4.17	7.21	10.89
36000	0.00	0.00	4.40	8.94	0.51	3.14	8.83	2.37	4.84	9.89
39000	0.00	0.00	1.25	8.90	0.64	1.93	8.71	0.71	3.61	6.94
42000	0.00	0.00	1.28	6.76	0.68	1.79	7.36	0.68	2.13	5.11
45000	0.00	0.00	1.20	5.90	0.55	1.63	6.54	1.19	1.91	5.20
48000	0.00	0.00	0.47	5.37	0.64	1.69	5.39	0.23	1.84	2.64
51000	0.00	0.00	0.22	3.33	0.28	1.46	3.16	0.74	1.62	1.22
54000	0.00	0.00	0.18	2.43	0.57	0.29	2.42	5.72	1.76	1.41
57000	0.00	0.00	0.01	1.82	0.42	0.27	1.48	2.87	1.06	1.22
60000	0.00	0.00	0.01	1.14	0.46	0.17	1.24	3.80	0.74	0.57
63000	0.00	0.00	0.00	0.60	0.37	0.09	0.51	4.92	1.03	0.68
66000	0.00	0.00	0.00	0.27	0.75	0.07	0.48	1.44	0.56	0.51
69000	0.00	0.00	0.00	0.25	0.71	0.18	0.27	1.95	0.13	0.35
72000	0.00	0.00	0.00	0.09	0.27	0.09	0.24	1.53	0.33	0.29
75000	0.00	0.00	0.00	0.09	0.43	0.02	0.08	0.34	0.34	0.10
78000	0.00	0.00	0.00	0.12	0.67	0.02	0.05	0.00	0.17	0.11
81000	0.00	0.00	0.00	0.02	0.46	0.05	0.10	0.00	0.59	0.08
84000	0.00	0.00	0.00	0.02	0.06	0.08	0.01	0.00	0.86	0.13
87000	0.00	0.00	0.00	0.02	0.11	0.02	0.01	0.40	0.14	0.04
90000	0.00	0.00	0.00	0.04	0.41	0.05	0.03	0.00	0.16	0.12
93000	0.00	0.00	0.00	0.21	0.16	0.00	0.02	0.00	0.13	0.11
96000	0.00	0.00	0.00	0.02	0.14	0.00	0.03	0.08	0.22	0.03
99000	0.00	0.00	0.00	0.02	0.05	0.08	0.02	0.71	0.02	0.05
102000	0.00	0.00	0.00	0.39	0.56	0.31	0.13	0.00	0.00	0.37

Table 68. Statewide Quad Axle Load Spectra

Axle Load (lb)	Vehicle Class									
	4		4		4		4		4	
12000	0.00	0.00	0.00	10.85	27.34	18.21	4.77	0.00	14.78	8.29
15000	0.00	0.00	0.00	3.91	8.72	6.68	3.52	0.00	4.66	2.56
18000	0.00	0.00	0.00	3.22	6.30	13.83	2.94	2.72	3.31	3.06
21000	0.00	0.00	0.00	4.57	6.60	10.70	2.27	16.20	5.90	2.04
24000	0.00	0.00	0.00	6.90	2.62	8.81	1.91	17.69	7.13	1.86
27000	0.00	0.00	0.00	7.74	5.86	6.19	2.55	10.22	6.20	2.22
30000	0.00	0.00	0.00	6.54	5.18	3.71	2.34	6.51	7.84	3.20
33000	0.00	0.00	0.00	4.61	3.54	1.08	3.47	9.77	2.08	6.76
36000	0.00	0.00	0.00	2.94	1.35	2.05	5.47	13.31	3.97	3.74
39000	0.00	0.00	0.00	3.88	4.80	4.52	9.09	10.48	9.08	4.61
42000	0.00	0.00	0.00	3.56	4.73	3.38	6.89	9.99	4.38	4.79
45000	0.00	0.00	0.00	2.82	5.68	2.40	10.90	2.53	2.93	5.77
48000	0.00	0.00	0.00	4.11	1.24	2.12	10.80	0.58	1.91	4.29
51000	0.00	0.00	0.00	4.83	2.22	0.72	9.04	0.00	0.37	5.44
54000	0.00	0.00	0.00	3.69	2.53	1.13	6.06	0.00	1.22	3.99
57000	0.00	0.00	0.00	2.84	1.25	2.85	4.23	0.00	0.13	4.85
60000	0.00	0.00	0.00	1.48	1.64	0.95	2.69	0.00	1.06	4.74
63000	0.00	0.00	0.00	1.36	2.01	1.80	2.46	0.00	0.13	4.72
66000	0.00	0.00	0.00	1.27	2.05	1.50	2.16	0.00	0.93	4.02
69000	0.00	0.00	0.00	1.33	0.51	1.60	1.78	0.00	2.45	4.60
72000	0.00	0.00	0.00	1.64	0.47	0.74	1.50	0.00	2.40	4.17
75000	0.00	0.00	0.00	1.28	1.03	0.81	1.23	0.00	3.14	1.83
78000	0.00	0.00	0.00	1.16	0.00	1.64	0.58	0.00	3.84	1.41
81000	0.00	0.00	0.00	1.65	0.00	0.70	0.20	0.00	4.12	1.00
84000	0.00	0.00	0.00	0.75	0.04	1.71	0.11	0.00	1.94	1.13
87000	0.00	0.00	0.00	1.89	0.21	0.17	0.08	0.00	1.31	1.01
90000	0.00	0.00	0.00	1.90	0.25	0.00	0.07	0.00	1.00	0.60
93000	0.00	0.00	0.00	2.42	0.20	0.00	0.14	0.00	0.17	0.58
96000	0.00	0.00	0.00	1.65	0.20	0.00	0.14	0.00	0.09	0.57
99000	0.00	0.00	0.00	1.20	0.64	0.00	0.09	0.00	0.26	0.27
102000	0.00	0.00	0.00	2.01	0.79	0.00	0.52	0.00	1.27	1.88

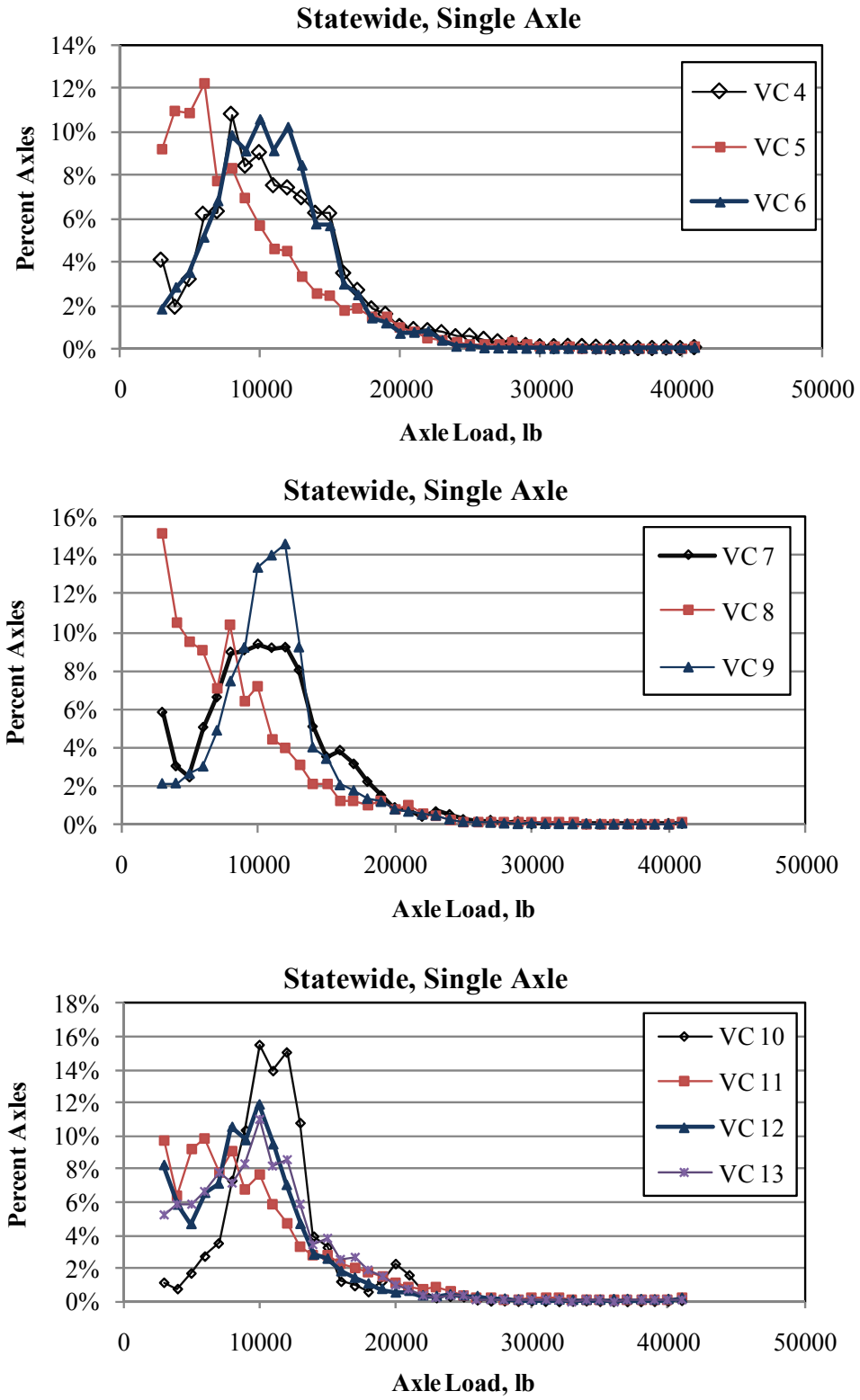

Figure 91. Statewide Single Axle Load Spectra

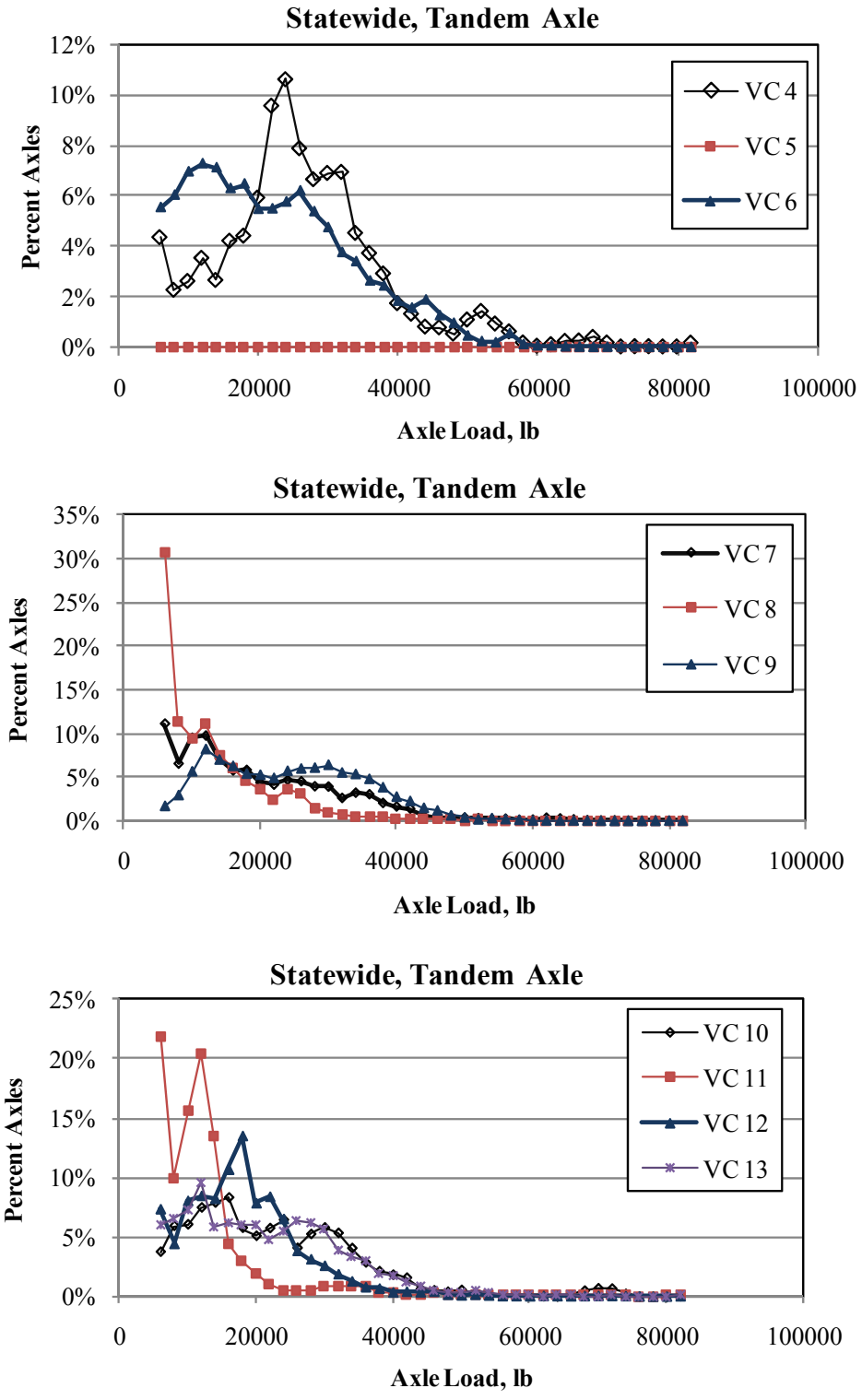

Figure 92. Statewide Tandem Axle Load Spectra

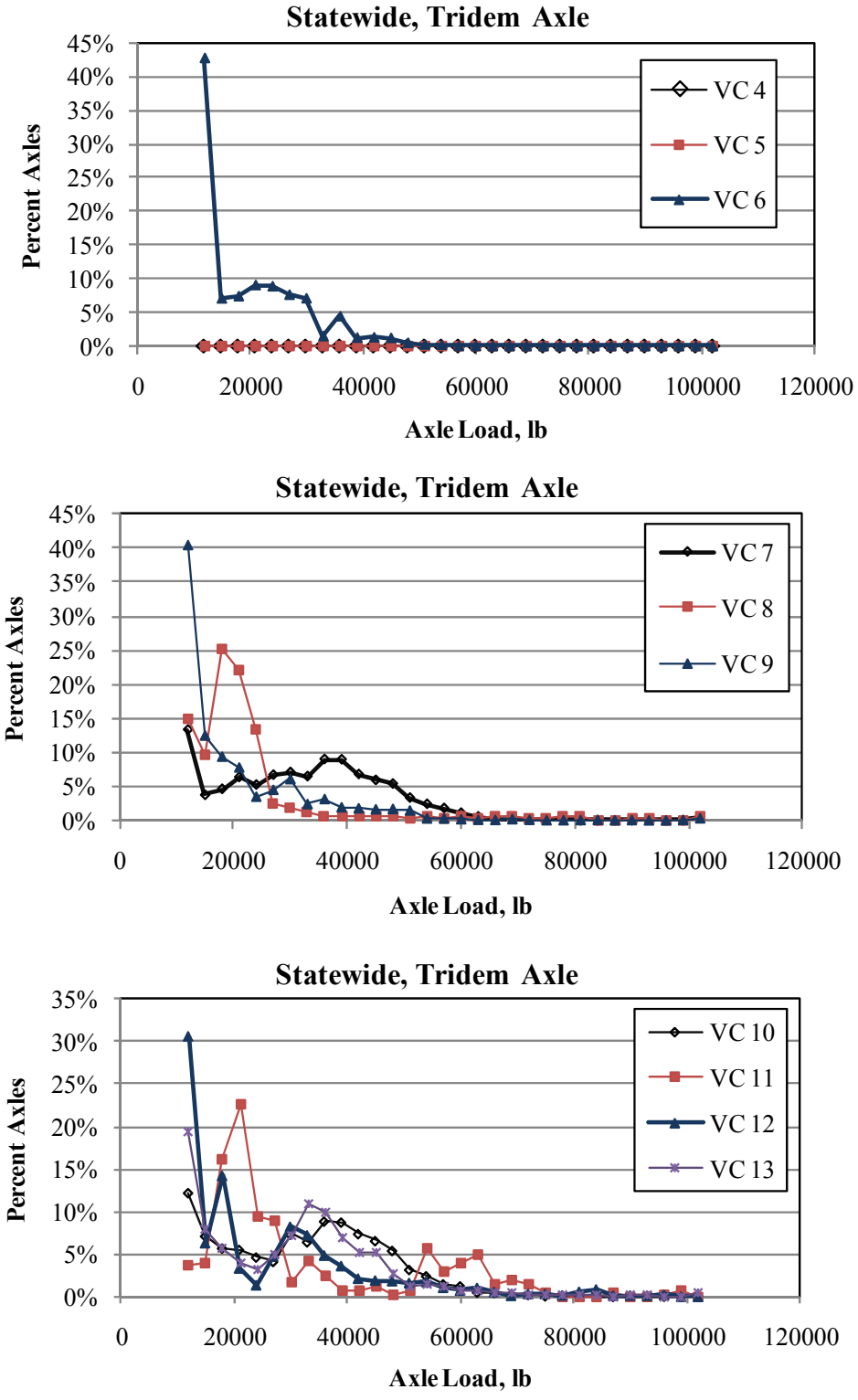

Figure 93. Statewide Tridem Axle Load Spectra

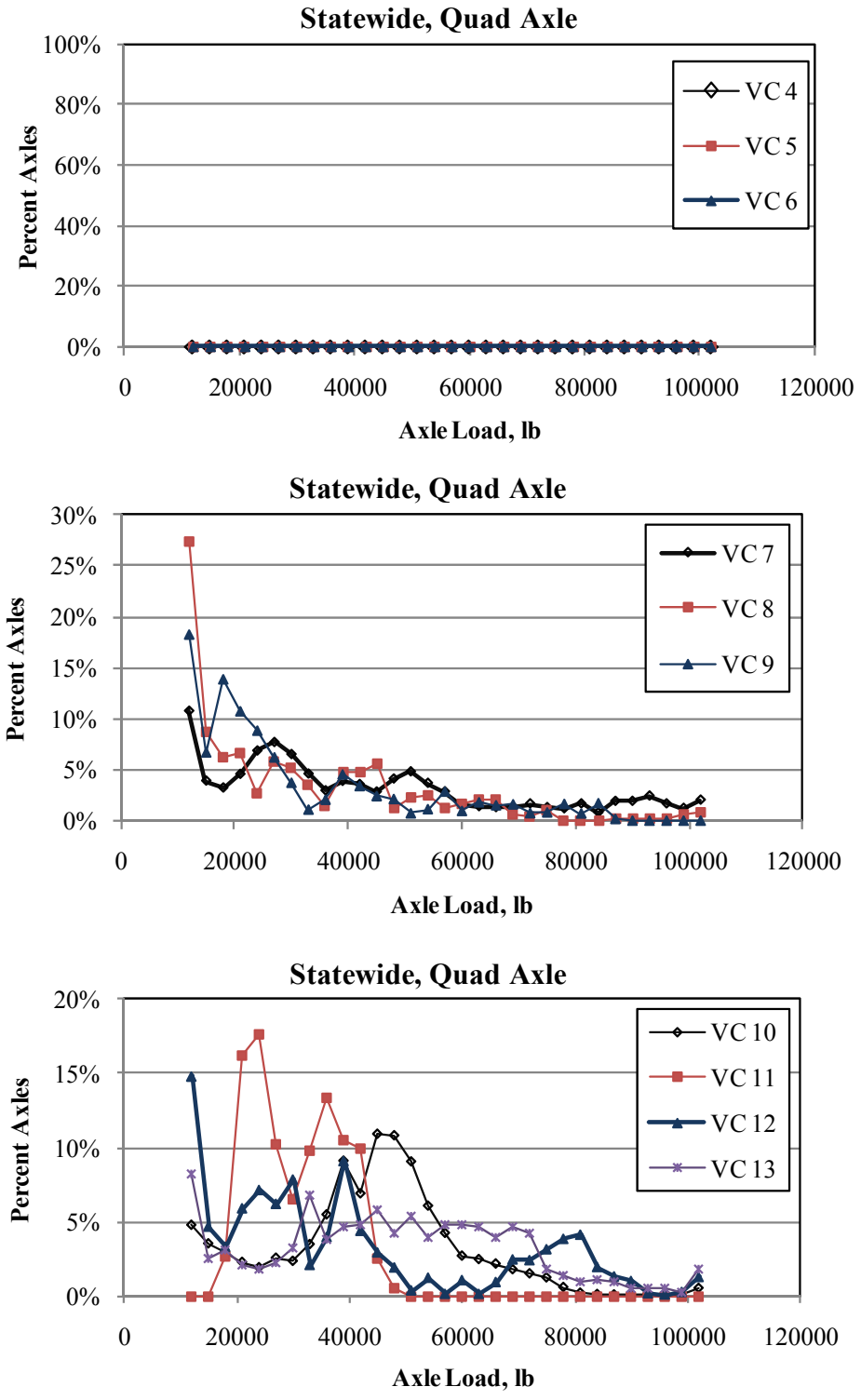

Figure 94. Statewide Quad Axle Load Spectra

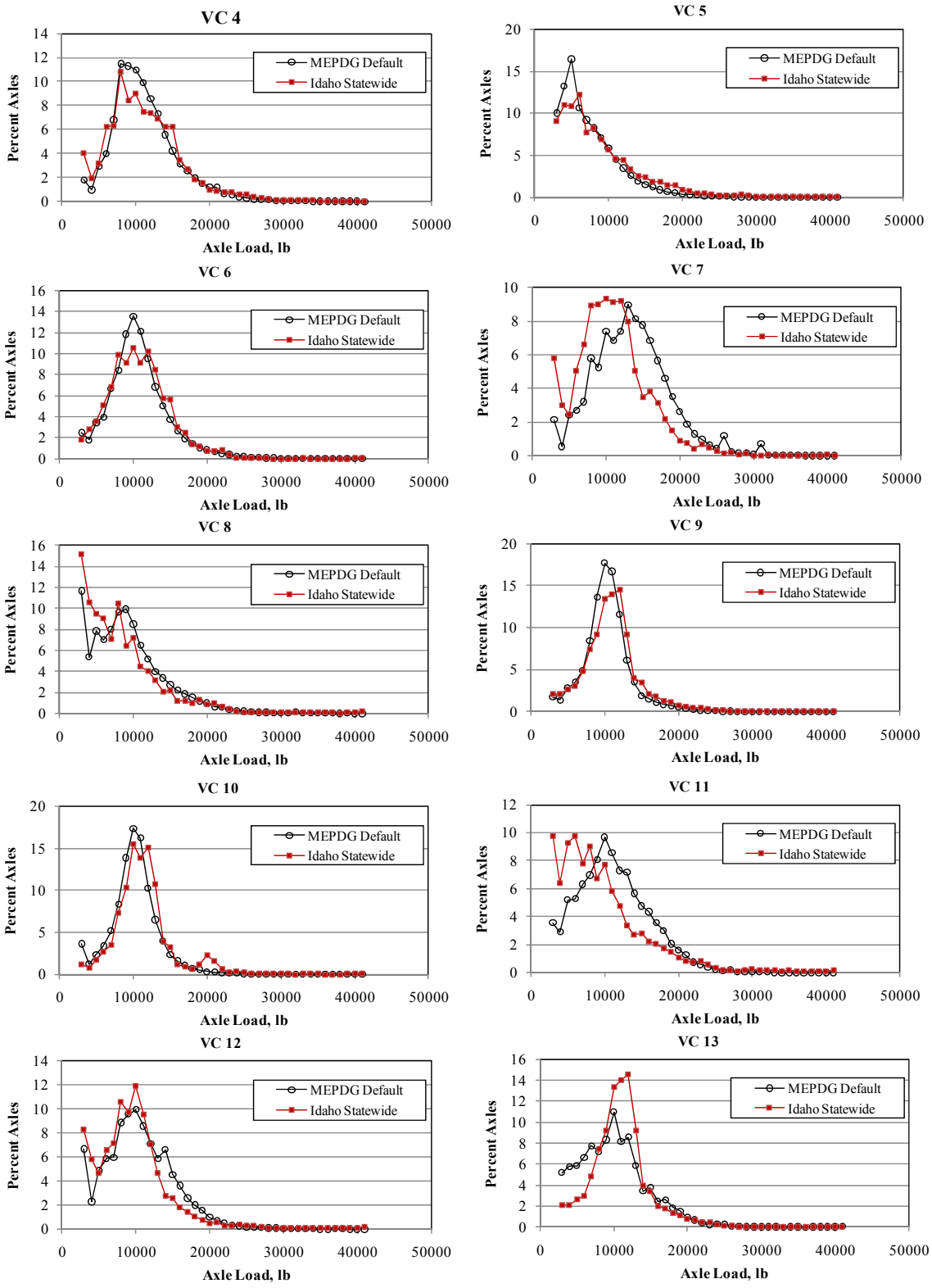

Figure 95. Comparison between Statewide and MEPDG Default Single Axle Load Spectra for Vehicle Classes 4 to 13

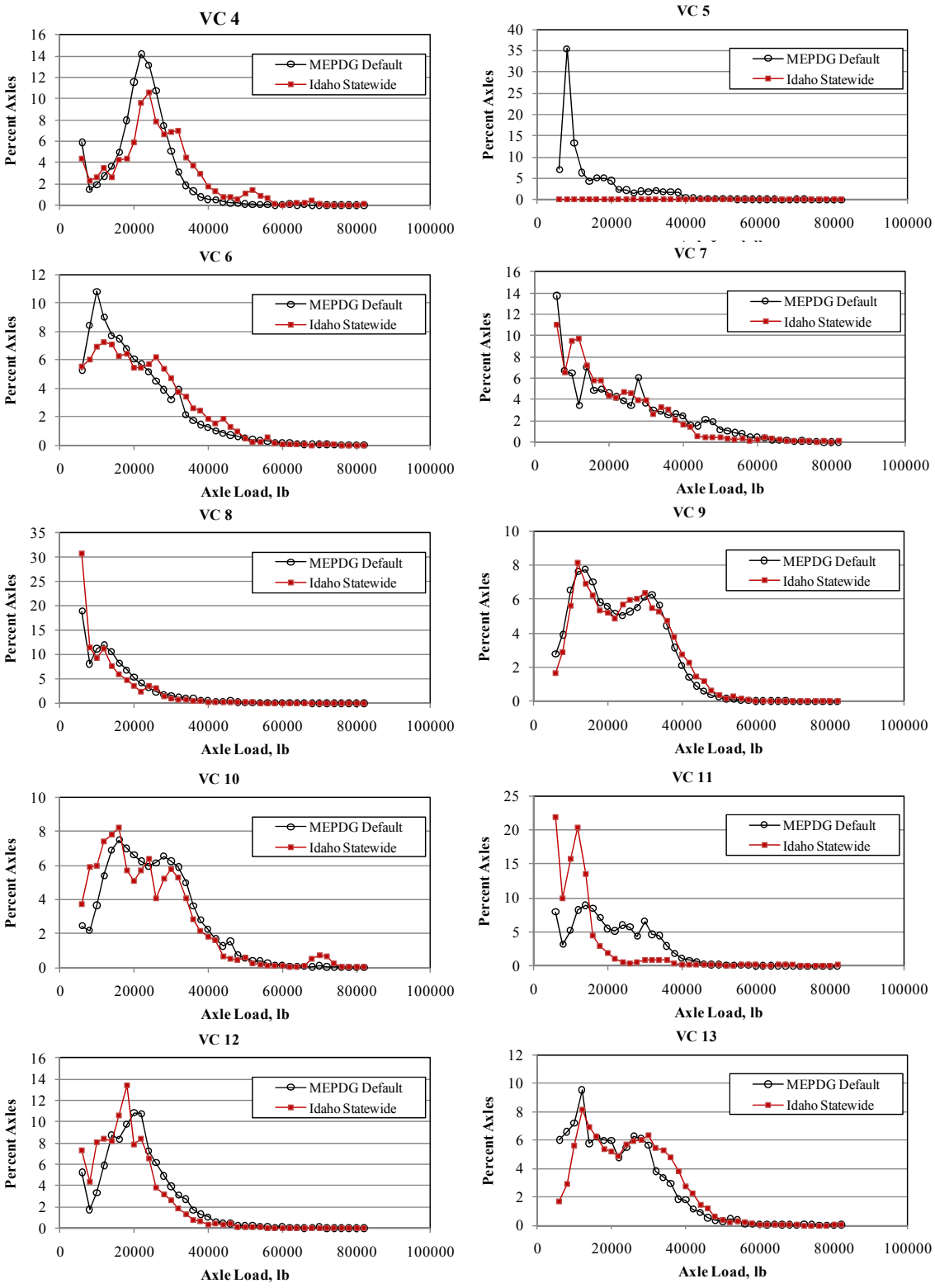

Figure 96. Comparison between Statewide and MEPDG Default Tandem Axle Load Spectra for Vehicle Classes 4 to 13

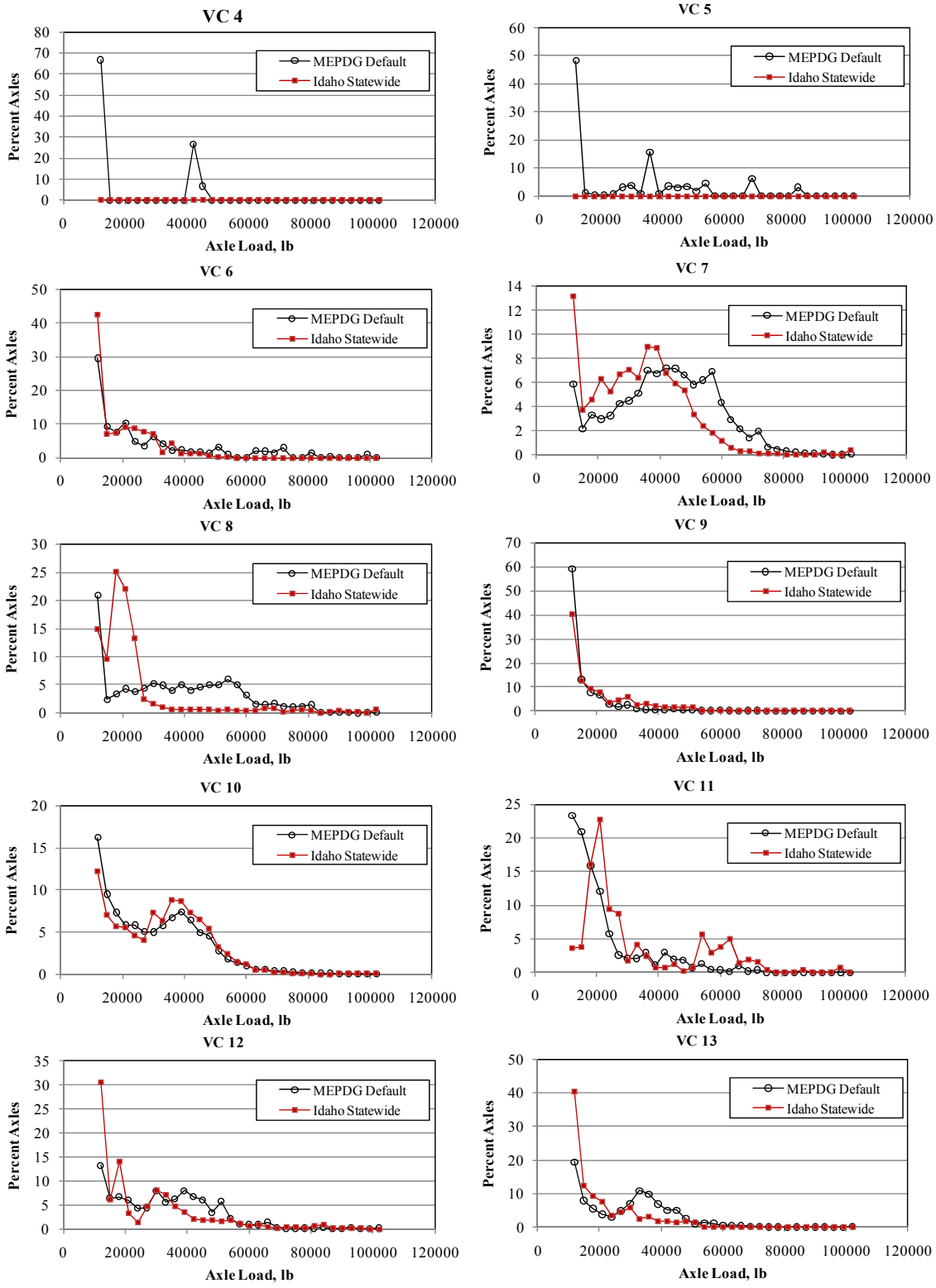

Figure 97. Comparison between Statewide and MEPDG Default Tridem Axle Load Spectra for Vehicle Classes 4 to 13

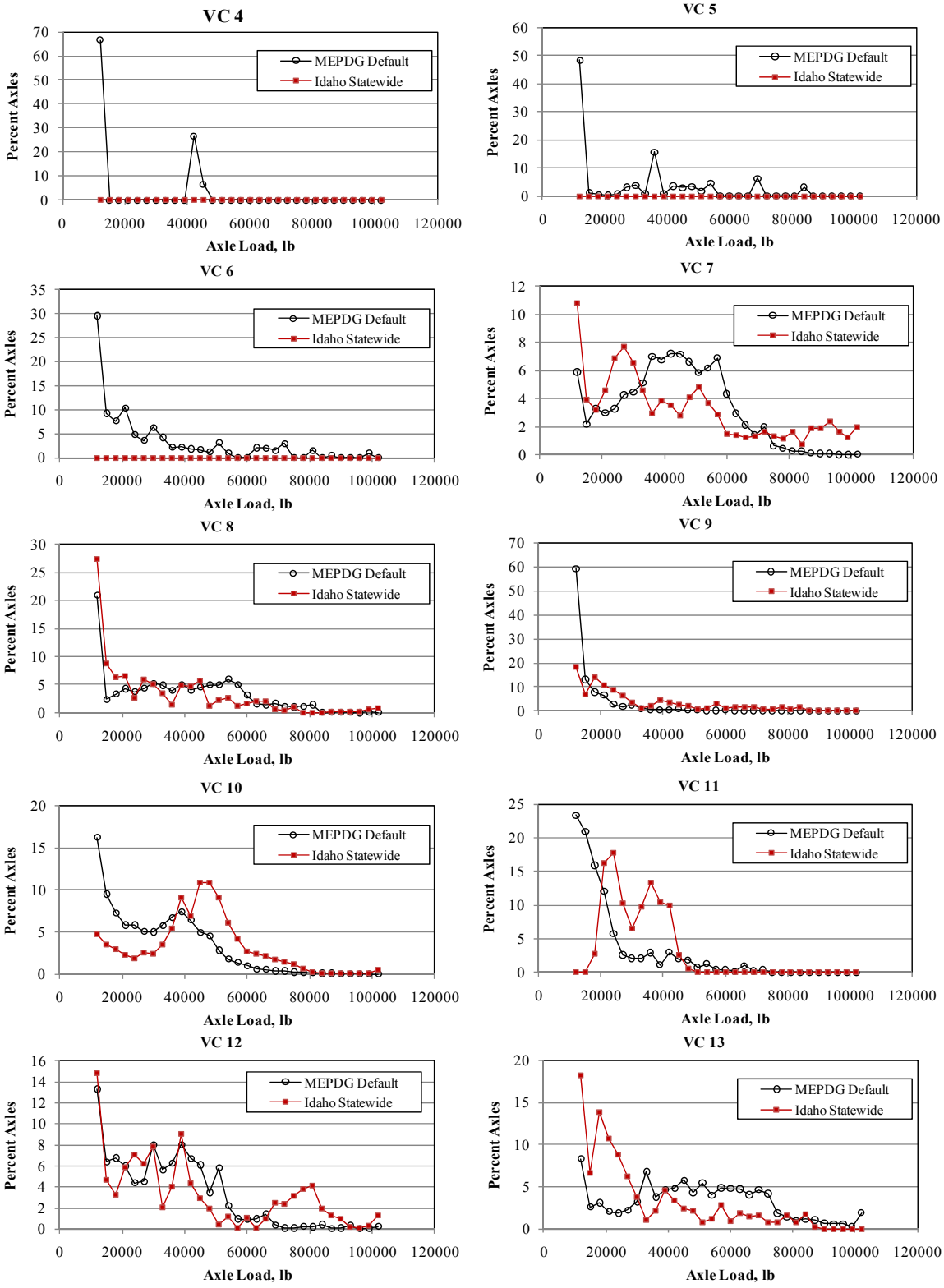

Figure 98. Comparison of Statewide and MEPDG Default Quad Axle Load Spectra for Vehicle Classes 4 to 13

Development of TWRG Axle Load Spectra

TWRG axle load distributions are summary load distributions that represent axle loads found on roads with similar truck weight characteristics (similar axle load distributions). In Idaho, based on the analysis of the data at the investigated WIM sites, 3 TWRGs were found. These TWRGs were established based on the similarity in the shape of the tandem axle load spectra of class 9 trucks. This truck class was selected as the majority of the analyzed WIM stations showed that the majority of truck volumes travel on Idaho roads belongs to this truck class. The TWRGs representing Idaho traffic loading characteristics are as follows:

- Primarily loaded- in which there is bimodal distribution of the axle weights with a large percentage of the trucks are heavily loaded.
- Moderately Loaded-in which there is a bimodal distribution of the axle weights with almost similar percentages of the heavy and light axle weights.
- Lightly loaded-in which there is a bimodal distribution of the axle weights with a large percentages of the trucks are empty or partially loaded.

The 3 TWRGs show unloaded and loaded peaks as shown in Figure 99 to Figure 101 for primarily, moderately, and lightly loaded trucks, respectively. A comparison between the average tandem axle load spectra of truck class 9 for the 3 TWRG is depicted in Figure 102. This figure shows that the primarily loaded truck group exhibit 2 peaks, one peak at 12,000 lb., and the other peak at 36,000 lb. The moderately loaded truck group exhibits 2 peaks with almost similar percentages; one at 12,000 lb. and the other one at 34,000 lb. Finally, the lightly loaded trucks have 2 peaks at 12,000 lb. and 28,000 lb.

The single, tandem, tridem, and quad axle load spectra for the primarily and moderately loaded TWRGs are summarized in Table 69 through Table 80, respectively. Table 81 illustrates the WIM sites belonging to each of the developed TWRG.

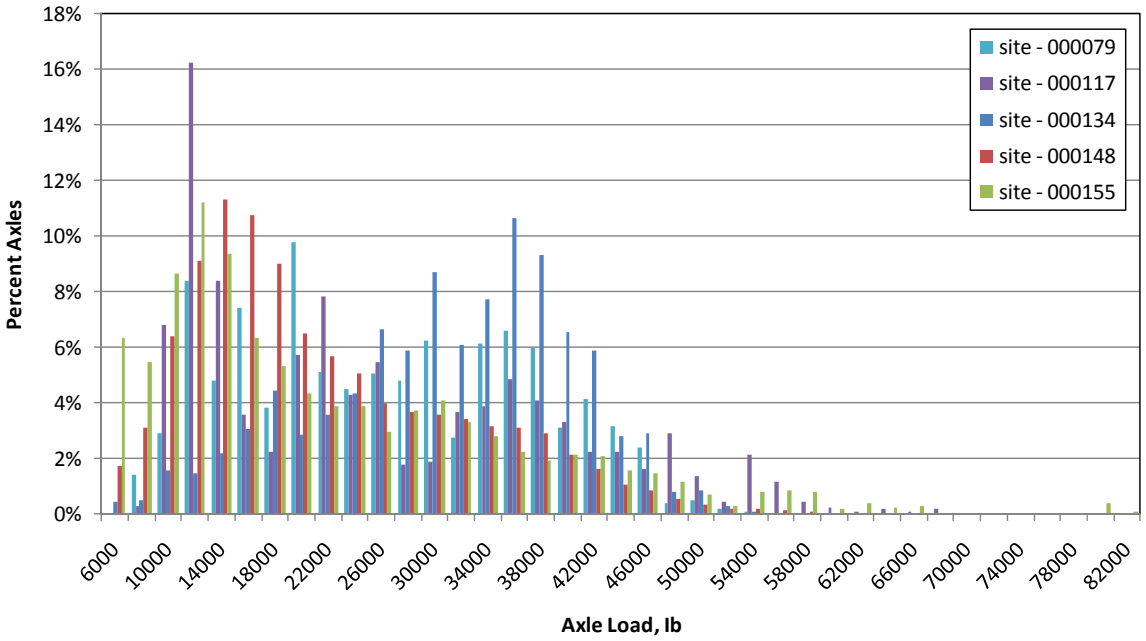

Figure 99. Tandem Axle Load Distribution for Class 9 Trucks, Primarily Loaded TWRG

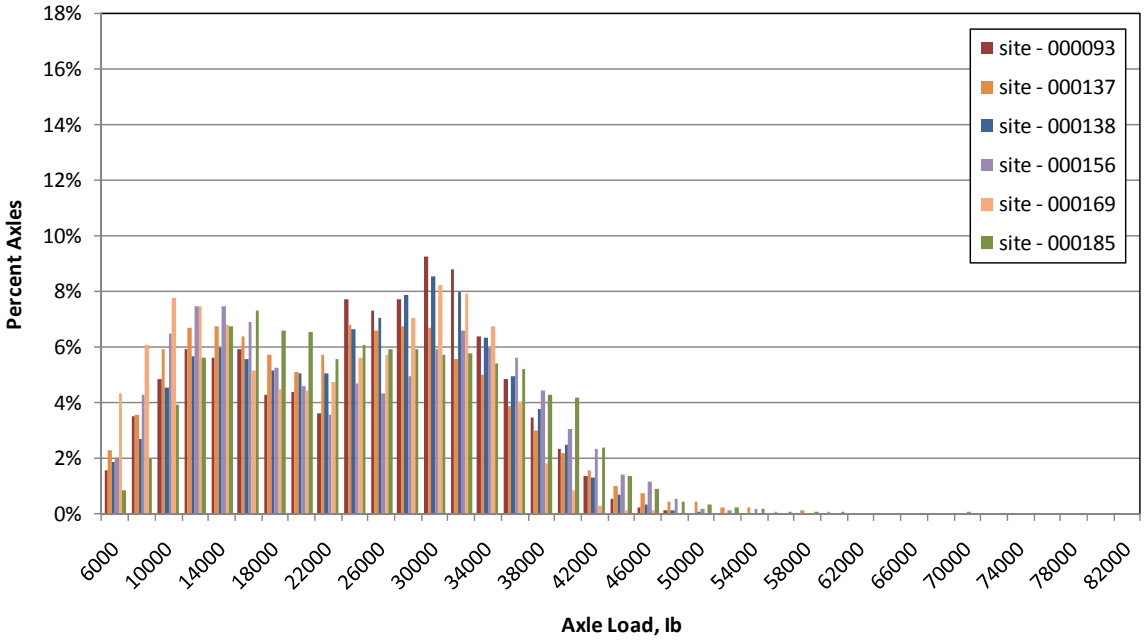

Figure 100. Tandem Axle Load Distribution for Class 9 Trucks, Moderately Loaded TWRG

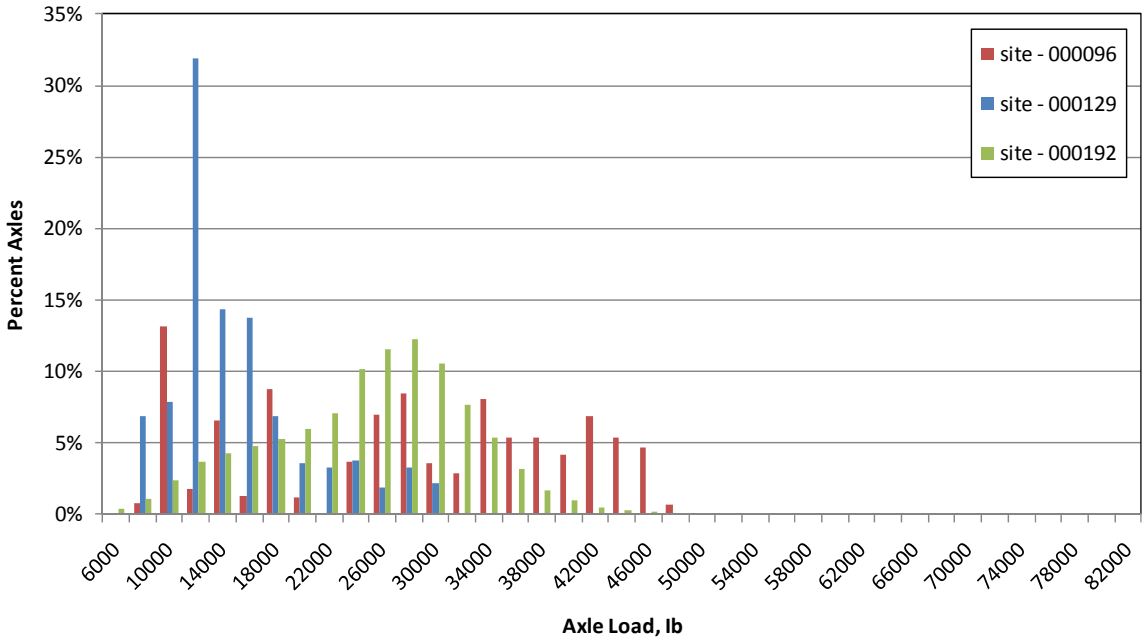

Figure 101. Tandem Axle Load Distribution for Class 9 Trucks, Lightly Loaded TWRG

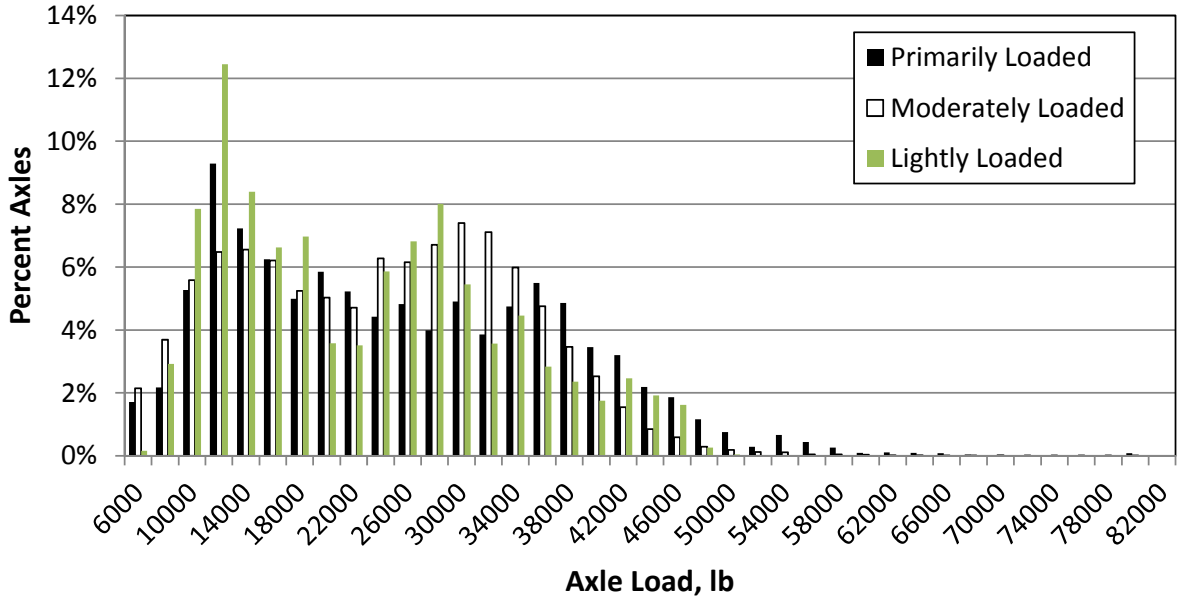

Figure 102. Comparison of Average Tandem Axle Load Distribution for Class 9 Trucks for the 3 TWRG

Table 69. Single Axle Load Spectra for the Primarily Loaded TWRG

Axle Load (lb)	Vehicle Class									
	4	5	6	7	8	9	10	11	12	13
3000	2.74	14.66	2.32	8.76	10.75	1.87	1.08	5.49	10.60	4.28
4000	1.08	16.44	3.81	3.11	9.48	2.58	1.04	1.88	7.33	2.98
5000	3.83	11.48	4.11	3.27	13.36	2.60	2.76	7.38	2.73	3.92
6000	7.04	11.73	4.12	4.90	9.48	3.38	1.72	11.53	6.12	8.17
7000	7.03	5.78	4.57	2.83	6.56	5.08	2.58	8.37	5.82	9.51
8000	12.80	6.56	7.40	6.10	10.22	8.57	7.67	8.94	9.81	7.50
9000	8.33	5.81	5.26	6.34	4.72	10.69	11.02	5.11	7.99	10.03
10000	7.24	4.48	7.07	7.23	6.82	13.47	16.90	7.09	14.20	11.80
11000	5.93	2.53	7.55	5.17	3.80	14.52	11.98	5.46	9.95	8.19
12000	3.64	2.23	12.07	9.87	4.39	11.90	10.07	5.17	6.60	7.58
13000	5.51	2.43	11.12	11.24	3.00	7.59	7.26	3.89	4.06	4.70
14000	7.75	1.75	8.17	7.02	2.81	3.49	3.13	4.05	2.09	3.77
15000	7.13	1.76	8.49	4.38	2.55	2.83	3.50	4.28	2.33	3.36
16000	3.97	1.26	3.02	2.69	1.17	2.11	0.93	3.56	1.38	2.29
17000	1.97	1.20	2.79	2.95	0.98	1.72	0.79	2.52	1.25	2.81
18000	2.13	1.08	1.18	3.09	0.95	1.45	0.63	2.11	0.91	1.93
19000	1.46	1.40	1.20	1.21	1.73	1.13	2.49	2.36	0.69	1.27
20000	0.93	1.15	0.84	1.43	0.98	0.85	5.83	1.85	0.44	1.04
21000	1.09	0.88	1.47	1.20	1.76	0.62	4.12	1.20	0.40	0.84
22000	1.06	0.52	1.74	0.82	0.98	0.70	1.54	0.82	0.35	0.49
23000	1.25	0.51	0.86	2.33	0.64	0.73	0.50	1.10	0.42	0.43
24000	1.04	0.40	0.20	1.64	0.33	0.42	0.70	0.98	0.41	0.60
25000	1.26	0.26	0.31	0.57	0.23	0.17	0.68	0.57	0.61	0.64
26000	0.78	0.35	0.04	0.42	0.22	0.25	0.23	0.33	0.59	0.24
27000	0.71	0.43	0.02	0.78	0.19	0.18	0.08	0.28	0.27	0.17
28000	0.55	0.76	0.01	0.03	0.21	0.11	0.07	0.25	0.26	0.14
29000	0.36	0.51	0.00	0.21	0.14	0.05	0.04	0.38	0.15	0.13
30000	0.13	0.27	0.00	0.03	0.14	0.17	0.09	0.64	0.15	0.14
31000	0.16	0.20	0.00	0.00	0.11	0.08	0.03	0.32	0.16	0.09
32000	0.28	0.15	0.00	0.00	0.10	0.06	0.00	0.15	0.14	0.08
33000	0.25	0.11	0.00	0.00	0.12	0.05	0.04	0.30	0.11	0.05
34000	0.17	0.11	0.00	0.00	0.12	0.12	0.11	0.29	0.13	0.10
35000	0.08	0.09	0.00	0.00	0.10	0.07	0.05	0.18	0.13	0.08
36000	0.07	0.10	0.01	0.00	0.09	0.04	0.01	0.19	0.19	0.06
37000	0.02	0.10	0.02	0.00	0.09	0.07	0.03	0.13	0.22	0.07
38000	0.00	0.06	0.00	0.03	0.09	0.06	0.03	0.14	0.21	0.07
39000	0.06	0.03	0.00	0.01	0.10	0.01	0.04	0.14	0.15	0.09
40000	0.03	0.10	0.07	0.22	0.12	0.04	0.05	0.19	0.23	0.10
41000	0.14	0.33	0.16	0.12	0.37	0.17	0.18	0.38	0.42	0.26

Table 70. Tandem Axle Load Spectra for the Primarily Loaded TWRG

Axle Load (lb)	Vehicle Class									
	4	5	6	7	8	9	10	11	12	13
6000	1.87	0	6.16	15.63	30.21	1.72	2.7	4.75	8.51	4.58
8000	1.82	0	5.53	7.76	13.38	2.17	9.29	8.44	3.4	5.67
10000	1.47	0	3.73	5.2	8.27	5.28	4.36	8.21	8.06	6
12000	3.92	0	4.12	7.78	8.1	9.3	4.09	12.6	4.83	12.96
14000	2.12	0	4.43	6.56	7.21	7.24	5.98	19.12	6.49	5.67
16000	3.71	0	4.89	5.99	6.04	6.25	8.88	10.35	11.4	6.72
18000	2.84	0	5.91	6.33	4.16	4.99	4.73	4.79	19.99	6.17
20000	4.52	0	5.23	4.69	2.61	5.86	4.29	4.32	9.14	6.22
22000	11.32	0	6.59	3.97	2.3	5.24	4.23	1.95	10.45	4.6
24000	13.62	0	7.28	4.73	5.6	4.42	5.17	1.53	5.57	5.25
26000	8.71	0	7.29	4.69	4.93	4.83	2.31	1.04	2.2	5.25
28000	5.41	0	5.88	3.89	1.86	3.99	3.67	1.9	1.26	5.68
30000	5.17	0	4.25	3.85	0.67	4.91	5.29	1.27	0.49	5.03
32000	5.99	0	3.17	2.15	0.48	3.86	7.41	1.51	0.72	2.8
34000	2.7	0	3.52	3.09	0.51	4.75	5.69	1.82	1.5	3.46
36000	2.37	0	2.54	2.73	0.5	5.5	3.42	3.2	0.78	3.71
38000	1.31	0	2.9	3.17	0.38	4.86	2.67	1.03	0.52	2.26
40000	1.88	0	2.46	1.67	0.24	3.45	2.64	1.11	0.4	2.16
42000	0.9	0	2.38	1.43	0.25	3.2	2.54	0.84	0.87	1.3
44000	1.33	0	3.32	0.31	0.27	2.19	0.8	0.88	0.66	1.04
46000	0.49	0	2.4	0.3	0.29	1.87	0.48	0.97	0.74	0.8
48000	1.03	0	2.02	0.55	0.21	1.16	0.7	0.73	0.27	0.6
50000	2.93	0	0.94	0.52	0.16	0.76	1.15	0.6	0.07	0.46
52000	4.08	0	0.4	0.34	0.22	0.29	0.41	0.36	0.14	0.27
54000	2.69	0	0.32	0.06	0.15	0.66	0.3	0.44	0.23	0.13
56000	1.75	0	1.51	0.46	0.14	0.44	0.15	0.77	0.1	0.11
58000	0.45	0	0.29	0.13	0.08	0.26	0.16	0.53	0.11	0.05
60000	0.07	0	0.13	0.03	0.04	0.1	0.21	0.56	0.09	0.2
62000	0.22	0	0.11	0.04	0.12	0.11	0.09	0.25	0.14	0.06
64000	0.66	0	0.05	0.1	0.06	0.09	0.03	0.49	0.1	0.14
66000	0.71	0	0.02	0.48	0.11	0.08	0.31	0.5	0.08	0.14
68000	1.06	0	0.01	0.22	0.09	0.05	1.33	0.55	0.12	0.07
70000	0.44	0	0.01	0.19	0.06	0.01	1.89	0.67	0.15	0.03
72000	0	0	0.05	0.1	0.01	0	1.81	0.38	0.15	0.14
74000	0	0	0.08	0.14	0.01	0	0.62	0.33	0.11	0.08
76000	0	0	0.02	0.09	0.03	0.01	0.06	0.13	0.06	0.03
78000	0	0	0.04	0.18	0.04	0	0.02	0.07	0	0.02
80000	0	0	0.01	0.15	0.1	0.08	0.02	0.23	0.02	0.02
82000	0.44	0	0.01	0.3	0.11	0.02	0.1	0.78	0.08	0.12

Table 71. Tridem Axle Load Spectra for the Primarily Loaded TWRG

Axle Load (lb)	Vehicle Class									
	4	5	6	7	8	9	10	11	12	13
12000	0.00	0.00	22.70	8.17	36.82	28.42	7.66	5.48	37.88	26.67
15000	0.00	0.00	6.88	3.72	8.75	17.22	4.88	5.76	4.45	6.26
18000	0.00	0.00	1.63	2.56	5.66	7.44	4.82	6.48	1.53	5.80
21000	0.00	0.00	6.99	7.57	8.72	4.36	6.61	6.48	2.88	4.23
24000	0.00	0.00	11.73	4.78	6.34	4.29	2.51	9.51	3.14	2.12
27000	0.00	0.00	15.01	3.84	2.42	8.30	3.44	12.95	2.93	6.14
30000	0.00	0.00	14.13	3.59	3.89	9.66	2.79	2.54	3.53	4.26
33000	0.00	0.00	2.91	4.55	2.70	3.73	2.38	6.26	3.31	8.77
36000	0.00	0.00	8.80	7.55	1.26	2.10	9.27	3.56	2.89	6.62
39000	0.00	0.00	2.49	11.05	1.60	0.77	11.03	1.07	3.14	5.87
42000	0.00	0.00	2.56	8.82	1.69	1.27	8.88	1.02	3.92	4.03
45000	0.00	0.00	2.40	6.47	1.36	1.29	8.91	1.78	5.33	3.63
48000	0.00	0.00	0.94	6.06	1.60	3.72	8.81	0.35	5.47	2.10
51000	0.00	0.00	0.44	5.69	0.69	2.32	4.85	1.12	2.18	1.19
54000	0.00	0.00	0.36	4.65	1.43	0.67	4.00	8.58	1.39	2.13
57000	0.00	0.00	0.02	2.30	1.05	0.35	2.63	4.30	1.20	1.98
60000	0.00	0.00	0.01	2.44	1.14	0.50	2.57	5.70	1.38	1.16
63000	0.00	0.00	0.00	1.26	0.91	0.29	0.90	7.38	1.95	1.43
66000	0.00	0.00	0.00	0.53	1.87	0.24	0.91	2.15	0.58	0.78
69000	0.00	0.00	0.00	0.85	1.78	0.60	0.62	2.93	0.38	0.78
72000	0.00	0.00	0.00	0.26	0.66	0.30	0.57	2.30	1.07	0.58
75000	0.00	0.00	0.00	0.11	1.08	0.08	0.15	0.51	1.12	0.05
78000	0.00	0.00	0.00	0.13	1.68	0.06	0.02	0.00	0.59	0.02
81000	0.00	0.00	0.00	0.07	1.14	0.18	0.26	0.00	2.16	0.18
84000	0.00	0.00	0.00	0.07	0.16	0.27	0.01	0.00	3.16	0.38
87000	0.00	0.00	0.00	0.02	0.28	0.07	0.01	0.60	0.51	0.15
90000	0.00	0.00	0.00	0.19	1.03	0.15	0.06	0.00	0.59	0.48
93000	0.00	0.00	0.00	0.91	0.41	0.02	0.05	0.00	0.49	0.43
96000	0.00	0.00	0.00	0.06	0.35	0.01	0.06	0.13	0.79	0.12
99000	0.00	0.00	0.00	0.03	0.14	0.27	0.04	1.06	0.06	0.19
102000	0.00	0.00	0.00	1.70	1.39	1.05	0.30	0.00	0.00	1.47

Table 72. Quad Axle Load Spectra for the Primarily Loaded TWRG

Axle Load (lb)	Vehicle Class									
	4	5	6	7	8	9	10	11	12	13
12000	0.00	0.00	0.00	12.99	27.34	18.10	3.43	0.00	14.78	18.51
15000	0.00	0.00	0.00	5.94	8.71	7.61	2.60	0.00	4.66	5.11
18000	0.00	0.00	0.00	5.44	6.30	10.46	2.71	2.72	3.31	1.52
21000	0.00	0.00	0.00	5.62	6.60	8.17	3.00	16.20	5.90	1.86
24000	0.00	0.00	0.00	5.58	2.62	9.44	1.95	17.69	7.13	0.68
27000	0.00	0.00	0.00	8.02	5.86	4.65	3.62	10.22	6.20	1.03
30000	0.00	0.00	0.00	9.60	5.18	3.84	2.23	6.51	7.84	1.41
33000	0.00	0.00	0.00	6.42	3.54	1.24	2.09	9.77	2.08	7.88
36000	0.00	0.00	0.00	2.73	1.35	2.95	2.92	13.31	3.97	5.24
39000	0.00	0.00	0.00	1.74	4.80	6.78	5.58	10.48	9.08	3.57
42000	0.00	0.00	0.00	2.92	4.73	5.07	4.87	9.99	4.38	2.29
45000	0.00	0.00	0.00	3.18	5.68	3.60	14.60	2.53	2.93	4.09
48000	0.00	0.00	0.00	2.00	1.24	3.17	16.27	0.58	1.91	3.42
51000	0.00	0.00	0.00	2.20	2.22	1.09	7.74	0.00	0.37	3.88
54000	0.00	0.00	0.00	3.71	2.53	1.69	3.99	0.00	1.22	3.28
57000	0.00	0.00	0.00	5.68	1.25	4.08	3.55	0.00	0.13	5.65
60000	0.00	0.00	0.00	3.56	1.65	0.00	3.09	0.00	1.06	3.52
63000	0.00	0.00	0.00	2.58	2.01	0.00	1.96	0.00	0.13	2.49
66000	0.00	0.00	0.00	1.25	2.05	0.00	1.25	0.00	0.93	1.78
69000	0.00	0.00	0.00	0.54	0.51	0.37	2.00	0.00	2.45	1.72
72000	0.00	0.00	0.00	0.42	0.47	0.97	3.45	0.00	2.40	2.09
75000	0.00	0.00	0.00	0.49	1.03	1.08	3.00	0.00	3.14	1.22
78000	0.00	0.00	0.00	0.36	0.00	2.11	1.34	0.00	3.84	2.06
81000	0.00	0.00	0.00	0.17	0.00	0.71	0.44	0.00	4.12	1.76
84000	0.00	0.00	0.00	0.19	0.04	2.57	0.26	0.00	1.94	2.52
87000	0.00	0.00	0.00	0.31	0.21	0.25	0.09	0.00	1.31	2.38
90000	0.00	0.00	0.00	0.71	0.25	0.00	0.04	0.00	1.00	1.27
93000	0.00	0.00	0.00	0.49	0.20	0.00	0.16	0.00	0.17	0.51
96000	0.00	0.00	0.00	0.55	0.20	0.00	0.35	0.00	0.09	1.00
99000	0.00	0.00	0.00	0.92	0.64	0.00	0.22	0.00	0.26	0.58
102000	0.00	0.00	0.00	3.69	0.79	0.00	1.24	0.00	1.27	5.68

Table 73. Single Axle Load Spectra for the Moderately Loaded TWRG

Axle Load (lb)	Vehicle Class									
	4	5	6	7	8	9	10	11	12	13
3000	5.66	7.18	1.80	4.76	18.54	1.88	1.28	12.76	7.42	7.04
4000	2.79	6.44	2.56	3.35	8.00	2.40	0.71	9.88	5.45	7.25
5000	2.89	7.57	3.70	2.19	7.93	2.55	1.24	11.33	6.36	6.16
6000	6.09	10.47	5.84	5.53	8.83	3.52	2.64	9.53	6.35	6.78
7000	6.24	8.85	6.86	7.87	7.27	4.30	4.28	7.55	8.39	5.51
8000	9.45	9.39	9.45	9.11	8.61	7.00	8.01	8.20	11.36	6.85
9000	7.99	7.44	9.56	8.92	8.09	7.45	9.79	6.45	10.93	7.37
10000	9.50	7.11	12.40	9.28	7.61	12.67	14.26	7.08	10.46	9.93
11000	7.72	5.66	10.30	9.46	5.38	12.78	15.08	5.41	8.78	7.71
12000	9.31	5.30	9.70	9.22	4.25	14.74	16.75	3.82	7.14	8.47
13000	7.60	4.33	7.64	7.89	3.65	10.62	11.46	2.81	4.90	6.76
14000	5.26	3.65	5.04	4.78	1.84	5.00	5.03	1.90	2.81	3.99
15000	5.62	3.36	4.76	2.90	2.11	4.07	3.87	2.03	2.53	4.69
16000	3.23	2.68	2.96	4.66	1.39	2.11	1.59	1.62	2.25	2.62
17000	3.21	2.76	2.48	3.45	1.41	2.16	1.27	1.83	1.49	2.60
18000	1.72	2.31	1.66	2.04	1.19	1.62	0.71	1.51	0.96	1.79
19000	1.77	1.90	1.35	1.73	1.08	1.56	0.56	1.21	0.64	1.48
20000	1.20	1.07	0.72	0.76	0.79	1.00	0.35	0.73	0.45	0.91
21000	0.76	0.84	0.44	0.72	0.56	0.92	0.26	0.73	0.35	0.78
22000	0.72	0.53	0.42	0.26	0.42	0.56	0.20	0.82	0.15	0.47
23000	0.41	0.52	0.14	0.19	0.31	0.43	0.13	0.81	0.18	0.25
24000	0.24	0.31	0.06	0.21	0.19	0.23	0.13	0.41	0.38	0.17
25000	0.15	0.10	0.05	0.17	0.10	0.15	0.06	0.20	0.13	0.16
26000	0.22	0.07	0.02	0.06	0.10	0.11	0.05	0.10	0.05	0.06
27000	0.07	0.05	0.01	0.05	0.07	0.07	0.03	0.23	0.07	0.06
28000	0.03	0.02	0.02	0.12	0.05	0.04	0.05	0.07	0.02	0.02
29000	0.02	0.01	0.02	0.17	0.04	0.02	0.02	0.03	0.00	0.02
30000	0.07	0.02	0.01	0.00	0.03	0.01	0.05	0.06	0.00	0.01
31000	0.04	0.02	0.00	0.02	0.04	0.02	0.03	0.10	0.00	0.01
32000	0.00	0.03	0.00	0.05	0.03	0.01	0.02	0.20	0.00	0.02
33000	0.01	0.01	0.03	0.05	0.02	0.00	0.03	0.09	0.00	0.01
34000	0.00	0.00	0.00	0.01	0.01	0.00	0.02	0.05	0.00	0.00
35000	0.00	0.00	0.00	0.00	0.03	0.00	0.01	0.17	0.00	0.00
36000	0.01	0.00	0.00	0.01	0.00	0.00	0.01	0.05	0.00	0.00
37000	0.00	0.00	0.00	0.01	0.01	0.00	0.00	0.07	0.00	0.04
38000	0.00	0.00	0.00	0.00	0.00	0.00	0.00	0.03	0.00	0.00
39000	0.00	0.00	0.00	0.00	0.00	0.00	0.00	0.02	0.00	0.00
40000	0.00	0.00	0.00	0.00	0.00	0.00	0.01	0.02	0.00	0.00
41000	0.00	0.00	0.00	0.00	0.02	0.00	0.01	0.09	0.00	0.01

Table 74. Tandem Axle Load Spectra for the Moderately Loaded TWRG

Axle Load (lb)	Vehicle Class									
	4	5	6	7	8	9	10	11	12	13
6000	6.47	0.00	5.56	9.97	31.80	2.15	4.94	28.29	6.79	8.27
8000	2.78	0.00	6.38	6.68	11.06	3.70	4.29	8.59	5.82	7.70
10000	3.58	0.00	8.27	11.95	9.76	5.59	7.82	18.10	8.25	8.54
12000	3.70	0.00	8.53	10.93	8.72	6.48	10.74	23.52	10.38	8.86
14000	2.98	0.00	8.39	7.85	8.22	6.56	10.21	12.62	9.06	7.30
16000	4.47	0.00	6.87	5.49	6.41	6.22	8.75	2.65	11.47	6.17
18000	4.77	0.00	6.61	5.76	5.50	5.25	6.35	2.39	9.71	5.33
20000	5.55	0.00	5.26	4.22	4.65	5.03	5.32	1.09	6.61	4.89
22000	7.59	0.00	4.89	3.93	2.98	4.72	5.08	0.12	5.63	5.15
24000	8.22	0.00	4.93	4.44	2.63	6.28	5.71	0.00	5.86	5.87
26000	7.01	0.00	5.22	4.23	2.21	6.16	4.69	0.00	4.60	5.60
28000	6.61	0.00	4.85	4.10	1.47	6.72	4.30	0.04	4.48	5.62
30000	7.73	0.00	4.92	3.42	1.17	7.41	4.43	0.87	4.45	5.47
32000	7.90	0.00	4.00	2.70	0.88	7.11	4.31	0.74	2.60	4.48
34000	5.97	0.00	3.54	2.87	0.80	5.99	3.29	0.66	1.20	3.48
36000	4.76	0.00	2.88	2.80	0.72	4.76	2.75	0.22	0.92	2.40
38000	4.07	0.00	2.35	1.50	0.47	3.47	2.01	0.09	0.91	1.66
40000	1.84	0.00	1.75	1.65	0.25	2.53	1.58	0.01	0.36	1.50
42000	1.74	0.00	1.29	0.97	0.06	1.55	1.23	0.00	0.15	0.64
44000	0.56	0.00	1.30	0.46	0.10	0.86	0.61	0.00	0.19	0.50
46000	1.02	0.00	0.79	0.23	0.05	0.59	0.65	0.00	0.24	0.24
48000	0.29	0.00	0.51	0.32	0.00	0.29	0.30	0.00	0.08	0.16
50000	0.15	0.00	0.26	0.43	0.01	0.18	0.28	0.00	0.10	0.06
52000	0.07	0.00	0.18	0.41	0.04	0.12	0.14	0.00	0.14	0.03
54000	0.01	0.00	0.15	0.36	0.00	0.11	0.06	0.00	0.00	0.03
56000	0.04	0.00	0.08	0.24	0.00	0.04	0.07	0.00	0.00	0.01
58000	0.02	0.00	0.03	0.17	0.01	0.04	0.02	0.00	0.00	0.01
60000	0.01	0.00	0.05	0.28	0.04	0.03	0.01	0.00	0.00	0.01
62000	0.03	0.00	0.06	0.62	0.00	0.02	0.02	0.00	0.00	0.01
64000	0.00	0.00	0.02	0.46	0.00	0.01	0.01	0.00	0.00	0.00
66000	0.00	0.00	0.02	0.14	0.00	0.01	0.01	0.00	0.00	0.00
68000	0.05	0.00	0.01	0.09	0.00	0.01	0.01	0.00	0.00	0.00
70000	0.01	0.00	0.03	0.05	0.00	0.01	0.00	0.00	0.00	0.00
72000	0.00	0.00	0.01	0.12	0.00	0.00	0.00	0.00	0.00	0.00
74000	0.00	0.00	0.01	0.06	0.00	0.00	0.01	0.00	0.00	0.01
76000	0.00	0.00	0.00	0.04	0.00	0.00	0.00	0.00	0.00	0.00
78000	0.00	0.00	0.00	0.06	0.00	0.00	0.00	0.00	0.00	0.00
80000	0.00	0.00	0.00	0.00	0.00	0.00	0.00	0.00	0.00	0.00
82000	0.00	0.00	0.00	0.00	0.00	0.00	0.00	0.00	0.00	0.00

Table 75. Tridem Axle Load Spectra for the Moderately Loaded TWRG

Axle Load (lb)	Vehicle Class									
	4	5	6	7	8	9	10	11	12	13
12000	0.00	0.00	93.81	12.62	0.00	46.12	16.06	0.00	28.69	17.88
15000	0.00	0.00	5.96	3.95	7.46	9.66	8.19	0.00	7.90	10.04
18000	0.00	0.00	0.23	5.55	41.03	8.38	5.36	0.00	21.61	6.93
21000	0.00	0.00	0.00	5.88	34.63	8.83	4.77	0.00	3.99	4.54
24000	0.00	0.00	0.00	5.23	14.97	3.35	4.27	0.00	0.78	3.85
27000	0.00	0.00	0.00	7.76	1.91	2.68	4.55	0.00	6.19	4.91
30000	0.00	0.00	0.00	8.25	0.00	5.15	7.07	0.00	10.83	7.88
33000	0.00	0.00	0.00	7.01	0.00	2.12	6.88	0.00	8.62	8.27
36000	0.00	0.00	0.00	8.95	0.00	4.18	8.72	0.00	4.97	8.36
39000	0.00	0.00	0.00	7.69	0.00	2.83	8.73	0.00	2.65	7.80
42000	0.00	0.00	0.00	6.61	0.00	2.26	7.85	0.00	0.18	5.44
45000	0.00	0.00	0.00	6.39	0.00	1.75	6.32	0.00	0.01	5.25
48000	0.00	0.00	0.00	5.72	0.00	0.95	4.16	0.00	0.19	3.06
51000	0.00	0.00	0.00	2.78	0.00	1.28	2.60	0.00	1.22	1.43
54000	0.00	0.00	0.00	1.88	0.00	0.15	1.68	0.00	1.65	1.42
57000	0.00	0.00	0.00	1.83	0.00	0.28	1.01	0.00	0.47	1.17
60000	0.00	0.00	0.00	0.76	0.00	0.03	0.61	0.00	0.05	0.41
63000	0.00	0.00	0.00	0.47	0.00	0.00	0.38	0.00	0.00	0.30
66000	0.00	0.00	0.00	0.20	0.00	0.00	0.29	0.00	0.00	0.20
69000	0.00	0.00	0.00	0.09	0.00	0.00	0.10	0.00	0.00	0.22
72000	0.00	0.00	0.00	0.05	0.00	0.00	0.08	0.00	0.00	0.23
75000	0.00	0.00	0.00	0.09	0.00	0.00	0.06	0.00	0.00	0.13
78000	0.00	0.00	0.00	0.14	0.00	0.00	0.10	0.00	0.00	0.16
81000	0.00	0.00	0.00	0.00	0.00	0.00	0.02	0.00	0.00	0.05
84000	0.00	0.00	0.00	0.01	0.00	0.00	0.02	0.00	0.00	0.06
87000	0.00	0.00	0.00	0.02	0.00	0.00	0.02	0.00	0.00	0.01
90000	0.00	0.00	0.00	0.00	0.00	0.00	0.02	0.00	0.00	0.00
93000	0.00	0.00	0.00	0.01	0.00	0.00	0.01	0.00	0.00	0.00
96000	0.00	0.00	0.00	0.02	0.00	0.00	0.01	0.00	0.00	0.00
99000	0.00	0.00	0.00	0.02	0.00	0.00	0.01	0.00	0.00	0.00
102000	0.00	0.00	0.00	0.02	0.00	0.00	0.05	0.00	0.00	0.00

Table 76. Quad Axle Load Spectra for the Moderately Loaded TWRG

Axle Load (lb)	Vehicle Class									
	4	5	6	7	8	9	10	11	12	13
12000	0.00	0.00	0.00	11.08	0.00	0.00	6.55	0.00	0.00	4.84
15000	0.00	0.00	0.00	3.49	0.00	0.00	3.89	0.00	0.00	1.60
18000	0.00	0.00	0.00	2.64	0.00	0.00	2.76	0.00	0.00	3.12
21000	0.00	0.00	0.00	4.07	0.00	0.00	2.45	0.00	0.00	2.42
24000	0.00	0.00	0.00	6.71	0.00	0.00	2.18	0.00	0.00	2.80
27000	0.00	0.00	0.00	6.68	0.00	0.00	2.65	0.00	0.00	3.26
30000	0.00	0.00	0.00	4.09	0.00	0.00	2.94	0.00	0.00	4.73
33000	0.00	0.00	0.00	3.87	0.00	0.00	4.46	0.00	0.00	7.50
36000	0.00	0.00	0.00	3.26	0.00	0.00	5.16	0.00	0.00	3.24
39000	0.00	0.00	0.00	5.12	0.00	0.00	6.88	0.00	0.00	5.04
42000	0.00	0.00	0.00	4.17	0.00	0.00	6.93	0.00	0.00	5.75
45000	0.00	0.00	0.00	2.96	0.00	0.00	7.75	0.00	0.00	6.34
48000	0.00	0.00	0.00	5.37	0.00	0.00	8.11	0.00	0.00	5.13
51000	0.00	0.00	0.00	6.36	0.00	0.00	9.60	0.00	0.00	7.18
54000	0.00	0.00	0.00	4.06	0.00	0.00	8.46	0.00	0.00	4.98
57000	0.00	0.00	0.00	1.99	0.00	0.00	5.27	0.00	0.00	5.40
60000	0.00	0.00	0.00	0.80	0.00	0.00	2.97	0.00	0.00	6.29
63000	0.00	0.00	0.00	0.69	0.00	0.00	3.37	0.00	0.00	6.71
66000	0.00	0.00	0.00	1.02	0.00	0.00	3.07	0.00	0.00	5.09
69000	0.00	0.00	0.00	1.19	0.00	0.00	2.11	0.00	0.00	2.43
72000	0.00	0.00	0.00	2.14	0.00	0.00	0.86	0.00	0.00	2.25
75000	0.00	0.00	0.00	1.51	0.00	0.00	0.48	0.00	0.00	1.00
78000	0.00	0.00	0.00	1.30	0.00	0.00	0.32	0.00	0.00	0.64
81000	0.00	0.00	0.00	1.16	0.00	0.00	0.13	0.00	0.00	0.74
84000	0.00	0.00	0.00	0.99	0.00	0.00	0.06	0.00	0.00	0.57
87000	0.00	0.00	0.00	2.55	0.00	0.00	0.10	0.00	0.00	0.34
90000	0.00	0.00	0.00	2.16	0.00	0.00	0.11	0.00	0.00	0.12
93000	0.00	0.00	0.00	3.35	0.00	0.00	0.09	0.00	0.00	0.08
96000	0.00	0.00	0.00	2.25	0.00	0.00	0.06	0.00	0.00	0.08
99000	0.00	0.00	0.00	1.43	0.00	0.00	0.05	0.00	0.00	0.11
102000	0.00	0.00	0.00	1.54	0.00	0.00	0.18	0.00	0.00	0.22

Table 77. Single Axle Load Spectra for the Lightly Loaded TWRG

Axle Load (lb)	Vehicle Class									
	4	5	6	7	8	9	10	11	12	13
3000	0.57	2.84	0.73	6.20	16.21	3.26	0.96	6.47	2.68	2.66
4000	0.29	10.63	1.62	0.92	20.68	0.67	0.41	1.71	1.50	8.03
5000	1.96	17.22	1.32	2.27	4.44	2.92	0.81	3.40	3.14	9.09
6000	2.90	17.37	4.73	2.21	8.66	1.08	5.32	5.26	9.75	3.29
7000	3.35	8.73	11.91	6.44	7.56	5.89	3.38	7.56	5.36	9.58
8000	9.61	9.23	17.16	13.55	16.28	6.30	4.35	14.13	9.26	7.46
9000	11.06	8.00	16.33	15.09	5.33	10.43	10.48	14.00	10.88	7.30
10000	14.11	4.71	11.56	13.97	6.79	14.81	16.01	13.58	10.64	12.03
11000	13.19	6.17	8.10	15.21	3.31	15.91	14.77	9.65	11.86	9.13
12000	12.84	6.95	8.07	7.58	2.25	19.54	21.10	8.61	8.33	10.91
13000	9.36	2.66	5.61	2.13	1.74	9.14	16.66	4.62	6.10	5.99
14000	5.04	1.24	2.94	2.89	1.01	2.75	2.49	3.17	5.95	1.69
15000	5.57	1.36	2.71	5.46	1.27	3.07	1.01	2.47	3.68	2.48
16000	2.48	0.78	2.87	1.22	0.68	1.80	0.78	1.24	0.79	2.63
17000	2.64	0.76	1.79	1.59	1.02	0.94	0.41	1.49	1.39	2.35
18000	1.19	0.32	0.95	1.47	0.61	0.49	0.22	1.63	2.09	1.93
19000	1.06	0.33	0.50	0.62	0.61	0.41	0.32	0.52	1.16	2.21
20000	0.36	0.20	0.32	0.41	0.51	0.18	0.12	0.23	0.96	0.93
21000	0.68	0.20	0.27	0.05	0.45	0.14	0.03	0.10	2.90	0.17
22000	0.50	0.13	0.14	0.40	0.21	0.06	0.05	0.00	1.11	0.13
23000	0.43	0.07	0.20	0.16	0.14	0.05	0.02	0.07	0.17	0.01
24000	0.16	0.02	0.00	0.07	0.09	0.03	0.03	0.08	0.14	0.00
25000	0.05	0.02	0.00	0.07	0.04	0.04	0.12	0.01	0.01	0.00
26000	0.06	0.02	0.08	0.02	0.02	0.03	0.01	0.00	0.15	0.00
27000	0.01	0.03	0.04	0.00	0.04	0.02	0.03	0.00	0.00	0.00
28000	0.01	0.00	0.05	0.00	0.01	0.00	0.00	0.00	0.00	0.00
29000	0.07	0.00	0.00	0.00	0.00	0.00	0.00	0.00	0.00	0.00
30000	0.07	0.00	0.00	0.00	0.00	0.01	0.00	0.00	0.00	0.00
31000	0.06	0.00	0.00	0.00	0.00	0.01	0.01	0.00	0.00	0.00
32000	0.00	0.00	0.00	0.00	0.01	0.00	0.00	0.00	0.00	0.00
33000	0.00	0.00	0.00	0.00	0.03	0.00	0.00	0.00	0.00	0.00
34000	0.00	0.00	0.00	0.00	0.00	0.01	0.00	0.00	0.00	0.00
35000	0.06	0.00	0.00	0.00	0.00	0.01	0.00	0.00	0.00	0.00
36000	0.08	0.00	0.00	0.00	0.00	0.00	0.00	0.00	0.00	0.00
37000	0.02	0.00	0.00	0.00	0.00	0.00	0.00	0.00	0.00	0.00
38000	0.04	0.00	0.00	0.00	0.00	0.00	0.00	0.00	0.00	0.00
39000	0.12	0.00	0.00	0.00	0.00	0.00	0.01	0.00	0.00	0.00
40000	0.00	0.00	0.00	0.00	0.00	0.00	0.04	0.00	0.00	0.00
41000	0.00	0.01	0.00	0.00	0.00	0.00	0.05	0.00	0.00	0.00

Table 78. Tandem Axle Load Spectra for the Lightly Loaded TWRG

Axle Load (lb)	Vehicle Class									
	4	5	6	7	8	9	10	11	12	13
6000	0.20	0.00	3.08	6.37	27.90	0.21	2.02	21.16	5.23	2.94
8000	0.53	0.00	5.41	2.65	6.60	2.48	2.11	20.59	0.58	5.66
10000	0.67	0.00	10.09	5.21	11.66	6.50	3.73	17.51	6.63	6.20
12000	1.12	0.00	10.50	7.38	30.71	10.25	4.00	18.74	13.19	3.03
14000	2.42	0.00	8.57	4.70	5.77	7.36	3.76	7.07	10.68	1.42
16000	4.37	0.00	7.46	6.69	4.55	6.18	4.32	2.83	2.28	4.99
18000	7.69	0.00	7.42	4.84	2.96	6.54	6.22	1.98	6.66	7.62
20000	12.92	0.00	7.30	4.67	2.50	4.18	6.36	1.56	9.34	8.55
22000	15.18	0.00	5.02	5.89	0.60	4.41	12.63	4.30	15.59	4.18
24000	14.41	0.00	5.18	5.98	1.16	6.95	12.75	1.82	14.66	4.76
26000	10.13	0.00	8.16	6.03	0.97	8.00	6.87	1.55	6.68	10.91
28000	11.15	0.00	6.62	3.37	0.53	9.07	13.50	0.89	3.45	8.82
30000	7.88	0.00	5.25	7.17	0.57	6.74	12.43	0.00	0.90	7.87
32000	4.42	0.00	4.18	3.50	0.44	4.60	2.96	0.00	2.81	4.21
34000	2.14	0.00	2.13	5.84	0.04	4.67	2.06	0.00	0.86	2.83
36000	2.06	0.00	1.49	5.50	0.00	2.92	1.54	0.00	0.00	2.71
38000	1.42	0.00	1.26	2.76	0.18	2.20	0.99	0.00	0.00	1.33
40000	0.38	0.00	0.16	1.89	0.24	1.57	0.38	0.00	0.00	1.72
42000	0.04	0.00	0.23	4.15	0.42	1.98	0.23	0.00	0.00	2.28
44000	0.24	0.00	0.33	2.06	0.19	1.52	0.43	0.00	0.00	1.83
46000	0.11	0.00	0.05	2.20	0.09	1.25	0.27	0.00	0.00	0.75
48000	0.00	0.00	0.00	0.56	0.30	0.23	0.10	0.00	0.00	0.20
50000	0.06	0.00	0.03	0.12	0.25	0.05	0.02	0.00	0.21	0.48
52000	0.12	0.00	0.08	0.03	0.09	0.03	0.14	0.00	0.25	2.08
54000	0.08	0.00	0.00	0.15	0.11	0.01	0.03	0.00	0.00	1.96
56000	0.00	0.00	0.00	0.20	0.22	0.02	0.01	0.00	0.00	0.44
58000	0.00	0.00	0.00	0.09	0.15	0.01	0.03	0.00	0.00	0.23
60000	0.00	0.00	0.00	0.00	0.05	0.01	0.00	0.00	0.00	0.00
62000	0.00	0.00	0.00	0.00	0.01	0.02	0.01	0.00	0.00	0.00
64000	0.00	0.00	0.00	0.00	0.18	0.01	0.00	0.00	0.00	0.00
66000	0.00	0.00	0.00	0.00	0.32	0.01	0.02	0.00	0.00	0.00
68000	0.00	0.00	0.00	0.00	0.18	0.01	0.03	0.00	0.00	0.00
70000	0.09	0.00	0.00	0.00	0.01	0.00	0.00	0.00	0.00	0.00
72000	0.00	0.00	0.00	0.00	0.05	0.00	0.00	0.00	0.00	0.00
74000	0.10	0.00	0.00	0.00	0.00	0.01	0.00	0.00	0.00	0.00
76000	0.07	0.00	0.00	0.00	0.00	0.00	0.00	0.00	0.00	0.00
78000	0.00	0.00	0.00	0.00	0.00	0.00	0.00	0.00	0.00	0.00
80000	0.00	0.00	0.00	0.00	0.00	0.00	0.00	0.00	0.00	0.00
82000	0.00	0.00	0.00	0.00	0.00	0.00	0.05	0.00	0.00	0.00

Table 79. Tridem Axle Load Spectra for the Lightly Loaded TWRG

Axle Load (lb)	Vehicle Class									
	4	5	6	7	8	9	10	11	12	13
12000	0.00	0.00	0.00	26.92	0.70	42.86	10.61	0.00	21.05	13.43
15000	0.00	0.00	9.70	2.38	15.43	15.16	8.87	0.00	0.58	2.37
18000	0.00	0.00	38.86	3.03	32.08	21.02	8.54	35.32	0.03	0.25
21000	0.00	0.00	33.08	6.44	23.79	11.78	5.23	55.06	0.00	0.50
24000	0.00	0.00	17.85	6.06	24.00	1.95	10.38	9.04	0.00	1.40
27000	0.00	0.00	0.51	5.63	3.24	3.90	4.30	0.52	0.23	2.61
30000	0.00	0.00	0.00	6.73	0.76	0.79	18.20	0.06	3.83	9.27
33000	0.00	0.00	0.00	6.86	0.00	0.08	13.97	0.00	9.03	24.88
36000	0.00	0.00	0.00	11.66	0.00	0.00	8.14	0.00	9.78	21.47
39000	0.00	0.00	0.00	11.84	0.00	0.06	3.43	0.00	11.69	5.27
42000	0.00	0.00	0.00	3.60	0.00	0.48	2.45	0.00	10.47	5.56
45000	0.00	0.00	0.00	1.89	0.00	1.92	1.87	0.00	4.99	7.57
48000	0.00	0.00	0.00	1.87	0.00	0.00	1.37	0.00	2.50	1.83
51000	0.00	0.00	0.00	1.86	0.00	0.00	1.02	0.00	2.65	0.41
54000	0.00	0.00	0.00	1.24	0.00	0.00	1.08	0.00	3.70	0.18
57000	0.00	0.00	0.00	0.77	0.00	0.00	0.29	0.00	4.83	0.14
60000	0.00	0.00	0.00	0.87	0.00	0.00	0.11	0.00	3.69	0.22
63000	0.00	0.00	0.00	0.13	0.00	0.00	0.06	0.00	5.43	0.92
66000	0.00	0.00	0.00	0.17	0.00	0.00	0.08	0.00	4.38	1.30
69000	0.00	0.00	0.00	0.05	0.00	0.00	0.00	0.00	0.28	0.19
72000	0.00	0.00	0.00	0.00	0.00	0.00	0.00	0.00	0.37	0.01
75000	0.00	0.00	0.00	0.00	0.00	0.00	0.00	0.00	0.35	0.04
78000	0.00	0.00	0.00	0.00	0.00	0.00	0.00	0.00	0.14	0.10
81000	0.00	0.00	0.00	0.00	0.00	0.00	0.00	0.00	0.00	0.08
84000	0.00	0.00	0.00	0.00	0.00	0.00	0.00	0.00	0.00	0.00
87000	0.00	0.00	0.00	0.00	0.00	0.00	0.00	0.00	0.00	0.00
90000	0.00	0.00	0.00	0.00	0.00	0.00	0.00	0.00	0.00	0.00
93000	0.00	0.00	0.00	0.00	0.00	0.00	0.00	0.00	0.00	0.00
96000	0.00	0.00	0.00	0.00	0.00	0.00	0.00	0.00	0.00	0.00
99000	0.00	0.00	0.00	0.00	0.00	0.00	0.00	0.00	0.00	0.00
102000	0.00	0.00	0.00	0.00	0.00	0.00	0.00	0.00	0.00	0.00

Table 80. Quad Axle Load Spectra for the Lightly Loaded TWRG

Axle Load (lb)	Vehicle Class									
	4	5	6	7	8	9	10	11	12	13
12000	0.00	0.00	0.00	0.00	0.00	18.43	1.77	0.00	0.00	0.01
15000	0.00	0.00	0.00	0.00	0.00	4.84	4.01	0.00	0.00	0.99
18000	0.00	0.00	0.00	0.16	0.00	20.58	3.88	0.00	0.00	6.60
21000	0.00	0.00	0.00	5.41	0.00	15.76	0.44	0.00	0.00	0.63
24000	0.00	0.00	0.00	14.03	0.00	7.56	1.04	0.00	0.00	0.09
27000	0.00	0.00	0.00	17.16	0.00	9.26	0.42	0.00	0.00	0.00
30000	0.00	0.00	0.00	18.85	0.00	3.42	0.72	0.00	0.00	0.00
33000	0.00	0.00	0.00	4.70	0.00	0.73	2.91	0.00	0.00	0.25
36000	0.00	0.00	0.00	0.51	0.00	0.26	10.88	0.00	0.00	2.49
39000	0.00	0.00	0.00	0.02	0.00	0.00	21.85	0.00	0.00	5.05
42000	0.00	0.00	0.00	0.00	0.00	0.00	10.33	0.00	0.00	6.20
45000	0.00	0.00	0.00	0.00	0.00	0.00	13.87	0.00	0.00	7.12
48000	0.00	0.00	0.00	0.00	0.00	0.00	9.33	0.00	0.00	2.29
51000	0.00	0.00	0.00	0.00	0.00	0.00	9.66	0.00	0.00	0.67
54000	0.00	0.00	0.00	0.00	0.00	0.00	2.49	0.00	0.00	0.79
57000	0.00	0.00	0.00	0.00	0.00	0.40	2.30	0.00	0.00	0.12
60000	0.00	0.00	0.00	0.03	0.00	2.86	1.18	0.00	0.00	0.02
63000	0.00	0.00	0.00	3.15	0.00	5.39	0.60	0.00	0.00	0.37
66000	0.00	0.00	0.00	3.85	0.00	4.50	1.02	0.00	0.00	4.21
69000	0.00	0.00	0.00	5.96	0.00	4.05	0.40	0.00	0.00	22.72
72000	0.00	0.00	0.00	1.47	0.00	0.30	0.00	0.00	0.00	18.94
75000	0.00	0.00	0.00	2.13	0.00	0.25	0.38	0.00	0.00	7.46
78000	0.00	0.00	0.00	2.99	0.00	0.71	0.03	0.00	0.00	3.62
81000	0.00	0.00	0.00	12.40	0.00	0.70	0.00	0.00	0.00	0.37
84000	0.00	0.00	0.00	0.54	0.00	0.00	0.00	0.00	0.00	0.47
87000	0.00	0.00	0.00	1.68	0.00	0.00	0.00	0.00	0.00	0.92
90000	0.00	0.00	0.00	4.08	0.00	0.00	0.00	0.00	0.00	1.31
93000	0.00	0.00	0.00	0.82	0.00	0.00	0.22	0.00	0.00	3.31
96000	0.00	0.00	0.00	0.06	0.00	0.00	0.01	0.00	0.00	2.02
99000	0.00	0.00	0.00	0.00	0.00	0.00	0.00	0.00	0.00	0.27
102000	0.00	0.00	0.00	0.00	0.00	0.00	0.26	0.00	0.00	0.69

Table 81. WIM Sites Associated with Idaho Truck Weight Road Groups

Idaho Truck Weight Road Groups (TWRG)	WIM Station
Primarily Loaded	79, 117, 134, 148, 155
Moderately Loaded	93, 137, 138, 156, 169, 185
Lightly Loaded	96, 129, 192

Number of Axles per Truck Type

The *TrafLoad* software outputs the average number of axles for each axle category and truck type. This number represents the total number of each axle type (single, tandem, tridem, and quad) divided by the total number of trucks. The statewide number of axles per truck type based on the analysis of the Idaho WIM data is illustrated in Table 82. A comparison of the developed statewide and MEPDG default number of axles per truck is shown in Figure 103. This figure shows that for all practical purposes, there is no significant difference in the number of single, tandem and tridem axles per truck for all truck classes. ITD data showed few quad axles for vehicle classes 7, 10, 11, and 13 while MEPDG has 0 percent quad axles for all truck types.

Table 82. Number of Axles per Truck Type

Truck Class	Average Number of Axles			
	Single	Tandem	Tridem	Quad
4	1.59	0.34	0.00	0.00
5	2.00	0.00	0.00	0.00
6	1.00	1.00	0.00	0.00
7	1.00	0.22	0.83	0.10
8	2.52	0.60	0.00	0.00
9	1.25	1.87	0.00	0.00
10	1.03	0.85	0.95	0.26
11	4.21	0.29	0.01	0.00
12	3.24	1.16	0.07	0.01
13	3.32	1.79	0.14	0.02

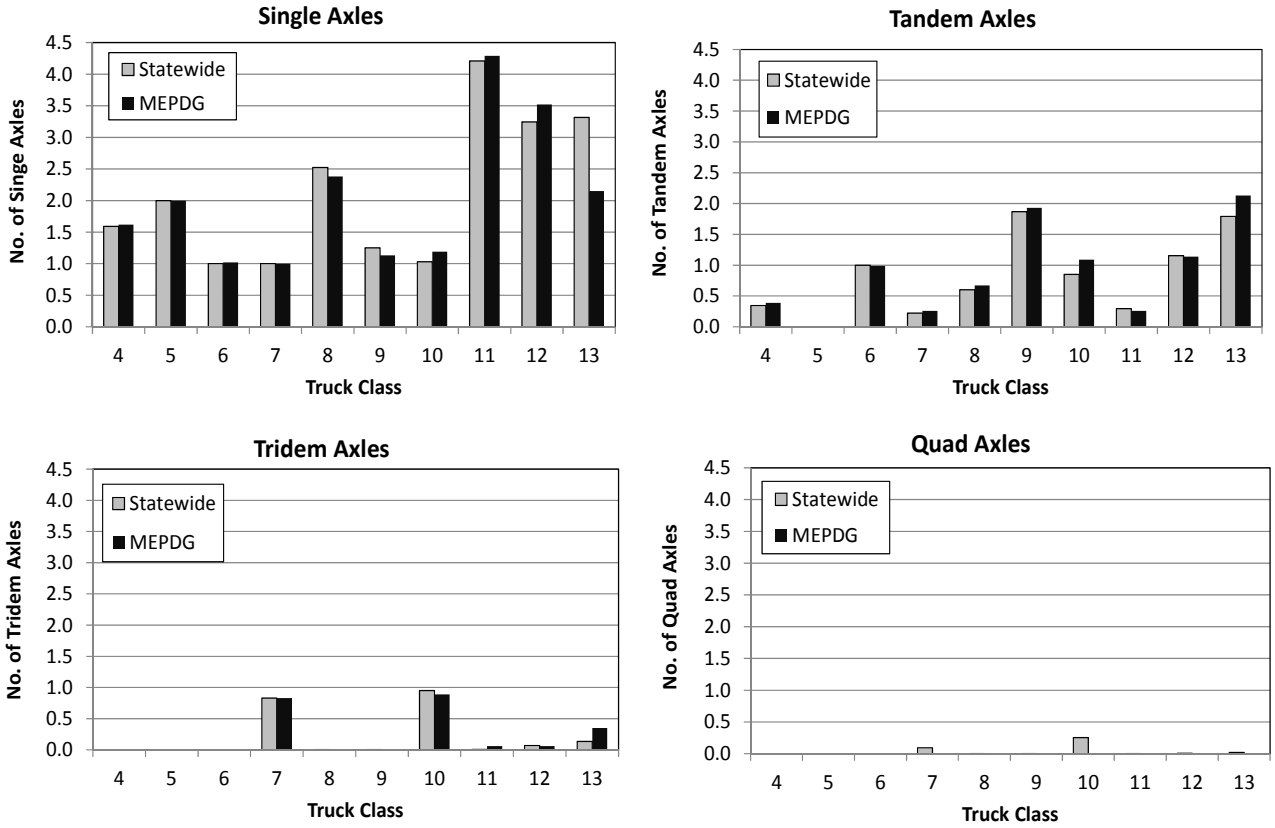

Figure 103. Comparison of Statewide and MEPDG Default Number of Axles per Truck for Vehicle Classes 4 to 13

Idaho Traffic Characterization Database

The developed traffic characteristics at the investigated WIM sites are provided in electronic format on a CD database. The database is explained in Appendix D. Traffic ALS data were developed for the 3 input levels in MEPDG. Site-specific data for level 1 at all WIM sites was developed. TWRG ALS (level 2) and statewide averages (level 3) were also developed based on the analyzed traffic data.

Distress Prediction for Statewide ALS versus National Defaults

The developed statewide ALS was compared to the default ALS in MEPDG, which was based on the nationwide LTPP database. A typical pavement section was selected for this comparative study. The pavement section properties and primary inputs used for this study are illustrated in Table 83. MEPDG software was run using the typical inputs shown in Table 83 with all inputs kept constant except for the ALS.

Table 83. Typical Design Inputs Used in the Analysis

Parameter	Input
General Information: Type of Design Reliability	 Flexible 50%
Design Life AADTT (in design lane) Axle Load Spectra Vehicle Class Distribution Monthly Adjustment Factor No. of Axles per Truck Operational Speed	20 years 150 Variable Default Default Default 60 mph
Climate	Pullman/Moscow
HMA Layer: Thickness, in. Mix	 6 ½" ITD SP-2 Mix, PG 58-28
Granular Base: Thickness, in. Modulus, psi	 8 40,000
Subgrade: Classification Modulus, psi	 CL 5,600

A comparison between predicted longitudinal and alligator fatigue cracking based on statewide versus MEPDG default ALS is shown in Figure 104 and Figure 105, respectively. These figures show that the developed statewide ALS yielded significantly higher cracking compared MEPDG default ALS. Figure 106 and Figure 107 illustrate the influence of the statewide compared to MEPDG default ALS on the total rutting, and AC layer rutting, respectively. These figures show that, in general, rutting is not as sensitive to ALS as cracking. Finally, the Influence of the statewide axle load spectra on the predicted IRI is shown in Figure 108. It can be inferred from this figure that there is no significant difference in predicted IRI based on statewide and MEPDG default ALS.

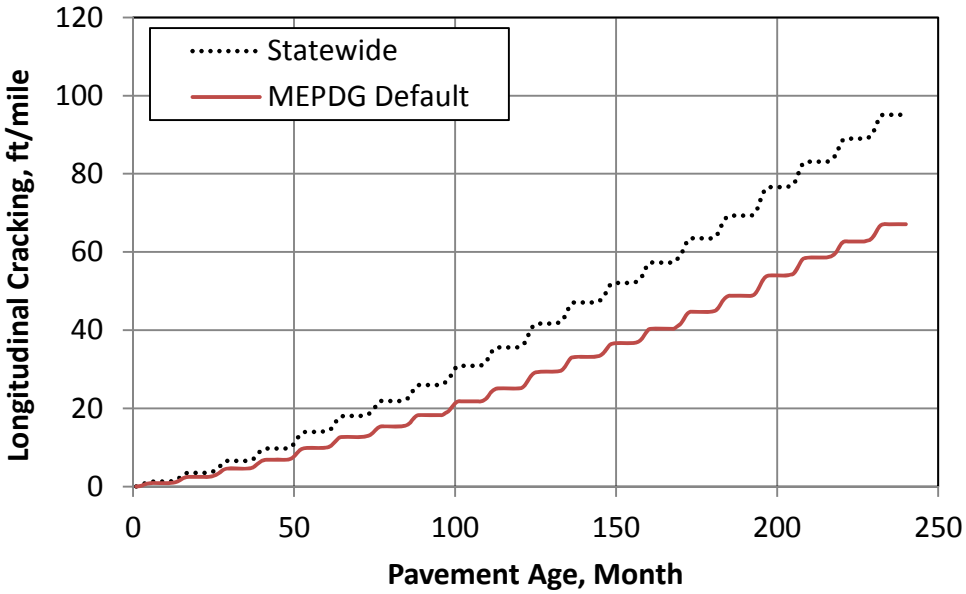

Figure 104. Influence of Statewide and MEPDG Default ALS on Predicted Longitudinal Cracking

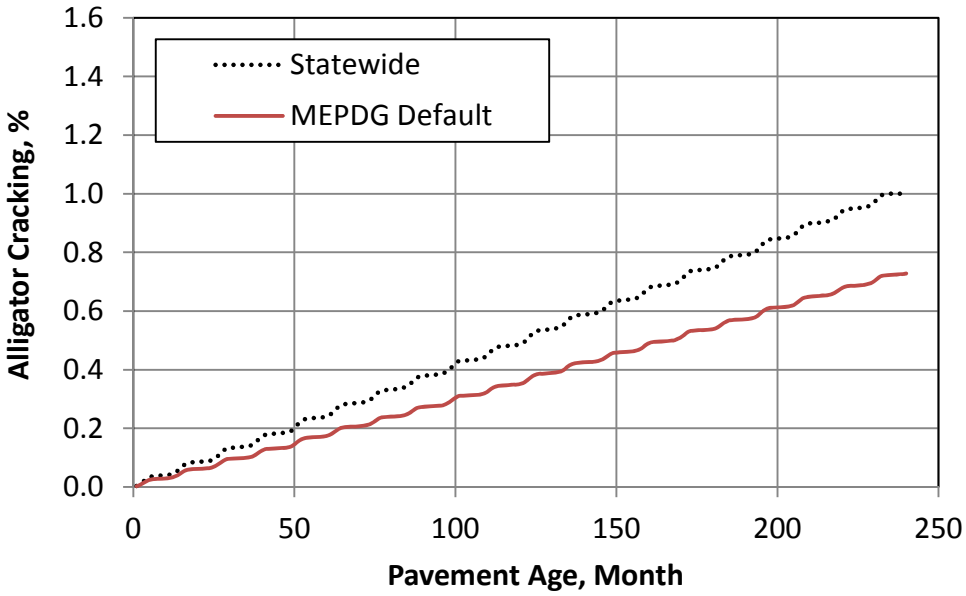

Figure 105. Influence of Statewide and MEPDG Default ALS on Predicted Alligator Cracking

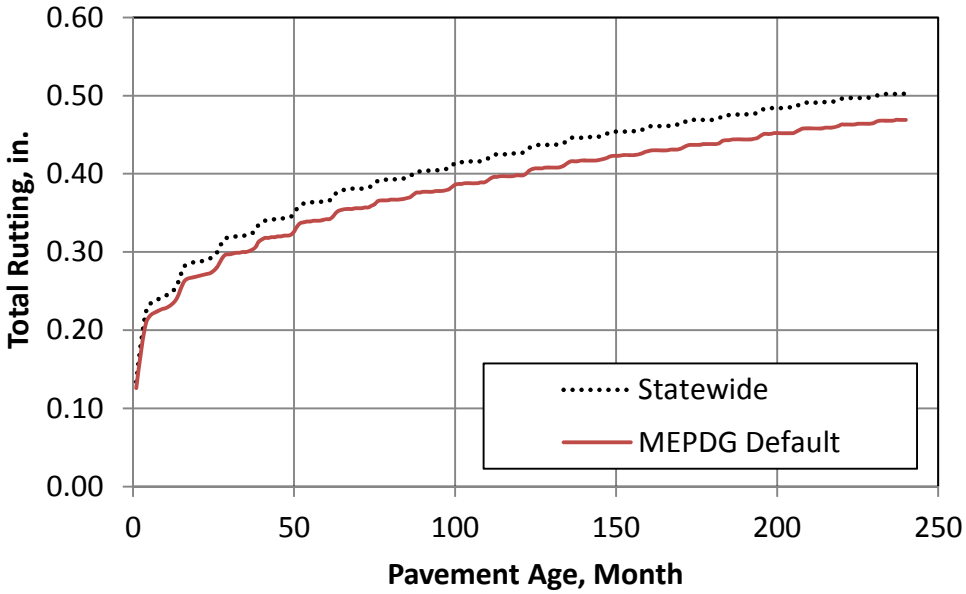

Figure 106. Influence of Statewide and MEPDG Default ALS on Predicted Total Rutting

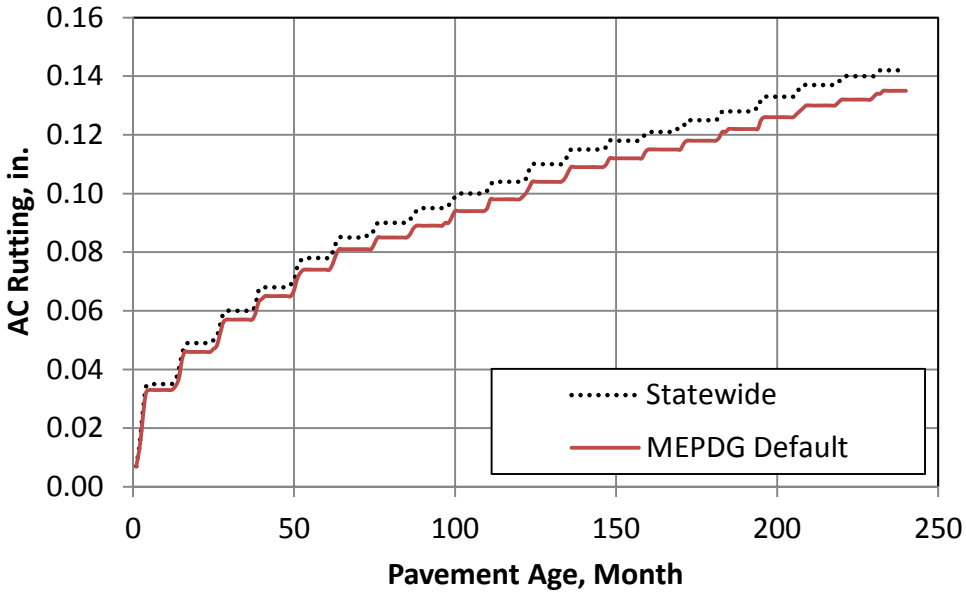

Figure 107. Influence of Statewide and MEPDG Default ALS on Predicted AC Rutting

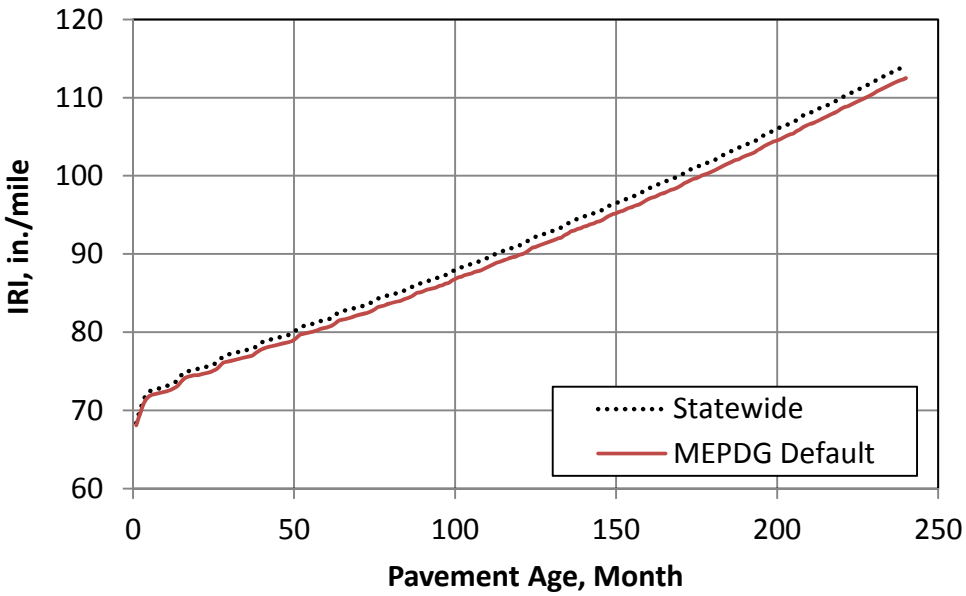

Figure 108. Influence of Statewide and MEPDG Default ALS on Predicted IRI

Impact of Traffic Input Level on MEPDG Practiced Performance

It is important to study the significance of the level of traffic inputs on the MEPDG predicted performance. A sensitivity study is conducted on a typical Idaho pavement section with level 1 (site-specific) versus level 3 (statewide/national or default) traffic data. The traffic data included in the study are ALS, VCD, MAF, and number of axles per truck. The pavement section properties and primary inputs used for this study are illustrated in Table 83. All other MEPDG inputs used in this analysis were taken as the MEPDG default values. The difference between the predicted distresses based on levels 1 and 3 inputs was normalized using the equation given in Figure 109.

$$NE = \frac{|X_{level\ 1} - X_{level\ 3}|}{X_{level\ 1}}.100$$

where:

NE = Absolute value of the normalized difference
$X_{level\ 1}$ = Predicted distress based on site-specific (level 1) inputs
$X_{level\ 3}$ = Predicted distress based on statewide/national default (level 3) inputs

Figure 109. Equation to Calculate the Normalized Error

Predicted Performance based on Site-Specific versus Developed Statewide ALS

The absolute normalized error values computed for MEPDG predicted longitudinal cracking, alligator cracking, AC rutting, total rutting, and IRI based on site-specific and developed statewide ALS are shown in Table 84. Large errors in predicted longitudinal cracking occurred as a result of using statewide ALS instead of site-specific ALS. The absolute normalized error (NE) for longitudinal cracking ranged from 5% to more than 100% with an average value exceeding 40%. For alligator cracking the error was also high with an average value of 31%. The average NE values for AC rutting, total rutting and IRI were generally very small especially for IRI. This data indicates that ALS has a significant influence on load-associated cracking and minor to negligible influence on rutting and IRI.

Table 84. Influence of Site-Specific versus MEPDG Default ALS on MEPDG Predicted Distresses and IRI

WIM Site ID	Absolute Normalized Error (NE), %				
	Longitudinal Cracking	Alligator Cracking	AC Rutting	Total Rutting	IRI
79	11.0	4.8	2.1	1.2	0.3
93	48.3	44.3	2.2	10.1	1.9
96	32.0	2.4	3.4	1.0	0.2
117	55.7	34.0	8.4	11.0	2.3
134	49.4	21.7	11.8	5.8	1.2
137	23.8	24.5	3.6	4.6	0.9
138	52.3	43.1	2.2	10.1	1.8
148	63.3	43.1	9.2	8.2	1.5
155	50.4	62.3	9.6	16.9	4.2
156	10.6	3.8	0.7	1.2	0.3
185	130.0	88.4	10.9	17.5	3.0
192	5.2	0.0	2.1	1.8	0.4
Average	44.3	31.0	5.5	7.4	1.5
Standard Deviation	32.0	26.0	3.9	5.6	1.2

Predicted Performance based on Site-Specific versus National Default VCD

To investigate the influence of site-specific (level 1) VCD versus equivalent MEPDG TTC group distribution (level 3), the WIM sites with VCD that matches any of the MEPDG 17 TTC groups were identified. For each WIM site data, 1 run was conducted using actual site-specific traffic data related to ALS, MAF, number of axles per truck, and VCD while the other run used the equivalent MEPDG TTC distribution instead of actual VCD.

Table 85 summarizes the computed normalized errors. The average error values shown in this table indicate that using the appropriate MEPDG TTC group may lead to satisfactory results in regard to

alligator cracking, rutting, and IRI (average NE of 7.1%, 3.9%, 2.6%, and 0.5%, respectively). On the other hand, higher average NE percent (20.9) occurred with respect to longitudinal cracking if MEPDG TTC group is used instead of actual VCD.

Table 85. Influence of Site-Specific VCD versus Equivalent MEPDG TTC Group Distribution on MEPDG Predicted Distresses and IRI

WIM Site ID	Absolute Normalized Error (NE), %				
	Longitudinal Cracking	Alligator Cracking	AC Rutting	Total Rutting	IRI
79	14.5	6.7	3.6	2.1	0.4
93	34.5	6.1	4.1	3.6	0.6
96	18.8	14.7	5.1	2.9	0.5
134	9.9	3.4	2.6	1.1	0.2
137	32.8	8.1	5.9	4.3	0.8
192	14.6	3.7	1.9	1.6	0.3
Average	20.9	7.1	3.9	2.6	0.5
Standard Deviation	10.3	4.2	1.5	1.2	0.2

Predicted Performance based on Site-Specific versus National Default MAF

Table 86 shows the comparison results of the computed absolute normalized error values for MEPDG predicted distresses and roughness when level 1 and level 3 MAF were used. This data shows a high average error of 26.3 percent in longitudinal cracking predictions. In addition, alligator cracking, and AC rutting show relatively small average absolute percent errors (8.8 and 7.1). Total rutting and IRI show very small average NE of only 2.7 and 0.5 percent, respectively.

Table 86. Influence of Site-Specific versus MEPDG Default MAF on MEPDG Predicted Distresses and IRI

WIM Site ID	Absolute Normalized Error (NE), %				
	Longitudinal Cracking	Alligator Cracking	AC Rutting	Total Rutting	IRI
79	0.0	0.6	0.7	0.2	0.0
93	0.9	1.0	0.7	0.2	0.1
96	5.3	1.6	3.5	1.0	0.2
117	73.4	34.2	21.1	7.6	1.6
134	4.4	0.8	0.0	0.0	0.0
137	2.8	0.6	0.0	0.0	0.0
138	26.7	10.7	6.7	3.8	0.6
148	29.1	16.8	12.2	5.1	1.0
155	111.0	8.5	16.3	4.9	1.1
156	15.6	1.9	4.0	0.6	0.2
185	20.6	14.4	9.9	4.1	0.8
192	25.8	14.6	10.4	4.6	0.8
Average	26.3	8.8	7.1	2.7	0.5
Standard Deviation	33.5	10.2	6.9	2.6	0.5

Predicted Performance based on Site-Specific versus Statewide Number of Axles per Truck

Table 87 shows the comparison results of the computed absolute normalized difference values for MEPDG predicted distresses and roughness when site-specific and the developed statewide MAF were used. This data indicates that, for all practical purposes, there is no significant difference in predicted distresses and IRI based on level 1and level 3 number of axles per truck. Thus, statewide/national number of axles per truck can be used without sacrificing accuracy of pavement performance predictions.

Table 87. Influence of Site-Specific versus MEPDG Default MAF on MEPDG Predicted Distresses and IRI

WIM Site ID	Absolute Normalized Error (NE), %				
	Longitudinal Cracking	Alligator Cracking	AC Rutting	Total Rutting	IRI
79	0.0	0.6	0.0	0.0	0.0
93	0.9	1.1	0.7	0.2	0.1
96	5.0	2.3	0.7	0.6	0.2
117	1.9	1.3	0.6	0.4	0.0
134	1.1	0.8	0.0	0.0	0.0
137	1.6	0.5	0.0	0.0	0.0
138	3.7	0.8	0.0	0.0	0.1
148	0.7	0.0	0.0	0.0	0.0
155	6.8	1.1	0.0	0.3	0.0
156	5.6	1.0	0.0	0.6	0.1
185	0.0	0.0	0.0	0.0	0.0
192	16.2	4.0	0.0	0.8	0.1
Average	3.6	1.1	0.2	0.2	0.0
Standard Deviation	4.4	1.0	0.3	0.3	0.1

Chapter 7
Idaho Climatic Database

Pavement performance is significantly affected by the environmental conditions, in particular temperature and moisture. Changes in moisture and temperature during the pavement service life greatly affect the strength of the pavement layers, and hence, its load carrying capacity. Sensitivity of pavement performance to input parameters described in Chapter 3 concluded that even climate differences within the state can have a significant influence on pavement performance. This chapter presents the climatic data required to run MEPDG. It also presents the climatic weather stations that can be used in Idaho.

MEPDG Required Climatic Data

The climatic inputs in MEPDG fall under the following categories:

- Weather-related information.
    - Hourly air temperature
    - Hourly precipitation
    - Hourly wind speed
    - Hourly percentage sunshine (used to define cloud cover)
    - Hourly relative humidity
- Ground water related information

The MEPDG software provides 851 weather station data, from the National Climatic Data Center (NCDC) database, containing up to 10 years (1995 to 2005) of the hourly air temperature, precipitation, wind speed, percentage sunshine, and relative humidity data distributed throughout the U.S.[18] Figure 110 presents a map that shows the distribution of the MEPDG built-in weather station data throughout the U.S. It should be noted that, if the design life is more than 10 years, the software takes the actual number of yearly climatic data and then repeats this data to achieve the required length of time (design life).

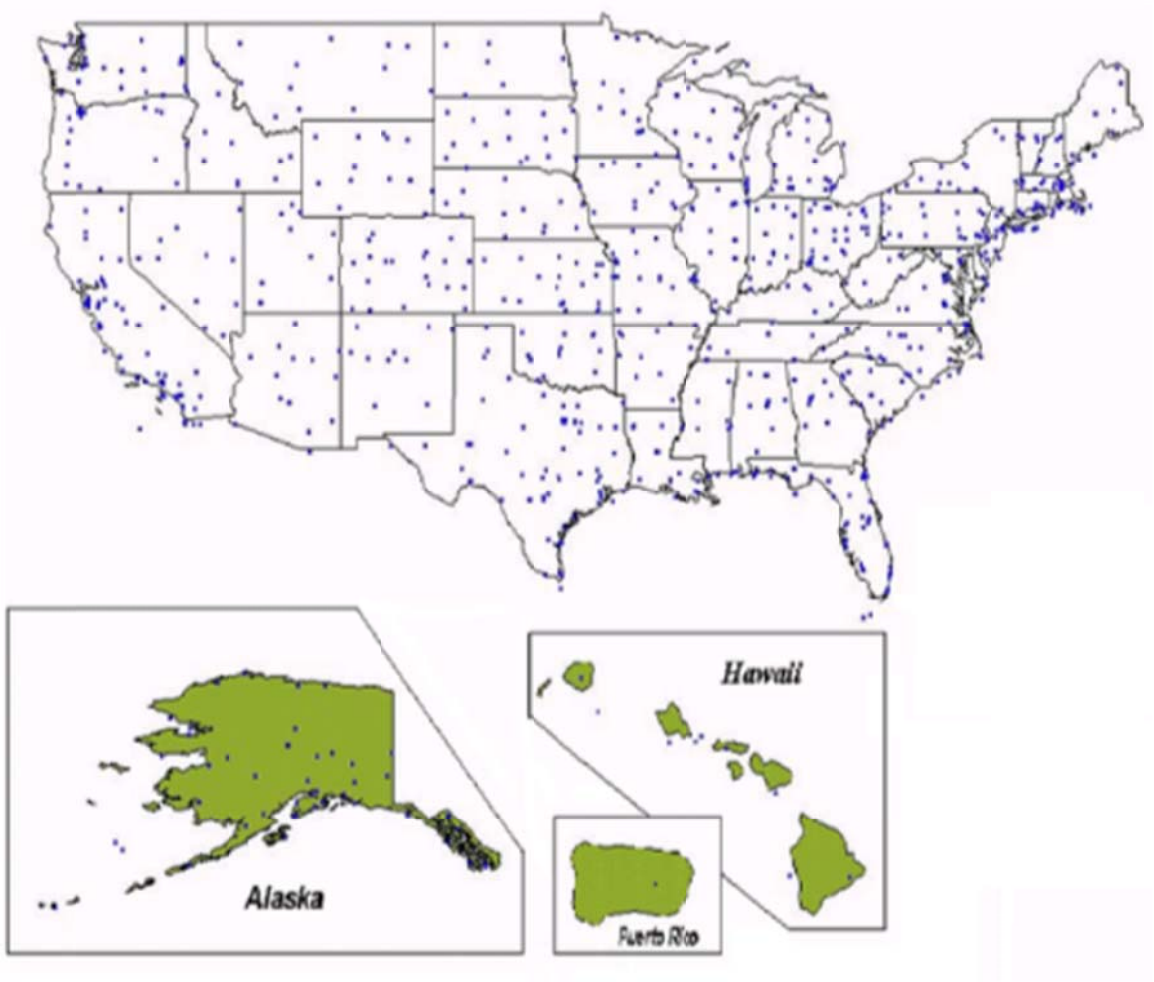

Figure 110. Locations of the Climatic Data Available in the MEPDG

To specify the climatic location for a specific project, users have 2 options as follows:

1) Import a previously generated climatic file.
2) Generate the climatic file using the available MEPDG built –in weather station database. A single weather station may be selected for projects within close proximity to a particular test section. When weather stations are unavailable within this proximity of the test section (project), the closest 6 surrounding weather stations populated automatically by the software may be selected and combined into a virtual weather station for the test section. To do that users are required to input the longitude, latitude, and elevation of the project site.

Idaho Climatic Database

In Idaho, 12 weather stations are included in the MEPDG national database. The location information and the number of months of available data as well as the missing data, if any, for these stations are summarized in Table 88. Additionally, there are about 20 weather station sites located in the surrounding states of Idaho that are in close proximity to the Idaho borders. Climatic data from these stations can also be used for Idaho. Table 89 summarizes the location information and the number of months of available climatic data and the missing data, if any, for these stations. It should be noted that, the software crashes if weather stations with missing data are used. Figure 111 depicts the locations of weather stations in Idaho and the surrounding states that can be used for Idaho.

Table 88. Summary of Idaho Weather Stations Currently Available in MEPDG Software Version 1.10

Weather Station	Station Location	Latitude (Degree.Minute)	Longitude (Degree.Minute)	Elevation (ft)	Months of Available Data	Months Missing in File
Boise	Boise Air Terminal/ Gowen Field Airport	43.34	-116.13	2861	116	0
Burley	Burley Municipal Airport	42.32	-113.46	4151	64	0
Challis	Challis Airport	41.31**	-114.13	5042	90	0
Idaho Falls	Idaho Falls Regional Airport	43.31	-112.04	4768	97	0
Jerome	Jerome County Airport	42.44	-114.28	4012	109	4*
Lewiston	Lewiston-Nez-Perce County airport	46.22	-117.01	1447	116	0
MC Call	McCall Municipal Airport	44.53	-116.06	5032	101	0
Mullan Pass	Mullan Pass	47.28	-115.38	6074	116	0
Pocatello	Pocatello Regional Airport	42.55	-112.34	4454	116	0
Rexburg	Rexburg-Madison County Airport	43.5	-111.53	4875	97	1*
Twin Falls	Joslin Field-Magic Valley Regional Airport	42.29	-114.29	4148	105	1*
Pullman /Moscow	Pullman/Moscow Regional Airport	46.44	-117.07	2540	93	0

* It is not preferable to use weather stations with missing data as it might cause the software to crash
** The latitude for Challis Airport should be 44.3 according to Google Earth and www.airnav.com. This should be corrected in MEPDG

.

Table 89. Summary of Weather Stations Located in Idaho Adjacent States Close to Idaho Borders Currently Available in the MEPDG Software Version 1.10

Weather Station	Station Location	State	Latitude (Degree.Minute)	Longitude (Degree.Minute)	Elev. (ft)	Months of Available Data	Months Missing in File
Baker City	Backer City Municipal Airport	OR	44.5	-117.49	3363	52	0
Burns	Burns Municipal Airport	OR	43.35	-118.57	4148	116	0
Meacham	Meacham	OR	45.31	-118.25	3729	94	0
Pendleton	Eastern Oregon Regional Airport	OR	45.42	-118.5	1516	116	1*
Ontario	Ontario Municipal Airport	OR	44.01	-117.01	2192	104	0
Deer Park	Deer Park Airport	WA	47.58	-117.25	2196	88	1*
Spokane	Spokane International Airport	WA	47.37	-117.32	2384	116	0
Spokane	Felts Field Airport	WA	47.41	-117.19	1979	89	0
Bozeman	Gallatin Field Airport	MT	45.47	-111.09	4468	116	0
Butte	Bert Mooney Airport	MT	45.58	-112.3	5539	64	0
Dillon	Dillon Airport	MT	45.16	-112.33	5221	105	0
Livingston	Mission Field Airport	MT	45.42	-110.27	4655	65	0
Missoula	Missoula International Airport	MT	46.55	-114.05	3202	114	0
Big Piney	Big Piney Marbleton Airport	WY	42.35	-110.07	6947	96	0
Evanston	Evanston-Unita County Burns Field Airport	WY	41.16	-111.02	7143	79	0
Logan	Logan-Cache Airport	UT	41.47	-111.51	4447	88	0
Ogden	Ogden-Hinckley Airport	UT	41.12	-112.01	4441	94	0
Salt Lake City	Salt Lake City International Airport	UT	40.47	-111.58	4224	108	11*
Elko	Elko Regional Airport	NV	40.5	-115.47	5079	61	0
Winnemucca	Winnemucca Municipal Airport	NV	40.54	-117.49	4300	116	1*

* It is not preferable to use weather stations with missing data as it might cause the software to crash

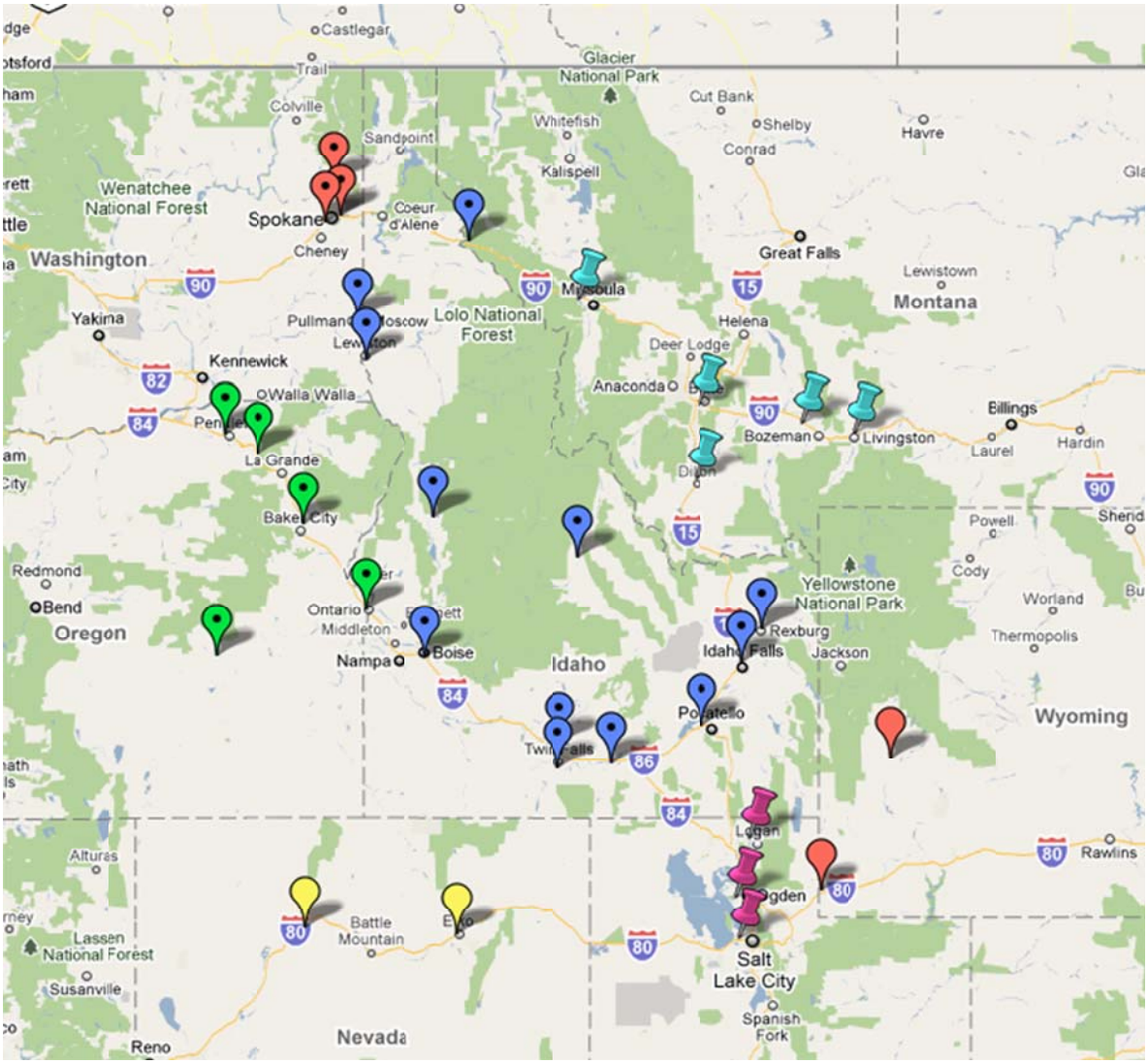

Figure 111. Location of Weather Stations Currently Available in MEPDG Software Version 1.10 that can be used for Idaho

A summary of the mean annual air temperature (MAAT), mean annual rainfall, average annual number of freeze/thaw cycles, average wind speed, and average sunshine of the MEPDG climatic locations in Idaho is shown in Table 90. A comparison of the climatic data for the MEPDG weather stations located in Idaho is shown in Figure 112 through Figure 116.

Table 90. Summary of the Climatic Data of the MEPDG Weather Stations Located in Idaho

Location	MAAT (ºF)	Mean Annual Rainfall (in.)	Freezing Index (ºF-days)	Average Annual Number of Freeze/Thaw Cycles	Average Wind Speed (mph)	Average Sunshine (%)
Boise	53.26	11.20	229.86	75	6.6	72.27
Burley	48.09	9.38	592.93	98	7.3	71.72
Challis	44.08	6.70	1400.51	119	3.7	67.69
Idaho Falls	44.93	8.57	1132.89	109	7.6	62.35
Pullman/Moscow	48.01	12.40	272.8	75	6.7	60.47
Lewiston	53.46	13.97	121.38	47	4.8	62.61
McCall	39.68	24.64	1471.71	140	3.5	57.43
Mullan Pass	37.62	37.67	1419.06	59	5.3	45.04
Pocatello	47.74	10.89	730.58	108	8.3	64.99

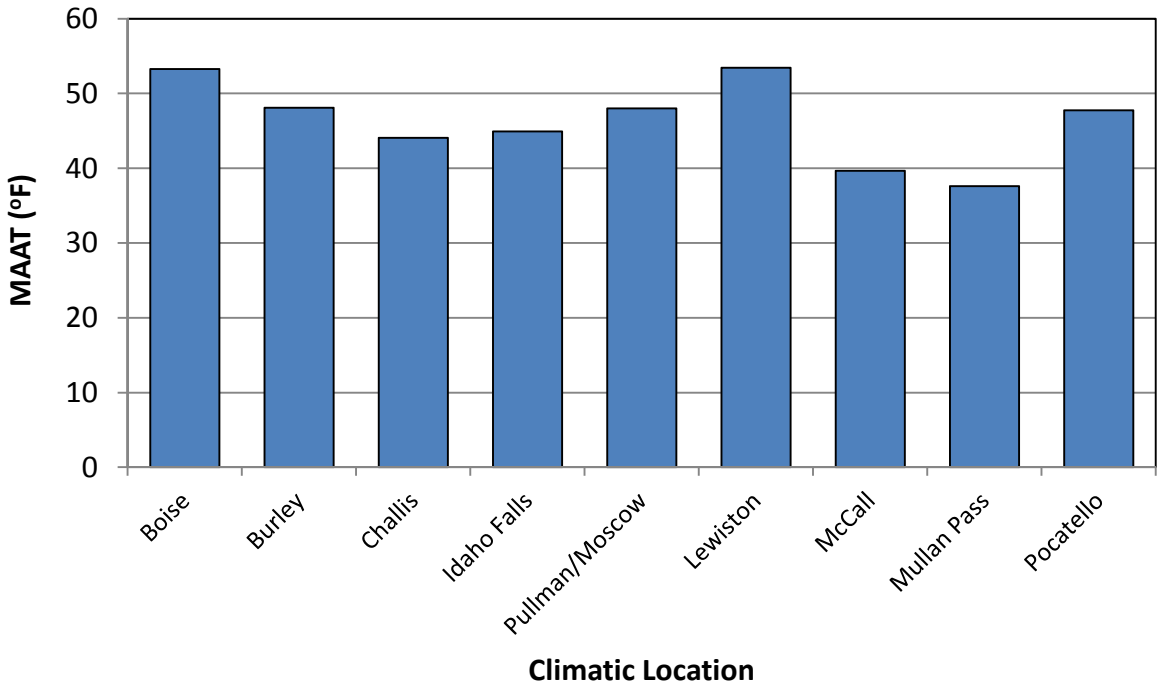

Figure 112. Comparison of MAAT for Different Climatic Locations in Idaho

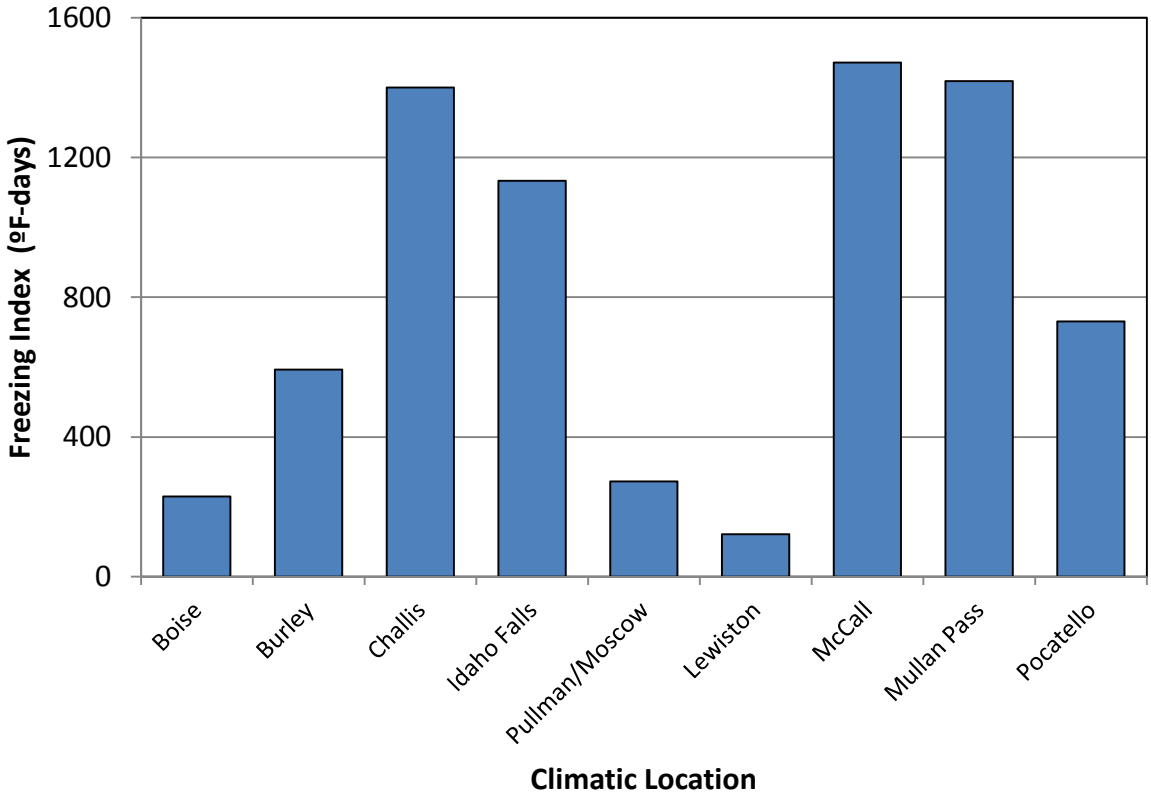

Figure 113. Comparison of Freezing Index for Different Climatic Locations in Idaho

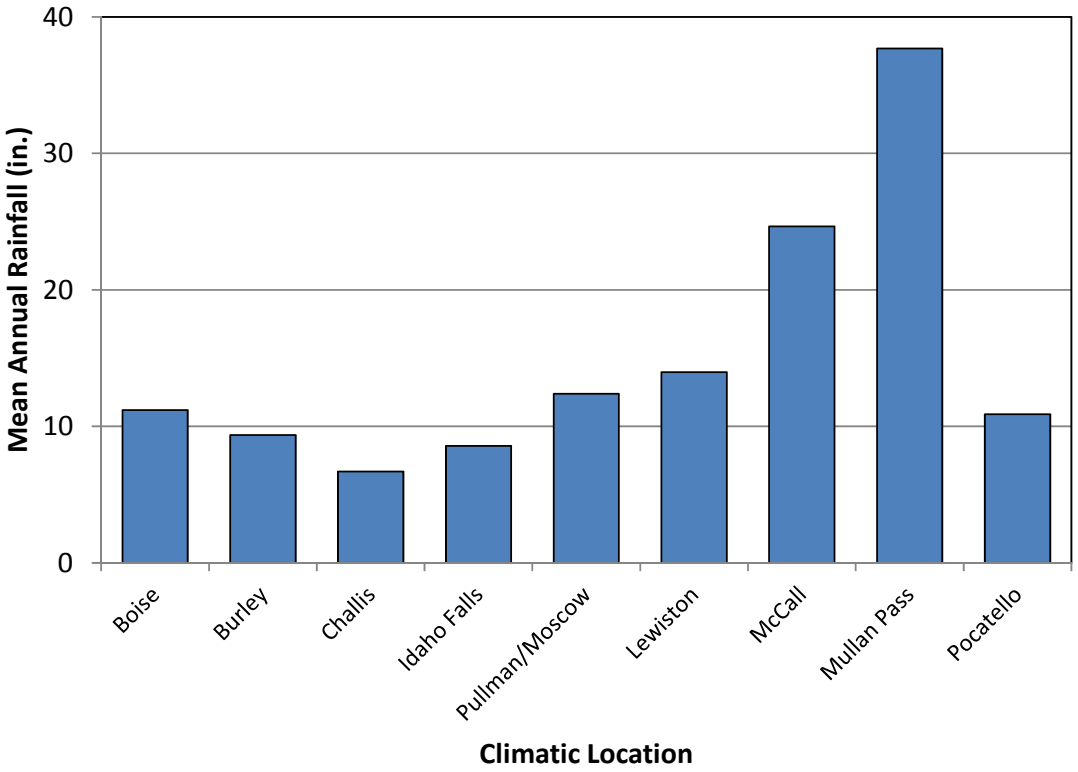

Figure 114. Comparison of Mean Annual Rainfall for Different Climatic Locations in Idaho

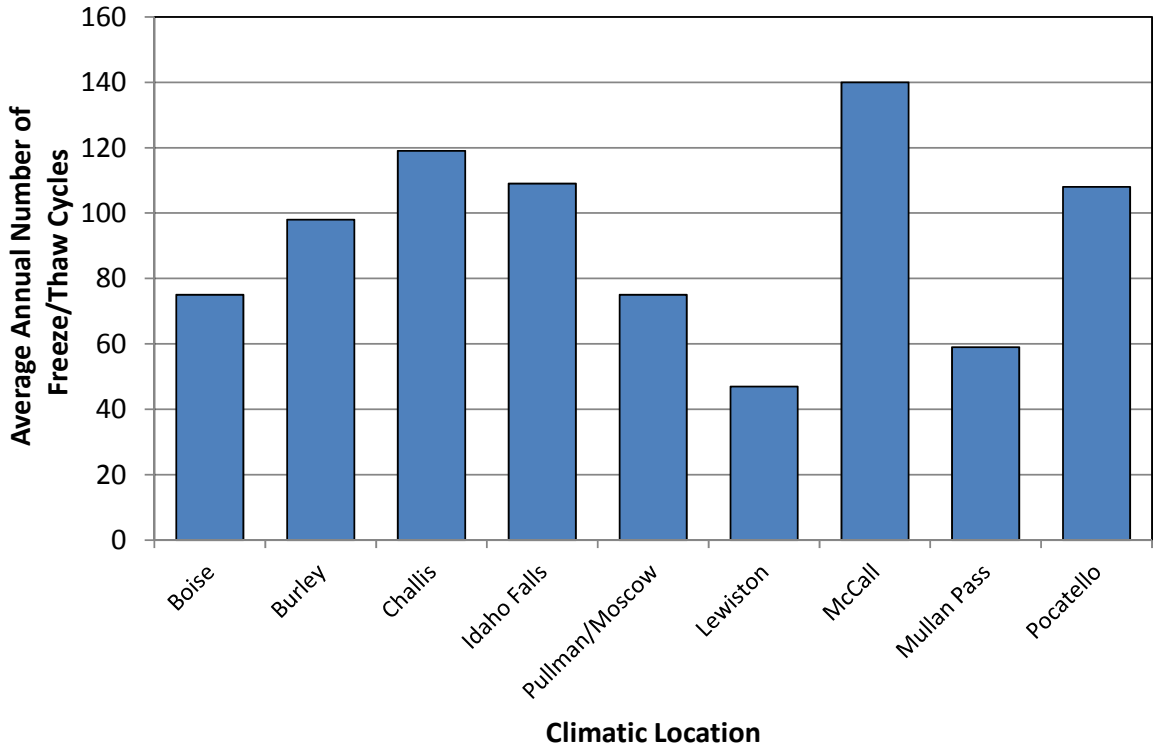

Figure 115. Comparison of the Average Annual Number Freeze/Thaw Cycles for Different Climatic Locations in Idaho

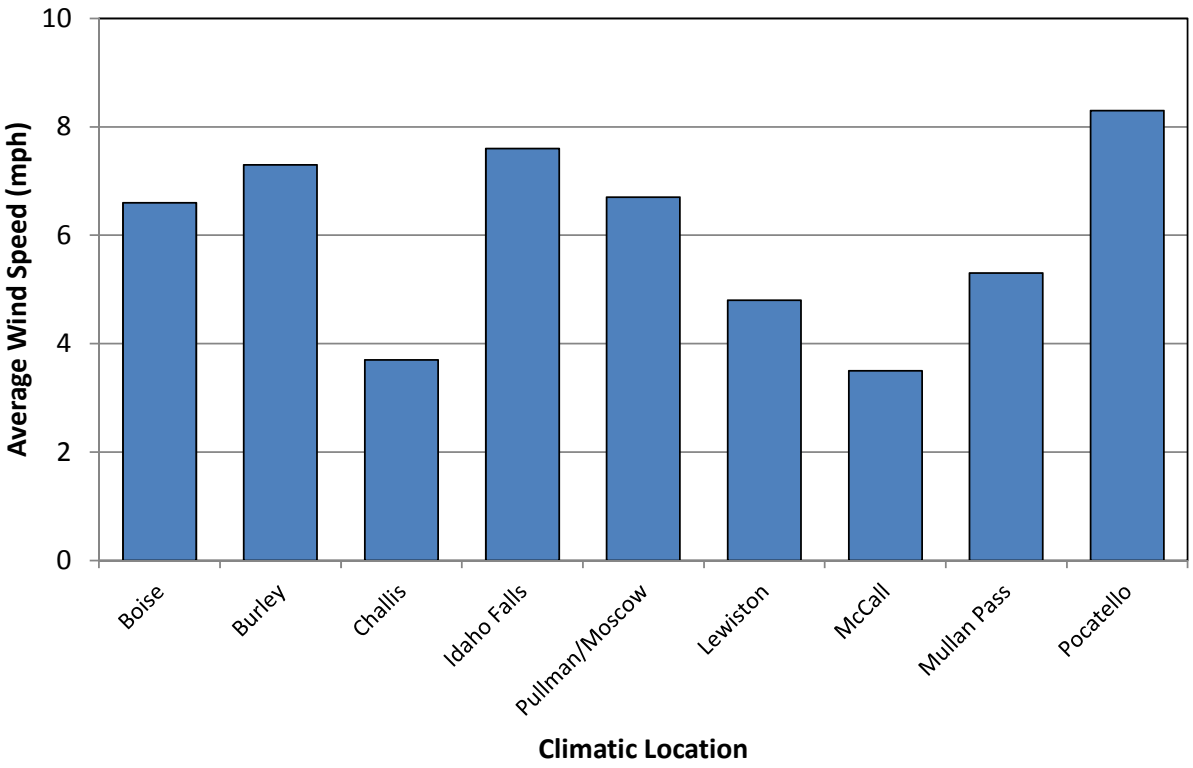

Figure 116. Comparison between the Average Wind Speed for the different Climatic Locations in Idaho

In order to facilitate the implementation of MEDPG in Idaho, the weather stations that can be used in each county of the state were identified. Table 91 shows weather stations that are in or near (within 100 miles) each county recommended to be used in design. The selection of the relevant weather station or stations for design shall be based on the actual longitude and latitude of the project site. Once the stations in proximity of the project site are identified, the MEPDG software interpolates the climatic data based on the actual elevations of these stations relative to the actual elevation of the project site.

Table 91. Recommended Weather Stations for Each Idaho County

County	Recommended MEPDG Weather Station
Ada	Boise, Ontario, Jerome, Joline, Mc Call
Adams	Mc Call, Baker, Meacham, Ontario, Lewiston
Bannock	Pocatello, Idaho Falls, Rexburg, Logan-Cache, Big Piney
Bear Lake	Pocatello, Ogden-Hinckley, Salt Lake, Evanston, Big Piney
Benewah	Deer Park, Spokane Felts Field, Spokane International Airport, Mullan Pass, Pullman/Moscow, Lewiston
Bingham	Pocatello, Idaho Falls, Rexburg, Jerome, Josline, Boise, Burley, Challis
Blaine	Challis , Idaho Falls, Pocatello, Jerome, Joline, Burley, Boise, Mc Call, Rexburg, Logan-Cache
Boise	Boise, Ontario, Challis
Bonner	Deer Park, Spokane Felts Field, Spokane International Airport, Mullan Pass, Pullman-Moscow
Bonneville	Idaho Falls, Rexburg, Pocatello, Big Piney
Boundary	Deer Park, Spokane Felts Field, Spokane International Airport, Mullan Pass
Butte	Idaho Falls, Pocatello, Rexburg, Jerome, Joline, Burley, Challis,
Camas	Challis, Jerome, Joline, Burley, Boise
Canyon	Ontario, Boise, Baker, Mc Call
Caribou	Pocatello, Idaho Falls, Rexburg, Logan-Cache, Big Piney
Cassia	Burley, Josline, Jerome, Pocatello, Winnemucca, Logan-Cache, Ogden-Hinckley
Clark	Rexburg, Idaho Falls, Challis, Pocatello, Dillon
Clearwater	Spokane Felts Field, Spokane International Airport, Mullan Pass, Pullman/Moscow, Lewiston, Missoula
Custer	Challis, Mc Call, Boise, Jerome
Elmore	Boise, Jerome, Mc Call, Challis, Jerome, Josline, Burley
Franklin	Pocatello, Logan-Cache, Ogden-Hinckley, Salt Lake, Evanston, Big Piney
Fremont	Rexburg, Idaho Falls, Pocatello, Dillon
Gem	Ontario, Boise, Baker, Mc Call
Gooding	Boise, Jerome, Josline, Burley, Ontario
Idaho	Mc Call, Challis, Boise, Idaho Falls, Rexburg
Jefferson	Rexburg, Idaho Falls, Pocatello
Jerome	Jerome, Josline, Burley, Pocatello

Table 91. Recommended Weather Stations for Each Idaho County *(Continued)*

County	Recommended MEPDG Weather Station
Kootenai	Deer Park, Spokane Felts Field, Spokane International Airport, Mullan Pass, Pullman/Moscow, Lewiston
Latah	Deer Park, Spokane Felts Field, Spokane International Airport, Mullan Pass, Pullman/Moscow, Lewiston
Lemhi	Challis, Dillon, Rexburg, Idaho Falls
Lewis	Lewiston
Lincoln	Jerome, Josline, Burley, Pocatello, Boise
Madison	Rexburg, Idaho Falls, Pocatello
Minidoka	Burley, Jerome, Josline, Burley, Pocatello, Idaho Falls
Nez Perce	Lewiston, Pullman/Moscow, Meacham
Oneida	Pocatello, Logan-Cache, Ogden-Hinckley, Salt Lake
Owyhee	Boise, Jerome, Josline, Burley, Ontario, Winnemucca, Elko
Payette	Ontario, Boise, Baker, Mc Call
Power	Burley, Josline, Jerome, Pocatello, Idaho Falls, Logan-Cache
Shoshone	Deer Park, Spokane Felts Field, Spokane International Airport, Mullan Pass, Pullman/Moscow, Lewiston, Missoula
Teton	Rexburg, Idaho Falls, Pocatello
Twin Falls	Boise, Jerome, Josline, Burley, Ontario, Winnemucca, Elko
Valley	Boise, Challis, Mc Call
Washington	Boise , Ontario, Mc call, Baker,

Ground Water Table in Idaho

Seasonal water table depth variations have a great impact on the in-situ moisture of the unbound base/subbase and subgrade materials. Thus, the depth to the GWT is required by EICM module in MEPDG to adjust the moister, hence the resilient modulus values of the unbound base/subbase and subgrade layers. Because of the significant role of GWT on the pavement foundation, when it is shallow, every attempt should be made to accurately estimate it. It is to be noted that GWT will have a minimal impact when greater than 10 ft. The effect of GWT has been diminished with the inclusion of the Thornwaith Moisture index.

For the state of Idaho, MEPDG level 1 GWT depth can be obtained from geotechnical investigation reports done at the project site. For MEPDG level 3, GWT depth is the best estimate of the annual average depth or the seasonal average depth which can be obtained from the United States Geological Survey's (USGS) website.[96] The National Water Information System (NWIS) web interface of the USGS

site maintains a comprehensive database of information on ground-water levels in the U. S.[96] In Idaho, the NWIS maintains GWT levels database for 662 active wells distributed all over the state. The locations of these wells are shown graphically in Figure 117. Table 92 shows the distribution of these wells in each county in Idaho.

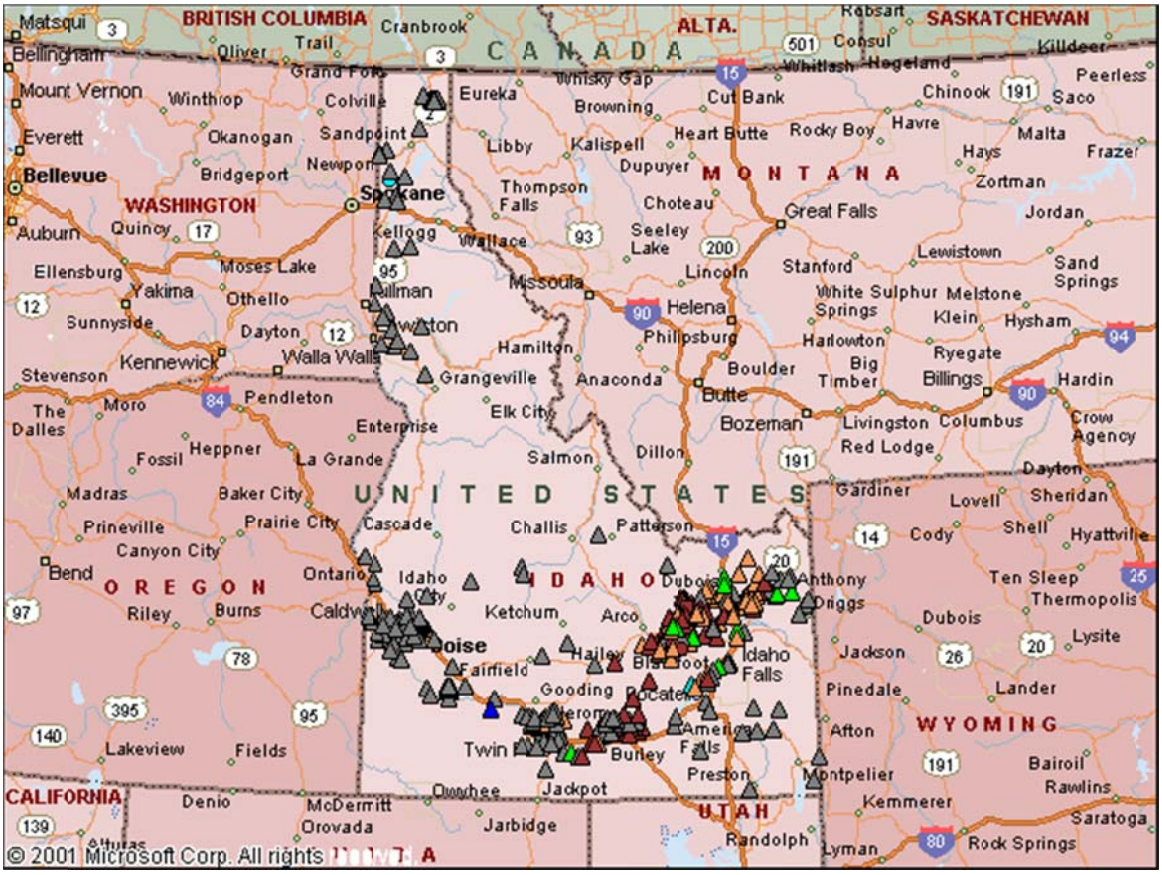

Map generated 4/12/2011 7:56:07 AM

Figure 117. Idaho Active Water Level Network Map[96]

Table 92. Idaho Counties, Depicted on the State Location Map, with Active Wells[96]

County	Well Count	Real-Time	Continuous	Periodic
Ada	26	1	-	25
Bannock	3	-	-	3
Bear Lake	2	-	-	2
Benewah	2	-	-	2
Bingham	28	1	-	27
Blaine	10	-	-	10
Boise	2	-	-	2
Bonner	5	-	-	5
Bonneville	7	-	-	7
Boundary	37	-	-	37
Butte	280	-	1	279
Camas	1	-	-	1
Canyon	20	-	-	20
Caribou	4	-	-	4
Cassia	5	-	-	5
Clark	2	-	-	2
Clearwater	1	-	-	1
Custer	3	-	-	3
Elmore	30	-	-	30
Franklin	1	-	-	1
Fremont	23	-	-	23
Gem	1	-	-	1
Gooding	13	-	-	13
Idaho	1	-	-	1
Jefferson	45	1	-	44
Jerome	18	-	-	18
Kootenai	5	1	-	4
Latah	4	-	-	4
Lemhi	1	-	-	1
Lewis	2	-	-	2
Lincoln	2	-	-	2
Madison	10	-	-	10
Minidoka	38	-	-	38
Nez Perce	3	-	-	3
Owyhee	4	-	-	4
Payette	2	-	-	2
Power	3	-	-	3
Teton	3	-	-	3
Twin Falls	13	-	-	13
Washington	2	-	-	2
Number of active wells	662	4	1	657

Chapter 8
Sensitivity Analysis of MEPDG Input Parameters

MEPDG requires a large number of input variables in order to analyze/design a pavement structure. Thus, it is important to determine which of these input variables have a significant impact on the MEPDG predicted performance. This helps DOTs to allocate funds to accurately estimate the most important input variables. It also facilitates the implementation of MEPDG.

A sensitivity analysis was performed with the objective of assessing the influence of MEPDG key input parameters on predicted performance for conditions typical to Idaho. The MEPDG software version 1.10 was used in this analysis. This chapter presents the results of the sensitivity analysis of the MEPDG based on typical Idaho conditions.

Input Parameters and Pavement Structure

Based on the thorough literature review results presented in this report, the following key variables were investigated in this sensitivity analysis:

- HMA and base layer thicknesses.
- HMA material properties.
- Subgrade soils properties.
- Traffic
- Environment

Reasonable practical ranges for MEPDG input parameters reflecting Idaho conditions were defined and used in the sensitivity analysis. Each selected input was varied at 3 or 4 values. The input parameters and the values used for each input are shown in Table 93. A typical flexible pavement cross-section was used in the study. It is a 2-layer pavement system with a single asphalt concrete layer and an unbound granular base layer resting on a subgrade soil. This is shown in Figure 118. The pavement cross section, used in this sensitivity analysis, was designed using the data representing the medium level for each variable as indicated in Table 93. ITD's design method for flexible pavements was used to compute the thicknesses of the pavement layers at the medium conditions. The design life was fixed to 20 years in all performed MEPDG simulation runs. The sensitivity runs were conducted by varying 1 input at a time while keeping all other inputs at the medium level.

Table 93. Inputs Evaluated in the MEPDG Sensitivity Runs

Input Parameter	Low	Medium	High	Very High
AADTT	50	350	3,250	8,000
Axle Load Spectra	Lightly loaded TWRG	Moderately Loaded TWRG	Primarily loaded TWRG	
Traffic Speed, mph	25	45	65	
Climatic Location (MAAT), (°F)	Mullan Pass (37.62)	Idaho Falls (44.93)	Burley (48.09)	Lewiston (53.46)
GWT Depth (ft)	3	10	100	
AC Thickness (in.)	2.0	4.8	6.0	10.0
AC Stiffness	(See Table 98)			
In-Situ Air Voids at Time of Construction (%)	4	6.7	10	
Effective Asphalt Content, (%)	8	10.17	14	
Base Layer Thickness (in.)	6	22	28	36
Base Layer Modulus (psi)		40,000		
Subgrade Modulus (psi)	3,000	9,000	16,000	29,500

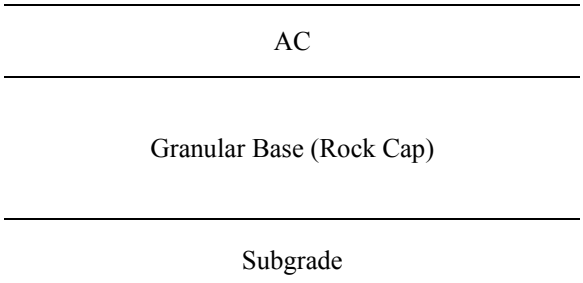

Figure 118. Pavement Structure used in the Sensitivity Analysis

Traffic

For the sensitivity runs, the traffic volume, expressed in AADTT, levels used are shown in Table 93. The equivalent 18-kips ESAL in 20 years, at 0 percent growth rate, for the AADTT shown in Table 93 are 0.33, 2.3, 16.5, and 52.7 million respectively. The percentage of trucks in the design direction was chosen as 56 percent as found from the analysis of the WIM data. The developed statewide number of axles per truck was used in the analysis. A total of 3 levels of ALS, based on the analysis of Idaho WIM data, were used in the sensitivity analysis. These cases are the primarily, moderately, and lightly loaded TWRG developed for Idaho. All other required traffic inputs were set to the MPEDG default values. The traffic inputs are summarized in Table 94 through Table 97. The monthly adjustment factors were for all truck classes were set to one (MEPDG default).

Table 94. Traffic Inputs

Traffic Input	Value
Number of Lanes in Design Direction	2
Percent of Trucks in Design Direction (%)	56
Percent of Trucks in Design Lane (%)	95
Design Lane (ft)	12
Mean Wheel Location (in.)	18
Traffic Wander Standard Deviation (in.)	10
Traffic Growth (%)	No growth

Table 95. AADTT Distributions by Vehicle Class

Truck Class	Percentage of Trucks
Class 4	0.9
Class 5	11.6
Class 6	3.6
Class 7	0.2
Class 8	6.7
Class 9	62
Class 10	4.8
Class 11	2.6
Class 12	1.4
Class 13	6.2

Table 96. Number of Axles per Truck

Truck Class	Number of Axles			
	Single	Tandem	Tridem	Quad
Class 4	1.67	0.33	0.00	0.00
Class 5	2.05	0.00	0.00	0.00
Class 6	1.04	1.04	0.00	0.00
Class 7	0.45	0.95	0.45	0.13
Class 8	2.59	0.63	0.00	0.00
Class 9	1.28	1.92	0.00	0.00
Class 10	1.06	0.87	0.98	0.25
Class 11	4.40	0.29	0.01	0.00
Class 12	3.39	1.19	0.07	0.01
Class 13	3.39	1.85	0.13	0.02

Table 97. Axle Configurations

Input	Value
Average Axle Width (Edge-to-Edge) (ft)	8.5
Dual Tire Spacing (in.)	12
Tire Pressure (psi)	120
Tandem Axle Spacing (in.)	51.6
Tridem Axle Spacing (in.)	49.2
Quad Axle Spacing (in.)	49.2

Properties of the Asphalt Concrete Mixtures

Based on the analysis of AC mixtures typically used in Idaho, 4 different AC mixtures with different stiffness values were used in this sensitivity analysis. These mixtures represent very high (SP-6), high (SP-5), medium (SP-3), and low (SP-1) stiffness mixtures. The properties of these mixtures are summarized in Table 98. The master curves for these AC mixtures are shown in Figure 119.

Table 98. Properties of the Asphalt Concrete Mixes

Variable	Low Stiffness	Medium Stiffness	High Stiffness
Air Voids (%)	7.53	6.78	6.87
Effective Binder Content (%)	13.65	10.41	9.39
% Retained ¾"	0	0	1
% Retained 3/8"	22	30	29
% Retained #4	47	50	51
% Passing # 200	6.8	4.7	4.7
PG Grade	58-34	70-28	76-28
Binder A	10.0350	9.7150	9.2000
Binder VTS	-3.3500	-3.2170	-3.0240

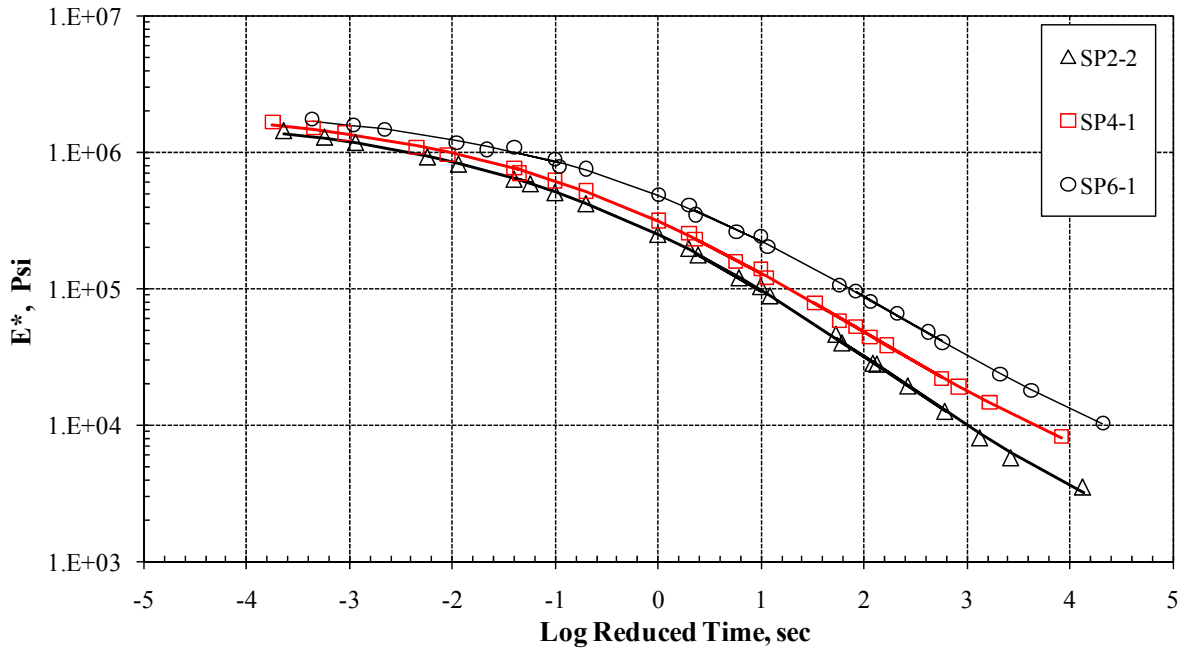

Figure 119. E* Master Curves used in the Sensitivity Analysis

For creep compliance and tensile strength, MEPDG default values based on the binder grade and mixtures properties were used in the analysis. The creep compliance and tensile strength values are shown in Table 99.

Table 99. Creep Compliance and Tensile Strength for the AC Mixes

Binder Grade	Loading Time (sec)	Low Temp (°F)			Tensile Strength at 14 °F, psi
		-4	14	32	
PG 58-34	1	5.3621e-007	7.86038e-007	1.04686e-006	384.74
	2	6.12977e-007	9.57863e-007	1.46254e-006	
	5	7.31577e-007	1.24395e-006	2.27551e-006	
	10	8.36313e-007	1.51588e-006	3.17907e-006	
	20	9.56043e-007	1.84724e-006	4.44141e-006	
	50	1.14102e-006	2.39897e-006	6.91022e-006	
	100	1.30437e-006	2.92338e-006	9.65412e-006	
PG70-28	1	3.90878e-007	5.9402e-007	8.15017e-007	487.6
	2	4.29446e-007	6.93401e-007	1.04337e-006	
	5	4.86331e-007	8.5074e-007	1.44624e-006	
	10	5.34317e-007	9.93072e-007	1.85144e-006	
	20	5.87038e-007	1.15922e-006	2.37016e-006	
	50	6.64798e-007	1.42225e-006	3.28534e-006	
	100	7.30394e-007	1.6602e-006	4.20582e-006	
PG 76-28	1	3.96416e-007	6.04278e-007	8.4481e-007	562.74
	2	4.32955e-007	7.00729e-007	1.06656e-006	
	5	4.86477e-007	8.52249e-007	1.45145e-006	
	10	5.31317e-007	9.88279e-007	1.83244e-006	
	20	5.80291e-007	1.14602e-006	2.31343e-006	
	50	6.52026e-007	1.39383e-006	3.14826e-006	
	100	7.12125e-007	1.6163e-006	3.97465e-006	

Unbound Base Layer and Subgrade Soils

The thickness of the unbound granular base layer was varied in the sensitivity analysis as shown in Table 93. Subgrade type and modulus were also varied. The selected subgrade R-values were taken from the historical ITD database. The subgrade resilient modulus values were then estimated using the developed M_r-R-value model. For the GW-GM subgrade, the modulus was taken from the default values recommended by MEPDG as it is granular material.[6] The properties of the granular base layer and subgrade soils used in the sensitivity analysis are shown in Table 100.

Table 100. Unbound Base and Subgrade Material Properties

Variable	Base Layer	Subgrade (Low)	Subgrade (Medium)	Subgrade (High)	Subgrade (Very High)
Classification	Permeable Aggregate (Rock Cap)	CH	CL	SM	GW-GM
R-Value	85	5	27	66	85
Modulus, psi	40,000	3,000	9,000	16,000	29500
PI	NP	39	9	1	NP
LL	6	65	29	23	25
% Passing #200	0	95	92	16	7
% Passing #40	0	97	99	63	15
% Passing #10	0	100	100	85	36
% Passing #4	0.3	100	100	89	50
% Passing 3/8”	5	100	100	92	66
% Passing ¾”	10				
% Passing 1½”	26.5				
% Passing 3”	100				
% Passing 3½”	100				

Results and Analysis

MEPDG software Version 1.10 was used in the sensitivity runs. The sensitivity of the MEPDG performance prediction models to each of the investigated input parameters was analyzed separately. MEPDG investigated prediction models are the longitudinal cracking, alligator cracking, rutting, and IRI models.

Longitudinal Cracking Sensitivity Analysis

The subsequent sections present the sensitivity of MEPDG predicted longitudinal cracking to each of the investigated parameters. All analyses are based on the longitudinal cracking predicted after 20-years of traffic loading.

AC Layer Thickness

The influence of changing the AC layer thickness on MEPDG predicted longitudinal cracking is shown in Figure 120. This figure shows that AC layer thickness between 3 and 5 inches yielded the highest amount of longitudinal cracking. Negligible amount of longitudinal cracking resulted at AC layers thicker than 7 inches or thinner than 2.5 inches.

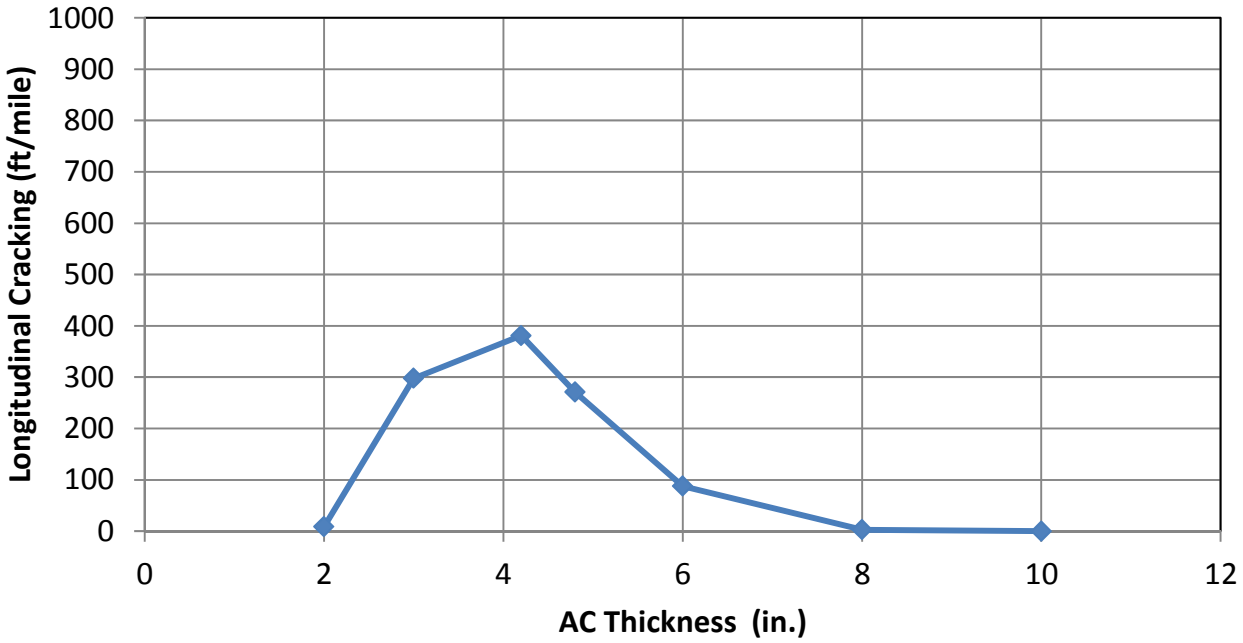

Figure 120. Influence of AC layer Thickness on Longitudinal Cracking

AC Mix Stiffness

Figure 121 depicts the effect of the AC mix stiffness on the longitudinal cracking distress predicted using MEPDG. This figure shows that as the mix stiffness increases the longitudinal cracking increases significantly. However, it should be noted that this behavior is AC thickness dependent. Literature studies showed that for pavement structures with thick AC layer(s), the longitudinal cracking decreases with the increase in the mix stiffness.[4, 8, 52]

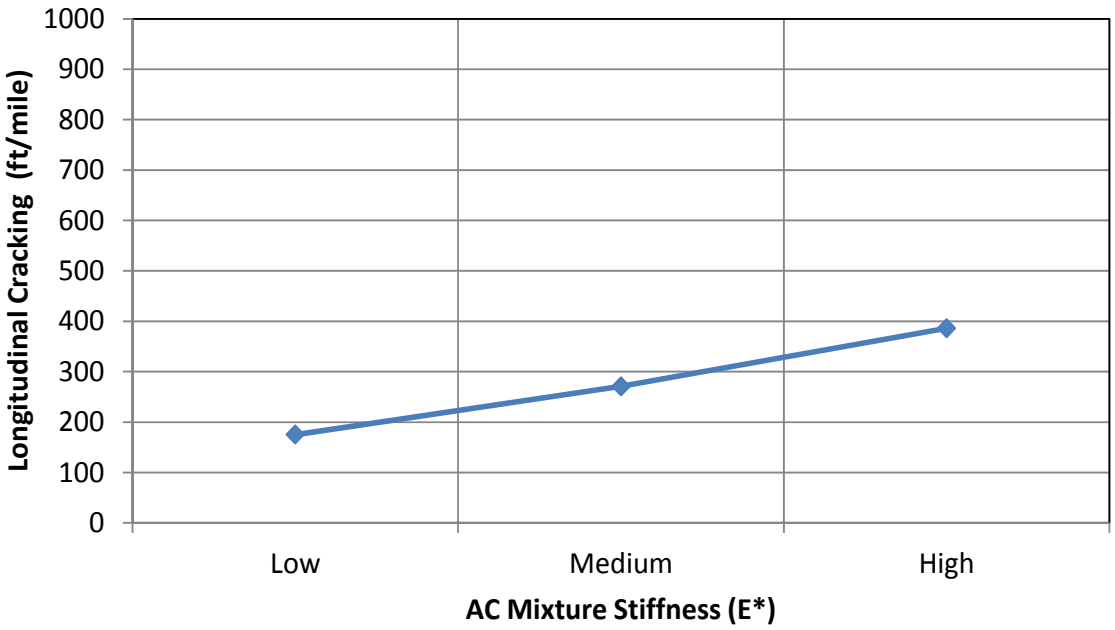

Figure 121. Influence of AC Mix Stiffness on Longitudinal Cracking

Effective Binder Content

The effective binder content is approximately 2 to 2.2 times the binder content by mix weight.[4] The influence of changing the effective binder content of the AC mix on longitudinal cracking is illustrated in Figure 122. This figure indicates that increasing the mix binder content significantly reduces the amount of longitudinal cracking.

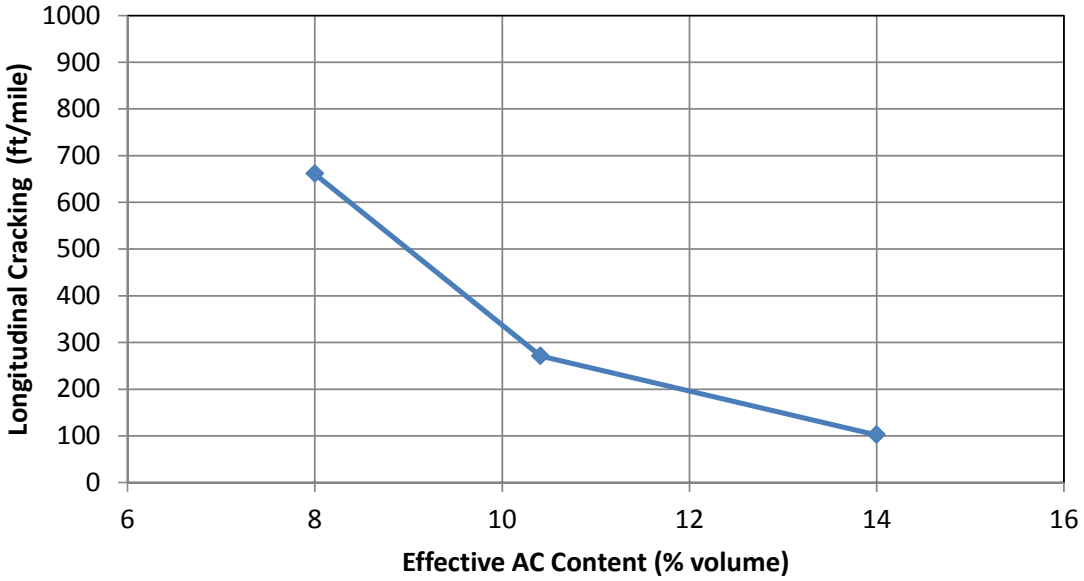

Figure 122. Influence of Effective Binder Content on Longitudinal Cracking

Mix Air Voids

The in-pace air voids content of the AC mix has a significant effect on longitudinal cracking. This is shown in Figure 123. As the percent air voids in the mix increases, the longitudinal cracking significantly increases.

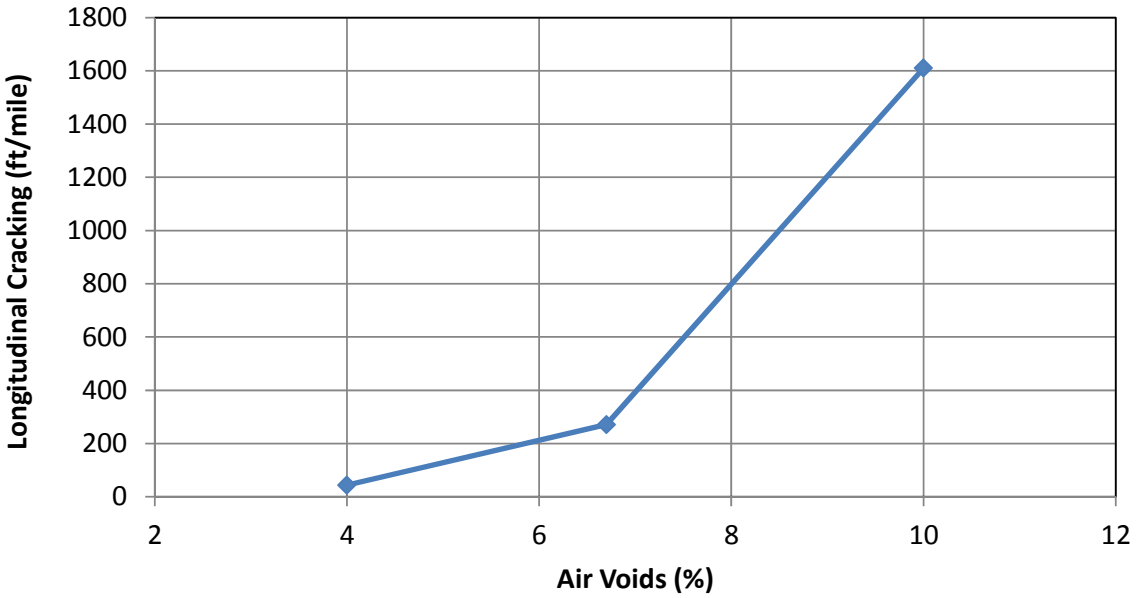

Figure 123. Influence of Mix Air Voids on Longitudinal Cracking

Base Layer Thickness

Figure 124 shows the longitudinal cracking after 20-years of traffic loading for 4 levels of granular base layer thickness. This figure shows a significant reduction in the amount of longitudinal cracking with the increase of the base layer thickness form 6 inches to 22 inches. An increase in the base layer thickness from 22 inches to 36 inches yielded a slight increase in the longitudinal cracking. This could be attributed to the increase in the overall stiffness of the foundation which leads to higher cracking.

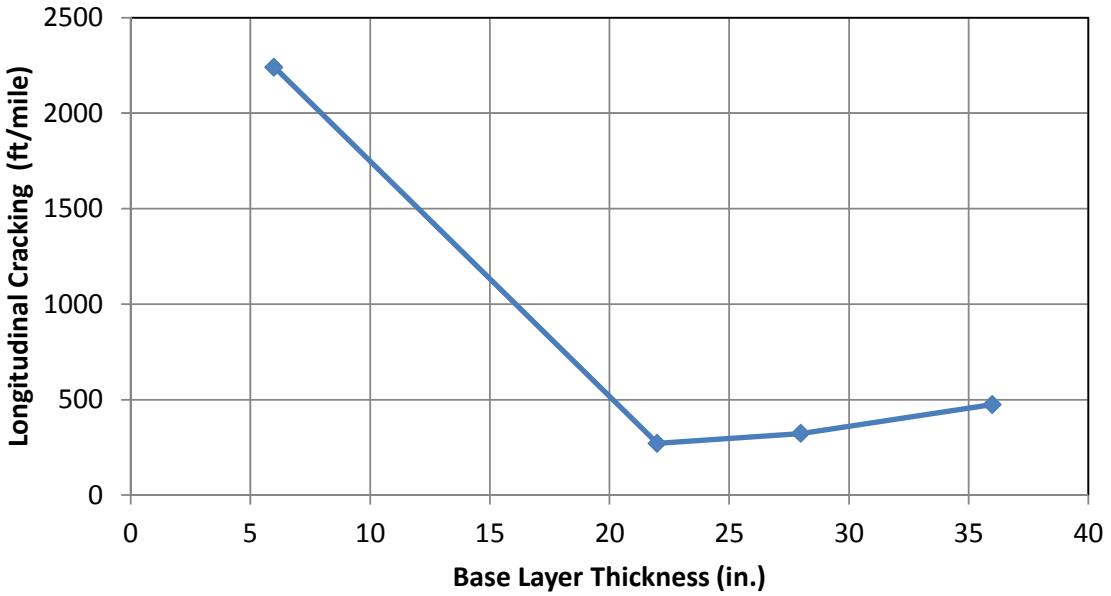

Figure 124. Influence of Granular Base Layer Thickness on Longitudinal Cracking

Subgrade Modulus

Figure 125 shows the longitudinal cracking after 20-years of traffic loading for 4 levels of subgrade modulus. The figure indicates that as the subgrade modulus increases, the longitudinal cracking significantly increases.

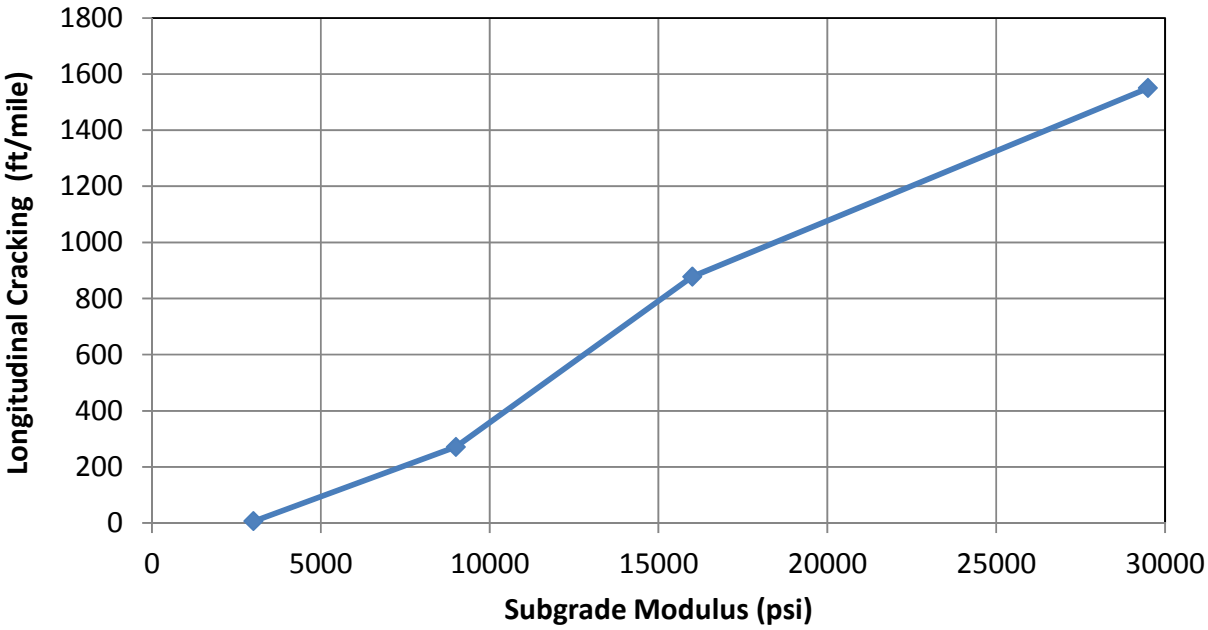

Figure 125. Influence of Subgrade Modulus on Longitudinal Cracking

Climate

MEPDG predicted longitudinal cracking after 20-years of traffic loading for 4 different climatic locations in Idaho is shown in Figure 126. This figure shows that climatic location conditions have a significant influence on longitudinal cracking. The amount of longitudinal cracking increases with the increase of the MAAT at the climatic location.

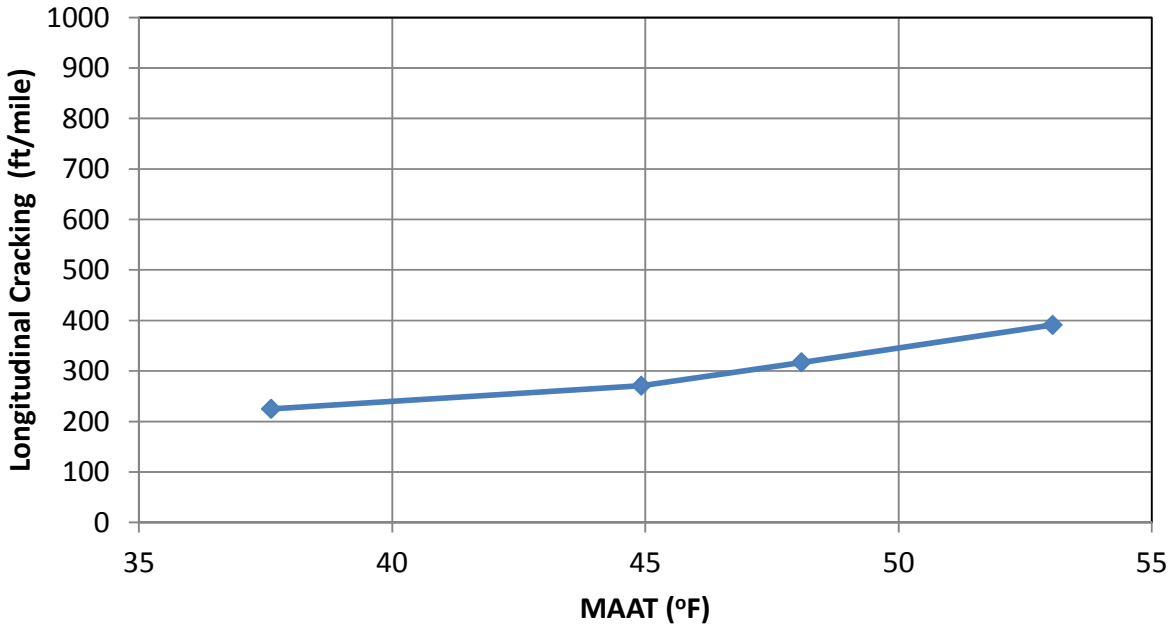

Figure 126. Influence of MAAT on Longitudinal Cracking

Ground Water Table Depth

Figure 127 depicts the longitudinal cracking for 3 different GWT levels. This figure shows an increase in longitudinal cracking with an increase in GWT depth. This occurs due to the increase in the subgrade stiffness with the increase in the GWT depth. MEPDG output shows an average subgrade modulus of 5040 psi and 6980 psi when the GWT depth was 3 ft. and 100 ft., respectively.

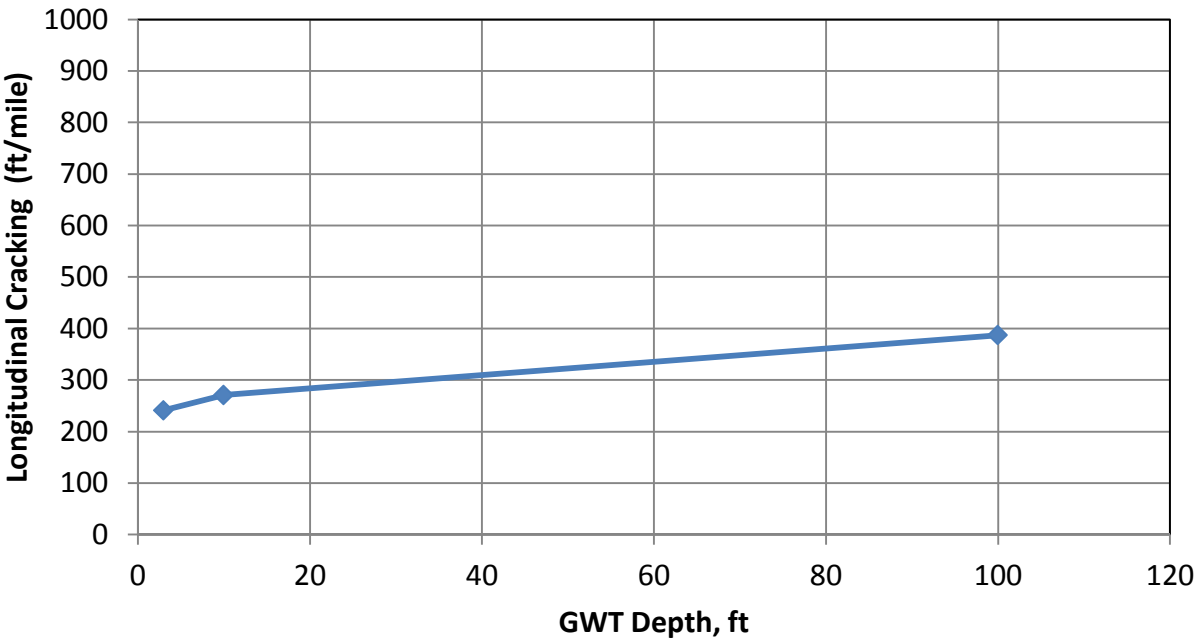

Figure 127. Influence of GWT Depth on Longitudinal Cracking

Axle Load Spectra

Figure 128 shows the relationship between longitudinal cracking and ALS. As ALS increases form light to heavy, a significant increase in longitudinal cracking occurs.

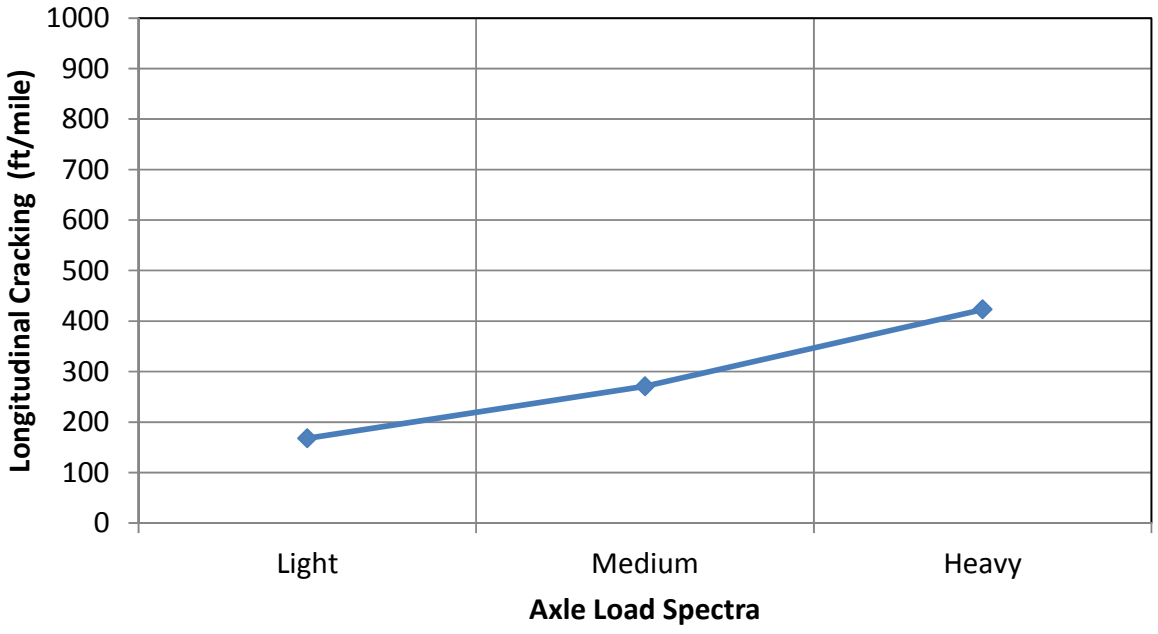

Figure 128. Influence of ALS on Longitudinal Cracking

Traffic Volume

The influence of traffic volume on longitudinal cracking is shown in Figure 129. Traffic volume has a highly significant influence on longitudinal cracking. As traffic volume increases, the amount of longitudinal cracking also increases significantly. This suggests that every effort should be exerted to estimate traffic volume precisely.

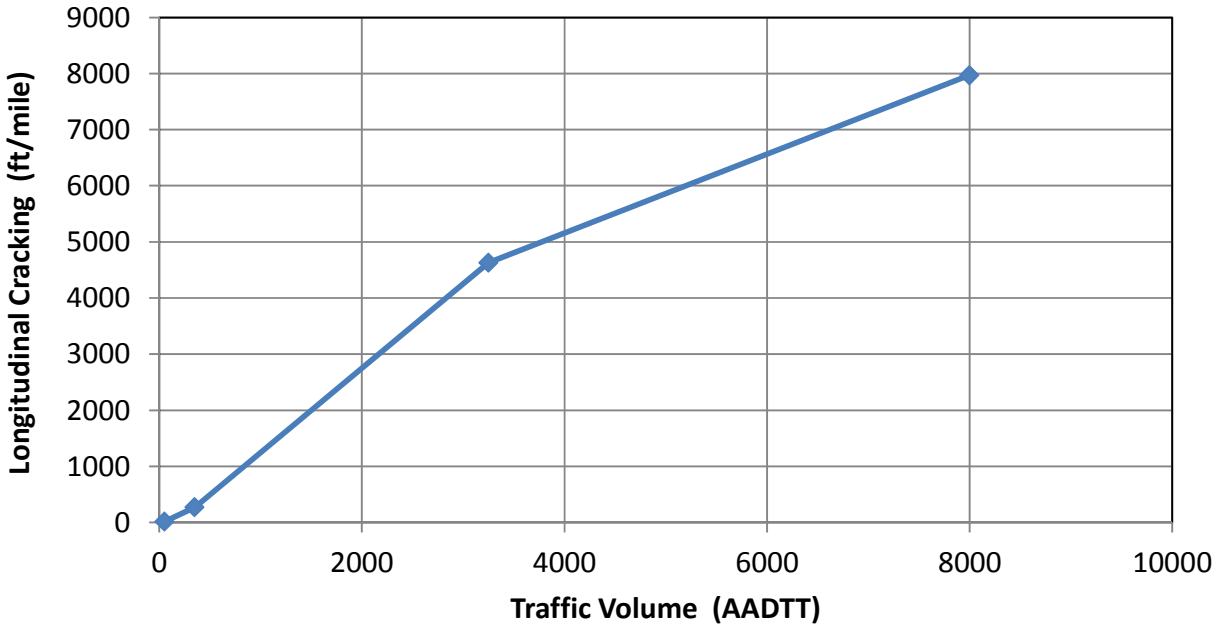

Figure 129. Influence of Traffic Volume on Longitudinal Cracking

Traffic Speed

Figure 130 shows the results of the sensitivity of longitudinal cracking to traffic speed. This figure shows that as the traffic speed increases from 25 to 65 mph, a decrease in longitudinal cracking occurs. However, the influence of traffic speed on longitudinal cracking is not significant. This figure also shows that the relationship between speed and longitudinal cracking is almost linear.

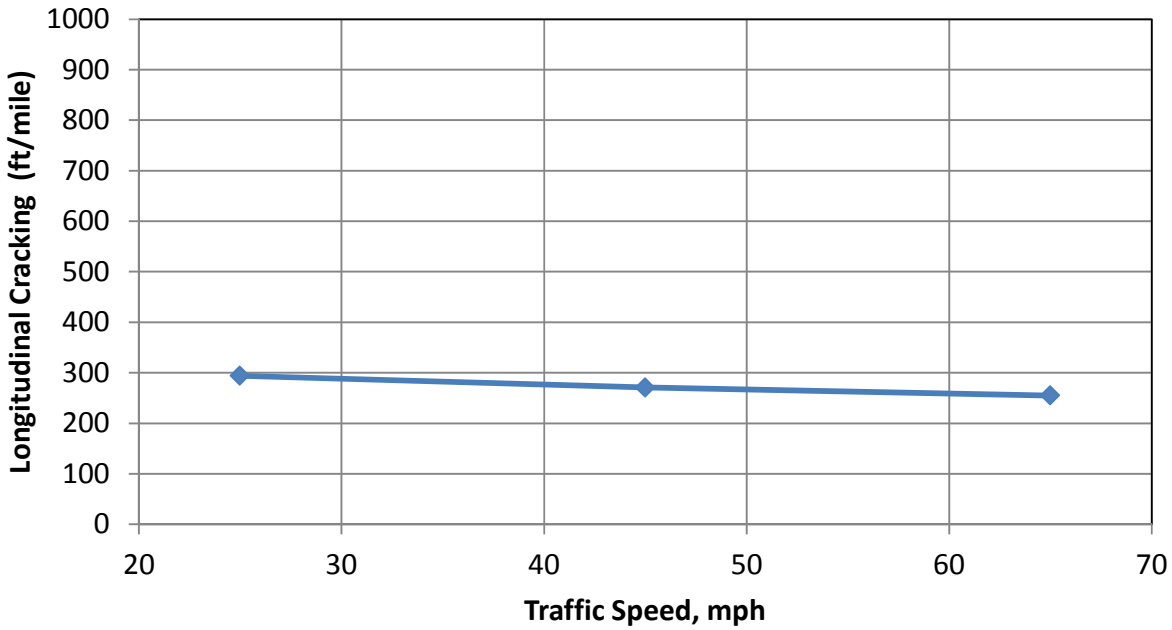

Figure 130. Influence of Traffic Speed on Longitudinal Cracking

Alligator Cracking Sensitivity Analysis

The subsequent sections describe the sensitivity of MEPDG predicted alligator cracking relative to each of the investigated parameters. All analyses are based on the alligator cracking predicted after 20-years of traffic loading.

AC Layer Thickness

The influence of changing the AC layer thickness on MEPDG predicted alligator cracking is shown in Figure 131. Similar to longitudinal cracking, this figure shows that AC layer thickness between 2 and 5 inches yielded the highest amount of alligator cracking. Negligible amount of alligator cracking resulted at AC layers thicker than 7 inches.

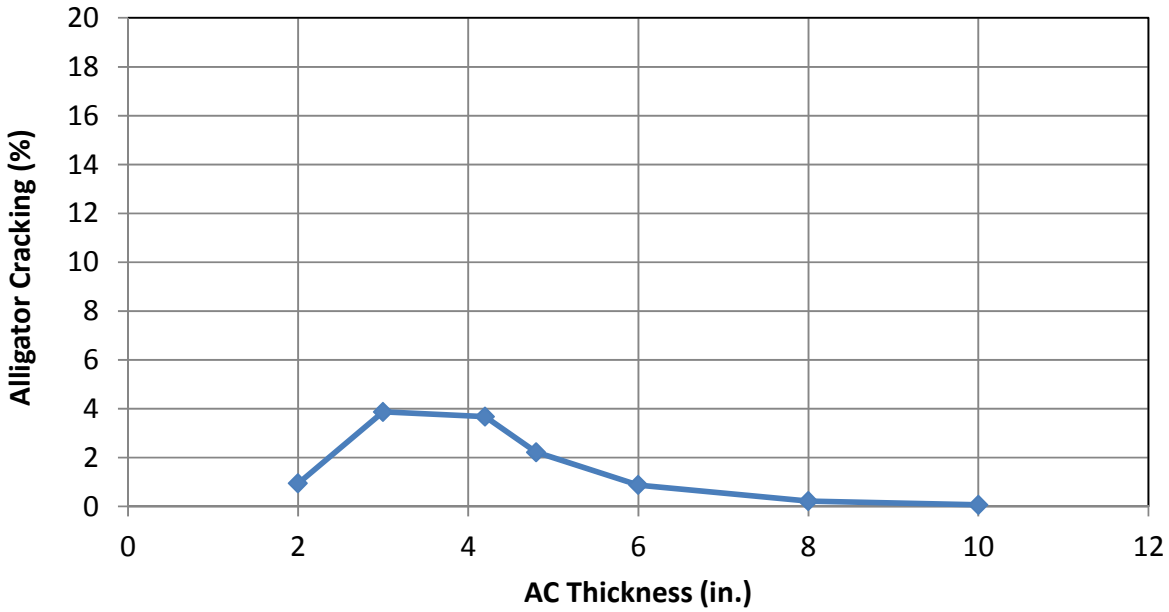

Figure 131. Influence of AC layer Thickness on Alligator Cracking

AC Mix Stiffness

Figure 132 illustrates the effect of changing the AC mix stiffness (low, medium, and high) on the alligator cracking distress predicted using MEPDG after 20-years of traffic loading. Similar to longitudinal cracking, this figure shows that as the mix stiffness increases the alligator cracking also increases. However, the influence of the mix stiffness on the alligator cracking distress is not as significant compared to the longitudinal cracking distress. It should be noted that this behavior is dependent on the thickness of the AC layer(s) as well.

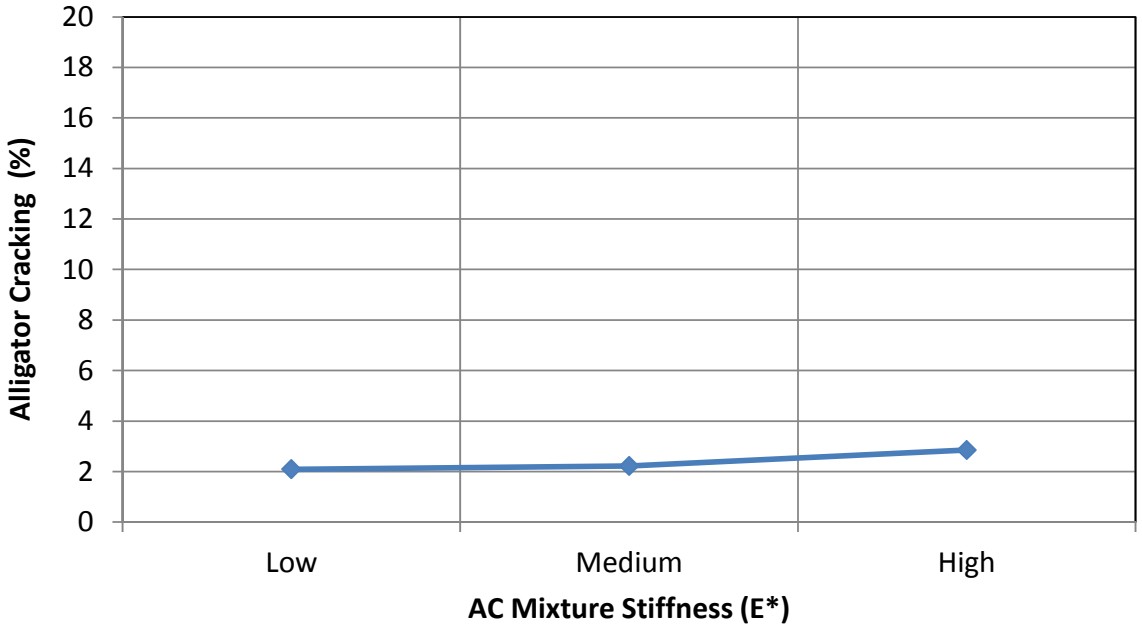

Figure 132. Influence of AC Mix Stiffness on Alligator Cracking

Effective Binder Content

The influence of changing the effective binder content of the AC mix on alligator cracking is illustrated in Figure 133. This figure shows that binder content has a significant influence on alligator cracking. Increasing the mix binder content significantly reduces the amount of alligator cracking.

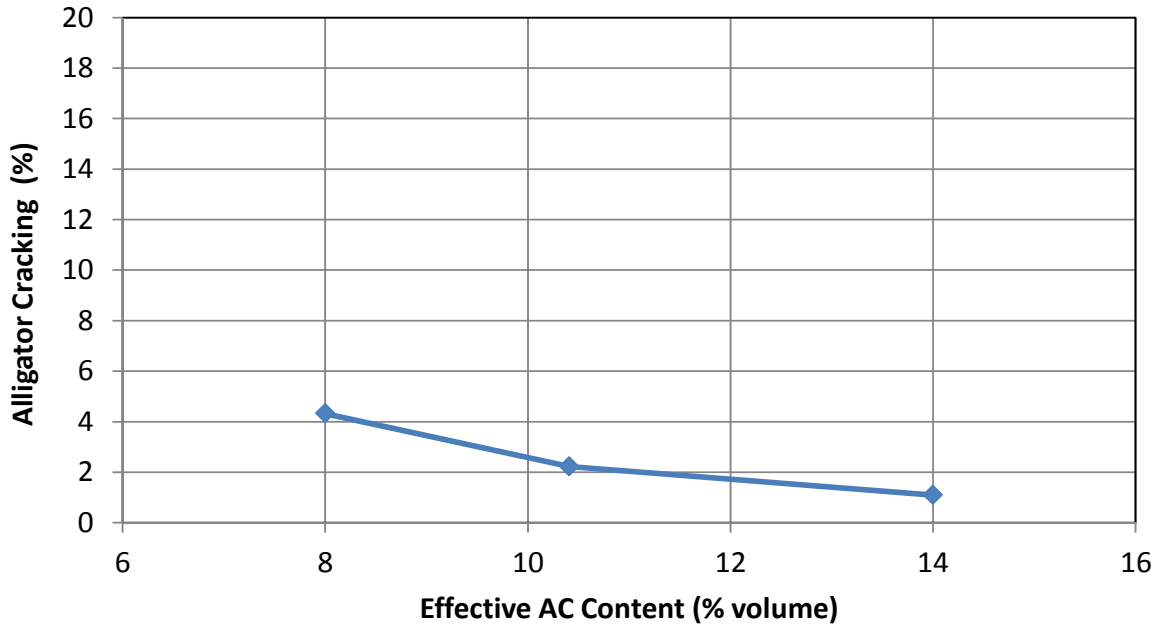

Figure 133. Influence of Effective Binder Content on Alligator Cracking

Mix Air Voids

Figure 134 shows that in-pace air voids content of the AC mix has a significant effect on alligator cracking. As the percent air voids in the mix increases, the alligator cracking significantly increases.

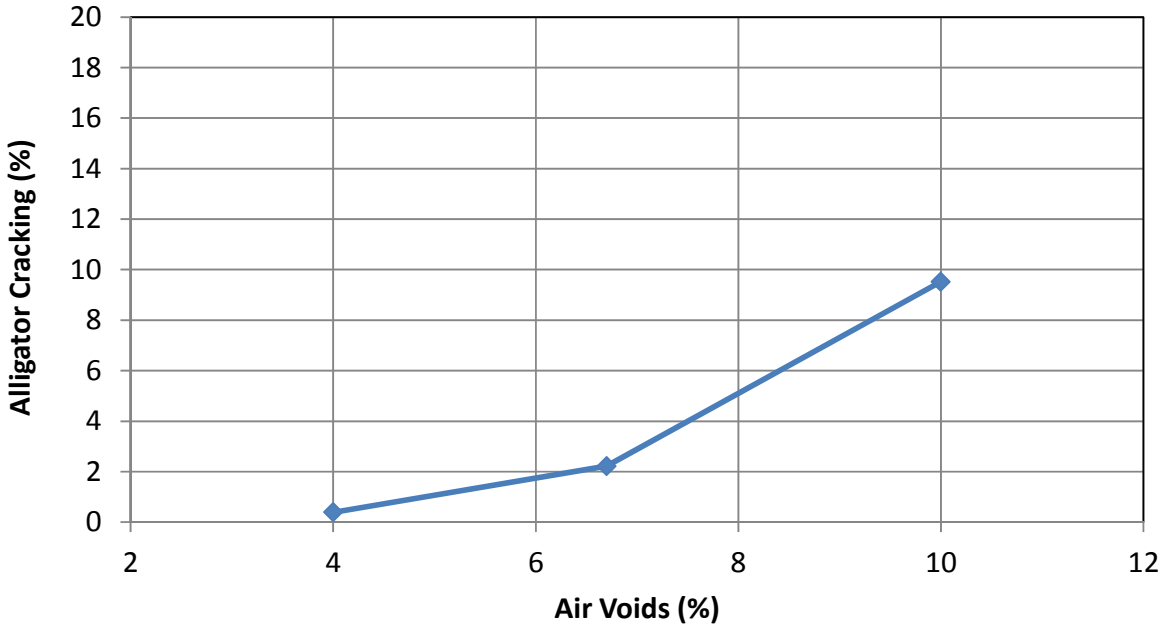

Figure 134. Influence of Mix Air Voids on Alligator Cracking

Base Layer Thickness

Figure 135 depicts the alligator cracking for 4 levels of granular base layer thickness. This figure shows a significant decrease in the amount of alligator cracking with the increase in the base layer thickness form 6 inches to 22 inches. Increasing the base layer thickness beyond 22 inches has no significant influence on the alligator cracking.

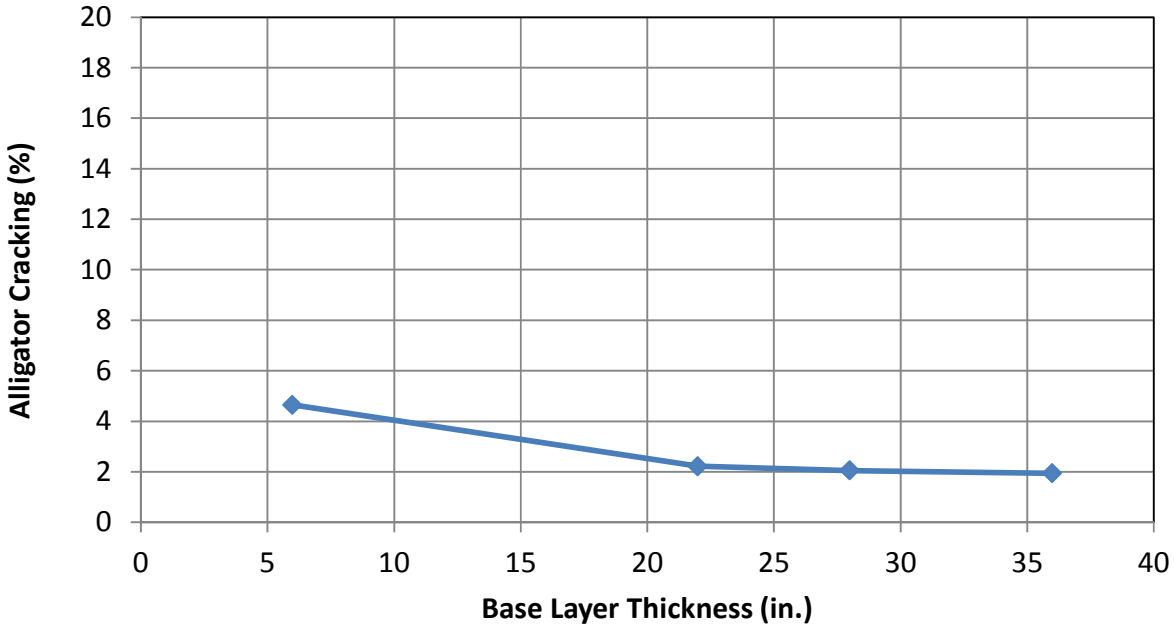

Figure 135. Influence of Granular Base Layer Thickness on Alligator Cracking

Subgrade Modulus

Figure 136 shows the alligator cracking after 20-years of traffic loading for 4 values of subgrade modulus. The figure indicates that as the subgrade modulus increases, the alligator cracking decreases.

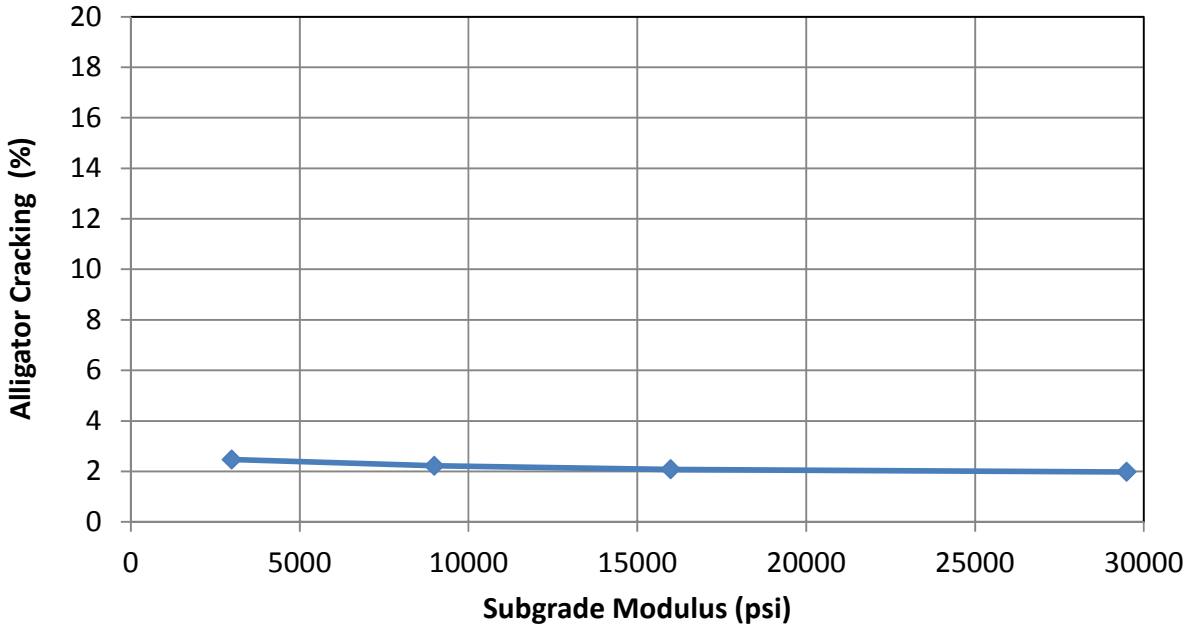

Figure 136. Influence of Subgrade Modulus on Alligator Cracking

Climate

The influence of the climatic site characteristics on MEPDG predicted alligator cracking after 20-years of traffic loading is shown in Figure 137. The figure shows that climatic location characteristics Affects alligator cracking. The amount of alligator cracking increases with an increase of MAAT at the climatic location.

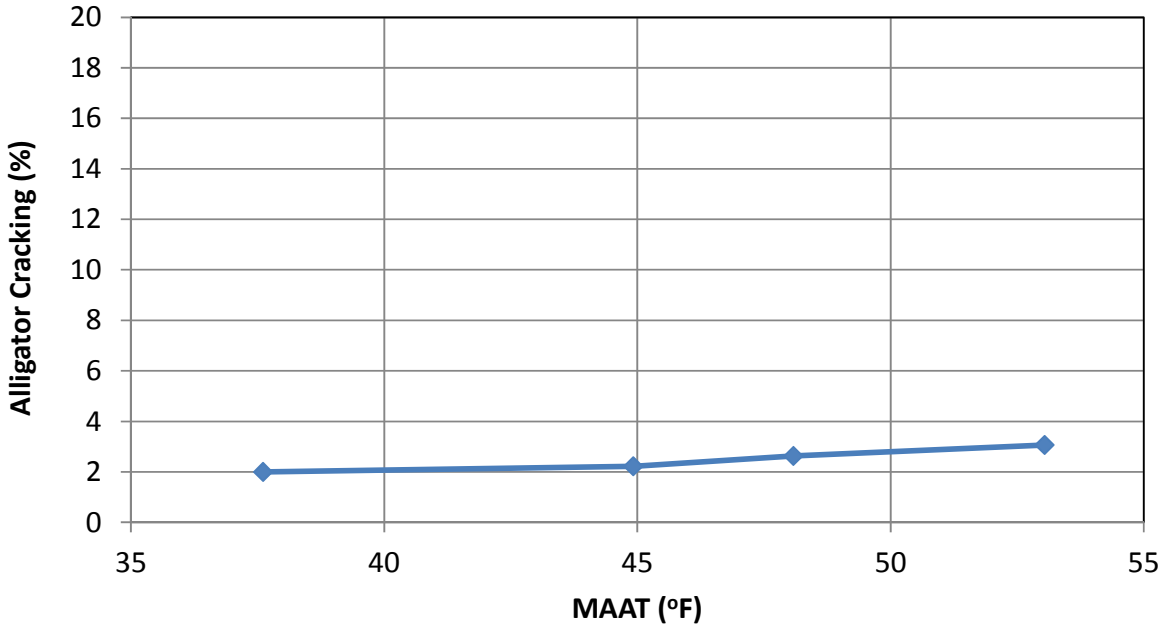

Figure 137. Influence of MAAT on Alligator Cracking

Ground Water Table Depth

Figure 138 shows the alligator cracking predicted at 3 GWT depth levels. This figure shows higher alligator cracking at shallow GWT depth. However, an increase in alligator cracking occurred when the GWT depth was increased from 10 to 100 ft. This trend seems to be wrong and could be a result of a software bug.

Figure 138. Influence of GWT Depth on Alligator Cracking

Axle Load Spectra

The influence of ALS on predicted alligator cracking is shown in Figure 139. Similar to longitudinal cracking, as the ALS increases from light to heavy, a significant increase in alligator cracking occurs.

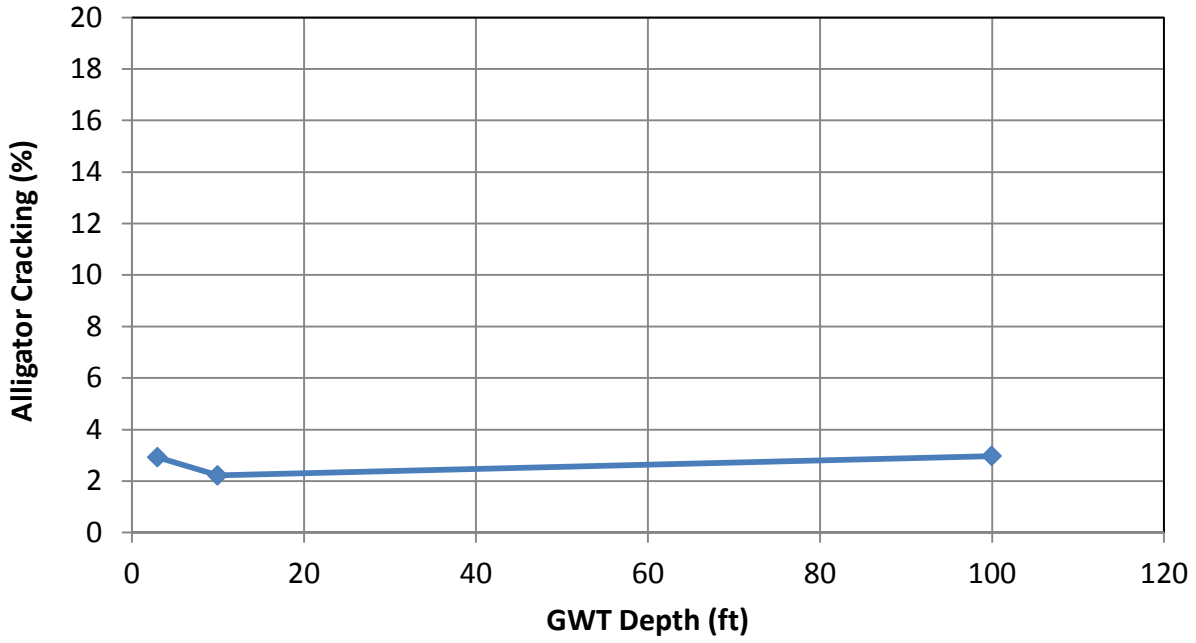

Figure 139. Influence of ALS on Alligator Cracking

Traffic Volume

The influence of traffic volume on alligator cracking is shown in Figure 140. Traffic volume has a very significant influence on alligator cracking. As traffic volume increases, the amount of alligator cracking increases significantly. Among all investigated variables, traffic volume has the highest influence on both types of load-associated cracking.

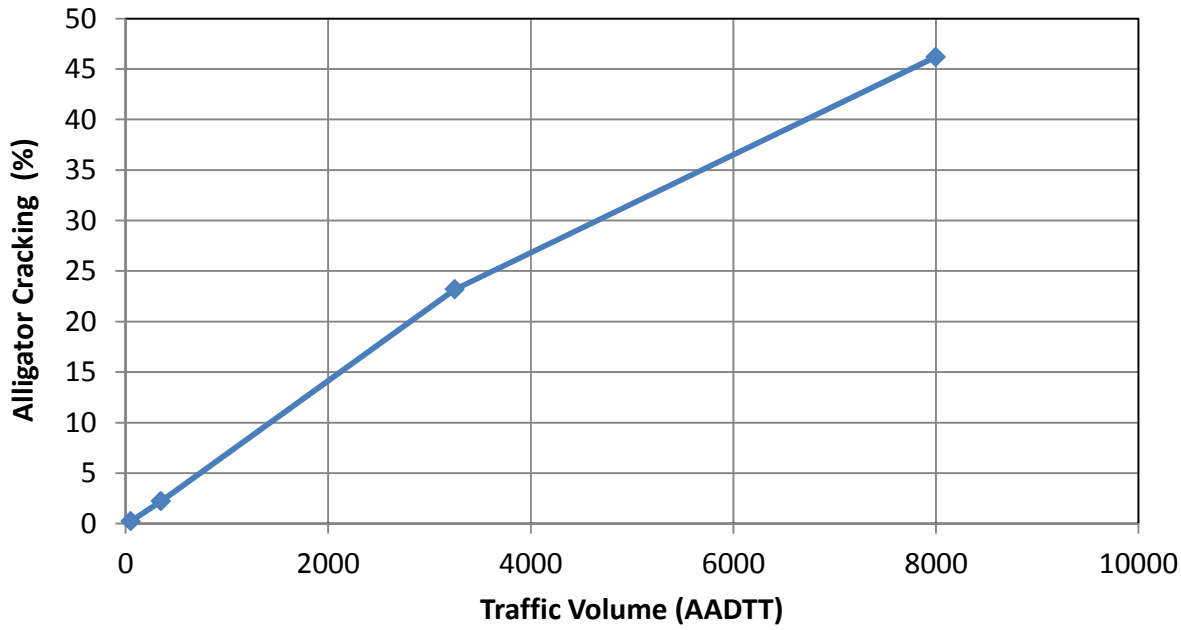

Figure 140. Influence of Traffic Volume on Alligator Cracking

Traffic Speed

Figure 141 shows the results of the sensitivity of alligator cracking relative to traffic speed. This figure shows that as the traffic speed increases from 25 to 65 mph, an increase in alligator cracking occurs. However the influence of traffic speed on alligator cracking is not overly significant. This figure also shows that the relationship between speed and alligator cracking is almost linear.

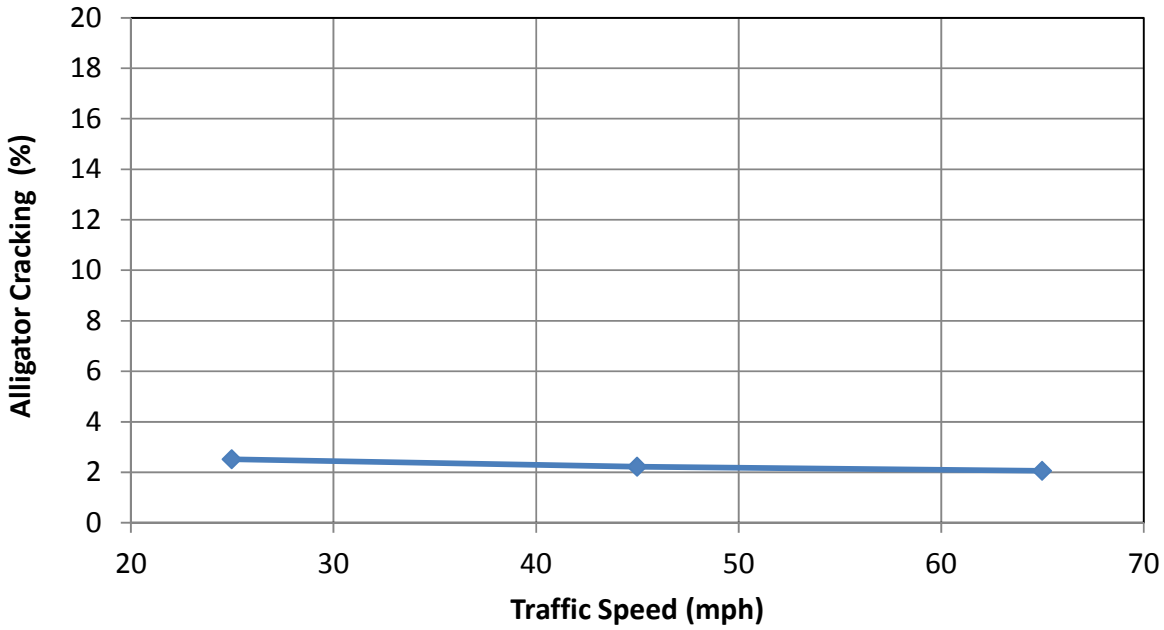

Figure 141. Influence of Traffic Speed on Alligator Cracking

Transverse Cracking Sensitivity Analysis

All performed MEPDG runs using the data presented in Table 93 produced 0 percent transverse cracking. This may be attributed to the used of level 3 data for the tensile strength and creep compliance of the HMA.

Rutting Sensitivity Analysis

The flowing subsections describe the sensitivity of MEPDG predicted rutting (AC, base, subgrade, and total rutting) to each of the investigated parameters. All analyses are based on the rutting predicted after 20-years of traffic loading.

AC Layer Thickness

The influence of changing the AC layer thickness on total, AC, base, and subgrade rutting is shown in Figure 142. This figure shows AC thickness affects rutting predicted in all layers. Consequently, the total rutting significantly decreased with the increase in the AC layer thickness.

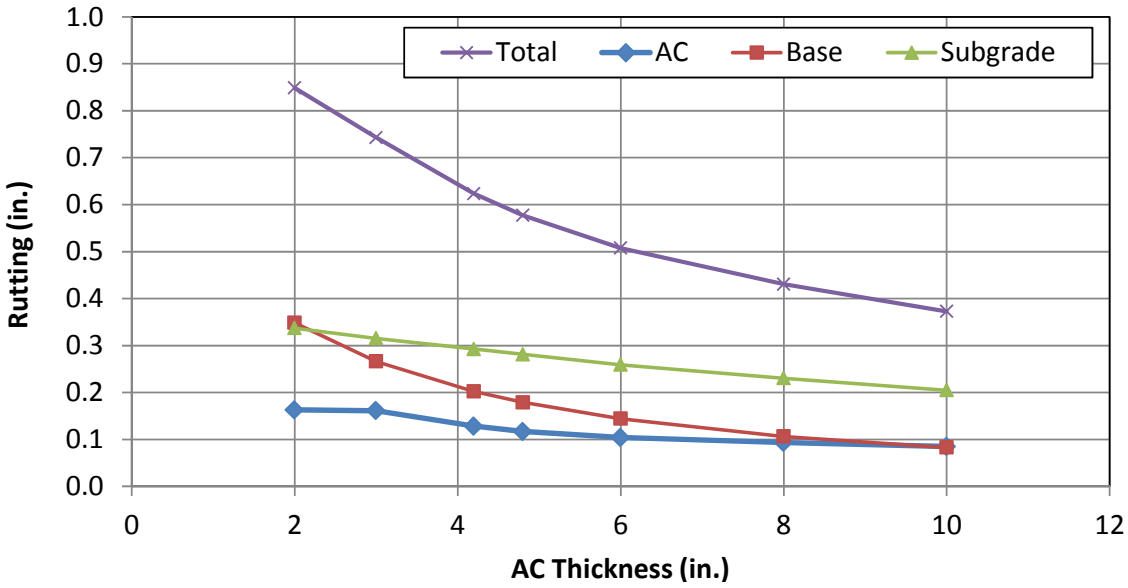

Figure 142. Influence of AC layer Thickness on Rutting

AC Mix Stiffness

Figure 143 illustrates the influence of increasing AC mix stiffness on MEPDG predicted rutting. This figure shows that as the mix stiffness increases both AC and total rutting deceases significantly. This figure also shows that the influence of AC mix stiffness is not significant on the MEPDG predicted base and subgrade rutting.

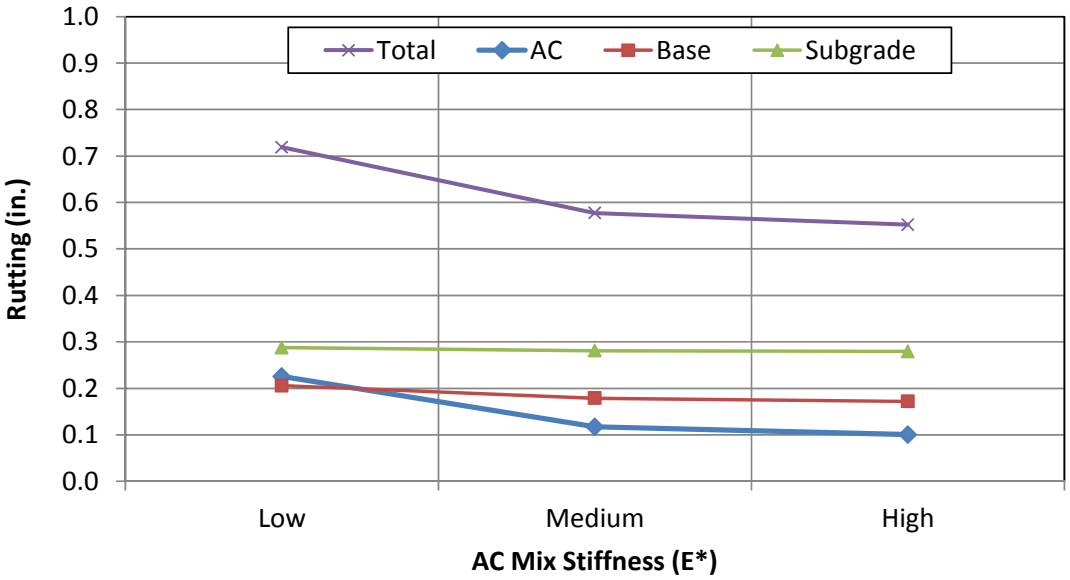

Figure 143. Influence of AC Mix Stiffness on Rutting

Effective Binder Content

The influence of changing the effective binder content of the AC mix on MEPDG predicted total, AC, base, and subgrade rutting is illustrated in Figure 144. This figure indicates that an increase in the mix binder content yields an increase in the AC rutting and consequently total rutting. However, this influence is not overly significant. It can also be concluded from this figure that both base and subgrade rutting were not affected by changes in the binder content of the mix.

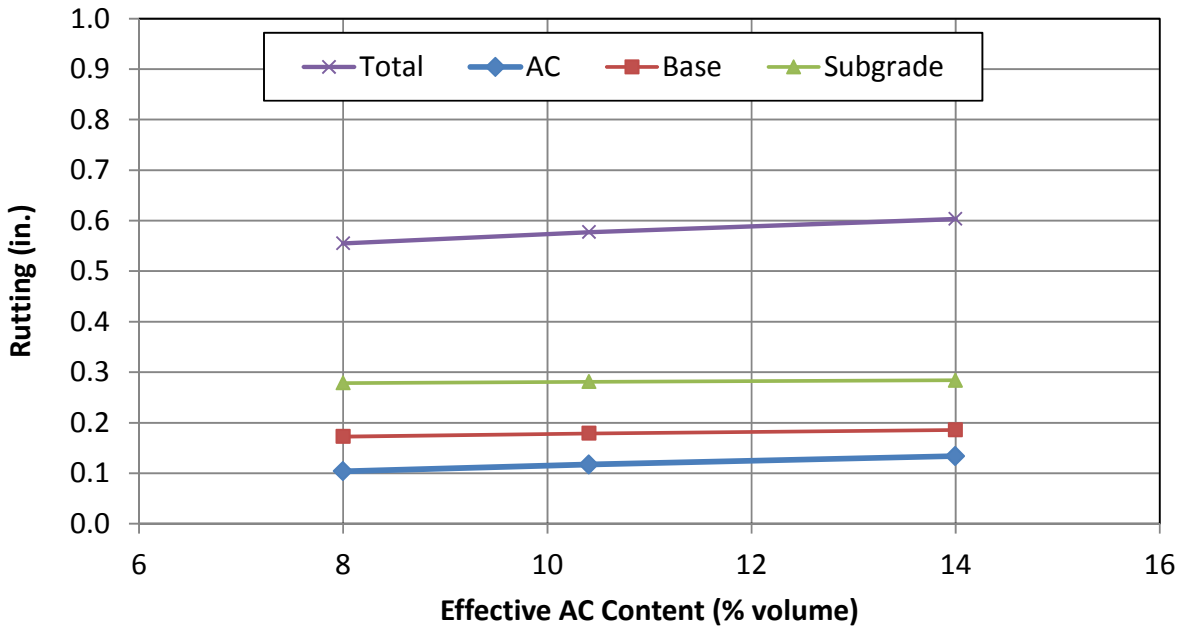

Figure 144. Influence of Effective Binder Content on Rutting

Mix Air Voids

The in-pace air voids content of the AC mix has a significant impact on AC rutting. This is shown in Figure 145. As the percent air voids in the mix increases, AC layer rutting increases. This figure also shows a significant increase in subgrade rutting and a slight increase in the base layer rutting due to the increase in the air voids.

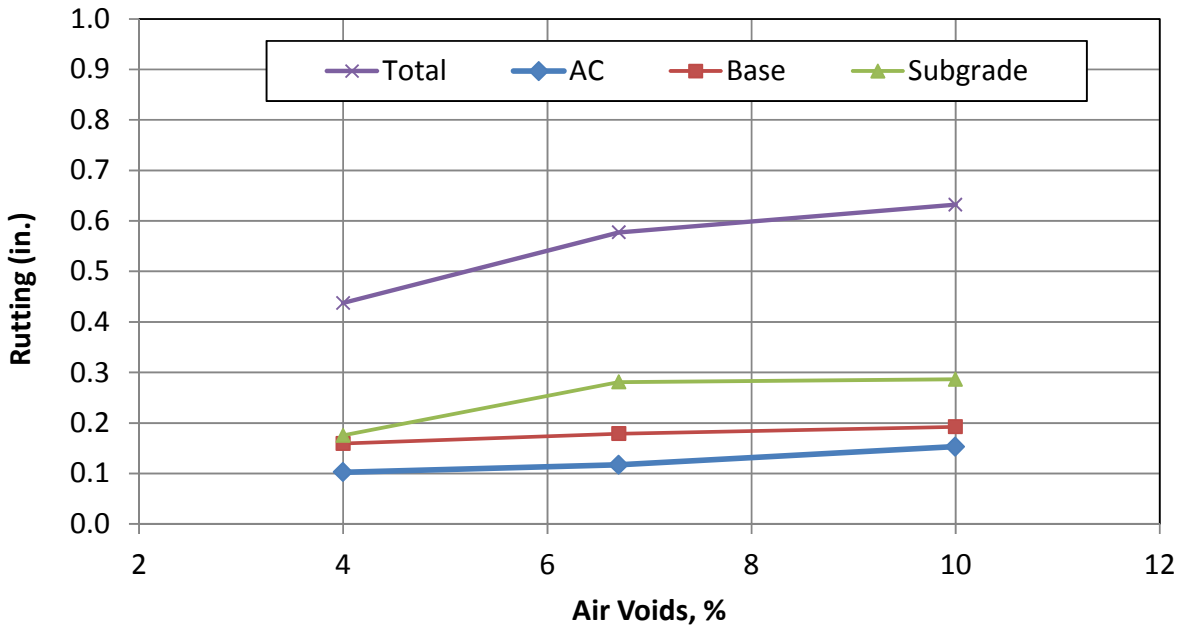

Figure 145. Influence of Mix Air Voids on Rutting

Base Layer Thickness

Figure 146 shows total and individual layers rutting after 20-years of traffic loading for 4 levels of granular base layer thickness. This figure shows some reduction in total rutting and a significant reduction in subgrade rutting. This figure also shows that as the base layer thickness increase, the base layer rutting also increases while the AC layer rutting does not change.

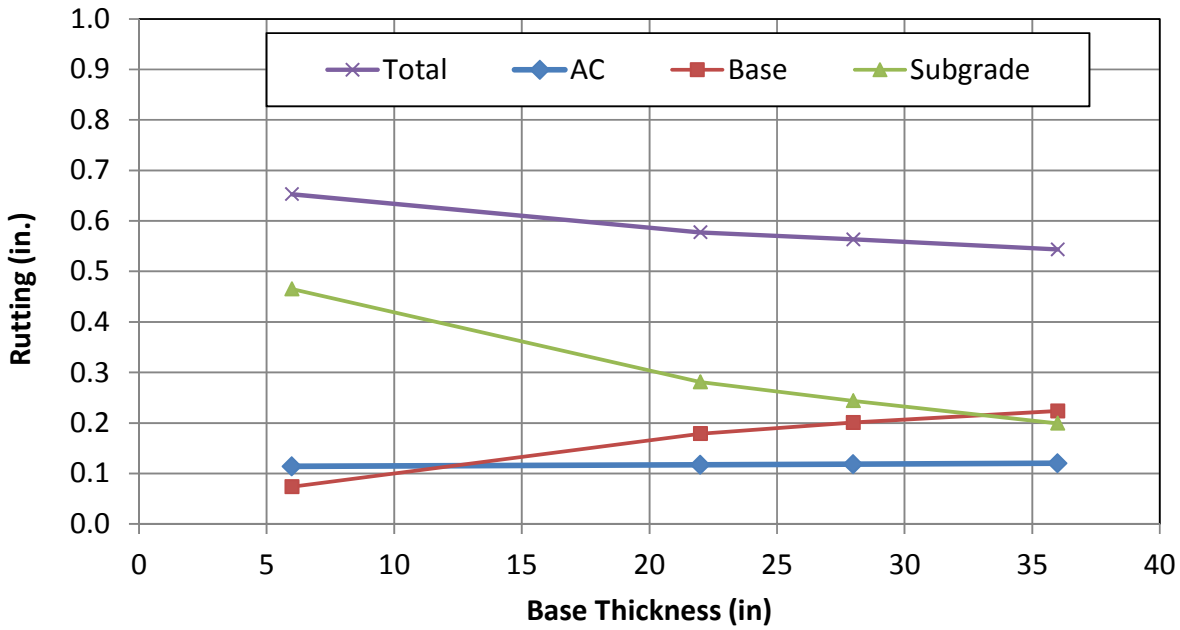

Figure 146. Influence of Granular Base Layer Thickness on Rutting

Subgrade Modulus

Figure 147 shows the influence of subgrade modulus on MEPDG predicted rutting. The figure indicates that as the subgrade modulus increases, the subgrade and hence total rutting decreases significantly. On the other hand, both AC and base layer rutting were not affected by the subgrade modulus.

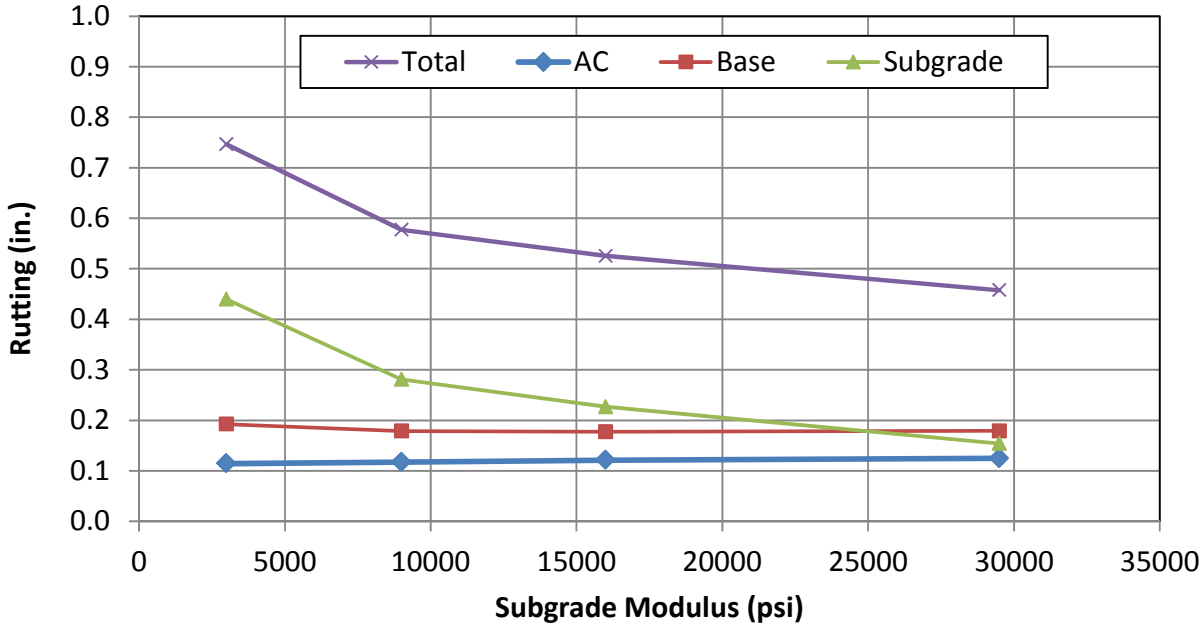

Figure 147. Influence of Subgrade Modulus on Rutting

Climate

MEPDG predicted rutting after 20-years of traffic loading for 4 different climatic locations in Idaho is shown in Figure 148. Both AC and total rutting increase significantly with the increase of the MAAT at the climatic location. Both base and subgrade rutting are not affected by the MAAT.

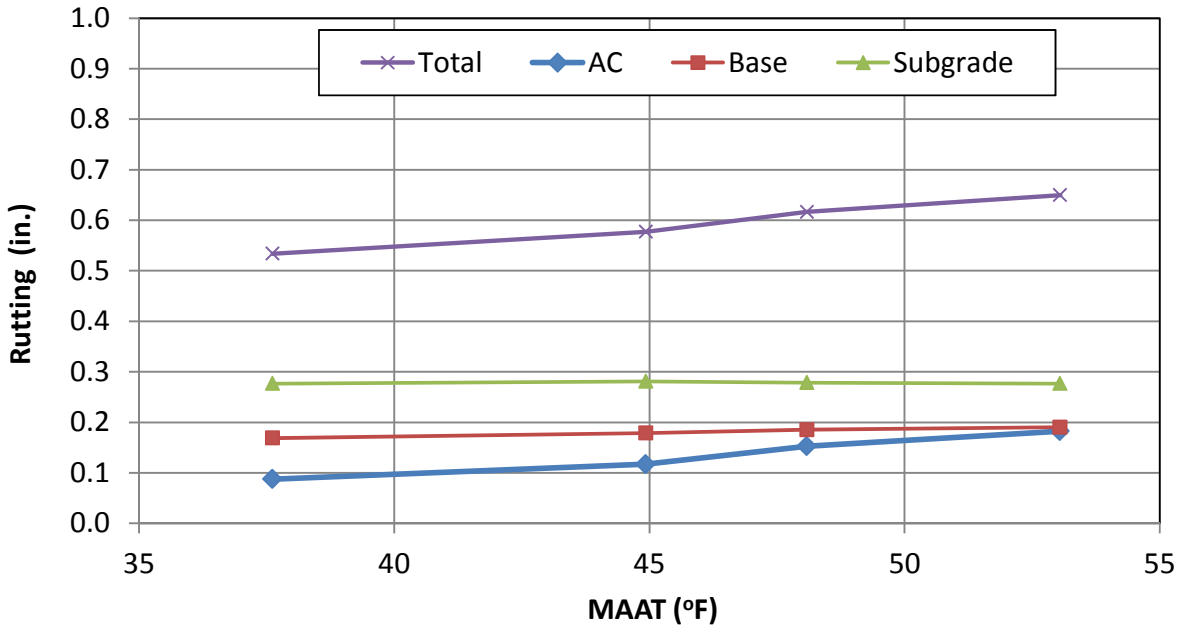

Figure 148. Influence of MAAT on Rutting

Ground Water Table Depth

Figure 149 shows the relationship between total and individual layers rutting and GWT depth level. This figure shows a decrease and then increase in both AC and total rutting with an increase in GWT depth. This trend is erroneous and may be an indication of some software bug.

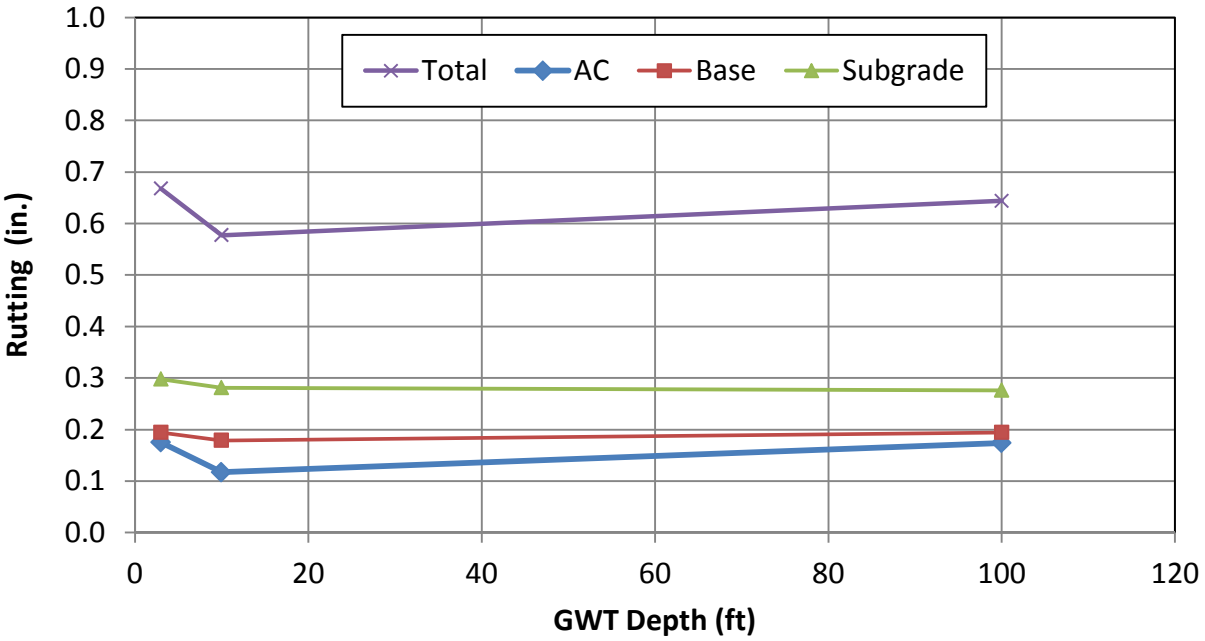

Figure 149. Influence of GWT Depth on Rutting

Axle Load Spectra

Figure 150 shows the relationship between rutting and ALS. As ALS increases form light to heavy, an increase in AC, base, and subgrade and hence total rutting occurs.

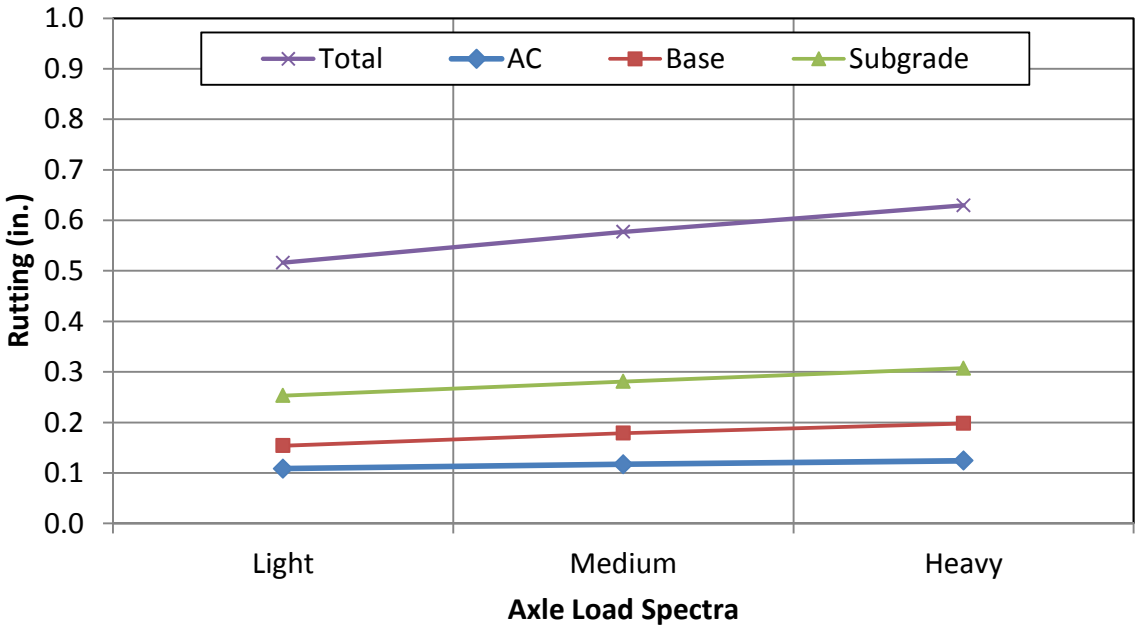

Figure 150. Influence of ALS on Rutting

Traffic Volume

The influence of traffic volume on MEPDG predicted rutting is shown in Figure 151. This figure shows that Traffic volume has a very significant influence on total and individual layers rutting. As traffic volume increases, the amount of total rutting increases significantly.

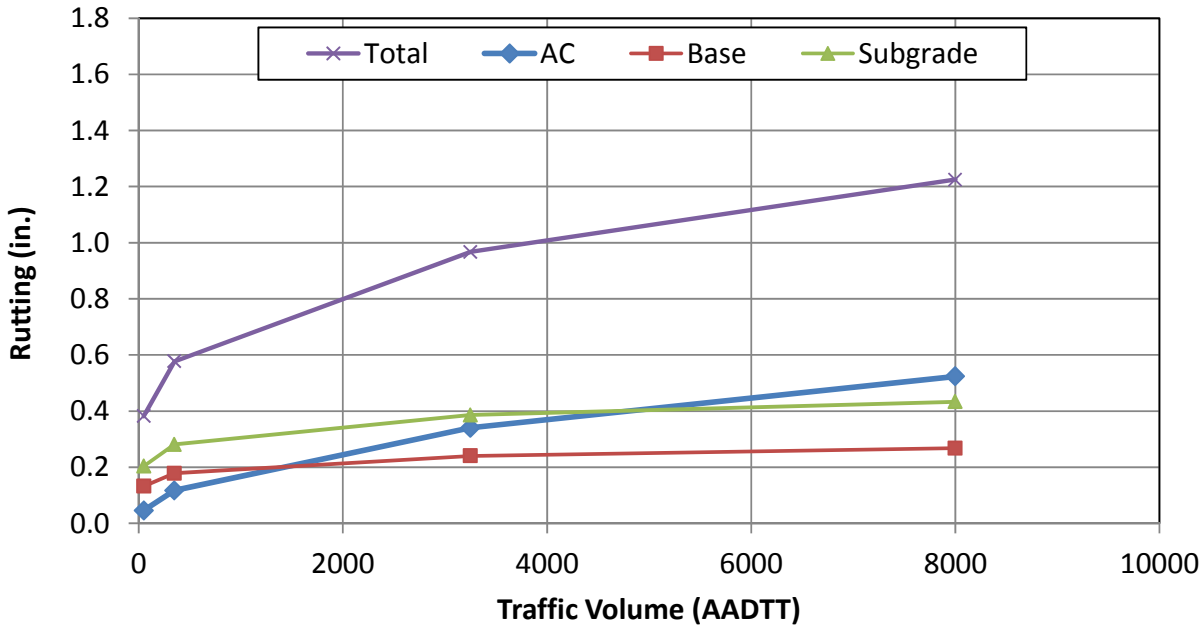

Figure 151. Influence of Traffic Volume on Rutting

Traffic Speed

Figure 152 shows the results of the sensitivity of MEPDG predicted rutting to traffic speed. This figure shows that as the traffic speed increases, a slight increase in AC and hence total rutting occurs. This figure also shows that traffic speed has no influence on both base and subgrade rutting.

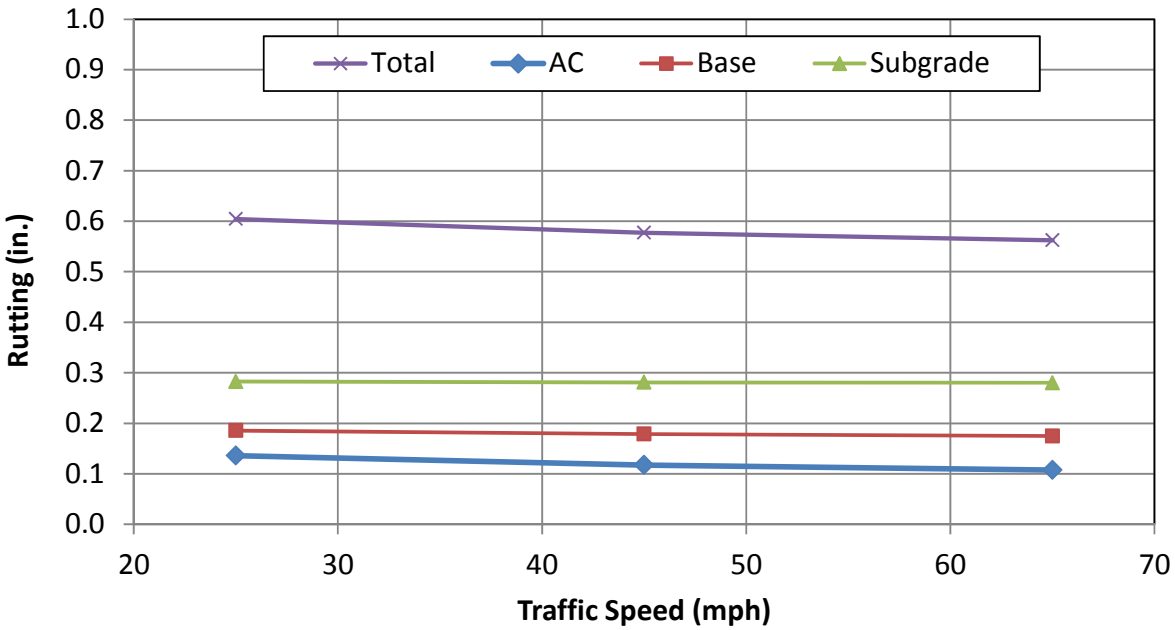

Figure 152. Influence of Traffic Speed on Rutting

International Roughness Index Sensitivity Analysis

The flowing subsections describe the sensitivity of MEPDG predicted IRI relative to each of the investigated parameters. All analyses are based on the IRI predicted after 20-years of traffic loading.

AC Layer Thickness

The influence of changing the AC layer thickness on MEPDG predicted IRI is shown in Figure 153. This figure shows a decrease in IRI with an increase in AC layer thickness.

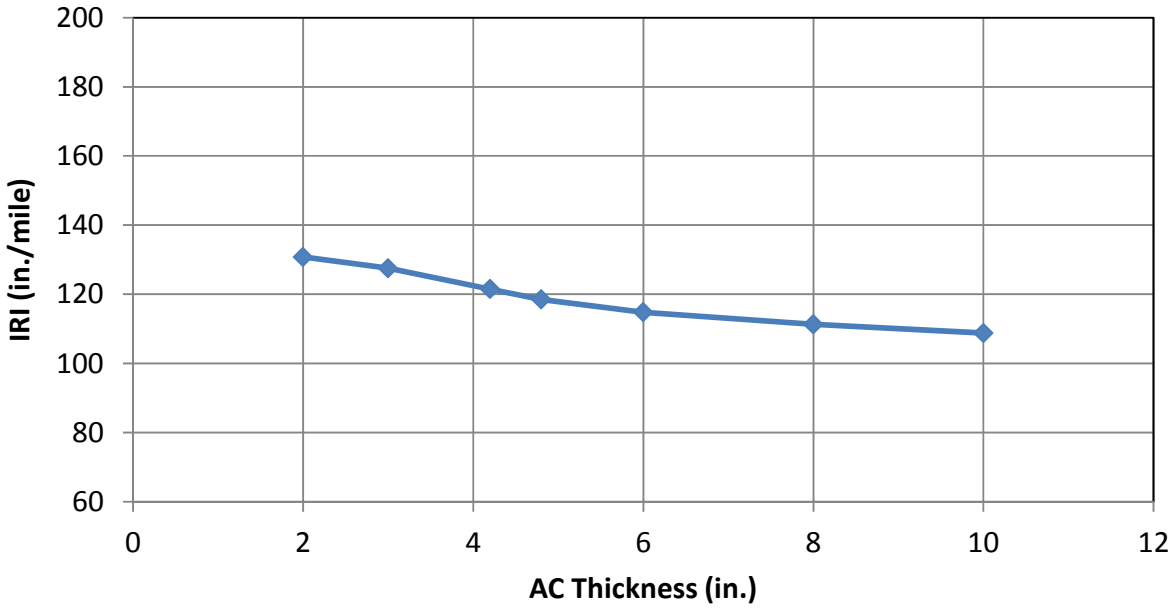

Figure 153. Influence of AC layer Thickness on IRI

AC Mix Stiffness

Figure 154 illustrates the influence of changing the AC mix stiffness (low, medium, and high) on the IRI predicted using MEPDG after 20-years of traffic loading. It can be inferred from this figure that mix stiffness has no significant influence on IRI.

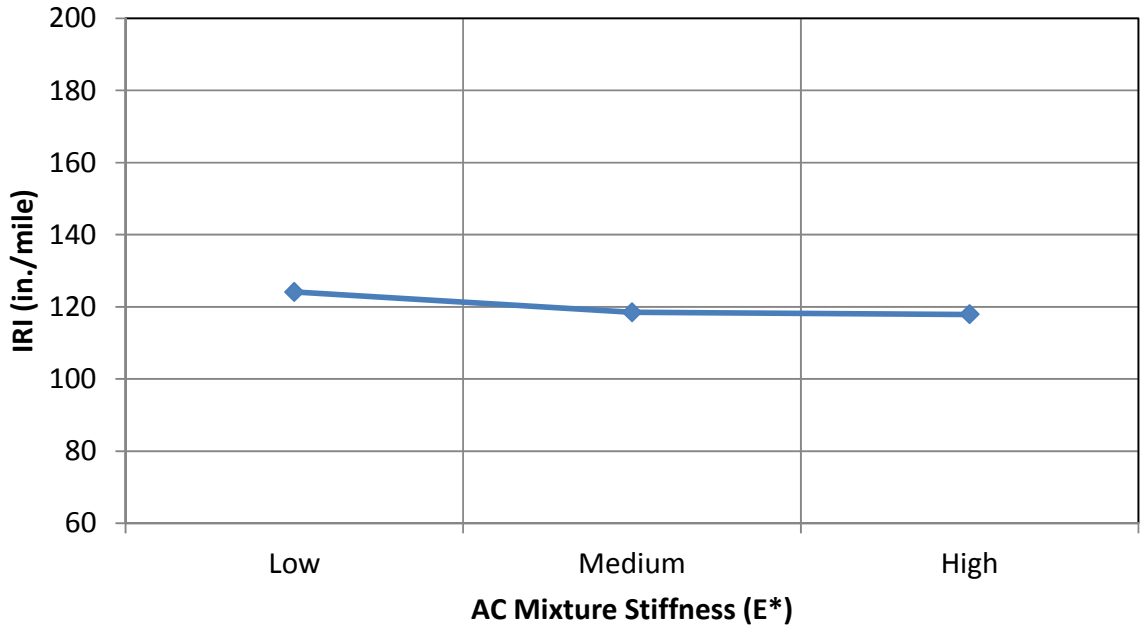

Figure 154. Influence of AC Mix Stiffness on IRI

Effective Binder Content

The influence of changing the effective binder content of the AC mix on IRI is illustrated in Figure 155. This figure shows that binder content has no significant influence on IRI.

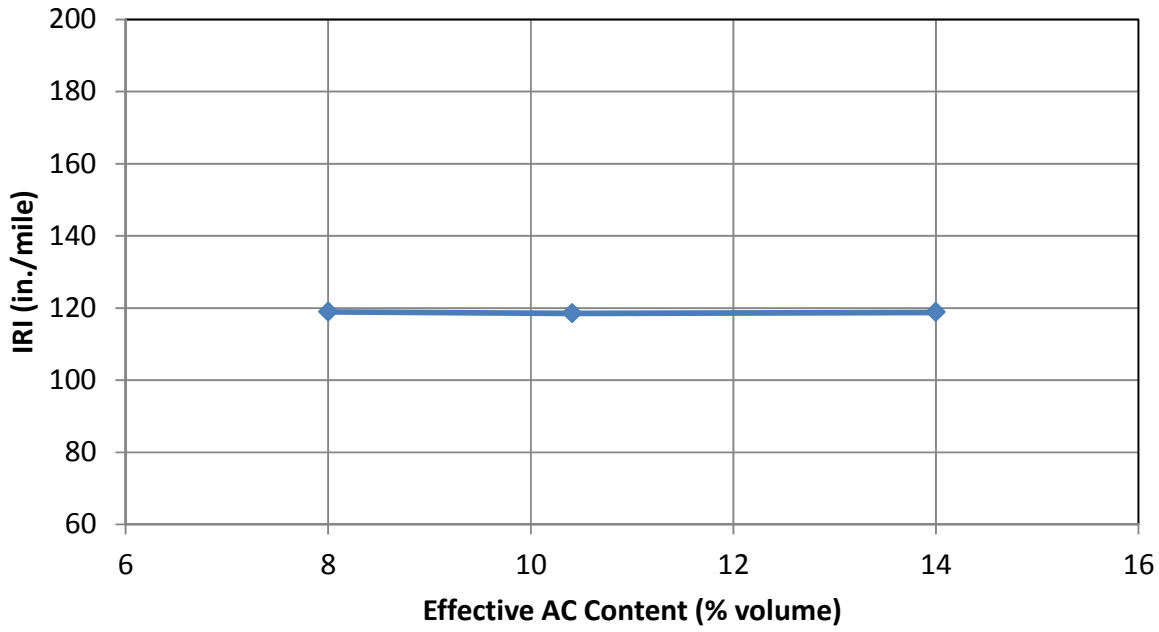

Figure 155. Influence of Effective Binder Content on IRI

Mix Air Voids

Figure 156 shows the relationship between in-pace air voids content of the AC mix and MEPDG predicted IRI. This figure shows a slight increase in IRI with an increase in percent air voids. However, the influence is not overly significant.

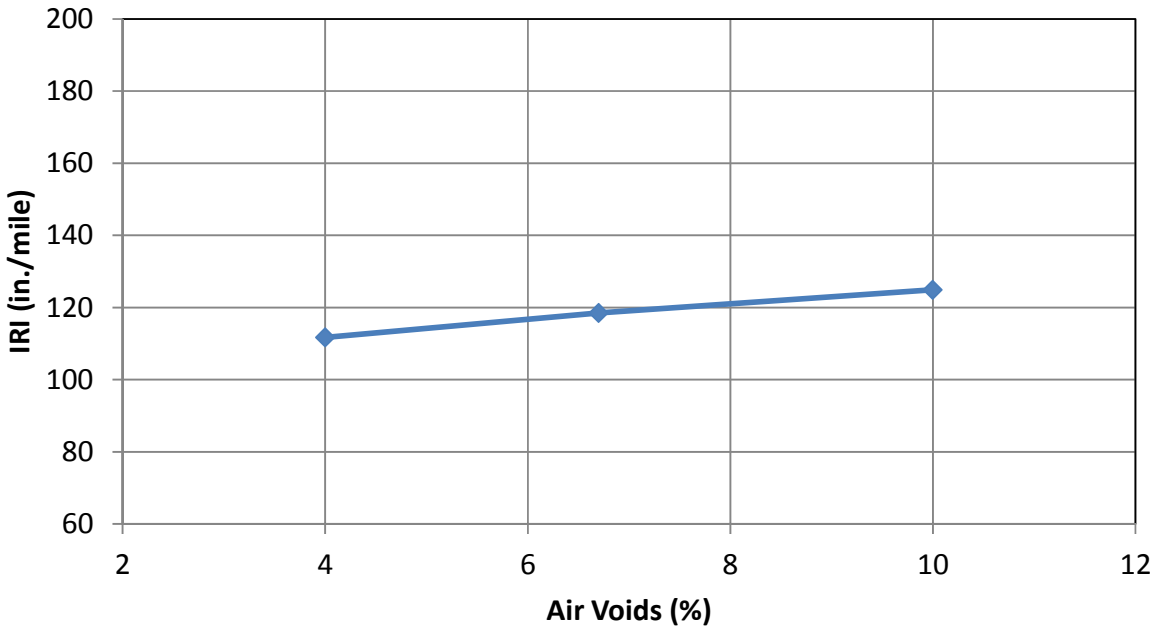

Figure 156. Influence of Mix Air Voids on IRI

Base Layer Thickness

Figure 157 depicts IRI for 4 levels of granular base layer thickness. This figure shows insignificant decrease in MPEDG predicted IRI with the increase in the base layer thickness.

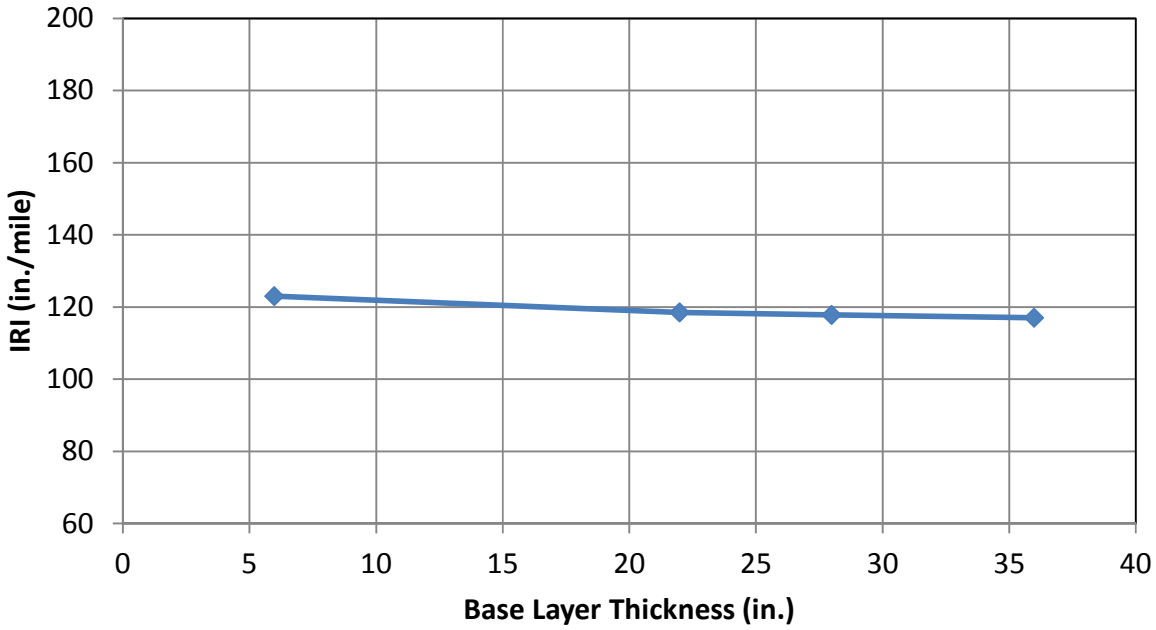

Figure 157. Influence of Granular Base Layer Thickness on IRI

Subgrade Modulus

Figure 158 shows IRI after 20-years of traffic loading for 4 values of subgrade modulus. The figure shows that as the subgrade modulus increases, IRI decreases.

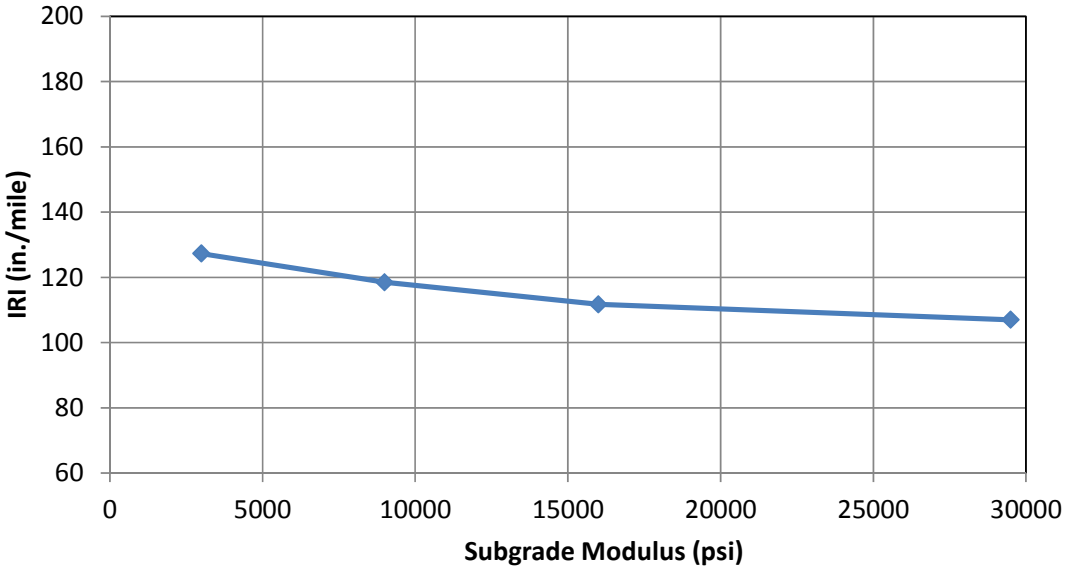

Figure 158. Influence of Subgrade Modulus on IRI

Climate

The influence of the climatic site characteristics on MEPDG predicted IRI after 20-years of traffic loading is shown in Figure 159. The figure shows that climatic location has no significant influence on IRI.

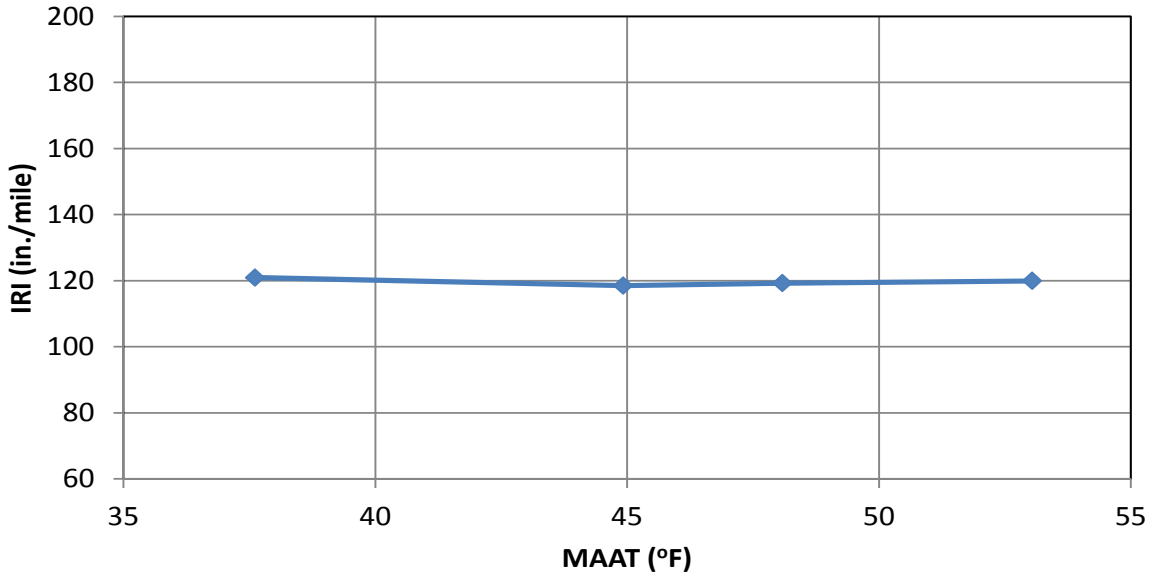

Figure 159. Influence of MAAT on IRI

Ground Water Table Depth

Figure 160 shows IRI predicted at 3 GWT depth levels after 20-years of traffic loading. This figure shows that GWT depth has insignificant influence on IRI.

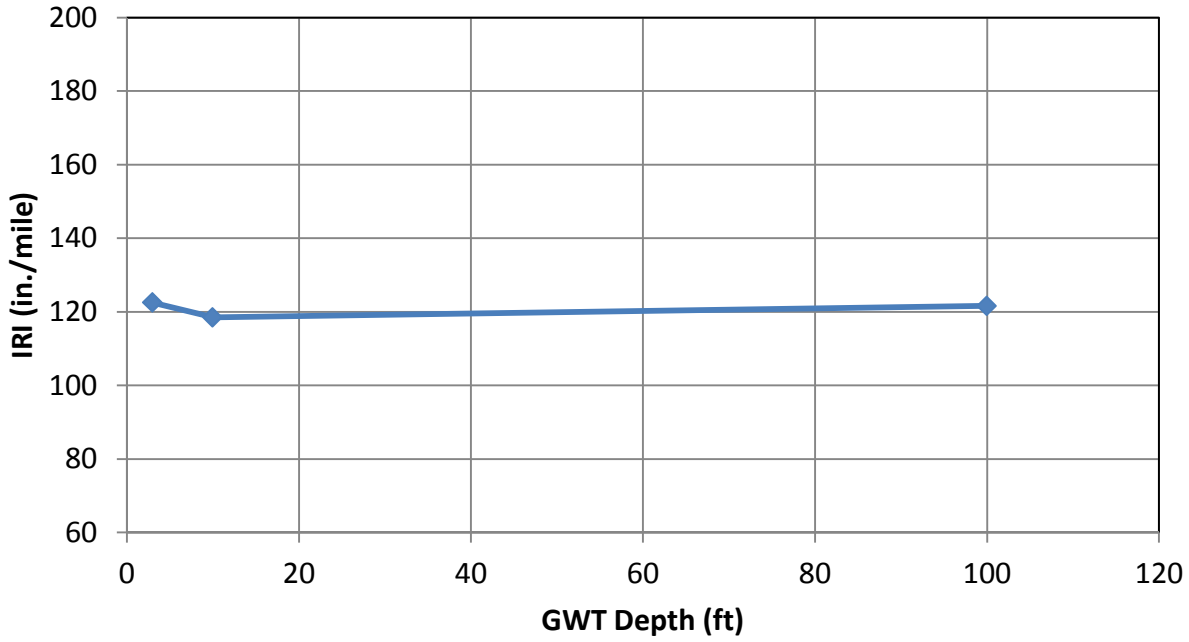

Figure 160. Influence of GWT Depth on IRI

Axle Load Spectra

Figure 161 shows the relationship between IRI predicted after 20-years of traffic loading and ALS. This figure clearly shows that ALS has insignificant influence on IRI.

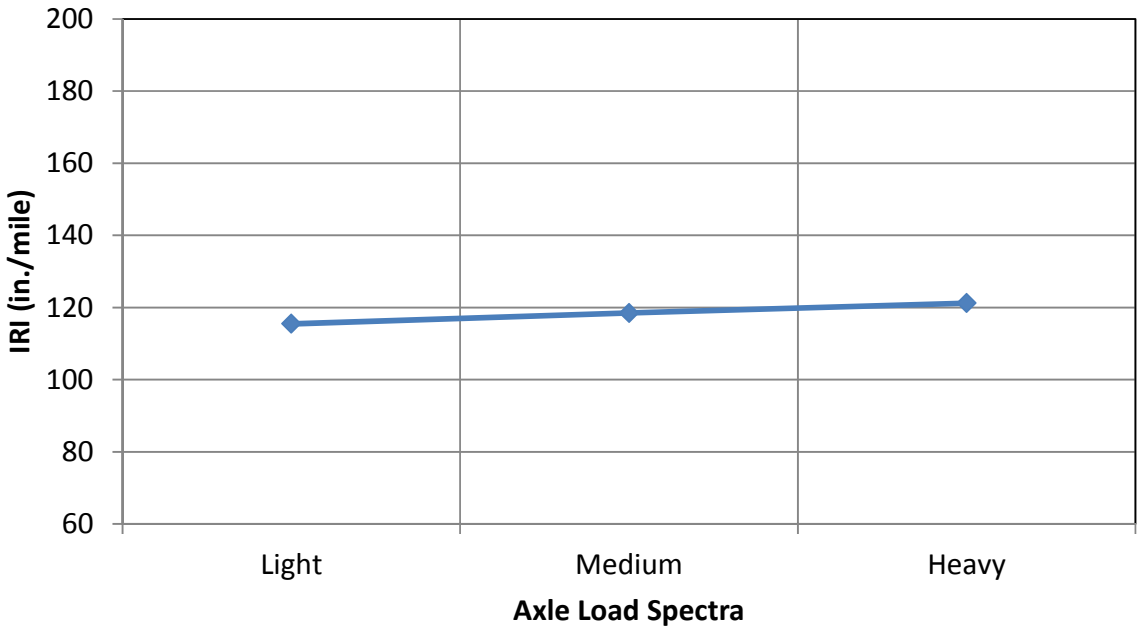

Figure 161. Influence of ALS on IRI

Traffic Volume

The influence of traffic volume on IRI predicted after 20-years of traffic loading is shown in Figure 162. As this figure shows, traffic volume has a very significant influence on IRI. As traffic volume increases, IRI increases significantly. Among all investigated variables, traffic volume has the highest influence on IRI.

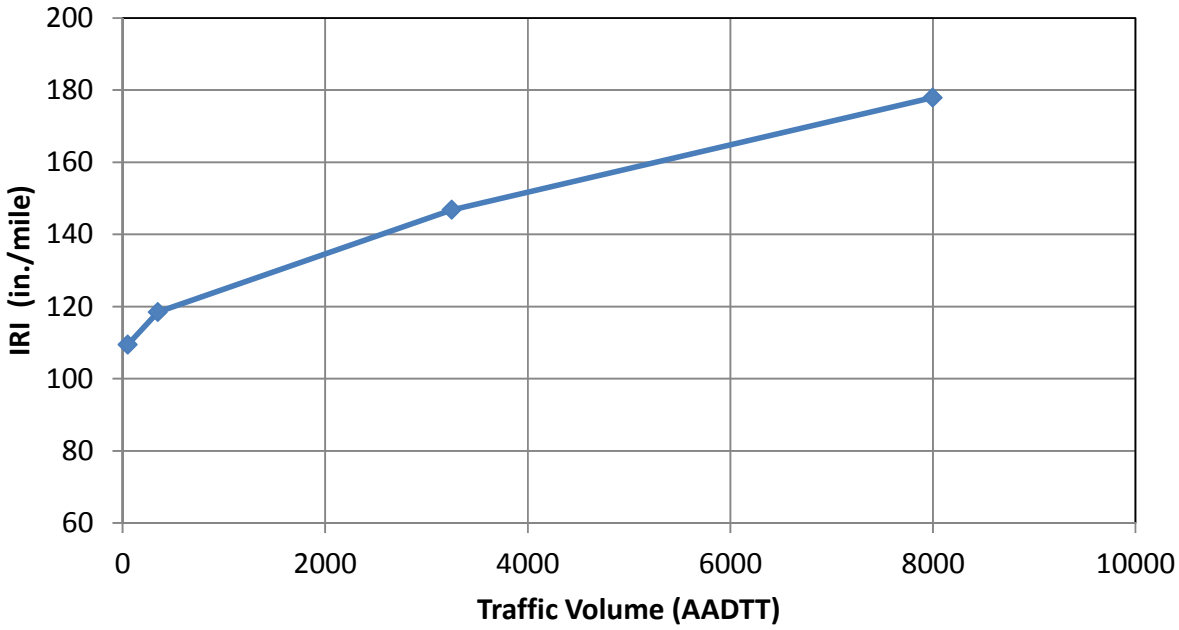

Figure 162. Influence of Traffic Volume on IRI

Traffic Speed

Figure 163 shows the results of the sensitivity of IRI relative to traffic speed. This figure clearly shows that traffic speed has insignificant influence on IRI.

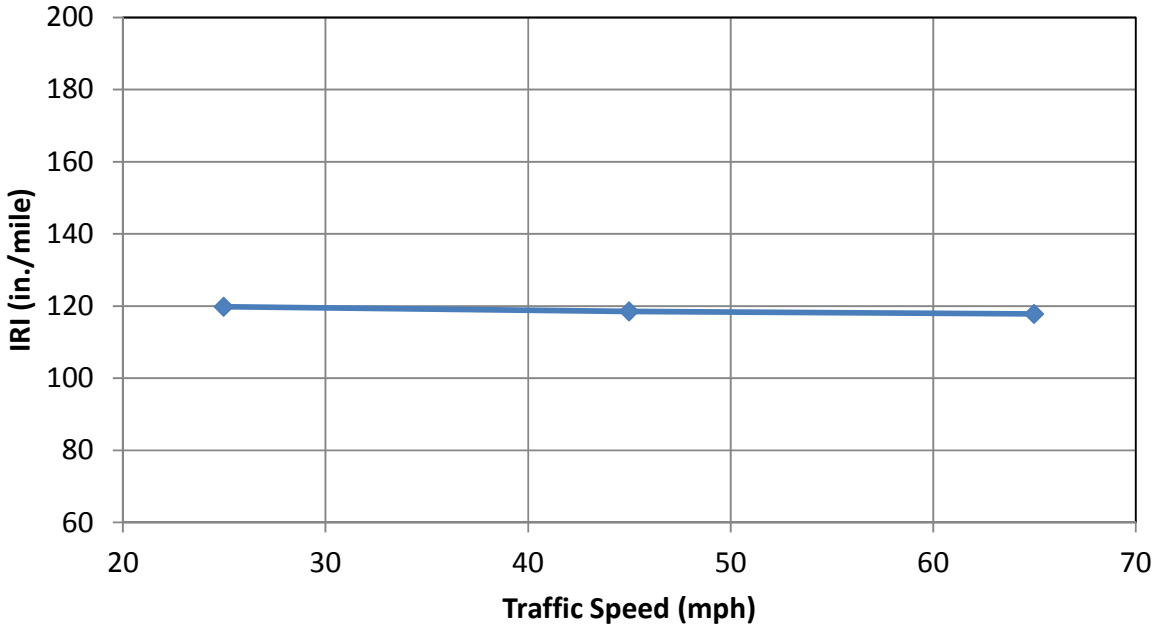

Figure 163. Influence of Traffic Speed on IRI

Summary of the Sensitivity Analysis

Based on the sensitivity analyses it was found that longitudinal cracking is extremely sensitive to most of the investigated parameters. Alligator cracking was found sensitive to extremely sensitive to most of the investigated parameters. IRI was not sensitive to most of the input parameters investigated in this study. Among all investigated parameters, traffic volume was found to be the most influencing input on MEPDG predicted distresses and IRI.

In order to identify the level of importance associated with each input parameter, results of the sensitivity analyses are summarized in Table 101. In this table the sensitivity of each distress is assigned a sensitivity level. The criteria used to define the sensitivity level of each of the distresses to the investigated input parameters is summarized in Table 102. This suggested criterion is based on the distress ratio (DS) which is the ratio of the largest to smallest predicted distress or IRI values.

Table 101. Summary of the Sensitivity Analysis

Input Parameter	Performance Models						
	Cracking		Rutting				IRI
	Longitudinal	Alligator	AC	Base	Subgrade	Total	
AC Thickness	ES	ES	VS	ES	VS	ES	LS
AC Mix Stiffness	ES	S	ES	LS	I	S	I
Effective Binder Content	ES	ES	LS	I	I	I	I
Mix Air Voids	ES	ES	S	LS	VS	S	LS
Base Layer Thickness	ES	ES	I	ES	ES	LS	I
Subgrade Modulus	ES	LS	LS	I	VS	VS	LS
Climate	VS	S	ES	LS	I	LS	I
GWT Level	VS	I	I	I	I	I	I
ALS	ES	ES	LS	LS	LS	LS	I
Traffic Volume	ES	ES	ES	ES	ES	ES	VS
Traffic Speed	LS	LS	LS	I	I	I	I

Table 102. Criteria used for Defining the Level of Sensitively

Sensitivity Level	Criteria
ES: Extremely Sensitive	DS ≥ 2.0
VS: Very Sensitive	1.6 ≤ DS < 2.0
S: Sensitive	1.3 ≤ DS < 1.6
LS: Low Sensitivity	1.10 ≤ DS < 1.3
I: Insensitive	DS < 1.1

Chapter 9
Performance and Reliability Design Criteria

Practically, there is a significant amount of uncertainly and variability related to pavement design, construction, traffic loading characteristics, traffic volume, climatic factors, and material properties. Thus, reliability is an important part of most of the pavement design procedures. In the AASHTO 1993 Design Guide reliability is defined as the probability that a pavement section designed using the process will perform satisfactory over the traffic and environmental conditions for the design period.[(1)] This definition is similar to that in MEPDG. Reliability analysis has been incorporated in MEPDG since its first release. It accounts for errors associated with the distress/IRI prediction models. These errors include all sources of variation related to the prediction such as material characterization, traffic, environmental conditions, and data used for calibration of the models.

This chapter presents the reliability concept in MEPDG. It also investigates the typical reliability values recommended to be used with MEPDG for design and analysis of flexible pavement systems.

MEPDG Reliability Concept

In MEPDG, the key outputs for flexible pavements are rutting, fatigue cracking, thermal cracking, and IRI. Thus, reliability is applied on these predicted distresses. Design reliability (R), within the context of MEPDG, is defined as the probability (P) that each of the key distress types and IRI will be less than a selected critical level over the design period.[(4)] This is shown in Figure 164.

R = P [Distress over Design Period < Critical Distress Level]

Figure 164. MEPDG Definition of reliability

Design process in MEPDG begins with a trail section. MEPDG then predicts key distress types and IRI over the design life of the pavement. These predictions are based on mean values (50 percent reliability) for all inputs. This is shown in Figure 165 for IRI as an example. The probability distributions of the predicted distresses and IRI about their mean values are important in establishing design reliability. These distresses and IRI are approximately normally distributed over ranges of the distress and IRI that are of interest in design.[(4)] Figure 165 illustrates the probability distribution for IRI. Distresses and IRI at a specific design reliability defined by the user are then calculated. This is shown in Figure 166 for IRI. Cracking and rutting at design reliability are calculated as shown in Figure 167 and Figure 168, respectively. Simply, the mean distress or IRI (at 50 percent reliability) is increased by a number of standard errors that apply to the reliability level selected. Figure 166 through Figure 168 show that for each distress type and IRI, design reliability is based on the standard error of estimate specific to the model. The standard error of estimate is obtained from the field calibration results of each of the distress prediction models and IRI. Reliability predictions at an arbitrary level ® above the mean predictions, for IRI as an example, are shown as dashed line in Figure 165.

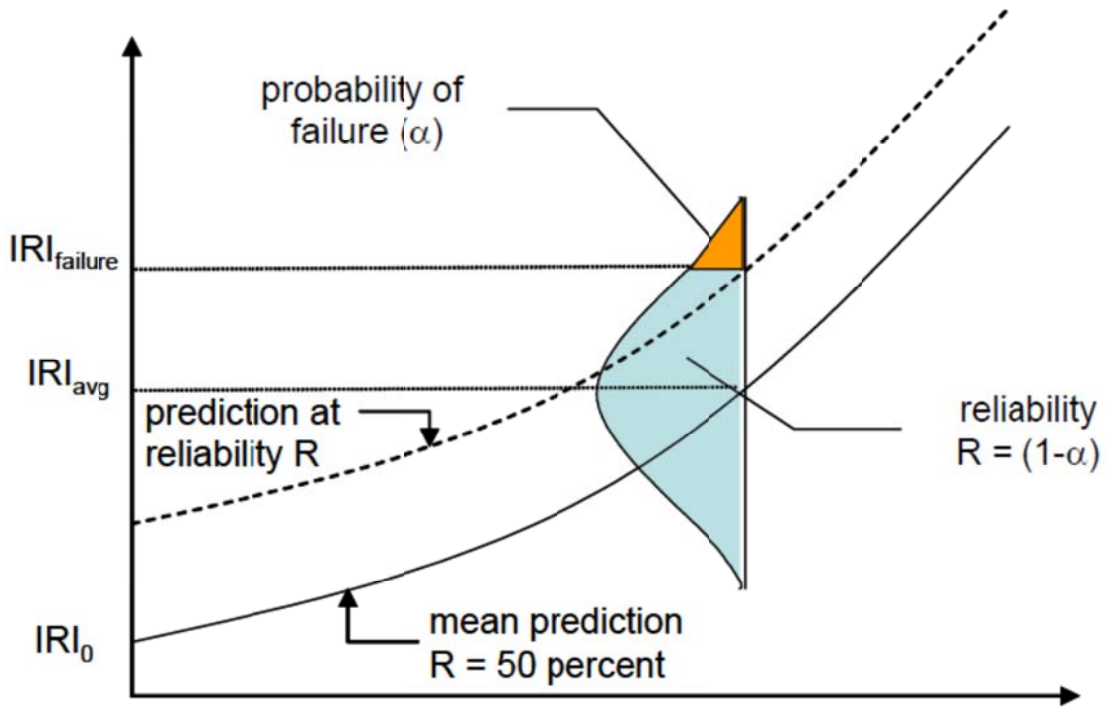

Figure 165. MEPDG Design Reliability Concept for Smoothness (IRI)[4]

$$IRI\_p = IRI\_mean + STDmeas * Zp$$

where:

IRI_p = IRI corresponding to reliability level p
IRI_mean = IRI predicted using the deterministic model with mean inputs (corresponding to 50 percent reliability)
STDmeas = standard deviation of IRI corresponding to IRI predicted using the deterministic model with mean inputs
Zp = standardized normal derivative corresponding to reliability level (mean = 0.0, and standard deviation = 1.0)

Figure 166. Equation to Calculate IRI at Selected Design Reliability

$$Cracking_p = Cracking_{mean} + STDmeas * Zp$$

where:

Cracking_p = Cracking corresponding to reliability level p
Cracking_mean = Cracking predicted using the deterministic model with mean inputs (corresponding to 50 percent reliability)
STDmeas = standard deviation of cracking corresponding to IRI predicted using the deterministic model with mean inputs
Zp = standardized normal derivative corresponding to reliability level (mean = 0.0, and standard deviation = 1.0)

Figure 167. Equation to Calculate Cracking at Selected Design Reliability

$$Rutting_p = Rutting_{mean} + STDmeas * Zp$$

where:

Rutting_p = Rutting corresponding to reliability level p
Rutting_mean = Rutting predicted using the deterministic model with mean inputs (corresponding to 50 percent reliability)
STDmeas = standard deviation of rutting corresponding to rutting predicted using the deterministic model with mean inputs
Zp = standardized normal derivative corresponding to reliability level (mean = 0.0, and standard deviation = 1.0)

Figure 168. Equation to Calculate Rutting at Selected Design Reliability

MEPDG versus AASHTO 1993 Reliability

MEPDG reliability definition varies from the previous versions of the AASHTO design guide in that it specifies each key distress and IRI directly in the definition.[97] AASHTO 1993 guide defines reliability in terms of predicted number of ESALs to terminal serviceability being less than the actual applied number of ESALs. This definition yields very high ESALs that are far beyond the capabilities of the AASHTO 1993 model. Thus, at high reliability levels, for heavy volumes of traffic loadings, AASHTO 1993 results in excessive pavement thicknesses compared to MEPDG.[97]

MEPDG Recommended Reliability Levels

MEPDG allows users to select different design reliability level s for each distress type and IRI. However, it is recommended to use the same reliability of all performance indicators.[4] The MEPDG recommend levels of design reliability for different functional classification of roadway are presented in Table 103.

Table 103. MEPDG Recommended Reliability Levels[6]

Functional Classification	Recommended Level of Reliability	
	Urban	Rural
Interstate/Freeways	95	95
Principal Arterials	90	85
Collectors	80	75
Local	75	70

Table 104 presents the performance criteria (threshold values) recommended for use with MEPDG for flexible pavement design based on the roadway functional class. These criteria are recommended for use with the reliability levels presented in Table 103.

Table 104. MEPDG Recommended Performance Criteria[6]

Distress	Threshold Value at Design Reliability
Terminal IRI (in./mile)	Interstate: 160 Primary: 200 Secondary: 200
AC Alligator Cracking (Percent Lane Area)	Interstate: 10 Primary: 20 Secondary: 35
Thermal Fracture (Transverse Cracking) (ft/mile)	Interstate: 500 Primary: 700 Secondary: 700
Total Rutting (in.)	Interstate: 0.40 Primary: 0.50 Others < 45 mph: 0.65

Investigating MEPDG Recommended Reliability Levels

This chapter focuses on investigating the suitability of MEPDG recommended reliability levels and design criteria to Idaho. In order to do that, it is first important to check the accuracy of the nationally calibrated MEPDG distress/IRI models predictions for Idaho pavements. LTPP flexible pavement sections in Idaho were identified and used to investigate the accuracy of the nationally calibrated MEPDG distress/IRI models.

Idaho LTPP Database

LTPP database is one of the most comprehensive and reliable sources of pavement data. This data matches MEPDG required input data. As part of the NCHRP 1-37A and NCHRP 1-40D projects, MEPDG performance models were calibrated based on LTPP data distributed throughout the U.S.[4, 98] In Idaho, there are 9 General Pavement Studies (GPS-1) LTPP flexible pavement sections. GPS-1 sites are asphalt pavements built on granular base layers. Each LTPP pavement section is 500 ft long. MEPDG required input data specific to the 9 GPS-1 LTPP sections in Idaho were collected. The latest LTPP Standard Data Release 24.0 DVD version was used as the source of data collection.[99] Each LTPP section in the database is identified by a state code and a SHRP ID. Idaho state code in the LTPP database is 16. The 9 GPS-1 Idaho sites are shown in Table 105. The complete LTPP data collected for this study is shown in Appendix F. LTPP data collection effort included pavement structure, AC aggregate gradation, asphalt binder properties, unbound materials properties, climatic data, cracking, rutting, and roughness.

Table 105. Idaho GPS-1 Sites

SHRP ID	Project Type	Pavement Type	County	Route #
1001	GPS-1	Conventional	Kootenai	95
1005	GPS-1	Conventional	Adams	95
1007	GPS-1	Conventional	Twin Falls	30
1009	GPS-1	Conventional	Cassia	84
1010	GPS-1	Conventional	Jefferson	15
1020	GPS-1	Conventional	Jerome	93
1021	GPS-1	Conventional	Jefferson	20
9032	GPS-1	Conventional	Kootenai	95
9034	GPS-1	Conventional	Bonner	95

Materials

Summary of LTPP database modules and associated tables for pavement structure, AC aggregate gradation, and asphalt binder data are shown in Table 106. MEPDG default values for thermal properties of the AC mixes were used.

Table 106. Summary of the Pavement Structure, AC Aggregate Gradation, and Asphalt Binder Data and their LTPP Database Sources

Data	LTPP Module	LTPP Table
AC and Granular Base Layer Thicknesses	Material_Test	SECTION_LAYER_STRUCTURE
Aggregate Gradation for AC Layer	Material_Test	TST_AG04
Binder Grade and Viscosity	Inventory	INV_PMA_ASPHALT
Bulk Specific Gravity of the Mix, G_{mb}	Material_Test	TST_AC02
Asphalt Content by Total Weight of Mix, P_b	Material_Test	TST_AC04
Binder Specific Gravity, G_b	Inventory	INV_PMA_ASPHALT
Bulk Specific Gravity of Aggregate, G_{sb}, G_{se}	Inventory	INV_PMA,
Effective Specific Gravity of Aggregate, G_{se}	Inventory	INV_PMA,
Theoretical maximum Specific Gravity, G_{mm}	Material_Test	TST_AC03

Table 107 summarizes the unbound granular materials and subgrade soils required inputs for MEPDG and the LTPP modules and associated tables used to collect this data. Resilient modulus is the MEPDG primary input for unbound granular materials and subgrade soils characterization. However, LTPP database does not contain the resilient modulus. Thus, MEPDG typical default modulus values (level 3) selected based on the AASHTO classification system were used in this analysis.

Table 107. Summary LTPP Database Sources for MEPDG Required Inputs Regarding Unbound Materials and Subgrade Soils

Data	LTPP Module	LTPP Table
Granular Base Gradation and Soil Classification	Material_Test	TST_SS01_UG01_UG0
Subgrade Gradation and Soil Calcification	Material_Test	TST_SS01_UG01_UG01
Subgrade Plasticity Index and Liquid Limit	Material_Test	TST_UG04_SS03
Subgrade Optimum Gravimetric Moisture Content and Maximum Dry Unit Weight	Material_Test	TST_UG05_SS05

Climate

In MEPDG there are built-in weather station data to be used with the software. In order to select the appropriate weather station(s) for a specific pavement section, the longitude, latitude and elevation of this section must be known. Data used to assign a climatic weather station for each LTPP section was determined from the LTPP database module and table as shown in Table 108. GWT depth data for each LTPP site were extracted from the NWIS of the USGS website.[96]

Table 108. LTPP Database Sources for MEPDG Required Inputs for Weather Station Selection

Data	LTPP Module	LTPP Table
Longitude, Latitude, and Elevation	Climate Summary Data	CLM_OWS_Location

Traffic

MEPDG primary traffic input data were extracted from the LTPP traffic module. This data were extracted from different tables in the LTPP database as shown in Table 109. It should be noted that 2 LTPP sections did not have the MEPDG required traffic inputs. Thus these 2 sections (1010 and 1021) were not included in the analysis.

Table 109. Summary of LTPP Database Sources for MEPDG Required Traffic Data

Data	LTPP Module	LTPP Table
AADTT	Traffic	TRF_MEPDG_AADTT_LTPP_LN
Vehicle Class Distribution	Traffic	TRF_MEPDG_VEH_CLASS_DIST
Monthly Adjustment Factors	Traffic	TRF_MEPDG_MONTH_ADJ_FACTR
Axle Load Spectra	Traffic	TRF_MEPDG_AX_ANL
Average Number of Axles Per Truck	Traffic	TRF_MEPDG_AX_PER_TRUCK

Performance

MPEDG predicts performance in terms of cracking, rutting, and IRI. For the selected LTPP sections, measured distresses and IRI data were extracted from the LTPP distress files located in the monitoring module. Table 110 presents a summary of the module, units of measurements, and table and field that cracking, rutting and IRI data were extracted from. It also shows the measurement units, in the LTPP database, of these distresses and IRI.

Table 110. Summary of LTPP Database Sources and Units for Distresses and IRI

Data	LTPP Module	LTPP Table	Field	Units
Longitudinal Cracking	Monitoring	MON_DIS_AC_REV	Long Crack WP L_L	m
			Long Crack WP L_M	m
			Long Crack WP L_H	m
Fatigue Cracking			Gator Crack A_L	m^2
			Gator Crack A_M	m^2
			Gator Crack A_H	m^2
Transverse Cracking			Trans Crack L_L	m
			Trans Crack L_M	m
			Trans Crack L_H	m
Rutting		MON_T_PROF_INDEX_SEC	Rut Depth Average of Right and Left wheel Path	mm
IRI		MON_PROFILE_MASTER	IRI_Average	m/km

Similar to the national calibration, both longitudinal and alligator cracking were represented by the sum of low, medium, and high severity cracking without any adjustment. This is shown in Appendix F. whereas the total transverse cracking was represented by the same weighing function used in the national calibration. This is also shown in Appendix F.

Results and Analysis

For each LTPP section, input data was prepared and MEPDG was run with the national calibration coefficients to predict performance over time. Comparisons of predicted performance at 3 reliability levels of 50, 85, and 95 percent for LTPP section 1007 are shown in Figure 169 through Figure 173. These figures illustrate the influence of using a design reliability upon predicted cracking, rutting and IRI. As the design reliability increases, predicted cracking, rutting, and IRI also increase.

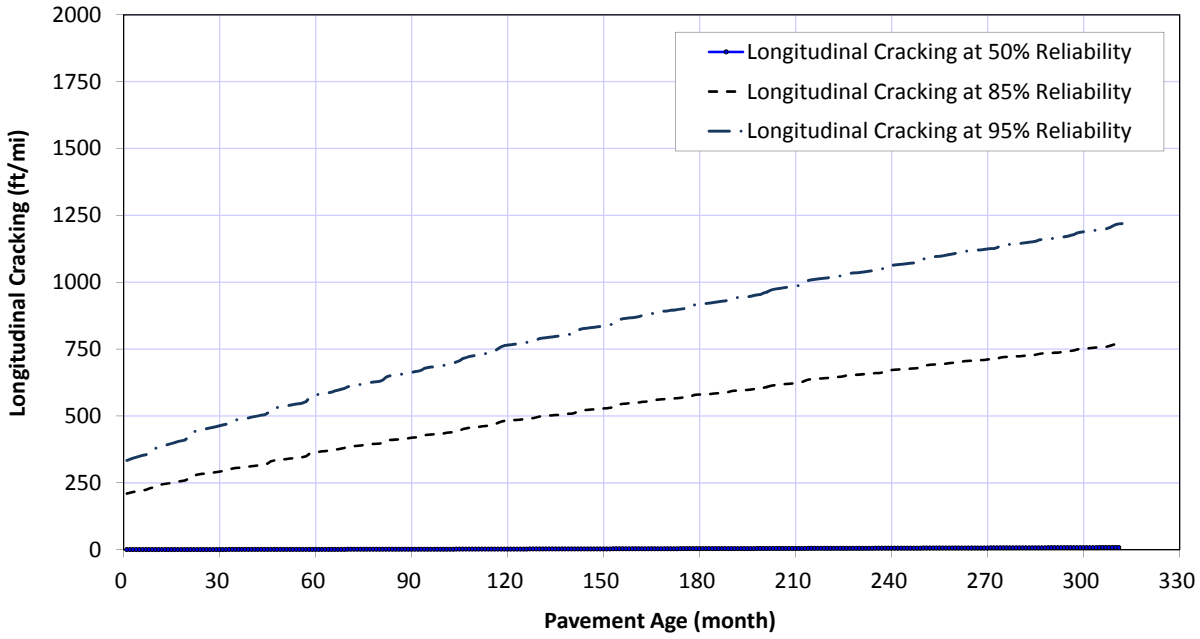

Figure 169. MEPDG Predicted Longitudinal Cracking at Different Reliability Levels for LTPP Section 1007

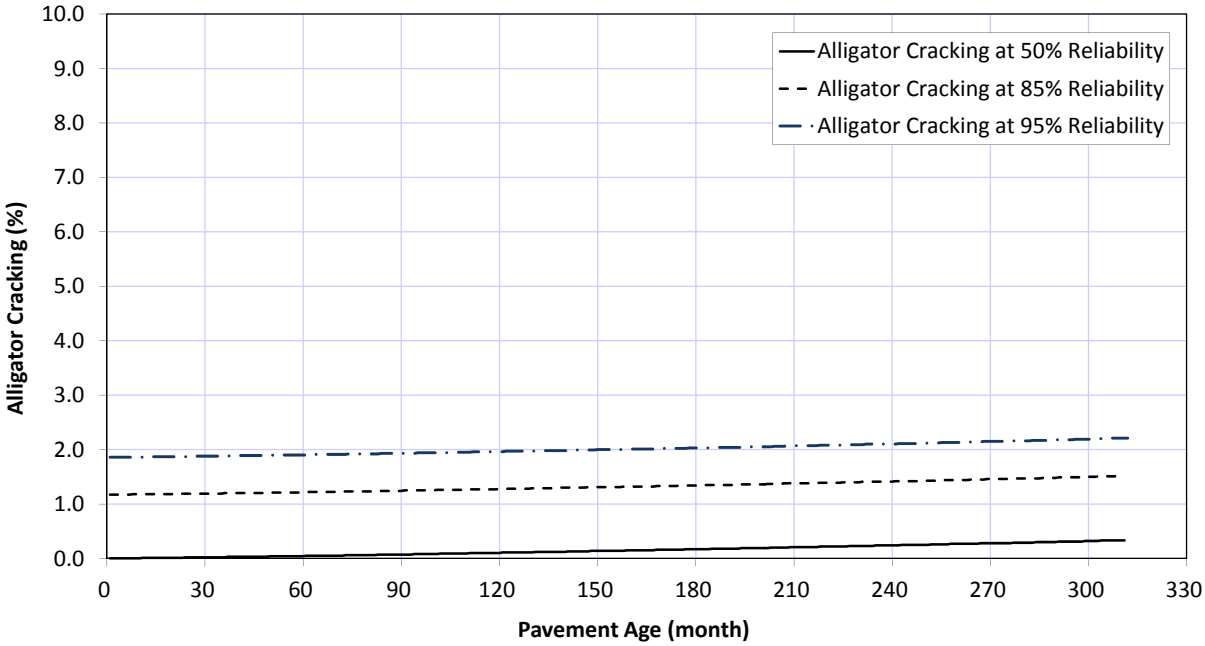

Figure 170. MEPDG Predicted Alligator Cracking at Different Reliability Levels for LTPP Section 1007

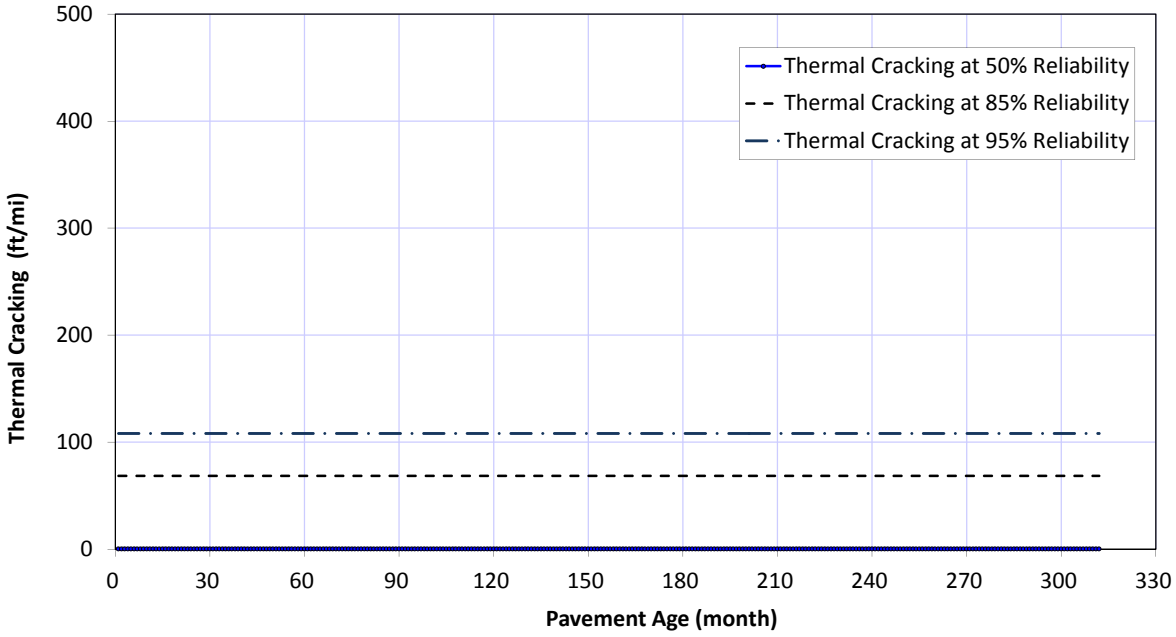

Figure 171. MEPDG Predicted Thermal Cracking at Different Reliability Levels for LTPP Section 1007

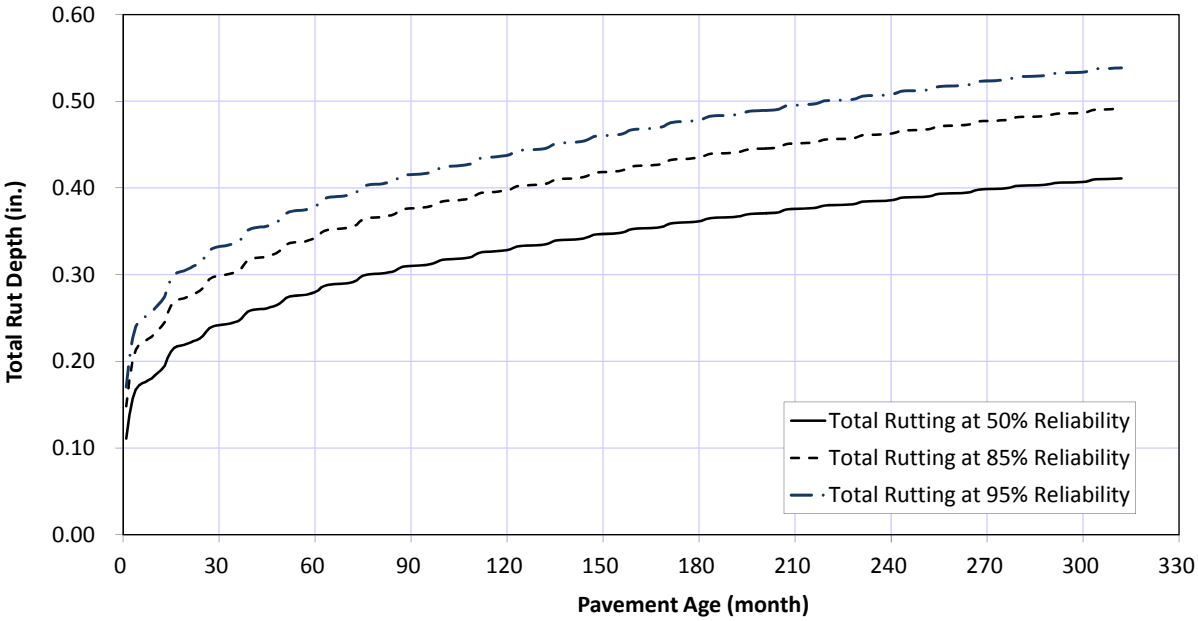

Figure 172. MEPDG Predicted Rutting at Different Reliability Levels for LTPP Section 1007

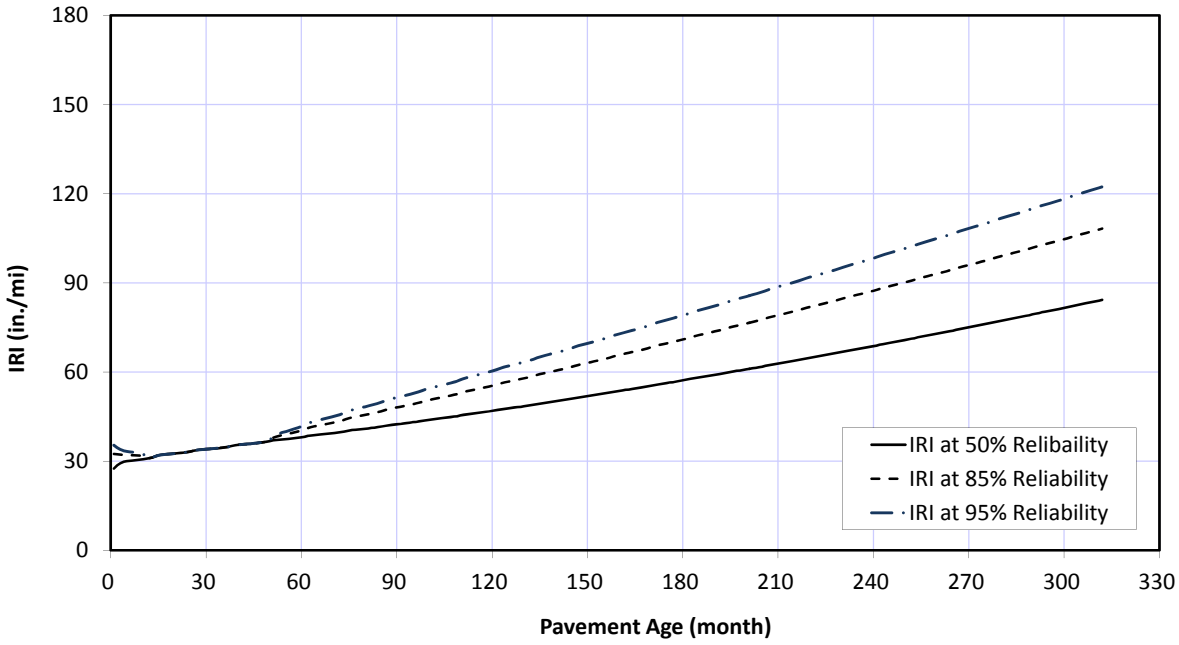

Figure 173. MEPDG Predicted IRI at Different Reliability Levels for LTPP Section 1007

Comparisons of predicted and measured longitudinal cracking, alligator cracking, and transverse cracking are shown in Figure 174 to Figure 176, respectively. Whereas Figure 177 and Figure 178 show measured versus predicted total rutting and IRI, respectively. Figure 174 to Figure 176 show that MEPDG predicted cracks are highly biased for all 3 types of cracks. Measured cracks are way more than MEPDG predicted cracks especially in case of transverse cracks. In fact MEPDG predicted 0 transverse cracks for most of the LTPP sections investigated in this study. Thermal cracking is dependent of the tensile strength and creep compliance properties of the asphalt mix. In all tested sections, these properties were not available and therefore level 3 data inputs were used. Hence, the prediction of 0 transverse cracking in these sections could be attributed to the use of level 3 data for tensile strength and creep compliance. Figure 177 show some bias at the high and low rutting values and some scatter at the low rutting values. The IRI comparison presented in Figure 178 shows highly biased IRI predictions at the low values and some scatter as well. These figures show that the national calibration coefficients do not represent Idaho conditions. Local calibration of MEPDG distress and IRI models should be performed. Thus, it is not feasible to investigate the current MEPDG reliability criteria and threshold values at this time.

In the meantime, it is suggested that ITD uses the current MEPDG recommended reliability levels and threshold values for distresses and IRI. Once distress and IRI models calibrated to Idaho conditions, these reliability levels and threshold values should be investigated and revised if warranted.

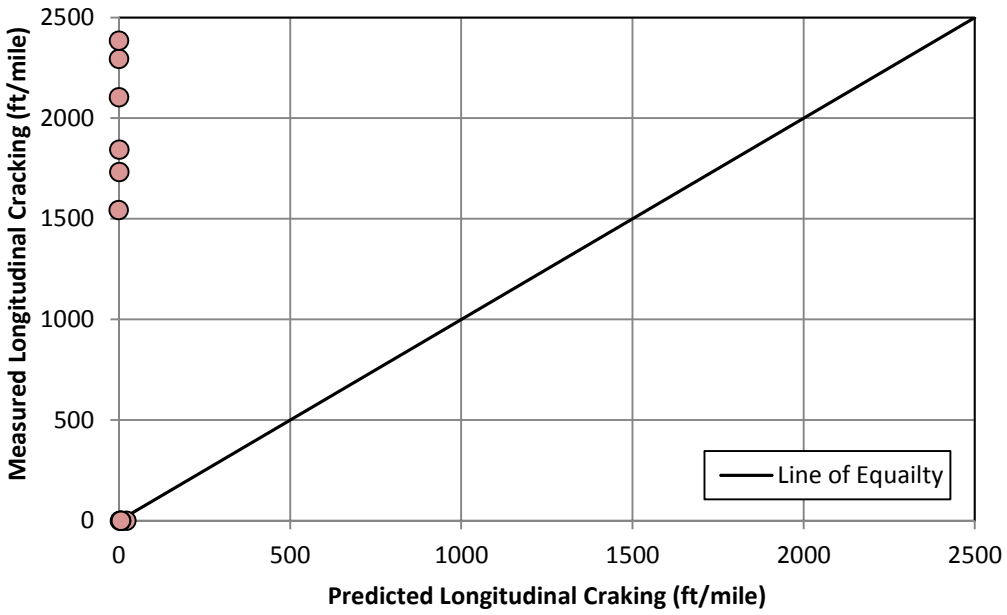

Figure 174. Comparison of Measured and Predicted Longitudinal Cracking

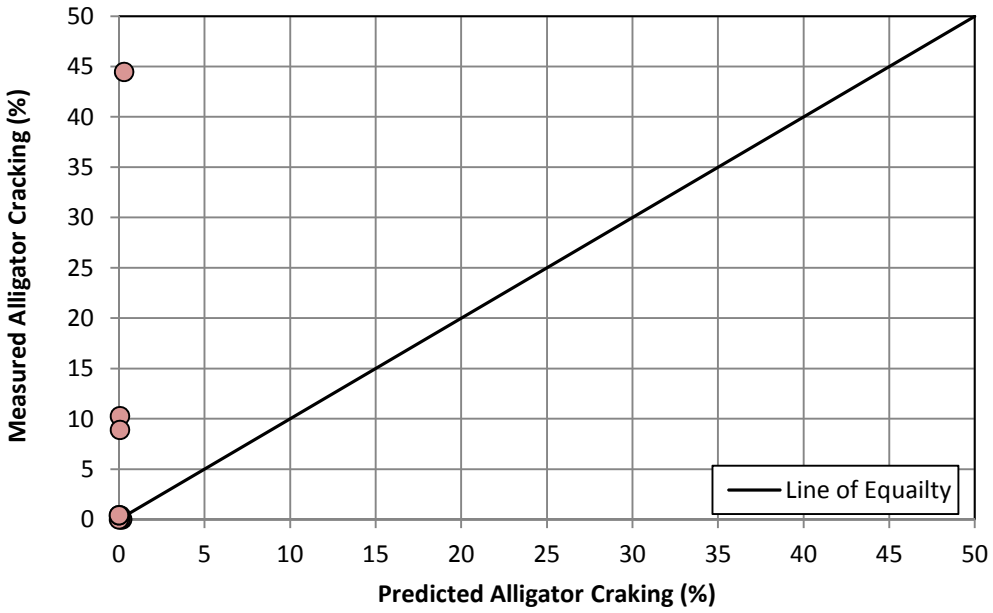

Figure 175. Comparison of Measured and Predicted Alligator Cracking

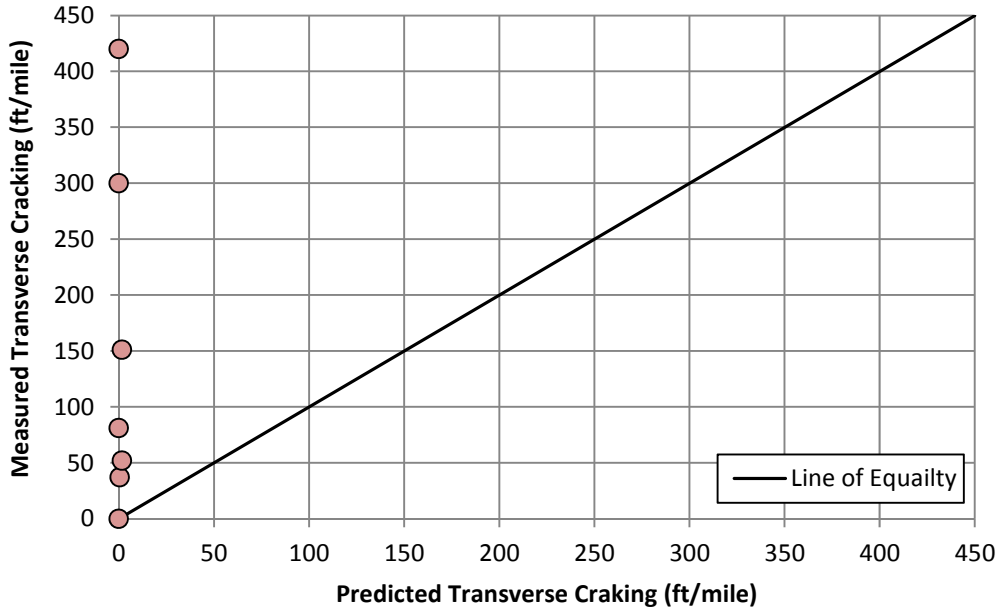

Figure 176. Comparison of Measured and Predicted Transverse Cracking

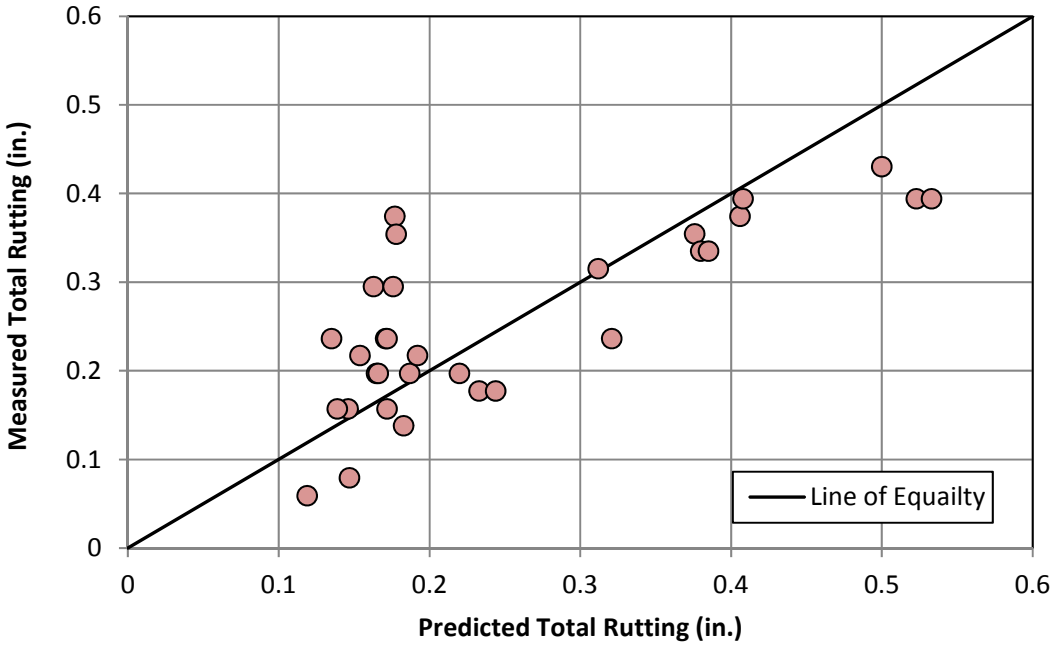

Figure 177. Comparison of Measured and Predicted Rutting

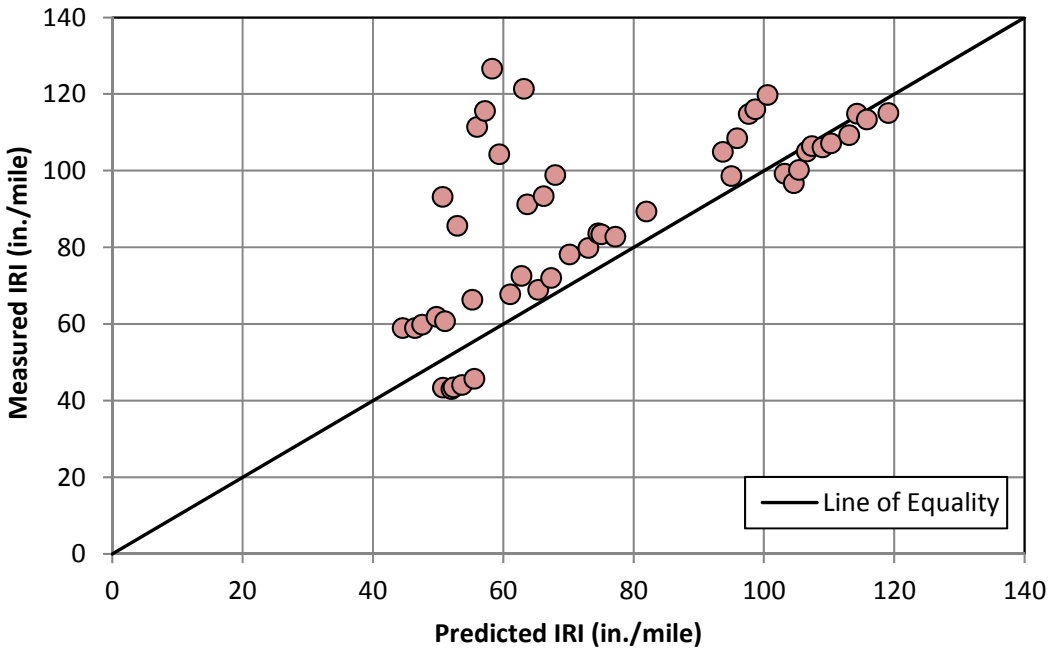

Figure 178. Comparison of Measured and Predicted IRI

Chapter 10
Local Calibration and Validation Plan

The current version of MEPDG contains pavement performance prediction models nationally calibrated using LTPP data distributed across the U.S. Results presented in the previous chapter showed that MEPDG national calibration coefficients yielded biased and inaccurate performance predictions, particularly for cracking, for Idaho conditions. Thus, for unbiased and more accurate MEPDG performance predictions, it is essential to develop local calibration coefficients. Well-calibrated performance models result in reliable pavement design and enable savings in maintenance and construction costs.

Calibration and Validation

The term calibration refers to mathematical process through which the total error (residual) or difference between observed and predicted values of distress in minimized.[100] Calibration of performance models can be done through reducing the bias and increasing the precision. Bias is defined as the systematic difference between observed and predicted performance. Precession is a measure of the closeness of predicted and observed performance. The concept of precision and bias is shown in Figure 179. The term validation refers to the process to confirm that the calibrated model can produce robust and accurate predictions for cases other than those used for model calibration.[100]

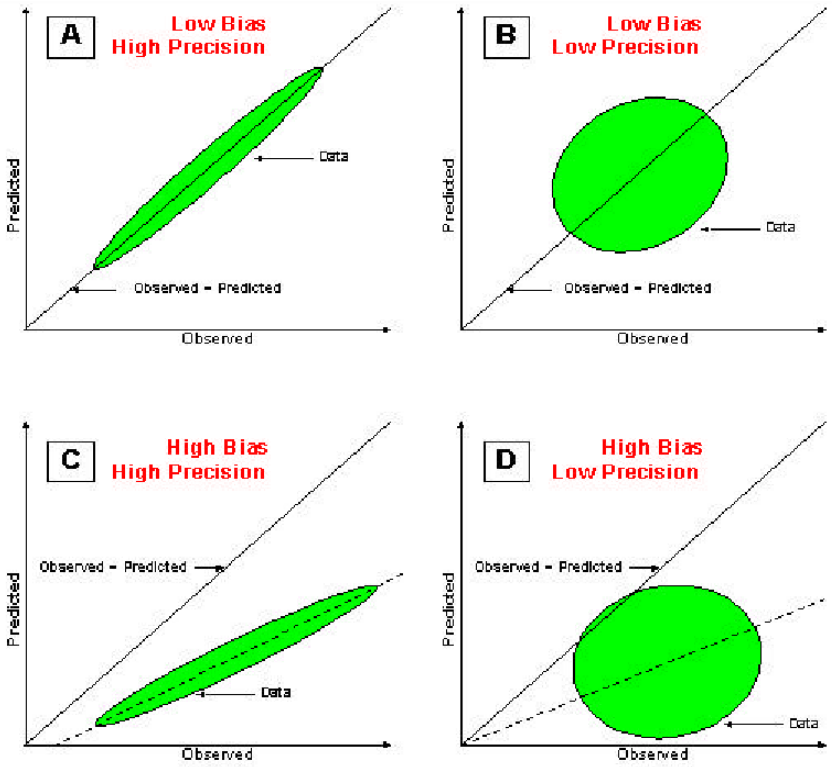

Figure 179. Precision and Bias[101]

Step by Step Plan for MEPDG Local Calibration and Validation

This section presents a plan for local calibration and validation of MEPDG for Idaho. This plan is based on guidelines presented in the Guide for the Local Calibration of MEPDG.[100] For all distress models and IRI, the developed plan consists of 11 steps. Description of these steps is presented in the subsequent sections.

Step 1: Hierarchical Input Level for Each Input Parameter

As previously presented, there are 3 hierarchical input levels in MPEDG. In Idaho, most of the MEPDG required input parameters are available at levels 2 and 3. Few inputs may be available at level 1 depending on the project. For example resilient modulus of subgrade is available at level 2. In-situ air voids, HMA creep compliance, indirect tensile strength, truck wander, and tire pressure are only available at level 3 (MEPDG default values). For some of the newer projects, HMA dynamic modulus and binder characterization data are available at level 1. In addition, for some sites, level 1 ALS, truck classification, truck volume, and monthly adjustment factors are available. Thus, it is recommended to use an appropriate mix of input levels (level 1 through level 3). The input level of each parameter should be consistent with ITD's day-to-day practices for characterizing pavement inputs for design.

Step 2: Experimental Factorial and Matrix or Sampling Template

Table 111 presents a sampling template suggested for selecting projects for local calibration and validation of MEPDG for Idaho. The simplified template is helpful is selecting different projects with diverse pavement structures, material types, and site conditions. It is recommended to include projects from all 6 districts in Idaho. This will ensure incorporating the different climatic characteristics and site conditions in the state. One may notice that, traffic and AC mix properties are not included directly in the sampling template. However, traffic is interrelated to the surface thickness and mix properties are interrelated to traffic. In addition, climate is interrelated to binder grade.

Table 111. Sampling Template for Local Calibration and Validation of Idaho Flexible Pavements

AC Thickness (in.)	Total Granular Base/Subbase Layer(s) Thickness (in.)	Subgrade Type					
		Coarse Subgrade			Fine Subgrade		
3 to 6	≤ 15						
	> 15						
> 6	≤ 15						
	> 15						

Step 3: Estimate Sample Size Required for Each Distress/IRI Model

For each distress and IRI model, both bias and precision are affected by the number of projects (sample size) used in the calibration process. Thus, it is important to determine the minimum number of projects required for each distress/IRI model calibration and validation. In order to determine the minimum number of projects it is important to know the model error, confidence level for statistical analysis, and threshold value at typical reliability level. In order to determine the number of projects for local calibration and validation of MEPDG performance models for Idaho, a 90 percent level of significance was assumed. The formula shown in Figure 180 was used to determine the minimum number of pavement sections required for each distress/IRI prediction model validation and local calibration.[23, 100]

$$n = \left(\frac{Z\alpha_{/2}\,\sigma}{e_t} \right)^2$$

$$e_t = Z\alpha_{/2} * S_e$$

where:

n = Minimum number of sections required for each distress/IRI prediction model validation and local calibration.
$Z\alpha_{/2} = 1.601$ for a 90 percent confidence interval.
σ = Performance indicator threshold (design criteria).
e_t = Tolerable bias at 90 percent reliability
S_e = Standard error of estimate.

Figure 180. Equation for Determination of Minimum Number of Samples for Local Calibration and Validation

Table 112 summarizes the minimum recommended number of pavement projects required for the local calibration and validation for each distress/IRI model. This table also presents the assumptions used in the computations. The threshold values shown in this table (σ) are based on recommendation form the MEPDG Manual of Practice.[6] The standard error of estimate for each distress/IRI model, shown in this table, is based on recommendations form the MEPDG Local Calibration Guide.[100] This table indicates that the minimum number of projects required for the IRI model calibration is 79 projects. This number is impractical. In MEPDG, IRI is a function of the other distresses. Thus, once cracking and rutting models are calibrated, the IRI model should yield reasonable predictions. It is then not necessary to use a large number of projects to calibrate the IRI model.

Table 112. Minimum Recommended Number of Pavement Projects for Local Calibration

Performance Indicator	σ	S_e	n
Alligator Cracking (%)	20	7	8
Longitudinal Cracking (ft/mile)	2000	600	11
Transverse Cracking, (ft/mile)	700	250	8
Rutting (in.)	0.4	0.1	16
IRI (in./mile)	160	18	79

To achieve this number of projects, LTPP and pavement projects from ITD's Pavement Management System (PMS) can be used. There are 7 LTPP (GPS-1) sections with complete data in Idaho. The rest of the projects can be recruited from the 6 districts in Idaho.

Step 4: Select Roadway Segments (Projects)

It is recommend that selected projects cover a range of distress values from poor to good conditions that are typical in Idaho. Each selected project should have at least 3 condition survey results in order to estimate the incremental increase in distress/IRI over time.[100] If available, it is recommended that the time history distress data represent at least a 10-year period.[100] This period is recommended to ensure that all time dependent material properties and the occurrence of distress are properly taken into account.

Step 5: Extract and Evaluate Distress and Project Data

Since projects from LTPP and ITD's PMS can be used it is important that distresses are measured in a consistent manner that is relevant to MEPDG. Because LTPP performance data was used in the national calibration effort of MEPDG, this data is compatible with MEPDG. ITD's total rutting and IRI survey methods are consistent with MEPDG predictions. On the other hand, ITD's cracking survey is different from LTPP method. Thus it is inconsistent with MEPDG cracking predictions. This is illustrated in Table 113.

It is suggested that ITD's implement the LTPP stress identification method so that distresses are compatible with MEPDG.[102] Thus, direct calibration and validation of the distress models can be done. Fortunately, since 1995 ITD's started collecting distress survey data using Pathway© profiler van technology.[104] Profiler vans drive the pavement and produce digital images (video files) of the pavement surface across the width and length of the roadway segment being evaluated. These video files can be used to conduct condition surveys compatible with MEPDG for projects selected for local calibration and validation.

Table 113. Comparison of ITD and LTPP Cracking Severity, Extent, and Measurement Method[102, 103]

Topic	ITD Definition	LTPP Definition
Alligator Cracking		
Low Severity	**Slight Severity:** Smaller than 1 ft in size	An area of cracks with no or only a few connecting cracks; cracks are not spalled or sealed; pumping is not evident.
Moderate Severity	**Moderate Severity:** 1 ft to 2 ft in size	An area of interconnected cracks forming a complete pattern; cracks may be slightly spalled; cracks may be sealed; pumping is not evident.
High Severity	**Heavy Severity:** 3 ft or more in size	An area of moderately or severely spalled interconnected cracks forming a complete pattern; pieces may move when subjected to traffic; cracks may be sealed; pumping may be evident.
Measurement	**Light Extent:** 10% or less of the total evaluation section having cracking. **Moderate Extent:** 10-40% of the total evaluation section having cracking. **Heavy Extent:** more than 40% of the total evaluation section having cracking.	Record square meters of affected area at each severity level.
Longitudinal Cracking		
Low Severity	Crack width is hairline up to 1/8".	Crack mean width is hairline up to ¼" or a sealed crack with sealant material in good condition and with a width that cannot be determined.
Moderate Severity	Crack width is 1/8" to ¼" or there is a dip 3" to 6" wide at the crack.	Any crack with a mean width > ¼" and ≤ ¾"; or any crack with a mean width ≤ ¾" and adjacent low severity random cracking.
High Severity	Crack width is more than ¼" or there is a distinct dip of 6" to 8" wide or there is vegetation in the crack.	Any crack with a mean width > ¾" or any crack with a mean width ≤ ¾" and adjacent moderate to high severity random cracking.
Measurement	**Light Extent:** 100 ft or less of cracking per 500 ft. **Moderate Extent**: 100-500 ft of cracking per 500 ft. **Heavy Extent:** more than 500 ft of cracking per 50 0ft.	Record separately the length in meters of longitudinal cracking in and outside the wheel path at each severity level. Record separately the length in meters of longitudinal cracking with sealant in good condition in and outside the wheel path at each severity level.
Transverse (Thermal) Cracking		
Low Severity	Crack width is hairline up to 1/8".	Crack mean width is hairline up to ¼", or a sealed crack with sealant material in good condition and with a width that cannot be determined.
Moderate Severity	Crack width is 1/8" to ¼" or there is a dip 3" to 6" wide at the crack.	Any crack with a mean width > ¼" and ≤ ¾"; or any crack with a mean width ≤ ¾" and adjacent low severity random cracking.
High Severity	Crack width is more than ¼" or there is a distinct dip of 6" to 8" wide or there is vegetation in the crack.	Any crack with a mean width > ¾"; or any crack with a mean width ≤ ¾" and adjacent moderate to high severity random cracking.
Measurement	**Light Extent:** 1-4 cracks per 500 ft. **Moderate Extent:** 4-10 cracks per 500 ft. **Heavy Extent:** more than 10 cracks in 500ft, or less than 50 ft in between cracks.	Record number and length of transverse cracks at each severity level. Also record length in meters of transverse cracks with sealant in good condition at each severity level.

Before using any field measured distress and IRI data, this data should be reviewed and evaluated to determine any anomalies and outliers. Once data are filtered from any anomalies and outliers it can be used in the calibration. For the selected projects, all required input data should be extracted. Data sources contain construction records, acceptance tests in quality assurance program, as-built construction plans and PMS.

Step 6: Conduct Field and Forensic Investigations

For Idaho local calibration effort, LTPP database and ITD's PMS data can be used. No field or forensic investigations are warranted.

Step 7: Assess Local Bias: Validation of Global Calibration Values to Local Condition

Run MEPDG with the global (national) calibration coefficients to predict performance. These runs should be performed at 50 percent reliability level. Compare predicted performance to measured performance to determine bias and standard error of estimate (S_e). This is to validate each distress prediction model for local conditions. Perform linear regression between measured and predicted distresses and IRI. Then evaluate the bias by performing the following hypothesis testing:

- Hypothesis 1: there is no bias or systematic difference between measured and predicted distresses/IRI.
- Hypothesis 2: the linear regression model developed using measured and predicted distresses/IRI has an intercept of 0.
- Hypothesis 3: the linear regression model developed using measured and predicted distresses/IRI has a slope of 1.

A rejection of any of the 3 hypotheses indicates bias in the predicted distresses/IRI. Passing all 3 hypotheses means no bias in the predictions.

Step 8: Eliminate Local Bias of Distress and IRI Prediction Models

If the previous step showed that any of the distress/IRI models yield biased predictions, this bias has to be eliminated. This can be done by developing local calibration coefficients for the biased models. Recommendations for the flexible pavement transfer function calibration parameters to be adjusted for eliminating the bias are given in Table 114.

Table 114. Recommendations for the Flexible Pavement Transfer Function Calibration Parameters to be Adjusted for Eliminating Bias[100]

Distress		Eliminate Bias
Total Rutting	HMA and Unbound Materials Layers	K_{r1}, β_{s1}, β_{r1}
Load Related Cracking	Alligator Cracking	C_2, K_{f1}
	Longitudinal Cracking	C_2, K_{f1}
	Semi-Rigid Pavements	C_2, β_{c1}
Non-Load Related Cracking	Transverse Cracking	β_{f3}
Roughness, IRI		C_4

Step 9: Assess the Standard Error of the Estimate

Compare the standard error determined from the data collected for calibration to the standard error from the national calibration effort. Perform statistical hypothesis testing to assess if there is no significant difference between the standard error for the national and local calibration.

Step 10: Reduce Standard Error of the Estimate

If statistical analysis in the previous step resulted in a significant difference between national and local calibration, local calibration factors should be re-adjusted. Recommendations for the flexible pavement transfer function calibration parameters to be adjusted for reducing the standard error are given in Table 115.

Table 115. Recommendations for the Flexible Pavement Transfer Function Calibration Parameters to be Adjusted for Reducing the Standard Error[100]

Distress		Reduce Standard Error
Total Rutting	HMA and Unbound Materials Layers	K_{r2}, K_{r3}, and β_{r2}, β_{r3}
Load Related Cracking	Alligator Cracking	K_{f2}, K_{f3}, and C_1
	Longitudinal Cracking	K_{f2}, K_{f3}, and C_1
	Semi-Rigid Pavements	C_1, C_2, C_4
Non-Load Related Cracking	Transverse Cracking	β_{f3}
Roughness, IRI		C_1, C_2, C_3

Step 11: Interpretation of Results, Deciding on Adequacy of Calibration Parameters

Run MEPDG at different design reliability levels to evaluate the standard error of estimate of the locally adjusted distress/IRI models. Evaluate if locally calibrated models produce reasonable design life at the reliability level of interest. If this is the case, the local calibration factors can be implemented. If not, the developed local calibration factors should be re-adjusted. This can be done by adding more projects to the calibration-validation projects, using more level 1 input parameters, and performing field forensic investigation.

Chapter 11
Summary, Conclusions, and Recommendations

Summary

The Mechanistic-Empirical Pavement Design Guide developed under the NCHRP Project 1-37A was originally released in 2004. This design guide uses mechanistic-empirical numerical models to analyze input data related to material, traffic, and climate to estimate damage accumulation over service life. This study was conducted to assist ITD in the implementation of MEPDG for flexible pavements. A thorough literature review of other state agencies, with focus on Idaho neighboring states, implementation efforts was conducted. Based on the presented review of the SHAs implementation and calibration activities of the MEPDG it was found that, for successful MEPDG implementation, a comprehensive input database (input libraries) for material characterization, traffic, and climate should be established. Distress/IRI prediction models should be locally calibrated based on the state conditions. Defining the sensitivity of each input as well as establishing reasonable ranges based on local conditions for each design key inputs are important. Finally, training pavement designers on the software is a very important task toward a successful MEPDG implementation.

The main research work in this study focused on establishing materials, traffic, and climatic database for Idaho MEPDG implementation. The primary HMA material input parameter, E*, was measured in the laboratory on 27 plant-produced mixes procured from various locations in Idaho. The mixes covered wide range of those typically used in Idaho for all Superpave specifications (SP1 to SP6). Gyratory Stability values of the tested mixes were also determined. DSR and Brookfield tests were also performed on 9 typical Superpave binder performance grades. For the tested mixtures and binders, level 1 and level 3 input data required by MEPDG were established. The influence of the binder characterization input level on the accuracy of MEPDG predicted E* was investigated. Based on the measured E* data, the prediction accuracy of the 1-37A η-based Witczak Model, 1-40D-G* based Witczak model, Hirsch model, and GS-based Idaho model was investigated.

For unbound materials, a total of 8233 historical R-value results along with routine material properties for Idaho unbound materials and subgrade soils were used to develop levels 2 and 3 unbound material characterization. For level 2 subgrade material characterization, 2 models were developed. First, a multiple regression model can be used to predict R-value as a function of the soil PI and percent passing No 200 sieve. Second, a M_r predictive model based on the estimated R-value of the soil was developed using literature M_r values measured in the laboratory. Hence, the models can be used to estimate the Mr value based on level 2 data input in the MEPDG. For level 3 unbound granular materials and subgrade soils, typical default average values and ranges for R-value, PI, and LL were developed.

For MEPDG traffic characterization, 12 to 24 months of classification and weight traffic data from 25 WIM sites in Idaho were analyzed. Level 1 ALS and traffic input parameters required by MEPDG were

established. Statewide and regional ALS and traffic adjustment factors were also developed. The impact of the traffic input level on MEPDG predicted performance was also studied.

Based on this research work, a master database for MEPDG required inputs was created. This database contains MEPDG key inputs related to materials, traffic, and climate. The developed database is stored in a simple user-friendly spreadsheet for quick and easy access of data.

Sensitivity of MEPDG predicted performance in terms of cracking, rutting, and IRI to key input parameters was conducted as part of this study. MEPDG recommended design reliability levels and criteria were investigated. Finally, a plan for local calibration and validation of MEPDG distress/IRI prediction models for Idaho conditions was established.

Conclusions

Based upon the results and analyses presented in this research, the following observations and conclusions are established:

- To facilitate MEPDG implementation in Idaho, a master database containing MEPDG required key inputs related to materials, traffic, and climate was created. This database is stored in a user-friendly spreadsheet with simple macros for quick and easy access of data.
- Based on the comparison of the overall prediction accuracy and bias of the 2 MEPDG Witczak E* prediction models (NCHRP 1-37A η-based and NCHRP 1-40D G*-based) along with the investigated 5 binder characterization cases the following conclusions are found:
    1. Overall, E* predicted from the 2 MEPDG models when using the 5 binder characterization cases showed bias and scatter in E* predictions especially at the higher and lower temperatures.
    2. The NCHRP 1-37A η-based E* predictive model along with cases 1, 2, 4, and 5 binder characterization produced relatively higher biased and less accurate E* estimates, compared to case 3 especially at the highest and lowest temperatures.
    3. Among the 5 binder characterization cases, the 1-40D G*-based E* predictive model along with case 1 binder characterization produced the best E* estimates based on the goodness of fit statistics. However, at the higher and lower temperatures, this model shows highly significant biased E* estimates.
    4. The NCHARP 1-40D G*-based E* model along with cases 2 and 4 binder characterization was found to slightly underestimate E* at low temperatures and highly overestimate E* at high temperatures. This model along with cases 3 and 5 binder characterization was found to significantly overestimate E* values at all temperatures.

5. The NCHRP 1-37A η-based E* model along with level 3 binder characterization (case 3) is the least biased methodology for E* prediction among the incorporated MEPDG E* models. However, this model was found to overestimate E* at the high temperatures.

- Based on the comparison of the overall prediction accuracy and bias of the MEPDG E* predictive models along with Hirsch and Idaho GS-based E* models, the following conclusions are found:

    1. In general, both Hirsch and MEPDG models significantly overestimate E* of the Idaho mixtures at the higher temperature regime.

    2. The GS-based Idaho E* predictive model predicts E* values that are in excellent agreement with the measured ones (S_e/S_y = 0.24 and R2 = 0.94). Among the 4 investigated models, the GS-based E* model was found to yield the lowest bias and highest accuracy in prediction.

- Two simple models for use in MEPDG level 2 inputs for subgrade soils characterization were developed. The first model estimates the R-value of the soil as a function of percent passing No 200 sieve and PI when direct laboratory measurement of the R-value is unavailable. The second model estimates the M_r from the R-value. The following conclusions and recommendations are made:

    1. The AI equation currently used for computation of M_r from R-value in the MEPDG for level 2 subgrade material characterization overestimates the resilient modulus.

    2. The literature M_r-R models investigated in this research significantly over or under estimate the modulus values.

    3. The proposed models yield better results compared to the current AI model used in MEPDG as well as other literature models.

    4. The developed M_r-R model allows the use of level 2 design input for the MEPDG subgrade material characterization.

- The following conclusions are made based on the analyses of Idaho WIM traffic data:

    1. For MEPDG traffic characterization, 12 to 24 months of classification and weight traffic data from 25 WIM sites in Idaho were analyzed using the *TrafLoad* software. Among the 25 sites, only 21 sites possessed enough classification data to produce level 1 traffic inputs for MEPDG. Only 14 WIM sites were found to have weight data that comply with the FHWA recommended procedure.

    2. The investigated data showed an average directional distribution and lane factors of 0.56±0.05 and 0.93±0.03 for the 4-lane roadways. These values agree quit well with the MEPDG recommended default values.

3. In general, class 9 followed by class 5 trucks represented the majority of the trucks travelling on Idaho roads.

4. The number of single, tandem, and tridem axles per truck for all truck classes based on Idaho data was found quite similar to MEPDG default values. Idaho data showed few percentages of quad axles for truck classes 7, 10, 11, and 13 compared to MEPDG default values which are all 0.

5. Statewide ALS and 3 TWRGs ALS were developed for Idaho based on the analysis of the weight data from the 14 WIM sites. The TWRGs were developed based on the similarity in the shape of the tandem axle load spectra of class 9 trucks.

6. The developed statewide axle load spectra yielded significantly higher longitudinal and alligator cracking compared to MEPDG default spectra. No significant difference was found in predicted AC rutting, total rutting, and IRI based on statewide and MEPDG default spectra.

7. High prediction errors were found for longitudinal cracking when statewide/national (level 3) axle load spectra, VCD, or MAF were used instead of site-specific (level 1) data.

8. Large prediction errors in alligator cracking were only found when statewide default ALS were used compared to site-specific spectra. Moderate errors were found when MEPDG typical default MAF or VCD were used instead of site-specific values.

9. The input level of the axle load spectra, MAF, VCD, and number of axles per truck had very low impact on predicted AC rutting and negligible impact on total rutting and IRI.

10. The input level of the number of axles per truck had negligible influence on MEPDG predicted performance.

- Based on the conducted sensitivity analyses the following conclusions are observed:

1. Longitudinal cracking was found extremely sensitive to most of the investigated parameters. These parameters are related to the HMA layer thickness and properties, base layer thickness, subgrade strength, traffic, and climate.

2. No thermal cracking was predicted for most of the performed MEPDG runs. This is attributed to the use of level 3 data inputs for tensile strength and creep compliance properties of the asphalt mixes. These properties directly affect thermal cracking of asphalt pavement.

3. Alligator cracking and total rutting were found mostly sensitive to extremely sensitive to most of the investigated parameters.

4. IRI was not sensitive to the majority of the parameters investigated in this study.

5. Among all investigated parameters, traffic volume (AADTT) was found to be the most influencing input on MEPDG predicted distresses and IRI.

- Analysis of LTPP projects in Idaho showed that MEPDG yielded highly biased predictions especially for cracking. Thus until these models are re-calibrated to Idaho conditions; the current MEPDG design reliability criteria cannot be examined.
- A plan for local calibration and validation of MEPDG distress and IRI models for Idaho conditions was developed. This plan closely follows the AASHTO Local Calibration Guide for MEPDG.

Recommendations

Based on the findings of this research the following are recommended:

- Based on the evaluation of level 1 and MEPDG level 3 E* predictions, MEPDG level 3 is not recommended to characterize Idaho HMA mixtures replacing level 1 due to the highly biased predictions especially at the high temperature values.
- Use Idaho GS-based E* predictive model for characterizing ITD HMA mixtures. This model can be used to predict E* at temperatures and frequencies of interest and then input these predicted values into MEPDG replacing the measured E* values as level 1.
- At least, 3 years of traffic data from WIM sites in Idaho should be analyzed to produce traffic data for MEPDG. This analysis should be performed every 3 to 5 years to ensure accurate traffic data. Such analysis should distinguish WIM sites based on similarities in axle load spectra. One way to do that is to develop Truck Road Weight Groups (TRWG) as per MEPDG guidelines.
- As the AADTT was found to be the most significant factor affecting MEPDG predicted distresses and IRI, every effort should be made to accurately determine this parameter.
- To ensure consistency with MEPDG distress prediction, it is recommended that ITD perform pavement condition surveys and update their distress survey method in accordance with LTPP method of data collection.
- Calibrate MEPDG distress/IRI prediction models to Idaho conditions.
- It is recommended that ITD use the current MEPDG design criteria and the associated design reliability values until local calibration of MEPDG distress/IRI models for Idaho conditions is performed. Once the models are locally re-calibrated, MEPDG recommended design criteria and reliability levels should be investigated.

References

1. **American Association of State Highways and Transportation Officials.** *AASHTO Guide for Design of Pavement Structures*, Washington, D.C: American Association of State Highways and Transportation Officials, 1993.
2. **Crawford, G.** "National Update of MEPDG Activities," *88th Annual TRB Meeting*, Washington, D.C.: Transportation Research Board, 2009.
3. **Federal Highway Administration.** *LTPP: Year in Review 2004.* Publication No: FHWA-HRT-04-125, U.S. Department of Transportation, Federal Highway Administration, 2004. http://www.fhwa.dot.gov/publications/research/infrastructure/pavements/ltpp/reports/04125/04125.pdf (Accessed on December, 2009).
4. **ARA, Inc., ERES Consultants Division**. *Guide for Mechanistic-Empirical Design of New and Rehabilitated Pavement Structures*. Prepared for National Cooperative Highway Research Program, NCHRP 1-37A Final Report, Washington, D.C.: March 2004.
5. **National Cooperative Highway Research Program.** *Mechanistic-Empirical Pavement Design Guide of New and Rehabilitated Pavement Structures.* Version 1.10, built August 31, 2009, NCHRP 1-37A Project, http://onlinepubs.trb.org/mepdg, (Accessed, December 2009).
6. **American Association of State Highways and Transportation Officials.** *Mechanistic-Empirical Pavement Design Guide: A Manual of Practice*. Interim Edition, American Association of Highways and Transportation Officials, July 2008.
7. **Schwartz, C.** *Implementation of the NCHRP 1-37A Design Guide.* Final Report, Volume 1: Summary of Findings and Implementation Plan, MDSHA SP0077B41, University of Maryland, College Park, MD, 2007. http://design.transportation.org/Documents/MDSHASummaryofFindingsandImplementationPlan-Volume1.pdf (Accessed on January, 2010)
8. **El-Basyouny, M.** *Calibration and Validation of Asphalt Concrete Pavements Distress Models for 2002 Design Guide* Ph.D. Dissertation, Arizona State University, Tempe, AZ, 2004.
9. **Witczak, M., S. El-Badawy S., and M. El-Basyouny.** *MEPDG Predictive Cracking Model Adjustment* Inter Team Technical Report, Arizona State University, Tempe, AZ, 2006.
10. **National Cooperative Highway Research Program.** *Release Notes for Version 1.10*, December 2009. http://onlinepubs.trb.org/onlinepubs/archive/mepdg/software.htm, (Accessed on December 2009).
11. **Witczak, M., M. El-Basyouny, M. Jeong, and S. El-Badawy.** *Final Revised Section Calibration Data for Asphalt Surfaced Pavement Recalibration under NCHRP 1-40D.* Inter Team Technical Report, Arizona State University, Tempe, AZ, 2007.
12. **Witczak, M., S. El-Badawy S., and M. El-Basyouny.** *Incorporation of the New (2005) E* Predictive Model in the MEPDG*. Inter Team Technical Report, Arizona State University, Tempe, AZ, 2006.
13. **Witczak, M., S. El-Badawy S., and M. El-Basyouny.** *Incorporation of Fatigue Endurance Limits into*

the MEPDG Analysis. Inter Team Technical Report, Arizona State University, Tempe, AZ, 2006.

14. **Witczak, M., C. Zapata, and M. El-Basyouny.** *Selection of Appropriate Resilient Modulus at Optimum Condition to be Used as a Design Input Parameter in the ME-PDG*. Inter Team Technical Report. Arizona State University, Tempe, AZ, 2006.
15. **Witczak, M., C. Zapata, and W. N. Houston.** *Models Incorporated into the Current Enhanced Integrated Climatic Model for Use in Version 1.0 of the ME-PDG (NCHRP 9-23 Project Findings and Additional Changes after Version 0.7)*. Inter Team Technical Report. Arizona State University, Tempe, AZ, 2006.
16. **Bari, J.** *Development of a New Revised Version of the Witczak E* Predictive Models for Hot Mix Asphalt Mixtures*. Ph.D. Dissertation, Arizona State University, Tempe, AZ, 2005.
17. **Bari, J., and M. Witczak. "**Development of a New Revised Version of the Witczak E* Predictive Models for Hot Mix Asphalt Mixtures*." Journal of the Association of Asphalt Paving Technologists,* Vol. 75 (2006): 381-417.
18. **Darter, M., J, Mallela, L. Titus-Glover, C. Rao, G. Larson, A. Gotlig, H. Von Quintus, L. Khazanovich, M. Witczak, M. El-Basyouny, S. El-Badawy, A. Zborowski, and C. Zapata.** *Research Results Digest 308: Changes to the Mechanistic-Empirical Pavement Design Guide Software through Version 0.900*. National Cooperative Highway Research Program, Transportation Research Board of the National Academies, September 2006. http://onlinepubs.trb.org/onlinepubs/nchrp/nchrp_rrd_308.pdf (Accessed on January, 2010)
19. **Brown, S.,** "Roadmap for Future Research on the Mechanistic Empirical Pavement Design Guide." *Journal of the Association of Asphalt Paving Technologists*, Vol. 77 (2008): 1037-1052.
20. **Federal Highway Administration.** *Lead States Group for the Implementation of Mechanistic-Empirical Pavement Design Guide.* U.S. Department of Transportation, Federal Highway Administration. http://www.fhwa.dot.gov/pavement/dgit/leadstates/leadstatesflyer.pdf (Accessed on December, 2009).
21. **Wagner, C.** *AASHTO MEPDG - What's in it for you?* Power Point Presentation at North Central Asphalt User/Producer Group, Springfield, Illinois, (January 2007). http://cobweb.ecn.purdue.edu/~spave/NCAUPG/Activities/2008/presentations/ (Accessed on March, 2010).
22. **Federal Highway Administration, Office of Pavement Technology,** *Design Guide Implementation Survey*. Washington, D.C.: Washington, D. C.: Federal Highway Administration, Office of Pavement Technology, 2004. http://www.fhwa.dot.gov/pavement/dgit/dgitsurvey.pdf. (Accessed on March, 2010).
23. **Darter, M., L. Titus-Glover, and H., Von Quintus.** *Implementation of the Mechanistic-Empirical Pavement Design Guide in Utah: Validation, Calibration, and Development of the UDOT MEPDG User's Guide*. Report No. UT-09.11, Applied Research Associates, Inc., 2009. http://utah.ptfs.com/awweb/main.jsp?flag=browse&smd=1&awdid=1, (Accesses on January, 2010).
24. **Darter, M., L. Titus-Glover, and H., Von Quintus.** *Draft User's Guide for UDOT Mechanistic-*

Empirical Pavement Design Guide. Report No. UT-09.11a, Applied Research Associates, Inc., 2009. http://utah.ptfs.com/awweb/main.jsp?flag=collection&smd=1&cl=all_lib&lb_document_id=27346 (Accessed on January, 2010).

25. **Von Quintus, H. and J. Moulthrop.** *Mechanistic-Empirical Pavement Design Guide Flexible Pavement Performance Prediction Models for Montana: Volume I Executive Research Summary*. FHWA/MT-07-008/8158-1 Final Report, 2007. http://www.archive.org/details/664B4642-A369-476C-BB5E-6196988FC74E, (Accessed on January, 2010).
26. **Von Quintus, H. and J. Moulthrop.** *Mechanistic-Empirical Pavement Design Guide Flexible Pavement Performance Prediction Models for Montana: Volume II Reference Manual*. *FHWA/MT-07-008/8158-1* Final Report, 2007.
27. **Von Quintus, H. and J. Moulthrop.** *Mechanistic-Empirical Pavement Design Guide Flexible Pavement Performance Prediction Models for Montana: Volume III Field Guide.* FHWA/MT-07-008/8158-1 Final Report, 2007.
28. **Witczak, M., El-Basyouny M., and S. El-Badawy.** Incorporation of NCHRP 1-40B HMA Permanent Deformation Model into NCHRP 1-40D," Inter Team Technical Report, Arizona State University, Tempe, AZ, 2006.
29. **Li, J., L. Pierce, and J. Uhlmeryer.** "Calibration of Flexible Pavement in Mechanistic-Empirical Pavement Design Guide for Washington State." *Transportation Research Board, Journal of the Transportation Research Board*, No. 2095 (2009): 73-83.
30. **Li, J., L. Pierce, M. Hallenbeck, and J. Uhlmeryer.,** "Sensitivity of Axle Load Spectra in the Mechanistic-Empirical Pavement Design Guide for Flexible Pavement Design." *Transportation Research Board, Journal of the Transportation Research Board*, No. 2093 (2009): 50-56.
31. **Elkins, L., and C. Higgins.** *Development of Truck Axle Spectra from Oregon Wight-In-Motion Data for Used in Pavement Design and Analysis.* SPR 635, FHWA-OR-RD-08-06 Final Report, Oregon State University, Corvallis, Oregon, 2008.
32. **Lu, Q., Y. Zhang, and J. Harvey.** "Evaluation of Truck Traffic Inputs for Mechanistic-Empirical Pavement Design in California," *Transportation Research Board, Journal of the Transportation Research Board*, No. 2095 (2009): 62-72.
33. **Witczak, M.,** *Development of Performance Related Specifications for Asphalt Pavements in the State of Arizona*. Final Report 402-2, Prepared for the Arizona Department of Transportation, Phoenix, AZ, May 2008. http://www.azdot.gov/TPD/ATRC/Publications/project_reports/PDF/AZ402-2.pdf (Accessed on February, 2010).
34. **Souliman, M.** *Calibration of the AASHTO MEPDG for Flexible Pavements for Arizona Conditions*. Master's Thesis, Arizona State University, Tempe, AZ, 2009.
35. **Hall, K., S. Beam, and M. Lee.** *AASHTO 2002 Pavement Design Guide Design Inputs Evaluation Study*. TRC-0302 Final Report, University of Arkansas, Fayetteville, AR, 2006.
36. **Tran, N., and K. Hall.** *Projected Traffic Loading for Mechanistic-Empirical pavement Design Guide.* TRC-0402 Final Report, University of Arkansas, Fayetteville, AR, 2006.

37. **Tran, N., and K. Hall.** "Development and Significance of Statewide Volume Adjustment Factors in Mechanistic Pavement Design Guide." *Transportation Research Board, Journal of the Transportation Research Board*, No. 2037 (2007): 97-105.

38. **Tran, N., and K. Hall.** "Development and Influence of Statewide Axle Load Spectra on Flexible Pavement Performance." *Transportation Research Board, Journal of the Transportation Research Board*, No. 2037 (2007): 106-114.

39. **Wang, K., K. Hall, Q. Li, V. Nguyen, and W. Gong, W.** *Database Support for the Mechanistic-Empirical Pavement Design Guide (MEPDG)*. TRC-0702 Final Report, University of Arkansas, Fayetteville, AR, 2009.

40. **Wang, K., K. Hall, Q. Li, V. Nguyen, and W. Gong, W.** "Database Support for the Mechanistic-Empirical Pavement Design Guide." *Transportation Research Board, Journal of the Transportation Research Board*, No. 2087 (2008): 109-119.

41. **Hall, K., D. Xiao, and K. Wang.** "Calibration of the MEPDG for Flexible Pavement Design in Arkansas." Paper No. 11-3562, TRB 90th Annual Meeting Compendium of Papers CD-ROM, 2011.

42. **Coree, B., H. Ceylan, and D. Harrington.** *Implementing the Mechanistic-Empirical Pavement Design Guide.* Technical Report, IHRB Project TR-509, Iowa State University, Ames, IA, 2005.

43. **Coree, B., H. Ceylan, and D. Harrington.** "Sensitivity Study of Iowa Flexible Pavements Using Mechanistic-Empirical Pavement Design Guide," Paper No. 06-2139, TRB 85th Annual Meeting Compendium of Papers CD-ROM, 2006.

44. **Romanoschi, A., and S. Bethu.** *Implementation of the 2002 AASHTO Design Guide for Pavement Structures in KDOT Part-II Asphalt Concrete Pavements.* K-TRAN: KSU-04-4 Part 2 Final Report, Kansas State University, Manhattan, Kansas, 2009.

45. **Von Quintus, H.** "Local Calibration of MEPDG - An Overview of Selected Studies." *Journal of the Asphalt Paving Technologists,* Volume 77 (2008): 935-971.

46. **Valesquez, R., K. Hoegh, I. Yut, N. Funk, G. Cochran, M. Marasteanu, and L. Khazanovich.** *Implementation of the MEPDG for New and Rehabilitated Pavement Structures for Design of Concrete and Asphalt Pavements in Minnesota*. Report No. MN/RC 2009-06, University of Minnesota, Minneapolis, Minnesota, 2009.

47. **Muthadi, N.,** *Local Calibration of the MEPDG for Flexible Pavement Design.* Master's Thesis, North Carolina State University, Raleigh, NC, 2007.

48. **Muthadi, N., and Kim, R.** "Local Calibration of Mechanistic-Empirical Pavement Design Guide for Flexible Pavement Design." *Transportation Research Board, Journal of the Transportation Research Board*, No. 2087 (2008): 131-141.

49. **Hoerner, T., K. Zimmerman, K. Smith, and A. Cooley.** *Mechanistic-Empirical Pavement Design Guide Implementation Plan*. SD2005-01 Final Report, Applied Pavement Technology, Inc., Urbana, IL, 2007.

50. **Flintsch, G., A. Loulizi, S. Diefenderfer, K. Galal, and B. Diefenderfer,** *Asphalt Materials Characterization in Support of Implementation of the Proposed Mechanistic-Empirical Pavement*

Design Guide. Report No. VTRC 07-CR10, Virginia Transportation Research Council, Charlottesville, VA, 2007.

51. **El-Badawy, S.,** "Recommended Changes to Designs not Meeting HMA Fatigue Cracking and Rutting Criteria." *6th International Engineering Conference, Civil and Architecture Engineering*, Sharm Elshekh, Egypt, 18-23 March (2008): pp. 261-272.
52. **ARA, Inc., ERES Consultants Division**. *Appendix II-2: Sensitivity Analysis for Asphalt Concrete Fatigue Alligator Cracking*. Guide for Mechanistic-Empirical Design of New and Rehabilitated Pavement Structures, NCHRP 1-37A Final Report, Washington, D.C.: March 2004.
53. **ARA, Inc., ERES Consultants Division**. *Appendix II-3: Sensitivity Analysis for Asphalt Concrete Fatigue Longitudinal Surface Cracking.* Guide for Mechanistic-Empirical Design of New and Rehabilitated Pavement Structures, NCHRP 1-37A Final Report, Washington, D.C.: March 2004.
54. **ARA, Inc., ERES Consultants Division**. *Appendix GG-2: Sensitivity Analysis for Permanent Deformation for Flexible Pavements.* Guide for Mechanistic-Empirical Design of New and Rehabilitated Pavement Structures, NCHRP 1-37A Final Report, Washington, D.C.: March 2004.
55. **ARA, Inc., ERES Consultants Division**. *Appendix CC-4: Development of a Revised Predictive Model for the Dynamic (Complex) Modulus of Asphalt Mixtures.* Guide for Mechanistic-Empirical Design of New and Rehabilitated Pavement Structures, NCHRP 1-37A Final Report, Washington, D.C.: March 2004.
56. **Garcia, G., and M. Thompson .** *HMA Dynamic Modulus Predictive Models-A Review*. FHWA-ICT-07-005 Report, Illinois Center for Transportation, University of Illinois, Urbana, IL, 2007.
57. **Ceylan, H., C. Schwartz, S. Kim, and K. Gopalakrishnan,** "Accuracy of predictive Models for Dynamic Modulus of Hot-Mix Asphalt." *Journal of Materials in Civil Engineering,* Vol. 21 No. 6 (2009): 286-293.
58. **Awed, A., S. El-Badawy, and F. Bayomy.** "Influence of the MEPDG Binder Characterization Input Level on the Predicted Dynamic Modulus for Idaho Asphalt Concrete Mixtures." Paper No. 11-1268, TRB 90th Annual Meeting Compendium of Papers CD-ROM, January 2011.
59. **El-Badawy, S., F. Bayomy, and A. Awed.** "Evaluation of the MEPDG Dynamic Modulus Prediction Models for Asphalt Concrete Mixtures." pp. 576-585 In: T&DI Congress 2011: 1st Integrated Transportation and Development for a Better Tomorrow. Chicago, IL: American Society of Civil Engineers, (2011).
60. **ASTM D2493.** *Standard Viscosity-Temperature Chart for Asphalts*. ASTM D2493/D2493M-09, Volume 04.03 Road and Paving Materials; Vehicle Pavement Systems, 2009.
61. **Dongre', R., L. Myres, J. D'Angelo, C. Paugh, and J. Gudimettla, J.** "Field Evaluation of Witczak and Hirsch Models for Predicting Dynamic modulus of Hot-Mix Asphalt." *Journal of the Association of Asphalt Paving Technologists,* Vol. 74, (2005): 381-434.
62. **Harran, G., and A. Shalaby.** "Improving the Prediction of the Dynamic Modulus of Fine-Graded Asphalt Concrete Mixtures at High Temperatures." *Canadian Journal of Civil Engineering*, Vol. 36, No. 2 (2009): 180-190.
63. **Birgisson, B., G. Sholar and R. Roque.** "Evaluation of Predicted Dynamic Modulus for Florida

Mixtures." *Journal of the Transportation Research Board*, No. 1929, (2005): 200-207.

64. **Bayomy, F., S. Jung, S., T. Weaver, R. Nielsen, A. Abu Abdo, S. Beak, and P. Darveshi.** *Development and Evaluation of Performance tests to enhance Superpave Mix Design and its Implementation in Idaho.* USDOT Assistance No. DTOS59-06-G-00029, ITD Project No. RP 181, National Institute for Advanced Transportation technology (NIATT), University of Idaho, Moscow, ID, 2010.
65. **AASHTO TP 62-07.** *Standard Method of Test for Determining Dynamic Modulus of Hot-Mix Asphalt Concrete Mixtures.* AASHTO TP 62-07, American Association of State Highway and Transportation Officials, Washington, D.C.: 2009.
66. **AASHTO PP 60-09.** *Preparation of Cylindrical Performance Test Specimens Using the Superpave Gyratory Compactor (SGC)*. AASHTO PP 60-09, Provisional Standards, American Association of State Highway and Transportation Officials. Washington, D.C.: 2009.
67. **AASHTO T315-06.** *Standard Method of Test for Determining the Rheological Properties of Asphalt Binder Using a Dynamic Shear Rheometer (DSR)*. American Association of State Highway and Transportation Officials, Washington, D.C.: 2006.
68. **AASHTO TP48-97.** *Standard Method of Test for Viscosity Determination of Asphalt Binder Using Rotational Viscometer.* American Association of State Highway and Transportation Officials, Washington, D.C.: 2006.
69. **AASHTO PP 62-09**. *Standard Practice for Developing Dynamic Modulus Master Curves for Hot Mix Asphalt*. Provisional Standards, American Association of State Highway and Transportation Officials, Washington, D.C.: 2009.
70. **Awed, A.** *Material Characterization of HMA for MEPDG Implementation in Idaho.* Master's Thesis, University of Idaho, Moscow. ID, 2010.
71. **Abu Abdo, A.,** *Development of Predictive Model to Determine the Dynamic Modulus for Hot Mix Asphalt.* Ph.D. Dissertation, University of Idaho, Moscow, 2008.
72. **Abu Abdo, A., F. Bayomy, R. Nielsen, T. Weaver, S.J. Jung, and M. Santi. "**Prediction of the Dynamic Modulus of Superpave Mixes" *Proceedings of the Bearing Capacity of Roads, Railways, and Airfields,* Tutumluer & Al-Qadi (eds), Taylor & Francis Group, London, 2009.
73. **Abu Abdo, A., F. Bayomy, E. Masad, and M. Santi.** "Evaluation of Aggregate Structure Stability Using the Superpave Gyratory Compactor." Paper No. 06-1402, TRB 85th Annual Meeting Compendium of Papers CD-ROM, 2006.
74. **Abu Abdo, A., F. Bayomy, T. Weaver, S. Jung, R. Nielsen and M. Santi.** "Development and Evaluation of Hot Mix Asphalt Stability Index." Paper No. 09-2076, TRB 88th Annual Meeting Compendium of Papers CD-ROM, 2009.
75. **Abu Abdo, A., F. Bayomy, T. Weaver, S. Jung, R. Nielsen and M. Santi.** "Development and Evaluation of Hot Mix Asphalt Stability Index." *International Journal of Pavement Engineering,* Vol. 11, No. 6 (2010): 529-539.
76. **Bahia, H., E. Masad, A. Stakston, S. Dessoukey, and F. Bayomy,** "Simplistic Mixture Design Using

the SGC and the DSR," *Journal of the Association of Asphalt Paving Technologists*, Vol. 72 (2003): 196-225.

77. **Bayomy, F., and A. Abu Abdo.** *Performance Evaluation of Idaho HMA Mixes Using Gyratory Stability.* Project No. SPR-0004(022) RP 175, National Institute for Advanced Transportation Technology, University of Idaho, Moscow, 2007.
78. **Bayomy, F., A. Abu Abdo, A., and M. Santi.** "Permanent Deformation Evaluation of Idaho Superpave Mixes Using the Gyratory Stability," Proceedings of the 8th International Conference on the Bearing Capacity of Roads, Railways and Airfields (BCRA'09), Champaign, Illinois. Volume 1, (2009): 295-303.
79. **Bayomy, F., E. Masad , and S. Dessouky.** *Development and Performance Prediction of Idaho Superpave Mixes*. Projcet No. SPR-0003(014) RP 148, National Institute for Advanced Transportation Technology (NIATT), University of Idaho, Moscow, Idaho, 2006.
80. **Dessoukey, S., E. Masad, and F. Bayomy .** "Evaluation of Asphalt Mix Stability Using Compaction Properties and Aggregate Structure Analysis." *The International Journal of Pavement Engineering,* Vol. 4, No. 2, (2003): 87-104.
81. **Dessouky, S., E. Masad, and F. Bayomy,** "Prediction of Hot Mix Asphalt Stability Using the Superpave Gyratory Compactor." *Journal of Materials in Civil Engineering*, Vol. 16, No. 6, (2004): 578-587.
82. **Pellinen, T.** *Investigation of the Use of Dynamic Modulus as an Indicator of Hot-Mix Asphalt Performance.* Ph.D. Dissertation, Arizona State University, Tempe, AZ, 2001.
83. **Christensen Jr., D. W., T. K. Pellinen, and R. F. Bonaquist.** "Hirsch Model for Estimating the Modulus of Asphalt Concrete," *Journal of the Association of Asphalt Paving Technologists*, Vol. 72, (2003): 97-121.
84. **Asphalt Institute.** *Research and Development of the Asphalt Institute's Thickness Design Manual (MS-1)*. 9th edition, Research Report No. 82-2, The Asphalt Institute, Executive Officers & Research Center, Asphalt institute Building, College Park, Maryland, 1982.
85. **Miller, S.,** *Developing Statistical Correlations of Soil Properties with R-Value for Idaho Pavement Design.* Report No. RP185-KLK553, National Institute for Advanced Transportation technology, University of Idaho, Moscow, Idaho, 2009.
86. **Arizona Department of Transportation.** *Materials Preliminary Engineering and Design Manual.* Arizona Department of Transportation, Highways Division, Materials Section, 3rd Edition, Phoenix, Arizona, 1989.
87. **Amos, B.,** *Arizona and Texas Pavement Design on Expansive Subgrade Soil: A Comparison*. Master's Thesis, Arizona State University, Tempe, AZ, 2009.
88. **El-Badawy, S., F. Bayomy, and S. Miller.** "Prediction of the Subgrade Resilient Modulus for Implementation of the MEPDG in Idaho." ASCE Geotechnical Special Publication No. 211. Jie Han and Daniel E. Alzamora, Eds., American Society of Civil Engineers, Reston, VA, (2011): 4762-4772.
89. **Kim, D., and J. Kim.** "Resilient Behavior or Compacted Subgrade Soils Under the Repeated Triaxial Test." *Construction and Building Materials.* Vol. 21, Issue 7, (2007): 1470-1479.

90. **George, K.** *Prediction of Resilient Modulus from Soil Index Properties.* Report No. FHWA/MS-DOT-RD-04-172, Department of Civil Engineering, the University of Mississippi, 2004. http://gomdot.com/Divisions/Highways/Resources/Research/pdf/Reports/InterimFinal/SS172.pdf (Accessed on May, 2010).

91. **Mohammed, L., K. Gaspard, A. Herath, and M. Nazzal.** *Comparative Evaluation of Subgrade Resilient Modulus from Non-destructive, In-situ, and Laboratory Methods*. Report No. FHWA/LA.06/417 Final Report, Louisiana Transportation Research Center, Baton Rouge, LA, 2007. http://ntl.bts.gov/lib/40000/40800/40857/fr_417.pdf, (Accessed on May, 2010).

92. **Khasawneh, M.** *Laboratory Characterization of Cohesive Subgrade Material*. Master's Thesis, University of Akron, 2005. http://etd.ohiolink.edu/view.cgi?acc_num=akron1124387175, (Accessed on May, 2010).

93. **Federal Highway Administration, Office of Highway Policy Information**. T*raffic Monitoring Guide*. U.S. Department of Transportation, Federal Highway Administration, Office of Highway Policy Information, Washington, D.C., 2001. http://www.fhwa.dot.gov/ohim/tmguide/pdf/tmg0.pdf, (Accessed on July, 2010).

94. **Cambridge Systematics, Inc.** *Traffic Data Collection, Analysis, and Forecasting for Mechanistic Pavement Design*. NCHRP Report 538, National Cooperative Highway Research Program, Transportation Research Board of the National Academies, Washington, D.C., 2005. http://www.trb.org/Main/Public/Blurbs/155210.aspx, (Accessed on July, 2010).

95. **Federal Highway Administration**, **Office of Infrastructure Research, Development and Technology.** *Guide to LTPP Traffic Data Collection and Processing.* Federal Highway Administration, Office of Infrastructure Research, Development and Technology, Virginia, 2001. http://www.fhwa.dot.gov/publications/research/infrastructure/pavements/ltpp/trfcol/trfcol.pdf, (Accessed on June, 2010).

96. **United States Geological Survey**. *National Water Information System: Web Interface*. http://nwis.waterdata.usgs.gov/id/nwis/gwlevels?search_criteria=lat_long_bounding_box&submitted_form=introduction, (Accessed on June, 2011).

97. **Darter M., L. Khazanovich, T., Yu, and J. Mallela. "**Reliability Analysis of Cracking and Faulting Prediction in the New Mechanistic –Empirical Pavement Design Procedure." *Transportation Research Board, Journal of the Transportation Research Board*, No. 1936, (2005): 150-160.

98. **Witczak, M., M. El-Basyouny, M. Jeong, and S. El-Badawy.** *Final Revised Section Calibration Data for Asphalt Surfaced Pavement Recalibration under NCHRP 1-40D*. Inter Team Technical Report, Arizona State University, Tempe, AZ, 2007.

99. **Federal Highway Administration.** *Long-Term Pavement Performance.* Standard Data Release 24.0, DVD Version, January, 2010.

100. **American Association of State Highway and Transportation Officials.** *Guide for the Local Calibration of the Mechanistic-Empirical Pavement Design Guide.* American Association of State Highway and Transportation Officials, 2010.

101. **Bennett, C., and W. Paterson.** *A Guide to Calibration and Adaptation of HDM-4. The Highway*

Development and Management Series. World Road Association, Volume 5: (2001). http://www.lpcb.org/lpcb-downloads/isohdm_other/2000_bennett_paterson_calibration_guide.pdf, (Accessed on July, 2011)

102. **Federal Highway Administration.** *Distress Identification Manual for the Long-Term Pavement Performance Program.* Publication No. FHWA-RD-03-031. U.S. Department of Transportation. Federal Highway Administration, 2003. http://www.fhwa.dot.gov/publications/research/infrastructure/pavements/ltpp/reports/03031/03031.pdf, (Accessed on May, 2011).

103. Idaho Transportation Department. *Idaho Transportation Department Pavement Rating Manual.* 2010.

104. Idaho Transportation Department. *Idaho Transportation System 2009 Performance Report.* Boise, ID: Idaho Transportation Department, Division of Transportation Planning, 2009, http://itd.idaho.gov/planning/pm/ITD_2009_Performance_Report.pdf, (Accessed on June, 2011).